UNIVERSITY OF CALIFORNIA

Santa Barbara

The Effects of Elevated Ocean Acidity and Temperature on the Physiological Integrity of the Larvae of the Cauliflower Coral, *Pocillopora damicornis*

A dissertation submitted in partial satisfaction of the

requirements for the degree Doctor of Philosophy

in Ecology, Evolution & Marine Biology

by

Emily Bethana Rivest

Committee in charge:

Professor Gretchen E. Hofmann, Chair

Professor Sally J. Holbrook

Professor Kathleen R. Foltz

Professor Peter J. Edmunds, California State University, Northridge

June 2014

The dissertation of Emily Bethana Rivest is approved.

_____
Sally J. Holbrook

_____
Kathleen R. Foltz

_____
Peter J. Edmunds

_____
Gretchen E. Hofmann, Committee Chair

June 2014

The Effects of Elevated Ocean Acidity and Temperature on the Physiological Integrity of the Larvae of the Cauliflower Coral, *Pocillopora damicornis*

ACKNOWLEDGEMENTS

I would like to first acknowledge my advisor, Dr. Gretchen Hofmann, for her steadfast support throughout my graduate career. I am grateful that she supported my desires to study the physiology of tropical reef corals and encouraged my quests to fund that research, whose study system differed from that of her lab core. She is truly an incredible mentor and an excellent role model. She showed me how to be a strong female scholar and how to be a compassionate teacher and mentor. She facilitated and curbed my ambition with finesse. I will always feel incredibly honored to have been her student and colleague.

Next, I would like to acknowledge Dr. Peter Edmunds for his expertise in coral physiology. My academic growth, project development, and writing have benefited tremendously from his depth and breadth of knowledge about corals and the coral reef ecosystem, his razor-sharp analytical skills, and his perspective. I am very grateful for his support of my research projects at field sites in Moorea, French Polynesia and in Taiwan. I would also like to thank Dr. Sally Holbrook for guidance during my dissertation. I appreciate her attention to detail and her support of my projects through the Moorea Coral Reef Long-Term Ecological Research Program. I also wish to acknowledge Dr. Kathleen Foltz for her compassionate mentorship and her guidance.

My dissertation research, much of which took place at international field stations, was made possible by the support of many people. I would like to thank Dr. Brian Rivest, Lydia Kapsenberg, Dr. Anderson Mayfield, Anna MacPherson, and Dr. Paul Matson for their support during my field seasons in Moorea. I am particularly thankful that my dad and I could collaborate on a research project there. My work in Moorea benefited from the field

operations support of Keith Seydel, Vinny Moriarty, Jessica Nielsen, and Chelsea Behymer. Many thanks to the staff of Gump Station for keeping the power and seawater pump on and for making my stay enjoyable. I am thankful for Chicken and Guinness, whose company I enjoyed. I wish to thank Dr. Chii-Shiarng Chen and his lab members for hosting me in his research lab at the National Museum for Marine Biology and Aquarium for two summers. Dr. Tung-Yung Fan and his lab members supported my dive operations in Taiwan as well as husbandry and experimentation with corals. I am grateful to the support and collaboration of Dr. Vivian Cumbo, Dr. Steeve Comeau, Aaron Dufault, Chris Wall, Sylvia Zamudio, and Aaron Ninokawa in Moorea and in Taiwan. Many thanks to Drs. Li-Hsueh Wang and Hsing-Hui Li and their students for their assistance in getting my life and lab work off the ground in Taiwan. I wish to thank the students at the National Museum of Marine Biology and Aquarium, for welcoming me, conversing with me in English, and helping me navigate rural southern Taiwan. I would like to thank Josh Hancock, Katrina Shao, Silke Bachhuber, Farallon Broughton, Fiona Luong, Yana Nebuchina, Steven Liao, and Raymond Lu for their assistance with sample analyses. I would like to acknowledge Dr. Xueying Han, Daniel Okamoto, and Dr. Stephen Gosnell for their support in statistical analysis. I would also like to thank Dr. Libe Washburn and Chris Gotschalk for their guidance with time series analysis and MatLab code. I am grateful for the support of Dr. Morgan Kelly for bioinformatics. I would like to thank the members of the Hofmann lab for their support in the development of the laboratory techniques I employed and their academic and social dialogue.

Lastly, I would like to acknowledge the support of my family. My father, Brian Rivest, has encouraged my intellectual curiosity and my love for biology since I can remember. I have enjoyed his empathy for my experiences during graduate school and for

his involvement in my research, directly in Moorea and indirectly through lots of phone conversations. My mother, Mary Jane Rivest, has been a dependable source of emotional comfort throughout this endeavor. I am grateful for her patience, her generosity, and her abundant love. My sister, Julie Rivest, has been my compatriate through it all. I am thankful for our kinship, the priority of our relationship, and the way she brings the silliness out of me! Without a doubt, my fiancé Silas Magee has been my holdfast while I have pursued a PhD. I am grateful for his support during my long research trips – for the Skype lunch/dinner meals – and particularly for his support during the writing of my prospectus and this thesis. I appreciate his innovative ideas for funding ("Will titrate for $$"), his enthusiasm for my career (Profy-wife), and his hugs.

VITA OF EMILY BETHANA RIVEST
June 2014

EDUCATION

2008 – 2014	**University of California, Santa Barbara** Doctor of Philosophy Ecology, Evolution and Marine Biology Advisor: Dr. Gretchen Hofmann
2004 – 2008	**Cornell University** Bachelor of Science Biology (Biochemistry), College of Agriculture and Life Sciences *Cum Laude* with High Honors in Research
2000 – 2004	**Dryden High School**, Dryden, NY

FELLOWSHIPS AND AWARDS

2014	University Award of Distinction, UC Santa Barbara
2014	Charles A. Storke Fellowship, Dept. Ecology, Evolution and Marine Biology (EEMB), UC Santa Barbara
2013-2014	Broida-Hirschfelder Graduate Fellowship, UC Santa Barbara Faculty Women's Club, UC Santa Barbara
2013	EEMB Graduate Fellowship, UC Santa Barbara
2012	EEMB Graduate Fellowship, UC Santa Barbara
2012	2012-13 Academic Senate Doctoral Student Travel Grant, UC Santa Barbara ($1400)
2012	Ellen Schamberg Burley Graduate Scholarship ($800)
2012	Journal of Experimental Biology Travelling Fellowship, "*Energetic costs of an acidic, warm environment: changes in lipid consumption of* Pocillopora damicornis *larvae*" (£1200)
2011	National Science Foundation – East Asia Pacific Summer Institutes – Taiwan
2010-2012	Luce *Environmental Science to Solutions* Fellowship
2009-2012	National Science Foundation – Graduate Research Fellowship
2008-2009	EEMB Graduate Fellowship Award, UC Santa Barbara
2007	Hughes Scholars Program, Cornell University

GRANTS IN SUPPORT OF RESEARCH

2012-present	National Science Foundation, Office of International Science and Engineering, Doctoral Dissertation Improvement Funding, "*The energetic cost of an acidic, warm environment: changes in lipid consumption of* Pocillopora damicornis *larvae*" PIs: GE Hofmann and EB Rivest ($9,595)

2011-present	Moorea Coral Reef LTER, PIs: GE Hofmann and EB Rivest ($18,900)
2009-2010	Moorea Coral Reef LTER Minigrant, "*Ocean acidification experiments on tropical marine invertebrate larvae using a portable CO_2 system*" PIs: GE Hofmann and EB Rivest, ($17,000)
2008-2009	Mildred E. Mathias Graduate Research Grant, UC Reserve System ($800)

PUBLICATIONS

Rivest, EB and GE Hofmann. 2014. Responses of the metabolism of the larvae of *Pocillopora damicornis* to ocean acidification and warming. *PLoS ONE* 9(4): e96172.

Gaitán-Espitia, JD, JR Hancock, JL Padilla-Gamiño, **EB Rivest,** CA Blanchette, DC Reed, GE Hofmann**.** Interactive effects of elevated temperature and pCO_2 on early-life-history stages of the giant kelp *Macrocystis pyrifera*. *Journal of Experimental Marine Biology and Ecology* 457: 51-58.

Hofmann, GE, CA Blanchette, **EB Rivest,** and L Kapsenberg. 2013. Taking the pulse of marine ecosystems: the importance of coupling long-term physical and biological observations in the context of global change biology. *Oceanography* 26(3):140–148.

Prather, CM, S Pellini, A Laws, **EB Rivest**, *et al.* 2012. Invertebrates, ecosystem services and climate change. *Biological Reviews Cambridge Philosophical Society* 88: 327-348.

Yu, PC, MA Sewell, PG Matson, **EB Rivest**, L Kapsenberg, and GE Hofmann. 2012. Growth attenuation with developmental schedule progression in embryos and early larvae of *Sterechinus neumayeri* raised under elevated pCO_2. *PLoS ONE* 8(1): e52448.

Hofmann, GE, JE Smith, KS Johnson, U Send, LA Levin, F Micheli, A Paytan, NN Price, B Peterson, Y Takeshita, PG Matson, ED Crook, KJ Kroeker, MC Gambi, **EB Rivest**, CA Frieder, PC Yu, and TR Martz. 2011. High-frequency dynamics of ocean pH: a multi-ecosystem comparison. *PLoS ONE* 6(12): e28983.

Rivest, EB, DM Baker, KL Rypien, and CD Harvell. 2010. Nitrogen source preference of *Aspergillus sydowii*, the causative agent of aspergillosis in sea fan corals. *Limnology and Oceanography* 55(1): 386-392.

In review/revision

Lunden, JL*, **EB Rivest* (*co-first authors)**, L Kapsenberg, TR Martz, CC Gotschalk, M O'Brien, CA Blanchette, and GE Hofmann. *Environmental Science & Technology*.

Rivest, EB and GE Hofmann. A sinking ship?: effects of high pCO_2 and temperature on lipid use and physiological condition of larvae of *Pocillopora damicornis.* *Journal of Experimental Biology.*

In preparation

Rivest, EB, C-S Chen, T-Y Fan, H-H Li, PJ Edmunds, and GE Hofmann. Climate change challenges the energy budgets of *P. damicornis* larvae, but effects differ between sites with unique environmental conditions. *Proc R Soc B*

Rivest, EB and GE Hofmann. Gene expression in *Pocillopora damicornis* larvae responds differently to multiple vs. single stressors, ocean acidification and warming.

Rivest, EB, C-S Chen, T-Y Fan, L-H Wang, PJ Edmunds, and GE Hofmann. Effects of ocean acidification and elevated temperature on oxidative state and ionic balance in the larvae of the coral *Pocillopora damicornis*.

PRESENTATIONS OF RESEARCH

Rivest, EB, C-S Chen, T-Y Fan, H-H Li, and GE Hofmann**.** Effects of multiple stressors on lipid consumption and fitness characteristics of coral larvae are linked to local environmental variability and release date. 2014 Ocean Sciences Meeting (ASLO, AGU, and TOS), Honolulu, HI (Poster, February 25, 2014).

Rivest, EB, GE Hofmann, CA Blanchette, and L Kapsenberg. Keeping a finger on the pulse of marine ecosystems: the investment of coupled long-term physical and biological observations to understand the consequences of a changing environment. 94th Annual Meeting of the Western Society of Naturalists, Oxnard, CA (15 minute oral presentation, November 8, 2013).

Bachhuber, SM, CS Sugano, MW Kelly, **EB Rivest**, and GE Hofmann. Effects of elevated pCO_2 conditions on larval development of red abalone, *Haliotis rufescens*. 90th Annual Meeting of the Western Society of Naturalists (Poster, November 8, 2013).

Rivest, EB, X Han, and S Davis. *Identifying alternative indicators for the detection of abrupt transitions in ecosystems*. Moorea Coral Reef Long Term Ecological Research All Investigators Meeting, Santa Barbara, CA (Invited seminar, October 2013).

Rivest, EB and co-authors. *Identifying alternative indicators for the detection of abrupt transitions in ecosystems: multivariate analyses and cross-site comparisons*. MCR LTER site review, Moorea, French Polynesia (Poster, July 9, 2013).

Rivest, EB and GE Hofmann. *Coupling environmental history with physiological performance: a new direction for ocean acidification research*. Moorea Coral Reef Long Term Ecological Research site review, Moorea, French Polynesia (Poster, July 9, 2013).

Rivest, EB. *Effects of a changing ocean: characteristic patterns in tropical coral larvae vary throughout the lunar cycle.* 2nd meeting of the Consortium for the Study of Ocean Change, UABC, Ensenada, Mexico (Invited seminar, June 18, 2013).

Rivest, EB and GE Hofmann. *Coupling environmental history with physiological performance: a new direction for ocean acidification research*. Marine Science Graduate Research Showcase, UC Santa Barbara, Santa Barbara, CA (Poster, April 23, 2013).

Rivest, EB and GE Hofmann. *Coupling environmental history with physiological performance: a new direction for ocean acidification research*. UCSB Graduate Research Showcase, Santa Barbara, CA (Poster, April 19, 2013).

Rivest, EB. *Astrology of a tropical reef coral: characteristic physiological patterns in larvae.* LTER Student Symposium: CCE-SBC-MCR. University of California, San Diego, Scripps Institution of Oceanography, San Diego, CA (15 minute oral presentation, March 16, 2013).

Rivest, EB. *Astrology of a tropical reef coral: characteristic physiological patterns in larvae*. 9th Annual EEMB Graduate Student Symposium. UC Santa Barbara, Santa Barbara, CA (15 minute oral presentation, February 2, 2013).

Rivest, EB, C-S Chen, T-Y Fan, H-H Li, PJ Edmunds, and GE Hofmann. *Energetic consequences of ocean acidification and warming for coral larvae.* The Society for Integrative and Comparative Biology 2013 meeting, San Francisco, CA (Poster, January 5, 2013).

Rivest, EB and GE Hofmann. *Coupling environmental history with physiological performance: a new direction for ocean acidification research*. Long Term Ecological Research Network All Scientists Meeting, Estes Park, CO (Poster, September 12, 2012).

Rivest, EB, C-S Chen, T-Y Fan, H-H Li, PJ Edmunds, and GE Hofmann. *Energetic consequences of ocean acidification and warming for coral larvae*. National Museum of Marine Biology and Aquarium, Checheng, Taiwan (Invited seminar, August 13, 2012).

Rivest, EB and GE Hofmann. *Metabolic plasticity in coral larvae under ocean acidification and warming*. 12th International Coral Reef Symposium, Cairns, Australia (15 minute oral presentation, July 13, 2012).

Rivest, EB. *What's a larva to do?: Physiological mechanisms for tolerating a changing ocean.* Centre de Recherches Insulaires et Observatoire de l'Environnement, Moorea, French Polynesia (Invited seminar, March 13, 2012).

Rivest, EB, C-S Chen, T-Y Fan, L-H Wang, PJ Edmunds, and GE Hofmann. *Effects of ocean acidification and elevated temperature on ion balance and oxidative state in the larvae of the coral* Pocillopora damicornis. NSF EAPSI Symposium, Hsinchu, Taiwan (Poster, August 19 2011).

Rivest, EB, C-S Chen, T-Y Fan, L-H Wang, PJ Edmunds, and GE Hofmann. *Effects of ocean acidification and elevated temperature on ion balance and oxidative state in the larvae of the coral* Pocillopora damicornis. National Museum of Marine Biology and Aquarium, Checheng, Taiwan. (Invited seminar, August 16, 2011).

Rivest, EB and GE Hofmann. *Live from Moorea: At Sea and In The Lab*. Long Term Ecological Research Graduate Symposium (MCR, SBC, CCE), Santa Barbara, CA (Poster, February 2011).

Rivest, EB and GE Hofmann. *Potential effects of ocean acidification on three tropical invertebrates, the coral* Pocillopora damicornis*, the sea urchin* Echinometra mathaei, *and the crown-of-thorns starfish* Acanthaster planci. Moorea Coral Reef Long Term Ecological Research All Investigators Meeting, Santa Barbara, CA (Poster, November 2009).

Rivest, EB and GE Hofmann. *The effect of pH stress during upwelling events on the gene expression of* Strongylocentrotus purpuratus*, the purple sea urchin*. 90th Annual Meeting of the Western Society of Naturalists, Monterey, CA (Poster, November 2009).

Rivest, EB and GE Hofmann. *Potential effects of ocean acidification on three tropical invertebrates, the coral* Pocillopora damicornis*, the sea urchin* Echinometra mathaei, *and the crown-of-thorns starfish* Acanthaster planci. The US Long Term Ecological Research Network All Scientists Meeting, Estes Park, CO (Poster, September 2009).

TEACHING EXPERIENCE

2014	**Teaching Assistant**, Field Studies in Marine Ecological Physiology, *UC Santa Barbara*
2013	**Guest lecturer**, "Introduction to Coral Reefs" INT 91: Marine Science, *UC Santa Barbara*
2013	**Guest lecturer**, "Ocean Acidification and Coral Reefs" EEMB 55: Global Change Biology, *UC Santa Barbara*
2013	**Teaching Assistant,** Field Studies in Marine Ecological Physiology, *UC Santa Barbara*
2010	**Teaching Assistant**, Introductory Biology Laboratory 3, *UC Santa Barbara*
2008	**Teaching Assistant**, Field Marine Ecology – Belize, *State University of New York, Cortland*

PROFESSIONAL EXPERIENCE

2012-present. **Project leader**, "Effects of ocean acidification and warming on lipid content and physiological integrity of larvae of the coral *Pocillopora damicornis*

in Taiwan," National Museum of Marine Biology and Aquarium, Taiwan. Conducted manipulative culturing experiments with coral larvae. Measured pH and temperature variability on a fringing reef. Extracted cellular lipid and quantified lipid classes using thin-layer chromatography and flame ionization detection. Photographed larvae and measured size metrics. Quantified total protein and symbiont density.

2012-present. **Project leader**, "Identifying alternative indicators for the detection of abrupt transitions in ecosystems." Workshop sponsored by the US Long-Term Ecological Research Network. Synthesized long-term data to identify and characterize known ecosystem transitions, exploring the use of alternative indicators and temporal scales. Developed a set of recommendations to improve collection of long-term time series data for the detection of ecosystem transitions.

2012-2013. **Graduate Student Researcher**, UC Santa Barbara, Santa Barbara, CA. Organized deployments of SeaFET sensors for Santa Barbara Coastal Long-Term Ecological Research program. Established and performed quality control procedures for data analysis. Assisted with data management.

2011-present. **Project Leader**, "Effects of ocean acidification and warming on lipid content and physiological integrity of larvae of the coral *Pocillopora damicornis* in Moorea, French Polynesia," UC Berkeley Richard B. Gump South Pacific Research Station, Moorea, French Polynesia. Conducted manipulative culturing experiments with coral larvae. Measured pH and temperature variability on a fringing reef. Extracted cellular lipid and quantified lipid classes using thin-layer chromatography and flame ionization detection. Photographed larvae and measured size metrics. Quantified total protein and symbiont density.

2011. **Project Leader**, "Effects of ocean acidification and warming on oxidative state and ion balance of larvae of the coral *Pocillopora damicornis*," National Museum of Marine Biology and Aquarium, Taiwan. Conducted manipulative culturing experiments with coral larvae. Measured total antioxidant potential and catalase activity using spectrophotometric assays. Measured activities of Na^+/K^+-ATPase using spectrophotometric assays.

2011. **Project Leader**, "Effects of ocean acidification and warming on the metabolism of larvae of the coral *Pocillopora damicornis*," UC Berkeley Richard B. Gump South Pacific Research Station, Moorea, French Polynesia. Conducted manipulative culturing experiments with coral larvae. Measured oxygen consumption, total protein content, and citrate synthase activity of larvae. Measured pH and temperature variability on a fringing reef.

2010-present. **Project Leader**, "Effects of ocean acidification and warming on gene expression of larval of the coral *Pocillopora damicornis*," UC Berkeley Richard B. Gump South Pacific Research Station, Moorea, French Polynesia. Conducted manipulative culturing experiments with coral larvae. Extracted and sequenced total RNA. Assembled transcriptome and identified differentially expressed genes.

2010-2012. **Project Participant**, "Testing for the fingerprint of climate change in the phenology of marine organisms." Workshop sponsored by UC Santa Barbara and the Henry Luce Foundation. Retrieved and archived phenology time series data. Project directed by B Haggerty.

2010-2011. **Project Participant and Field Team Member**, "Effects of ocean acidification on the larvae of the sea urchin *Sterechinus neumayeri*," McMurdo Station, Antarctica. Performed missions to collect seawater samples through sea ice over Ross Sea. Performed seawater chemistry analyses. Assisted with sea urchin culturing experiments. Project directed by Dr. GE Hofmann.

2009-2011. **Project Participant**, "Invertebrate effects on ecosystem services under climate change." Workshop sponsored by the US Long-Term Ecological Research Network. Developed a manuscript for publication that provided (1) a review of the potential roles of invertebrates in providing ecosystem services, and (2) a discussion of the effects of global climate change on invertebrate impacts on ecosystem services. Project directed by CM Prather.

2007. **Hughes Scholars Program; Undergraduate Research**, Cornell University, Ithaca, NY. Evaluated the nutrient limitation and nitrogen source preference of the coral pathogenic fungus *Aspergillus sydowii*. Measured fungal growth and morphology. Compared nitrogen assimilation using stable isotope analysis. Project directed by Dr. CD Harvell.

2006. **Undergraduate Research**, Cornell University, Ithaca NY. Assessed the nutritional requirements of the fungus *A. sydowii*. Measured fungal growth and used stable isotope techniques. Project directed by Dr. CD Harvell.

2006. **Research Assistant**, Cornell University, Ithaca, NY. Performed fungal growth experiments. Extracted DNA from fungal isolates. Project directed by Dr. CD Harvell.

PROFESSIONAL ACTIVITIES, OUTREACH, AND SERVICE

2013	**Ambassador of UCSB graduate research**, 2013 Graduate Research Advocacy Day, University of California Office of the President, Sacramento, CA
2013	**Panel facilitator**, EEMB Graduate Student Panel, EEMB 510: Professional Development, UC Santa Barbara, Santa Barbara, CA
2013	**Instructor**, Science Communication Workshop for Graduate Students, Moorea Coral Reef Long Term Ecological Research All Investigators Meeting, Santa Barbara, CA
2013	**Instructor**, 2nd workshop for the Consortium for the Study of Ocean Change, UABC, Ensenada, Mexico
2013	**Co-organizer,** 9th Annual Graduate Student Symposium, UC Santa Barbara, Dept. Ecology, Evolution and Marine Biology, Santa Barbara, CA
2012	**Instructor**, A Day with Coral Biologists. National Museum of Marine Biology and Aquarium, Taiwan.
2012-present	**Reviewer for professional journals:** PLoS ONE, Marine Ecology Progress Series, Coral Reefs
2011-present	**Chair of professional development committee and active member**, Graduate Student Advisory Council, Dept. Ecology, Evolution and Marine Biology, UC Santa Barbara, Santa Barbara, CA

2011	**Volunteer**, MCR LTER Education and Outreach booth, Earth Day Festival, Santa Barbara, CA
2011	**Instructor**, "The ocean is changing: climate change and its effects on marine organisms." MCR LTER Outreach, UC Santa Barbara, Santa Barbara, CA
2011	**Presenter**, Research showcase for French Polynesian science teachers, MCR LTER Outreach, University of California Berkeley Richard B Gump South Pacific Research Station, Moorea, French Polynesia
2010	**Volunteer**, MCR LTER Education and Outreach booth, Earth Day Festival, Santa Barbara, CA
2010	**Presenter**, "The ocean is changing: climate change and its effects on marine organisms." MCR LTER Outreach, UC Santa Barbara, Santa Barbara, CA
2008 – 2011	**Instructor**, Family Ultimate Science Experience Workshop, UC Santa Barbara, Santa Barbara, CA
2007 – 2008	**Mentor**, Expanding Your Horizons Workshop, Cornell University, Ithaca, NY

RELEVANT GRADUATE COURSEWORK

2013	Bioinformatics Short Course, Genome Center and Bioinformatics Core Facility, UC Davis
2013	MARINE Short Course on Ocean Policy, Stanford University, Center for Ocean Solutions (Profs. M Caldwell, L Crowder, A Erickson, J Kittinger)
2011	Science Communication, UC Santa Barbara (Prof. S Airame)
2010	Writing Science, UC Santa Barbara (Prof. J Schimel)
2009	Larval Biology course, Friday Harbor Laboratories, University of Washington (Profs. R Strathmann, R Emlet)
2009	Biomechanics, Ecological Physiology and Genetics of Intertidal Communities, PISCO, Hopkins Marine Station, Stanford University (Profs. M Denny, G Somero, S Palumbi)

AFFILIATIONS WITH PROFESSIONAL ORGANIZATIONS

American Academy of Underwater Science
Association for the Sciences of Limnology and Oceanography
Consortium for the Study of Ocean Change (CSOC)
Ocean Margin Ecosystems Group of Acidification Studies (OMEGAS)
Society for Integrative and Comparative Biology
California Current Acidification Network
Western Society of Naturalists

ABSTRACT

The Effects of Elevated Ocean Acidity and Temperature on the Physiological Integrity of the Larvae of the Cauliflower Coral, *Pocillopora damicornis*

by

Emily Bethana Rivest

Ocean acidification (OA) and rising sea surface temperatures will likely shape the structure and function of coral reefs in the future (Fig. 1). Understanding the sensitivity of corals to ongoing shifts in pCO_2 and temperature is imperative as coral are the engineers of the coral reef ecosystem. Specifically, coral larvae may be a life history stage of corals that is particularly vulnerable to environmental stress. Shifts in physiological processes in response to environmental conditions may affect the success of larval dispersal and recruitment.

The aim of this dissertation was to examine the physiological plasticity of coral larvae in response to two potentially interacting anthropogenic stressors – OA and warming. *Pocillopora damicornis* (Linnaeus, 1758) was an excellent study organism for this research given its ubiquitous Indo-Pacific distribution, reef-building role, and long dispersal potential. To accomplish the objectives of this dissertation, I conducted laboratory experiments in which *P. damicornis* larvae were exposed to seawater of different pCO_2 and temperature conditions. *P. damicornis* larvae were collected from populations in Moorea, French Polynesia and southern Taiwan.

To understand the consequences of OA and warming on the physiology of *P. damicornis* larvae, I employed a holistic approach, examining the response of a suite of physiological processes from the levels of gene expression up to the level of the whole organism. I used metabolic rate and lipid utilization as whole-organism techniques for assessing the effects of OA and warming on larval energy consumption. Planulae released after the peak of spawning experienced metabolic suppression under high-temperature, high-pCO_2 conditions. There was evidence of biochemical limits of increasing oxidative capacity to satisfy elevated energy demands under future ocean conditions. Measurements of lipid utilization suggested that the metabolic costs of tolerating OA and warming will be greatest when both environmental stressors occur simultaneously. Larvae released at the peak of spawning will experience greatest changes in lipid content in response to OA and warming, with associated changes in buoyancy that affect their dispersal potential.

The organism-level studies revealed physiological plasticity within coral larval energy consumption. Biochemical and transcriptomic techniques were used to better understand the underlying mechanisms. *P. damicornis* larvae increased their total antioxidant potential in response to oxidative stress under exposures to high pCO_2 but not elevated temperature. Furthermore, OA-induced hypercapnia caused increased acid-base regulation, observed through elevated pNPPase activity of Na^+/K^+-ATPase. As was observed at the whole-organism level, physiological traits varied between cohorts of larvae. Finally, comparisons of gene expression profiles revealed down-regulation of genes under single-stressor treatments but up-regulation of genes when high-pCO_2 and high-temperature co-occurred.

An important facet of my dissertation research was to provide environmental context for the results of my biological experiments. I deployed autonomous pH and temperature sensors on the fringing reefs where the experimental corals were collected. The time series of pH and temperature approximated the conditions of the water mass bathing the reef to which the study organisms were acclimatized and into which the larvae would have been released. These environmental data confirmed that control treatments in the laboratory experiments were within the range of conditions experienced on the reef. The elevated pCO_2 treatment levels were not observed in the present-day time series. Additionally, pH and temperature regimes differed between reefs in Moorea and Taiwan. pH and temperature were on average lower in Taiwan and more variable in Moorea. Temperature was on average lower and more variable in Taiwan. These results highlight the importance of generating such an environmental context for study species. Environmental data informed metrics of biological performance of individuals at these sites as well as the potential heterogeneity of phenotypes across the biogeographic species range, products of local adaptation to regimes of pH and temperature.

TABLE OF CONTENTS

LIST OF FIGURES

LIST OF TABLES

I. Introduction

Future ocean change: ocean acidification and warming

Ocean acidification (OA) and ocean warming are expected in marine ecosystems as consequences of continued anthropogenic fossil fuel use, with significant changes already detected in the surface ocean (Feely, 2008). Atmospheric CO_2 concentrations are rising at about 0.5% per year, and atmospheric pCO_2 is expected to increase from present-day levels of ~396 ppm (2013 atmospheric mean; Tans & Keeling, 2014) to about 936 ppm by the end of the century (RCP8.5, IPCC, 2013). The surface ocean absorbs about one-third of this anthropogenic CO_2 (Sabine et al., 2004), which dissociates into HCO_3^- and H^+, causing seawater pH to decrease. Consequently, surface ocean pH may drop by ~0.3 units by 2100 (IPCC, 2013). This lower pH drives H^+ to combine with carbonate ions, CO_3^{2-}, to form more HCO_3^-. The resulting decrease in $[CO_3^{2-}]$ will cause long-term decreases in the calcium carbonate saturation state, $\Omega = [Ca^{2+}][CO_3^{2-}]/K'_{sp}$ (Doney, 2010). As carbonate becomes less saturated, the precipitation of calcium carbonate for calcification of structures like shells and skeletons becomes increasingly difficult and energetically costly (*e.g.* Cohen and Holcomb, 2009). Additionally, the projected changes in ocean chemistry will challenge marine organisms by disturbing their acid-base physiology, the processes maintaining intracellular chemical homeostasis (Fabry et al., 2008).

Concurrently with acidification, the surface temperature of the oceans is rising as Earth's climate warms. By 2100, average sea surface temperatures (SSTs) are expected to increase by ~2°C relative to the period 1980-2005 (IPCC, 2013). Temperature and ocean acidification may affect the same physiological processes, perhaps synergistically. Our

knowledge about biological tolerances to interacting stressors is increasing, particularly with regard to OA and temperature (for recent reviews, see Hendriks et al., 2010; Hofmann et al., 2010; Kroeker et al., 2010; Somero, 2010; Byrne, 2011; Sunday et al., 2012). High pCO_2 can exacerbate the effects of elevated temperatures by narrowing thermal tolerance windows (Pörtner, 2008; Walther et al., 2009; Hofmann and Todgham, 2010; Lannig et al., 2010). For example, thermal sensitivity of heart rates of the spider crab, *Hyas araneus*, increased as pCO_2 rose (Walther et al., 2009). A significant interaction of pCO_2 and temperature has been reported for processes including mortality, calcification, dissolution rate, metabolism/aerobic scope, motility, and community composition (Rosa and Seibel, 2008; Martin and Gattuso, 2009; Munday et al., 2009; Rose et al., 2009; Comeau et al., 2010; Rodolfo-Metalpa et al., 2010; Wood et al., 2010).

For early life history stages of marine invertebrates, fertilization appears to be robust to the interaction of elevated temperature and pCO_2 (Byrne et al., 2010). However, responses of physiological processes of marine invertebrate larvae to increases in pCO_2 and temperature have been inconsistent between studies (O'Donnell et al., 2009; Parker et al., 2009, 2010; Sheppard Brennand et al., 2010; Walther, 2010). This variation in response to OA and its interaction with temperature may be due to differential sensitivities of particular physiological processes, like calcification, as well as specific differences in sensitivity to these environmental stressors between species or between broader taxonomic groups (***i.e.*** calcifiers vs. non-calcifiers; Kroeker et al., 2010; Byrne, 2011).

The vulnerability of tropical reef corals to ocean acidification and warming

Understanding the sensitivities of reef-building corals to the ongoing simultaneous shifts in pCO_2 and temperature is imperative (Fig. 1) as corals are the engineers of the coral reef ecosystem that provides habitat for an incredible diversity of organisms as well as food, income, and coastline security to millions of humans. Tropical reef corals may be particularly vulnerable to changes in their abiotic environment. Thermal stress presents a major threat to coral reefs as the oceans warm (Hoegh-Guldberg, 1999). Thermotolerance limits of coral can be passed by only a few degrees of ocean warming (Jokiel and Coles, 1990; Middlebrook et al., 2008). The coral holobiont may be more sensitive because the symbiosis between *Symbiodinium* and coral is fragile. In response to thermal stress, bleaching often occurs, where the density of endosymbiont *Symbiodinium* and/or chlorophyll within the coral decreases. As a result, the coral animal loses a vital source of energy used to maintain normal function and to withstand future stress (*e.g.* Hoegh-Guldberg, 1999). OA may act synergistically with warming to lower the temperature threshold for bleaching in reef-building corals, magnifying the threat of bleaching (Anthony et al., 2008).

The majority of coral studies focused on the effects of OA have examined changes in rates of calcification and primary productivity. For corals, the saturation state of aragonite (the calcium carbonate mineral used to form coral skeletons) in tropical oceans may drop by 30% by 2100, causing a similar drop in calcification (Kleypas et al., 1999a; Hoegh-Guldberg et al., 2007; Jokiel et al., 2008; Marubini et al., 2008; Kroeker et al., 2010). However, corals may be able to use pH regulation and bicarbonate ions in their calcification fluid to maintain higher calcification rates under OA conditions (McCulloch et al., 2012; Comeau et al., 2013). High pCO_2 causes bleaching and loss of productivity in *Porites* and *Acropora* species

Figure 1. The effects of elevated ocean acidity and temperature on the physiological integrity of coral larvae. Ocean acidification (OA) and warming are among the environmental stressors that will influence the vitality of coral reefs. While OA and warming are known to decrease calcification and cause bleaching in corals, their interactive effects on coral larvae are less understood. In my dissertation research, I examined a variety of processes involved in the physiological plasticity of the larvae of the cauliflower coral, *Pocillopora damicornis*.

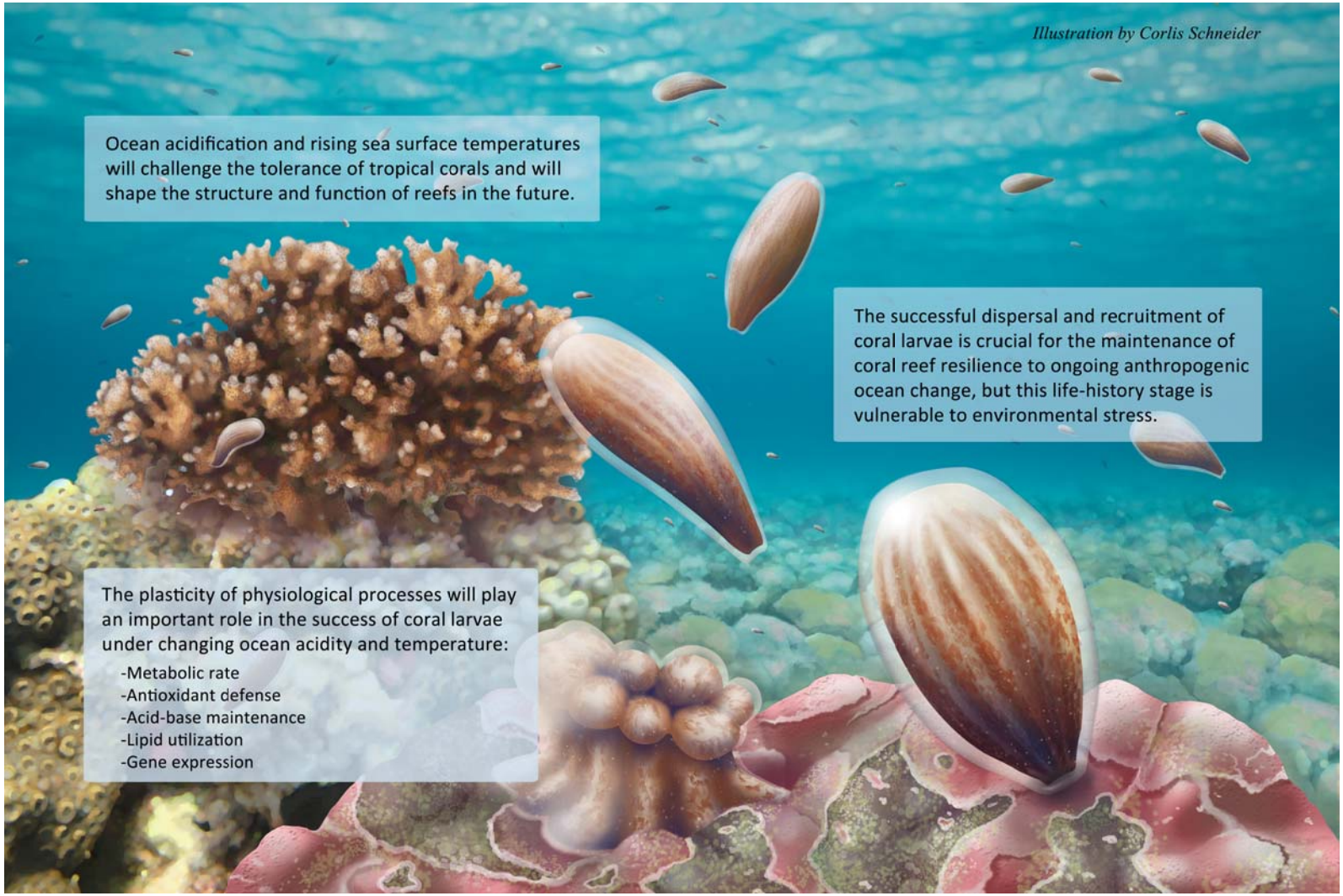
Illustration by Corlis Schneider
Ocean acidification and rising sea surface temperatures will challenge the tolerance of tropical corals and will shape the structure and function of reefs in the future.
The successful dispersal and recruitment of coral larvae is crucial for the maintenance of coral reef resilience to ongoing anthropogenic ocean change, but this life-history stage is vulnerable to environmental stress.
The plasticity of physiological processes will play an important role in the success of coral larvae under changing ocean acidity and temperature:
-Metabolic rate
-Antioxidant defense
-Acid-base maintenance
-Lipid utilization
-Gene expression

(Anthony et al., 2008), but both positive and negative responses in productivity have been documented (Kroeker et al., 2010). Recent transcriptomic works suggests that down-regulation of genes in calcification-related pathways and up-regulation of genes encoding proteins involved in ion transport in *P. damicornis* (Vidal-Dupiol et al., 2013), but this response may be species-specific as different results were observed in *Acropora millepora* (Kaniewska et al., 2012; Moya et al., 2012).

Poignantly, when both elevated temperature and pCO_2 are considered, coral decline is predicted to be up to 45% more than in a scenario with only elevated sea surface temperature (Buddemeier et al., 2008; Silverman et al., 2009). For tropical corals, high pCO_2 and elevated temperature interact to not only increase the risk for warm-water bleaching (Anthony et al., 2008; Wooldridge, 2009) but also further decrease individual and community calcification rates (Reynaud et al., 2003; Silverman et al., 2007). Additionally, thermal limits of survival may be decreased under OA conditions (Rodolfo-Metalpa et al., 2011).

The weak link in the chain? The intersection of larval physiology and dispersal

Due to the energy requirements and sometimes limited physiological capacity of dispersing early life stages, larvae are especially vulnerable to changing environmental conditions (Pechenik, 1999; Kurihara, 2008; Byrne, 2011). For example, the metabolic demands of coral larvae are high while they are actively swimming and locating optimal settlement sites (Okubo et al., 2008). According to a plethora of studies, ocean acidification has deleterious effects on various biological processes of young marine invertebrates: sperm motility and speed in echinoderms and coral (Havenhand et al., 2008; Morita et al., 2010), fertilization success in coral (Albright et al., 2010), oysters (Parker et al., 2009), and sea

urchins (*e.g.* Kurihara and Shirayama, 2004; Havenhand et al., 2008), larval metabolic rate in coral (Albright and Langdon, 2011; Nakamura et al., 2011) and sea urchins (O'Donnell et al., 2010), stress response and gene expression in sea urchins (O'Donnell et al., 2009, 2010; Todgham and Hofmann, 2009), larval development and growth in crustaceans (*e.g.* Arnold et al., 2009; Findlay et al., 2009), echinoderms (*e.g.* Kurihara and Shirayama, 2004; Dupont et al., 2008; O'Donnell et al., 2010), and mollusks (Kurihara et al., 2007; Ellis et al., 2009; Parker et al., 2009), calcification of larval parts in mollusks (Kurihara et al., 2007; Ellis et al., 2009) and echinoderms (Dupont et al., 2008), and larval survival of coral (Dupont et al., 2008; Clark et al., 2009) and echinoderms (Okubo et al., 2008).

Understanding how OA and warming will affect early life history dispersing stages of marine invertebrates will enable better predictions of the trajectories of these species, including shifts in their distributions, as the ocean becomes more acidic. The persistence of coral reefs is partially dependent on the successful dispersal and recruitment of coral larvae. There is currently a lack of information on the ecological ramifications of the physiological responses of coral larvae to changing environmental conditions with respect to effects on dispersal distance and recruitment success. In general, successful dispersal and recruitment of planktonic larvae maintains and links populations of marine invertebrate populations (Roberts, 1997; Jones et al., 1999; Underwood and Keough, 2001), influencing the size and distribution of these populations throughout the ocean (*e.g.* Thorson, 1950; Strathmann, 1985; Roughgarden et al., 1987). This input of the next generation also rejuvenates degraded reef communities via new settlers and supports standing genetic variation through the addition of new genotypes (Amar et al., 2007). The distance over which larvae can disperse is determined physically by the speed and direction of ocean currents and biologically by the

vertical position of larvae in the water column (buoyancy), swimming behavior, length of time in the plankton (larval duration), and the period during which the larvae are able to settle (settlement-competency period; Pechenik, 1990; Morgan, 1995; Young, 1995; Harii and Kayanne, 2003; Szmant and Meadows, 2006; Shanks, 2009).

Buoyancy, larval duration, settlement-competency period, and thus larval dispersal, are affected by larval energetics – the balance between demand for energy, the amount of endogenous energy, and the ability to utilize external sources of energy. Most coral planulae are lecithotrophic, rich in maternally derived lipids (*e.g.* Ward, 1992) whose energy stores largely determine the length of their larval duration and competency period (Richmond, 1987; Arai et al., 1993; Harii et al., 2002, 2007; Wellington and Fitt, 2003; Alamaru et al., 2009). A major biochemical component of planulae, lipids can compose 34%- 85% of larval biomass (Richmond, 1987; Harii et al., 2007; Norström and Sandström, 2010). Lipids (*e.g.* Shilling et al., 1996; Nates and McKenney, 2000; Moran and Manahan, 2004; Sewell, 2005) and protein (Vavra and Manahan, 1999; Marsh et al., 2001) serve as endogenous sources of energy for these larvae and are steadily used throughout dispersal (Richmond, 1987; Ben-David-Zaslow and Benayahu, 2000; Harii et al., 2007, 2010). Larvae can also acquire energy sources by absorbing dissolved organic material from the surrounding seawater (*e.g.* Jaeckle and Manahan, 1989a, 1989b; Ben-David-Zaslow and Benayahu, 2000; Moran and Manahan, 2004). Throughout their planktonic duration, larvae use these sources of energy for basic cellular processes such as protein synthesis (Marsh et al., 1999; Vavra and Manahan, 1999), ion regulation (Leong and Manahan, 1999; Marsh et al., 1999), swimming (*e.g.* Pechenik et al., 1993; Wendt, 2000), and the production of juvenile tissues.

The biological responses of larvae to OA and temperature described above will likely affect their dispersal through the depletion of energy stores and a reduction in larval buoyancy. Up-regulation of stress response pathways and increased maintenance of homeostatic processes is energetically costly, and consumption of energy stores (*i.e.* lipid and protein) or shifts in the allocation of metabolic energy may slow developmental timing, reduce growth, and impair competency to settle. Additionally, as lipid are consumed to fuel physiological responses to environmental stress, reduction of triacylglycerol and wax ester stores will reduce larval buoyancy, altering the physical transport of larvae by currents. As a consequence of reduced energy stores and buoyancy, larvae may disperse shorter distances or may terminate in the plankton. Through studies of the physiological response of larvae to anthropogenic change in the ocean, we will be better able to predict how OA and warming may alter the population dynamics of *P. damicornis* and the diversity of coral reef communities.

The role of physiological plasticity in the maintenance of physiological integrity under future ocean change

There are four general ways in which species may respond to future ocean change. First, species may migrate to areas with more hospitable conditions. For non-motile species, or if poor environmental conditions extend beyond the species range, acclimatization or adaptation may provide a means for tolerance. Adaptation generally occurs over longer time scales through genetic change as a function of evolution. Under shorter time scales, acclimatization allows organisms to compensate for the physiological effects of changes in their environment. During acclimatization, organisms rely on the plasticity of their suite of

phenotypes or of their physiological processes in order to tolerate new environmental conditions. If none of these options are viable, species may become locally or globally extinct.

As OA and warming progress, species may not have time to adapt to changing environmental conditions. They may, instead, rely on their physiological plasticity to maintain normal physiological function (Fig. 1). Changes in gene expression, particularly in gene regulatory networks, may allow organisms to adjust their physiology to a changing environment (Hofmann and Todgham, 2010; Evans and Hofmann, 2012). For example, in an estuarine goby, tolerance to sublethal thermal stress was achieved in part by up-regulating cellular repair pathways while down-regulating cellular proliferation pathways (Logan and Somero, 2011). Beyond changes in gene expression, corals may be able to gain tolerance by shifting their hosted communities of *Symbiodinium*. For example, corals can acclimatize to warmer seawater by harboring more of *Symbiodinium* clade D, the more heat-resistant group, which can increase coral thermotolerance by 1.0-1.5ºC (Berkelmans and van Oppen, 2006). Physiological plasticity through an increase in abundance of enzymes that regulate acid-base status also likely plays an important role in acclimatization to conditions of decreased pH and increased temperature. The way by which OA and warming may interact to impair calcification and metabolism may be through a reduction in intracellular pH. Organisms may be able to compensate by increasing the abundance of enzymes that regulate pH within cells, such as Na^+/K^+-ATPase (*e.g.* Deigweiher et al., 2008), or by regulating carbonate chemistry at the site of calcification (Hofmann and Todgham, 2010). Shifts in protein turnover, behavior, growth and morphology, and metabolic rate also contribute to acclimatization of corals to changing ocean conditions (Gates and Edmunds, 1999).

Study organism of choice: the cauliflower coral Pocillopora damicornis

For my dissertation research, I selected the cauliflower coral, *Pocillopora damicornis* (Linnaeus, 1758) as the ideal study organism for addressing the physiological consequences of OA and warming on dispersing planulae. This branching scleractinian coral is the most common pocilloporid and is widely distributed throughout shallow-water habitats of the Indian and Pacific oceans (Veron, 2000). It has been extensively studied and maintained in aquaria. *P. damicornis* broods lecithotrophic, free-swimming planula larvae (Fig. 1), which are released every month according to the lunar cycle, though the timing varies by geographic location (*e.g.* Harriott, 1983; Richmond and Jokiel, 1984; Fan et al., 2002) and with abiotic factors such as temperature, salinity, sedimentation, and light regime (reviewed by Baird et al., 2009). These planulae are mostly clonal, asexually produced by the parent colony, but some, even within the same cohort, are sexual and genetically distinct (Yeoh and Dai, 2009). The larvae contain endosymbiotic *Symbiodinium* upon release, vertically transmitted from the parent (Harrison and Wallace, 1990), though endosymbiont density can vary by three-fold within a cohort (Gaither and Rowan, 2010). In about 15% of coral species including *P. damicornis*, *Symbiodinium* supplement the energy available to coral larvae via transfer of metabolites (Richmond, 1981; Harrison and Wallace, 1990; Harii et al., 2010).

P. damicornis larvae are ~70% lipid by dry weight, with total lipid composed of wax esters (60%), triacylglycerol (16.5%), phospholipid (3.2%) and other lipids (Richmond, 1987; Harii et al., 2007). The large fraction of triacylglycerol provides a rapid source of energy for *P. damicornis* larvae as they are competent to settle and metamorphose within hours of release (pers. observation; Isomura and Nishihira, 2001). Though local retention is common (Adjeroud et al., 2013; Torda et al., 2013), these energy sources are adequate for *P.*

damicornis larvae to retain competency in the plankton for more than 100 days, enough time to be carried by currents throughout the tropical Pacific Ocean (Richmond, 1987). During their pelagic duration, they mainly rely on their stored lipid and translocated metabolites from the *Symbiodinium* to fuel their dispersal, settlement, and metamorphosis into the first polyp (Harii et al., 2010); however, uptake of dissolved organic matter (*e.g.* Jaeckle and Manahan, 1989b) and partial metamorphosis into a feeding planktotrophic larva during the pelagic duration are possible (Richmond, 1985).

Given its ubiquitous Indo-Pacific distribution, reef-building role, and long dispersal potential, it is imperative to know how *P. damicornis* will fare in a warmer, acidic ocean. If *P. damicornis* larvae are negatively impacted by future ocean conditions, the long-range dispersal potential of this species may be reduced (Richmond, 1987).

Biogeographic context: Moorea and Taiwan

For my dissertation research with larvae of *P. damicornis*, I worked with two study populations. The first was in Moorea, French Polynesia, a volcanic island within the Society Island archipelago in the south-central Pacific Ocean. The island is surrounded by a barrier coral reef, which protects an inshore lagoon as well as a fringing reef. There are several passes in the barrier reef that allow seawater exchange between the lagoon and the open ocean. The study site was located on the fringing reef on the north shore of Moorea, approximately 500 m alongshore from a pass through the barrier reef. Seasonal climate in Moorea is characterized by dry (May to October) and rainy (November to April) seasons. Winds can contribute to seawater circulation patterns on the North shore, where easterly trade winds are common. During the wet season, prevailing winds come from the north-east;

during dry season, the island shades the North shore from the prevailing southeasterly tradewinds.

The second study population was in southern Taiwan. Nanwan Bay, Taiwan is a semi-enclosed basin, 14 km across, at the southern tip of the island nation. It is bounded by two capes with the Pacific Ocean to the east and the Taiwan Strait to the west. Fringing reefs and sandy beaches line the coast, with several seamounts in the middle of the bay. On the east side of the bay, near Hobihu and the study site, there is no shallow continental shelf. Circulation patterns in Nanwan Bay are driven by tides, with added influence of high winds during monsoon/typhoon season (June-October).

Framing biological data with relevant environmental history

The study of OA has been greatly enhanced by monitoring natural pH dynamics in different marine near-shore environments. Recently, the challenge of acquiring high-frequency, long, continuous environmental datasets that estimate these changing conditions for study populations of benthic species has been overcome with the advent of autonomous oceanographic sensors that record pH, called SeaFETs (Martz et al., 2010). Deployed and tested in sites ranging from tropical to polar, these sensors have shown that calculations of global ocean pH underestimate the natural variation in seawater pH occurring between marine ecosystems (Hofmann et al., 2011; Frieder et al., 2012; Price et al., 2012; Boatta et al., 2013). With these sensors, the research community can now collect high-frequency environmental data to complement IPCC projections and to provide details of the conditions that adults and larvae experience *in situ* (Yu et al., 2011). Within marine ecosystems, we are beginning to appreciate how regional scale variation might influence biological responses to

environmental change and the adaptive potential of populations (Hauri et al., 2009; Fabricius et al., 2011; Pandolfi et al., 2011; Waldbusser et al., 2011; Yu et al., 2011; Kelly and Hofmann, 2012).

Data from SeaFETs have shifted scientific consensus away from the idea that OA is a homogenous, global environmental stressor. The acidification of the local ocean and its effects may manifest in site-specific ways because not all populations of the same species experience the same variability of present-day environmental conditions. For example, SeaFETs deployed within the Moorea Coral Reef and Santa Barbara Coastal Long-Term Ecological Research (LTER) sites have documented marked differences in pH regimes across a variety of spatial scales (Hofmann et al., 2013). pH variability through time differed between kelp forest habitats in the Santa Barbara channel only 54 km apart, despite similar species diversity and mean pH values at both sites. In Moorea, SeaFET sensors documented different pH variability across a transect of the barrier reef, a spatial scale of ~1 km. These data highlight the spatially complex mosaic of pH conditions that a study population may experience. Differences in pH variability across these small spatial scales (1-50 km) may foster a diversity of pH-related phenotypes within or among breeding populations, increasing the potential for resilience of species to future changes in environmental pH at regional scales. Additionally, the deployments provide an environmental context for interpreting the results of laboratory experiments where organisms are exposed to pCO_2 conditions. The LTER SeaFET deployments highlight the need to co-locate pH and other autonomous sensors with biological experiments as a holistic approach to studying global change biology in the coastal ocean (Price et al., 2012; Hofmann et al., 2013, 2014).

It is becoming increasingly clear that studies, such as those my dissertation research comprises, that present changes in biological processes at the levels of species and developmental stage in the context of environmental data are valuable for understanding how future environmental change might alter populations (Hofmann et al., 2013). Understanding the variability of pH and temperature to which study populations are adapted or acclimatized is important for predicting responses to future scenarios of OA and warming, including potential for acclimatization and adaptation of marine species to future OA (Kelly and Hofmann, 2012). Several studies using autonomous sensors have successfully used variability of environmental pH as environmental context for measurements of biological performance and ecosystem processes (Price et al., 2012; Padilla-Gamiño et al., 2013; Frieder, 2014; Gaitán-Espitia et al., 2014; Hofmann et al., 2014). These types of studies, including the work presented here, serve to ground our understanding of the future biological and ecological effects of OA by providing a frame of reference of the present-day regime experienced by the study population as well as a better understanding of the spatial and temporal variability in conditions and responses through which the effects of changing ocean conditions on marine ecosystems will manifest.

Statement of the problem

The overarching goal of my thesis research was to examine the physiological plasticity of the larvae of *P. damicornis* in response to two potentially interacting anthropogenic stressors – ocean acidification and warming. To generate a well-rounded picture of the combined effects of ocean acidification and elevated ocean temperature on

larval physiology, I employed methods focused on different levels of physiological function. Metrics such as lipid utilization and oxygen consumption provided an overview of the response of the organism - a summary of the effects of multitudes of cellular and molecular processes. Such a broader scope can provide useful insight into how the environmental stress will affect the ecological function of the organism, its reproductive capacity and fitness, and its dispersal potential. However, these metrics at the organism level do not provide information of the mechanisms by which the environmental stress challenges physiology. By including laboratory techniques such as colorimetric enzyme activity assays and transcriptomics, I aimed to learn *how* the organism is physiologically plastic - what changes are made at the molecular level to preserve function and survival under the environmental stress.

I accomplished my central objective to examine the plasticity of coral larvae to future ocean conditions using two approaches. First, I conducted experiments which exposed coral larvae to levels of pCO_2 and temperature. The studies I performed explored how coral larvae might respond to future ocean conditions by examining the mechanistic underpinning of such a response at multiple levels of biological organization – the organism (**Chapter II**), the biochemical (**Chapters III, IV**), and the transcriptome (**Chapter V)**. Secondly, I used oceanographic sensors to document the variability of pH and temperature in the fringing reef habitats of my study populations (**Chapter VI**) in order to provide a relevant context of the environmental conditions to which the experimental animals may have been acclimatized. My dissertation represents a holistic approach to global change research, providing biological data that is grounded with knowledge of present-day environmental conditions.

Chapter II assesses the effects of OA and warming on the aerobic metabolism of *P. damicornis* larvae. Larvae from consecutive spawns were collected and exposed to levels of pCO_2 and temperature in the laboratory. Proxies of metabolic rate – O_2 consumption and citrate synthase activity – were then measured. Additionally, pH and temperature variability of the water mass bathing the fringing reef were recorded using autonomous sensors during the course of the experiment. This study has been published in the journal *PLoS ONE* (Rivest and Hofmann, 2014), and the oceanographic data have also been contributed to a synthesis of natural pH variation in marine ecosystems (Hofmann et al., 2011). The data are available in the Moorea Coral Reef Long Term Ecological Research data catalog (Rivest, 2014). I hypothesized that OA would decrease larval metabolic rates while temperature would increase larval metabolic rates.

Chapter III presents one of the first studies of oxidative stress responses and acid-base regulation in coral larvae. *P. damicornis* larvae were incubated in controlled laboratory conditions of pCO_2 and temperature after which their total antioxidant potential and Na^+/K^+-ATPase activity were measured. OA and temperature may interact to challenge larval physiology by causing an increased production of reactive oxygen species as well as a decrease in intracellular pH. This study aimed to detect a biochemical response in larvae to compensate for these harmful departures from intracellular homeostasis under conditions of OA and warming. I hypothesized that OA and warming would cause oxidative stress and would disturb intracellular pH, resulting in elevated antioxidant potential and elevated acid-base regulation at high pCO_2.

Chapter IV investigates whether OA and warming affect the use of stored energy in *P. damicornis* larvae. Lipids, protein, and *Symbiodinium* provide energy that planulae use to fuel their metabolism, including homeostatic maintenance, growth, and dispersal. Larvae were exposed to controlled levels of pCO_2 and temperature in the laboratory. Lipid composition and metrics of physiological status, such as total lipid, total protein, density of *Symbiodinium* and size, were measured before and after these incubations. Responses of larvae were compared between cohorts released on consecutive days as well as between cohorts released from different biogeographic locations to investigate the heterogeneity of biological responses across a single brood and across the species' biogeographic range. Part of this chapter is currently in revision at the *Journal of Experimental Biology*. I hypothesized that energy storage lipids and physiological status of larvae would decrease under OA and warming and that these responses to the environmental stressors would differ between larval cohorts and study sites.

Chapter V explored a mechanism of physiological plasticity – gene expression. RNA sequencing was used to gain a broad overview of changes in gene expression in coral larvae after 24 –hour laboratory exposures to pCO_2 and temperature levels. The up- and down-regulation of particular genes and pathways is informative of potential mechanisms behind acclimatization of corals to future ocean change. I hypothesized that larvae would differentially express genes when exposed to OA and warming versus ambient conditions.

Chapter VI represents a major field component of my dissertation. Autonomous oceanographic sensors recording pH (SeaFETs; Martz et al., 2010), temperature, salinity, and

depth were deployed at study sites in Moorea, French Polynesia and Taiwan to complement the biological studies described in **Chapter IV**. My extensive work with SeaFET sensors throughout my dissertation has contributed to multiple publications (Hofmann et al., 2011, 2013; Gaitán-Espitia et al., 2014; Rivest and Hofmann, 2014; Lunden, Rivest et al., in review), has helped develop standard operating procedures for collecting and managing these data (Lunden, Rivest et al., in review), and has helped to establish the critical role of environmental data in ocean acidification research. I hypothesized that regimes of pH and temperature would differ between the study sites.

II. Responses of the metabolism of the larvae of *Pocillopora damicornis* to ocean acidification and warming

Introduction

In this study, I explored the physiological responses of larvae of stony coral, animals whose thermal physiology limits can be exceeded by small increases in water temperature above seasonal averages (1-2°C; Jokiel and Coles, 1990; Middlebrook et al., 2008) or can span a 10°C temperature range, as a result of local adaptation, seasonal acclimatization, or thermotolerance of hosted *Symbiodinium* clades (Oliver and Palumbi, 2011). To provide an assessment of the sensitivity of coral larvae to future ocean conditions, I measured how pH and temperature interact to influence the metabolic status of the larvae of the cauliflower coral, *Pocillopora damicornis*. To provide a relevant *in situ* environmental context for the study site, I determined the natural variation of pH and temperature on the natal coral reef during the month in which these larvae developed and released.

Although the response of coral larvae to elevated pCO_2 and temperature is difficult to predict, in ectothermic animals, environmental stressors commonly elicit metabolic depression – a regulated reduction in metabolism in response to stress-related cues (Hand, 1991; Sokolova, 2013). Strategically, suppression of metabolism may be an effective adaptive strategy in the short-term because it prevents mortality by increasing tolerance (Hand and Hardewig, 1996). However, when extended over long periods, low metabolic rates will likely impair growth and reproduction, decreasing fitness of the species (Sokolova et al., 2012; Sokolova, 2013).

For corals and their early life history stages, metabolic depression may be a likely response to rising ocean acidity and temperature (Pandolfi et al., 2011; Edmunds et al., 2013). Respiration rates of many life history stages increase with temperature (Coles and Jokiel, 1977; Edmunds et al., 2001; Edmunds, 2005), but narrowing of thermal tolerance windows under OA (Pörtner, 2008; Walther et al., 2009; Hofmann and Todgham, 2010; Lannig et al., 2010) may cause metabolism to decline at more conservative thermal extremes. If so, conditions of high CO_2 and high temperature conditions may delay or prevent larval growth and metamorphosis, increasing time in the plankton while decreasing recruitment, post-settlement success, and fitness. While elevated temperature is known to shorten the pelagic larval duration of coral larvae (*e.g.* Edmunds et al., 2001; Nozawa and Harrison, 2007), metabolic depression induced by the interacting stressors may prevent larvae from accomplishing this energetically-costly transformation. Larvae of some broadcast-spawning and brooding corals experience metabolic suppression at high pCO_2 (Albright and Langdon, 2011; Nakamura et al., 2011) while other species are more tolerant (Chua et al., 2013). Recent studies on larvae from a Taiwan population of *P. damicornis* have found variable responses of metabolism to elevated temperatures and a lack of response to elevated pCO_2 (Cumbo et al., 2013a, 2013b; Putnam et al., 2013). My study builds on these findings by exploring responses to the same stressors in a population in Moorea that is genetically distinct from the population studied in Taiwan (Forsman et al., 2013). I also used pCO_2 levels appropriate for current environmental variability and future projections and measured complementary molecular responses. I used environmental data collected on the reef at the study site to identify extreme conditions experienced in the field and as a context for

interpreting biological responses of coral larvae to future ocean scenarios of carbonate chemistry and temperature.

The life history strategy of corals like *P. damicornis* may provide a form of defense against the negative consequences of interacting climate change stressors on the species as a whole (*e.g.* Putnam et al., 2010; Cumbo et al., 2012, 2013a). Based on their spawning date, larval cohorts differ in terms of their inherent fitness-related traits. For example, Putnam *et al.* (2010) found that larval size, symbiont density, and symbiont photophysiology vary significantly between cohorts of *P. damicornis* larvae. In another species of brooding coral, *Porites astreoides*, larval cohorts differed in symbiont density and potential for autotrophy (Edmunds et al., 2001). As a result, larvae that spawn on different dates in the lunar cycle may have dissimilar responses to environmental stress. While the overall proportion of successful offspring is reduced consequently, this strategy for spreading risk may increase the likelihood that some offspring have phenotypes better suited for future ocean conditions.

Studies of larval metabolism can contribute to our ability to predict the future impact of ocean acidification and warming on corals through estimates of physiological plasticity, the ability of an organism to vary the rates of physiological processes in order to maintain homeostasis as environmental conditions change (Cohen et al., 2012; Kelly et al., 2012). Making use of its existing physiological repertoire to tailor its phenotype at the cellular and molecular level to a new environmental condition, the organism has the potential for acclimatization and longer-term persistence (Hofmann and Todgham, 2010; Evans and Hofmann, 2012). In this study, I explored plasticity of physiological responses of coral larvae from a reef in French Polynesia to elevated pCO_2 and temperature. The study was motivated by three questions. First, what is the response of *P. damicornis* larvae to conditions of

decreased pH and warming, measured using two indices of metabolism - rates of oxygen consumption and citrate synthase activity? Second, are there differences in larval sensitivity to environmental change between cohorts that are released from adult colonies at different times? Third, what is the present-day exposure of *P. damicornis* to natural variability of pH and temperature on the natal reef?

Materials and methods

All research, including fieldwork in Moorea, French Polynesia (17°28'49.08"S, 149°47'56.04"W), was performed under an annual research permit issued by the French Polynesia Ministry of Research to EBR.

Collection of coral larvae

Larvae were collected from adult colonies following their lunar pattern of reproduction (Fan et al., 2006). On the new moon (March 4, 2011), eight colonies of *P. damicornis* were collected at ~1-2m depth from a fringing reef site. Due to the proximity of the collection site to the oceanographic instruments, the pH and temperature histories of the adult colonies were characterized for the month prior to collection during which the larvae developed. Each colony was maintained in an aquarium at University of California Berkeley Richard B. Gump South Pacific Research Station with indirect natural sunlight and a slow flow of coarsely filtered seawater. Temperatures in the aquaria averaged 28.4 ± 0.4°C throughout the spawning period. Overnight, larvae were captured in mesh-lined cups that received the outflow of each aquarium. Daily at dawn, larvae from each colony were

collected, counted, pooled, and randomly assigned to experimental treatments. Although there was daily variation in larval output between colonies, low release levels in general necessitated the use of all larvae in the daily experiments. As a result, there were uneven contributions of genotypes in the experimental larval pool each day, which preclude any distinction between genotypic responses and species-level responses to OA and temperature. Data presented here were collected from experiments conducted with larvae released on March 13 ("Day 9"), March 14 ("Day 10"), and March 15 ("Day 11").

Experimental incubations

Two CO_2 treatments were used: Ambient-pCO_2 (~450 µatm CO_2) and High-pCO_2 (~950 µatm CO_2). The low treatment represents an environmental condition that released larvae may currently experience at the study site (approximated by environmental data), while the high treatment represents a level of dissolved pCO_2 that is outside the present-day pH minima of the seawater bathing the fringing reef and that is a surface ocean average expected by the year 2100 (IPCC, 2013). These conditions approximate those at the reef scale (*i.e.* km) and not what may be experienced and manipulated within the boundary layers of the adult corals. pCO_2 levels were combined with two experimental temperatures, 27.8°C and 30.6°C. The control temperature (27.8°C) approximates the 5-year average seawater temperature at the Moorea Coral Reef Long Term Ecological Research (Leichter, 2014) fringing reef monitoring site close to the collection site for adult *P. damicornis* as well as seawater temperature during the month preceding and including the release of larvae used in this experiment (verified by oceanographic instruments in this study). The elevated

temperature represents the average surface ocean temperature by year 2100 as predicted by global temperature projections (IPCC, 2013).

Treatments were created as described in Edmunds *et al.* (2012) in a MCR LTER facility, with one aquarium for each treatment combination of pCO_2 and temperature. Tank replication was not possible due to unexpected equipment failure. The closed-circuit aquaria were filled with 20μm-filtered seawater, 16% of which was replaced daily. Gas mixtures of the two desired CO_2 levels were created following Edmunds *et al.* (2012) and bubbled directly into aquaria. Saturation of pCO_2 in the seawater was reached before each daily experiment was performed. Individual Aqua Logic aquarium heaters and a chill loop maintained tank temperature treatments at +/- 0.4°C. Aquaria were darkened with aluminum foil to exclude photorespiratory CO_2 release. The four treatments created by this experimental set-up are defined as ambient temperature-ambient pCO_2 (ATAC), ambient temperature-high pCO_2 (ATHC), high temperature-ambient pCO_2 (HTAC), and high temperature-high pCO_2 (HTHC).

To verify and monitor the physical parameters of the treatments, the chemistry of the seawater in the aquaria was analyzed daily. pH, temperature, salinity, and total alkalinity of seawater in each aquarium were measured during the incubations.

Seawater temperature was measured throughout the experimental exposures (5-6 times) using a thermocouple (0.1°C resolution, T-type, Omega Digital Thermometer, Model HH81A). Seawater salinities were measured using a conductivity meter (YSI 3100). Seawater pH was measured using a spectrophotometric method with indicator dye, *m*-cresol purple (SOP 6b; Dickson et al., 2007). Total alkalinity (A_T) was measured using an automated, open-cell potentiometric titration (SOP 3b; Dickson et al., 2007) with a Mettler-

Toledo T50 titrator and a DG115-SC pH probe (Mettler-Toledo). Titrations were performed using certified acid titrant (~0.1M HCl, 0.6M NaCl; A. Dickson Laboratory, Scripps Institute of Oceanography), and a non-linear least-squares approach was used to calculate A_T (Fangue et al., 2010). For each day of the experiment, analyzed certified reference materials from A. Dickson Laboratory were accurate within 10 μmol kg^{-1} (*i.e.* 0.1-0.4%). pH at 25°C, A_T, temperature, and salinity were used to calculate the pH and pCO_2 of the treatments using CO2calc (Robbins et al., 2010), with CO_2 constants K1, K2 from Mehrbach *et al.* (1973) refit by Dickson and Millero (1987) and pH expressed on the total scale (mol kg-SW^{-1}).

Assessment of physiological responses

To assess how larval metabolism responds to OA and warming, larvae were placed in 10 mL serum vials (Wheaton Science Products, Inc.) that contained seawater filtered to 0.2μm from aquaria at all four combinations of temperature and pCO_2. For each treatment combination, there were 6 vials containing 5 larvae each and two blank vials. Each vial was sealed with Parafilm® so that no air bubbles remained inside.

The number of larvae per vial was optimized as follows to minimize the standard deviation in the oxygen consumption per larva between replicates and to ensure that the concentration of O_2 dropped over the incubation period within our range of detection (0.1 nmol O_2 min^{-1}) without becoming limiting for the larvae (data not shown here). A preliminary test was conducted to determine whether O_2 exchange differed through two vial-capping methods: gas-permeable Parafilm® and gas-impermeable plastic screw caps. The effect of pCO_2 and temperature on this gas exchange was also tested. The amount of O_2 exchange through the Parafilm® on vials vs. a plastic screw cap was affected only by pCO_2

level (two-way ANOVA, $F_{2,99} = 1.057$, $p = 0.003$). Parafilm®, not plastic screw caps, was used to cap vials in this experiment. However, blank vials were used in all treatments to account for background respiration, so this oxygen exchange did not contaminate the biological signal in each treatment. Exchange of CO_2 through Parafilm® was not estimated; any exchange occurring would serve to equilibrate the carbonate chemistry conditions between the vial and the treatment aquarium, both of which had the same pCO_2 treatment.

To account for any change in chemistry as treatment water was passed through a 0.2 μm filter and used to fill the vials, treatment water was measured before and after the vials were loaded (see Table 1, rows 'Vials'). The loaded vials were incubated for 6 hours in the dark treatment aquarium (the source for the water used to fill the vials). Due to the time needed to read the oxygen concentration in the vials post-incubation, loading of the vials for each treatment was staggered by one hour with the order randomized daily. Vials were cleaned and re-used for respirometry incubations on subsequent days.

In order to measure oxygen concentration, approximately 325 μL of the seawater in each vial was injected into a glass custom-built optrode cell. One measurement of oxygen consumption was made per vial. A built-in water jacket surrounding the optrode cell was connected to a re-circulating water bath held at the same treatment temperature of the vials being analyzed. After two minutes, the oxygen concentration was read in triplicate (Microx TX3, Presens GmbH, Regensberg, Germany). Oxygen consumption over the 6-hour incubation was calculated (nmol O_2 $larva^{-1}$ min^{-1}), and batches of 5 larvae from each respiration vial were preserved for analysis of total protein in order to account for variation of larval mass within a daily cohort. *Symbiodinium* numbers were not accounted for. Their abundance could alter holobiont rates of O_2 consumption through their rates of dark

respiration or through their contribution of intermediate metabolites for the Krebs cycle within the animal host (Gordon and Leggat, 2010). However, variation in endosymbiont density is unlikely to affect the biomass-standardized rate of respiration (Gaither and Rowan, 2010). *Symbiodinium* densities of *P. damicornis* larvae released on these lunar days in 2012 (described in Chapter 4) ranged from ~3,000 to 13,000 cells per larva. Based on measured respiration rates in free-living *Symbiodinium*, the symbionts in these larvae may account for 4-15% of holobiont oxygen consumption for *P. damicornis* larvae (4-17 pmol O_2 min^{-1}; clades A and B, Brading et al., 2011).

To complement oxygen consumption rates, citrate synthase (CS) activity was quantified to gauge changes in oxidative capacity of larvae (*i.e.* the catalytic potential of oxidative metabolism; Emmett and Hochachka, 1981) in response to the pCO_2 x temperature treatments. Additional larvae were needed in order to perform analyses of CS activity. These larvae were taken from the same pool used to stock the respirometry vials. They were incubated for 6 hours simultaneously with those in the respirometry vials and then frozen at -80°C. Within each treatment, these larvae were incubated at a density of 1 larva mL^{-1} in three flow-through 50 mL Falcon tubes enhanced with 100 µm-mesh windows.

CS activity in homogenates of larvae of *P. damicornis* was measured spectrophotometrically according to Srere (1969) as modified by preliminary tests to determine optimal pH and substrate concentrations. In these preliminary tests, the metabolic machinery within *Symbiodinium* in the larvae consumed biochemical substrates, likely oxaloacetate, causing absorbance of the mercaptide ion at 412 nm to decrease. To prevent this, *Symbiodinium* cells were separated from homogenates prior to initiation of the CS reaction. CS activity was tested across a range of pH of the 50 mM histidine buffer (7.0 - 8.6

at 28.0°C, $n = 7$); pH had a significant effect on CS activity (one-way ANOVA; $F_{6,12} = 4.011$; $p = 0.015$). pH 7.8 was chosen for this assay based on pairwise Student's t tests and an *a priori* knowledge of the low intracellular pH of coral cells (*e.g.* Kuhl et al., 1995; Venn et al., 2009). Substrate concentrations of acetyl-coenzyme A (0.3-0.6 mM, $n = 7$), DTNB (0.1-0.35 mM, $n = 6$), and oxaloacetate (0.35-0.65 mM, $n = 7$) were also optimized and verified to be non-limiting. Results presented here for CS activity in larvae were from measurements made at 28.0 ± 0.1°C, the control temperature for culturing and respiration.

To quantify CS activity, larvae were first homogenized on ice in 50 mM histidine pH 7.8 using a pestle followed by further physical disruption using a pipettor. Centrifugation (5 min at 400xg) was used to separate *Symbiodinium* cells from animal homogenate with minimal animal mitochondria in the pellet (Alberts et al., 2002). Aliquots of the homogenates were preserved for later analysis of total protein. Triton X-100 was added to the remaining homogenate at a final concentration of 0.25% v/v. At 28.0°C ± 0.1°C, the control temperature for culturing and respiration, absorbance at 412nm of the reaction was measured with and without oxaloacetate, with final concentrations of 0.4mM acetyl coA, 0.25 mM DTNB, and 0.5 mM oxaloacetate. Measurements of CS activity were performed twice for each tube of larvae ($n = 2$ technical replicates). Rates of CS activity are expressed as mmol min^{-1} $larva^{-1}$ and are also standardized by total protein to represent protein-specific activities (nmol min^{-1} g animal $protein^{-1}$; Bradford, 1976; Jaeckle and Manahan, 1989).

Total protein values were used to normalize data for oxygen consumption and CS activity. Following sonication, total protein content of larvae was determined using a Bradford assay (Bradford, 1976; Jaeckle and Manahan, 1989b).

Temperature coefficient Q_{10} values were calculated to determine if the sensitivity of larval metabolism to temperature changed under different pCO_2 levels. Q_{10}, commonly used to describe the sensitivity of reaction rates to temperature, is the factor by which the reaction rate increases following a 10-degree increase in temperature. To calculate this coefficient, the following formula was used: $Q_{10} = (R_2/R_1)^{(10/(T_2-T_1))}$, where R is the rate of reaction at Temperature 1 or Temperature 2. Q_{10} values of biological reaction rates are commonly between 2 and 3 (*e.g.* Hochachka and Somero, 2002). Values below 2 indicate a decrease in temperature sensitivity while values above 3 indicate hypersensitivity of the reaction to changes in temperature.

Statistical analysis

All data were analyzed using R version 3.0.1 (R Core Team 2013). In all cases, statistical assumptions of normality and homogeneity of variance were tested using quantile-quantile (Q-Q) plots and Levene's test and were met. A one-way ANOVA in which pCO_2 and temperature were fixed factors was used to compare physical conditions between treatments. With pCO_2, temperature, and day of release as fixed factors, effects on larval- and protein-specific rates of oxygen consumption, CS activity, and total and animal protein levels were estimated using linear mixed-effect models (nlme package in R; Pinheiro and Bates, 2000). To account for possible similarities between larvae incubated in the same container, "tube" was considered a random factor in all statistical analyses. Model selection was performed incrementally following Burnham and Anderson (2002): at each iteration, the simpler model was chosen if the model AIC value did not increase by 2 or more and if there was not a significant difference in the model log likelihood ratio. To determine which factors

in the models were significant, a type III sum of squares was conducted on selected models fit using maximum likelihood (Zuur et al., 2009; Crawley, 2013). When significant differences were detected among treatments, orthogonal contrasts were performed as post-hoc analyses using the multcomp package in R (Hothorn et al., 2008). Tukey's HSD was used for models without significant interactions between terms. When significant interactions were present, post-hoc analyses were performed using linear contrasts with Bonferroni corrections for multiple comparisons.

Collection of environmental data

pH and temperature time series were generated on a fringing reef in Moorea, French Polynesia. pH was recorded continuously from January 28 to March 19, 2011 on the fringing reef approximately 90 m from the collecting location of adult ***P. damicornis*** parents. An autonomous data logger based on a Honeywell Durafet® pH sensor, called a SeaFET (Martz et al., 2010), was deployed at 17°28'49.08"S, 149°47'56.04"W. The SeaFET was deployed at 3.3 m depth and suspended approximately 0.6 m off the sandy bottom; the instrument measured pH voltage at 10-minute intervals, averaging data over 30-second periods. The sensor reference anomaly oscillated between ±0.01and no detectable drift of the instrument occurred. Additionally, output of continuous operation of this sensor over a 6-month period has been shown to match frequent discrete samples of seawater chemistry (Martz et al., 2010). Adjacent to the SeaFET were two Seabird thermisters (SBE 39), synced with the SeaFET to simultaneously record temperature.

Following deployment, the SeaFET electrodes were calibrated using discrete seawater samples collected *in situ*, justified based on sensor characteristics previously demonstrated

(Martz et al., 2010). On February 25, 2011, a SCUBA diver using a Niskin bottle collected a single calibration sample adjacent to the SeaFET in concurrence with its voltage reading. Temperature of the seawater *in situ* was measured using an alcohol thermometer. pH, total alkalinity (A_T), and salinity were measured in four replicates (see below) within 1-2 hours of sample collection. Average A_T and salinity values were used to generate *in situ* pH, Ω_{arag}, Ω_{calc}, and pCO_2 values using CO2calc (Robbins et al., 2010). For purposes of calculation, salinity and total alkalinity were assumed constant throughout the 2-month deployment, allowing me to generate a real-time graph of pCO_2 variation over a coral reef. These assumptions were necessary because these parameters could only be measured using discrete samples. To estimate the error introduced in the pCO_2 calculations by the assumptions, we used discrete bottle samples to estimate changes in the carbonate chemistry, salinity, and TA at the deployment site following a rain event.

Data access

Environmental (accn #: knb-lter-mcr.2004) and physiological (accn #: knb-lter-mcr.2008) datasets generated by this study are publicly available in the LTER Metacat data catalog, mirrored in DataONE.

Results

Larval production

During the period of this experiment, *P. damicornis* colonies released planula larvae for 16 days following the new moon in March 2011 with variation in the number of larvae

released (Fig. 2). The peak day of larval release was Lunar Day 9 (Fig. 2). Larval release was not counted on Lunar Days 7 and 8 due to a tsunami warning and a power outage.

Physiological response of larvae to controlled pH variation

On several days during larval release (Lunar Days 9 – 11), I tested the performance of *P. damicornis* larvae using two indicators of metabolism – oxygen consumption and CS activity.

To assess the response of coral larvae to present and future pCO_2 and temperature levels, larvae were exposed to a set of conditions in the lab where the temperature and seawater chemistry in the experimental aquaria were carefully controlled (Table 1). Experimental treatment conditions remained stable throughout the course of the experiment and were similar within treatments, despite slight differences between aquarium and vial conditions. Temperature and tank pH differed between treatments ($F_{3,69} = 1960.59$, $p < 0.001$; $F_{3,23} = 3813.58$, $p < 0.001$). pH of seawater within the respirometry vials also varied significantly with treatment ($F_{3,23} = 2663.83$, $p < 0.001$), though absolute vial pH was slightly different from tank pH due to filtration and handling while vials were filled. While pH differed between tanks and vials within each treatment (ATAC: $F_{1,11} = 41.37$, $p < 0.001$; ATHC: $F_{1,11} = 15.04$, $p = 0.003$; HTAC: $F_{1,11} = 4.88$, $p = 0.052$; HTHC: $F_{1,11} = 27.31$, $p < 0.001$), the pCO_2 treatment conditions did not overlap. Salinity was significantly higher in the HTHC treatment ($F_{3,11} = 6.67$, $p = 0.014$), while A_T did not vary significantly between temperature and CO_2 combinations. Similarly, pCO_2 was significantly different between treatments in tanks ($F_{3,11} = 1247.34$, $p < 0.001$) and in vials ($F_{3,11} = 651.93$, $p < 0.001$).

Figure 2. Release of *Pocillopora damicornis* larvae in March 2011. Larval release increased following the new moon and then decreased after lunar day 9. Numbers of larvae released per colony (n = 8 colonies) are described by bar segments of different colors.

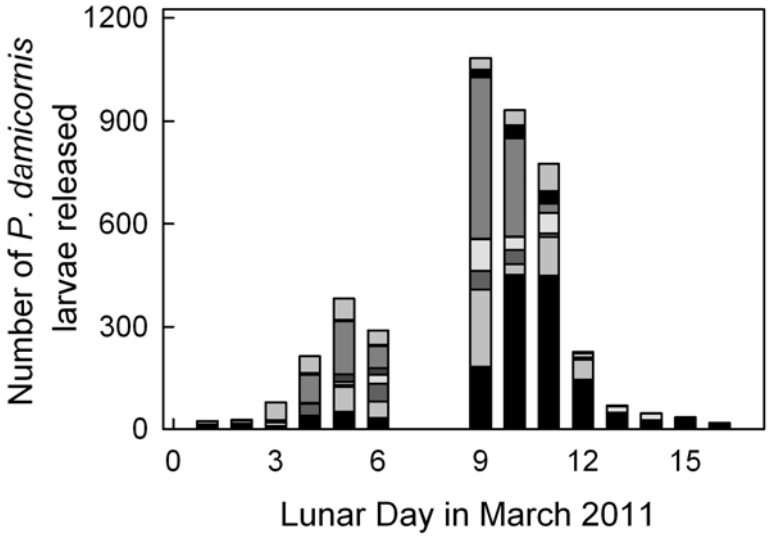

Table 1. Summary of physical conditions in treatment aquaria and vials for experiments conducted on Days 9-11.

Treatment		Temperature (°C)	Salinity (ppt)	pH	A_T (µmol kg^{-1})	pCO_2 (µatm)
ATAC	Tank	27.5	35.33	8.018	2353 ± 13	436 ± 6
	Vials			7.995		464 ± 6
HTAC	Tank	30.7 ± 0.1	35.40	7.985	2364 ± 7	477 ± 4
	Vials			7.994		466 ± 6
ATHC	Tank	28.1	35.43	7.714	2354 ± 16	996 ± 12
	Vials			7.726		965 ± 16
HTHC	Tank	30.44 ± 0.1	35.63 ± 0.1	7.736	2383 ± 5	952 ± 10
	Vials			7.759		895 ± 11

Data are presented as mean ± SE, except where SE < 0.1. For all parameters, $n = 3$.

pCO_2 levels of tanks and vials within treatments were different (ATAC: $F_{1,5} = 11.32$, $p = 0.028$; ATHC: $F_{1,5} = 2.30$, $p = 0.204$; HTAC: $F_{1,5} = 2.53$, $p = 0.187$; HTHC: $F_{1,5} = 14.93$, $p = 0.018$), but both tanks and vials grouped by treatment (Ambient- or High-pCO_2).

Patterns of oxygen consumption, used as an indirect measure of metabolism, revealed that larvae were sensitive to projected end-of-the-century ocean chemistry. Oxygen consumption of *P. damicornis* larvae varied between 0.0826 ± 0.006 nmol $larva^{-1}$ min^{-1} (Day 11 ATHC) and 0.1394 ± 0.009 nmol $larva^{-1}$ min^{-1} (Day 10 ATHC). With no significant interactions between fixed effects, larval specific oxygen consumption varied significantly by pCO_2, temperature, and day (Table 2). In general, rates of oxygen consumption per larva were higher at Ambient-pCO_2 (vs. High-pCO_2; Tukey's HSD; $p = 0.013$; Fig. 3A) and at 30.6°C (vs. 27.8°C; Tukey's HSD; $p < 0.001$). Additionally, larvae released on Day 10 respired more quickly than larvae released on the other two days (Tukey's HSD; $p < 0.001$ for both). Larval rates of oxygen consumption were on average 22.4% higher at 30.6°C vs. 7.8°C. The significant effect of CO_2 across days is driven by the lower oxygen consumption rates at 30.6°C on Day 11. At 30.6°C, Day 11 larvae at High-pCO_2 consumed oxygen 19.2% more slowly than larvae at Ambient-pCO_2, compared with 7.6% on Day 9 and 0.1% on Day 10 (Fig. 3A).

To complement calculations of metabolic rate on a per larva basis, oxygen consumption was standardized by total holobiont protein. Protein-specific rates account for differences in mass between replicates and treatments whereas larval-specific metabolism allows for interpretation of physiological response in ecological units, at the level of the whole animal. When protein-specific rates of oxygen consumption were compared, elevated

Table 2. Analysis of oxygen consumption rates for *P. damicornis* larvae among treatments, standardized to number of larvae (nmol larva $^{-1}$ min^{-1}) and to total protein (pmol µg protein^{-1} min^{-1}).

Dependent variable	Effect	X^2	Degrees of Freedom	*p*
Larval-specific oxygen consumption (nmol larva^{-1} min^{-1})	pCO_2	6.662	1	**0.010**
	T	51.863	1	**<0.001**
	Day	54.140	2	**<0.001**
Protein-specific oxygen consumption (pmol µg protein^{-1} min^{-1})	pCO_2	0.088	1	0.767
	T	5.1395	1	**0.023**
	Day	18.234	2	**<0.001**
	TxDay	5.379	2	0.068
Total protein (µg larva^{-1})	pCO_2	4.186	1	**0.041**
	T	2.469	1	0.116
	Day	20.110	2	**<0.001**

Comparisons were made using type III sum of squares with pCO_2, temperature (T) and day of release (Day) as fixed effects. Interaction terms that were removed from the model are not shown here.

Figure 3. Oxygen consumption of *Pocillopora damicornis* larvae over 6-hour exposures to combinations of pCO_2 and temperature. Mean ± SE (n = 6) rates of oxygen consumption standardized by number of larvae for those released on Days 9-11 (A) and standardized by total protein for larvae released on Days 9-11 (B). Larval respiration is significantly higher at 30.6°C (vs. 27.8°C), at Ambient-pCO_2 (vs. High-pCO_2) and on Day 10. Protein-specific rates are significantly higher at 30.6°C on Day 11 only. Refer to Table 2 for statistical details. Symbols are offset to improve clarity: Ambient-pCO_2 at 450 µatm (circles), High-pCO_2 at 950 µatm (triangles), 27.8°C (blue), and 30.6°C (red).

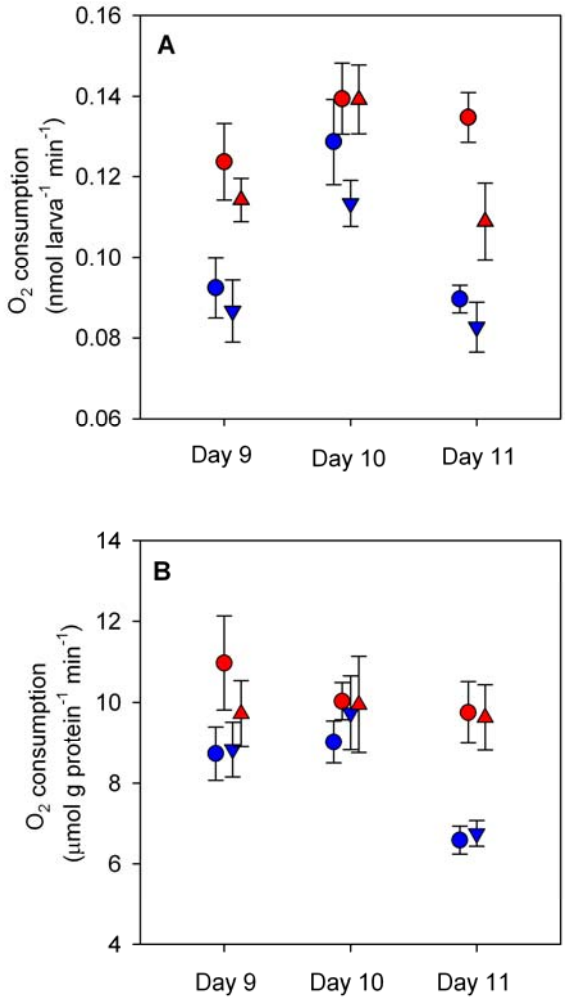

pCO_2 no longer caused a significant decrease in oxygen consumption for larvae released on Days 9-11 (Table 2, Fig. 3B). Effects of T and Day remained significant (Table 2). Post-hoc analysis of the marginally significant interaction (TxDay, Table 2) revealed significant effects of temperature on Day 11 (linear contrast with Bonferroni correction; $Z = -4.045$, $p < 0.001$), but no difference between temperatures on Days 9 and 10. The effect of temperature on protein-specific rates of oxygen consumption on Day 11 was 2-fold greater than on the other days.

Citrate synthase (CS) activity was measured as a proxy for the number of intact mitochondria and to quantify the capacity of larval aerobic metabolic machinery (Moyes, 2003). With respect to numbers of larvae, coral animal CS activity differed by Day, marginally by T and not by pCO_2. Despite a significant interaction between T and Day (Table 3), post-hoc analyses using linear contrasts with Bonferroni corrections showed insignificant differences between temperature groups on each day. On Day 9, elevated temperature raised CS rates slightly while on Day 11, CS activity was suppressed by elevated T and/or pCO_2 in general (Fig. 4A). When coral animal CS activities were normalized to total protein from the animal fraction of the larval holobiont, activities ranged from 1.36 ± 0.3 nmol g animal protein^{-1} min^{-1} (Day 11 HTAC, Fig. 4B) to 1.63 ± 0.04 nmol g animal protein^{-1} min^{-1} (Day 10 HTAC). Protein-specific CS activities varied significantly by T x Day, and pCO_2xTxDay (Table 3). Determined using post-hoc analyses of linear contrasts with Bonferroni corrections, there were no significant contrasts among treatment groups on Day 9. Day 10 CS activity HTAC was significantly greater than ATAC ($Z = 3.513$, $p = 0.008$) and ATHC ($Z = 3.753$, $p = 0.003$). On Day 11, protein-specific CS activity for

Table 3. Analysis of citrate synthase (CS) activity for *P. damicornis* larvae among treatments, standardized to number of larvae (mmol larva $^{-1}$ min^{-1}) and to animal protein content (nmol g animal protein^{-1} min^{-1}).

Dependent variable	Effect	X^2	Degrees of Freedom	*p*
Larval-specific CS activity (mmol larva^{-1} min^{-1})	pCO_2	0.014	1	0.906
	T	3.428	1	0.064
	Day	21.776	2	**<0.001**
	TxDay	8.706	2	**0.013**
Protein-specific CS activity (nmol g animal protein^{-1} min^{-1})	pCO_2	0.008	1	0.928
	T	0.164	1	0.686
	Day	3.081	2	0.214
	pCO_2xT	0.821	1	0.365
	pCO_2xDay	3.131	2	0.209
	TxDay	40.128	2	**<0.001**
	pCO_2xTxDay	8.173	2	**0.017**
Total animal protein (µg larva^{-1})	pCO_2	0.191	1	0.662
	T	6.578	1	**0.010**
	Day	37.198	2	**<0.001**
	TxDay	12.014	2	**0.003**

Comparisons were made using type III sum of squares with pCO_2, temperature (T) and day of release (Day) as fixed effects. Interaction terms that were removed from the model are not shown here.

Figure 4. Citrate synthase activity of *Pocillopora damicornis* larvae over 6-hour exposures to pCO_2 and temperature. Mean ± SE (n = 6) rates of citrate synthase (CS) activity standardized by number of larvae for those released on Days 9-11 (A) and standardized by animal protein content for larvae released on Days 9-11 (B). Refer to Table 3 for statistical details. Symbols are offset to improve clarity: Ambient-pCO_2 at 450 µatm (circles), High-pCO_2 at 950 µatm (triangles), 27.8°C (blue), and 30.6°C (red).

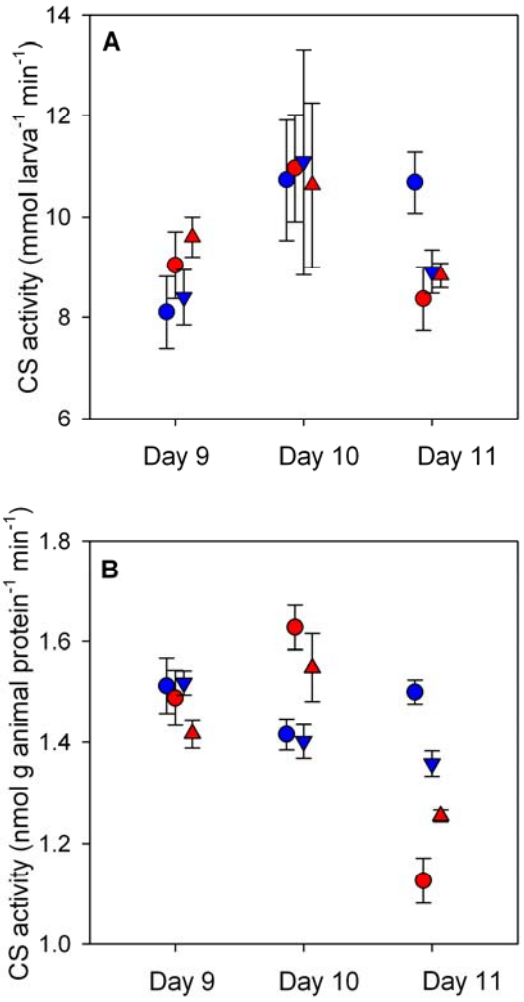

ATAC was significantly greater than for both high-temperature treatments (HTAC: $Z = 6.207$, $p < 0.001$; HTHC: $Z = 4.063$, $p = 0.001$). Treatment groups ATHC and HTAC were also significantly different ($Z = 3.829$, $p = 0.002$). While protein-specific rates of CS activity do not yield information regarding relative amounts of CS with respect to the pool of total animal protein, they reflect differences in activity per enzyme unit, changes in the proportion of CS within total protein, or a combination of both.

Total protein values were used to assess a measure of fitness and to normalize metabolic performance under combinations of control and elevated temperature and pCO_2. Total holobiont protein varied significantly by pCO_2 and by Day (Table 2), with highest densities in larvae released on Day 10 and 11 (vs. Day 9; Tukey's HSD, $p < 0.001$, 0.021, respectively). Larvae incubated at High-pCO_2 had slightly lower densities of total protein than at Ambient-pCO_2 (Fig. 5A; Tukey's HSD; $p = 0.049$). Total animal protein responded differently to changes in temperature depending on day of release (Table 3) and in general was lower in larvae released on Day 9 (Fig. 5B). Main effects of temperature and day were also significant (Table 3). Post-hoc analysis of the significant interaction (TxDay, Table 3) revealed significant effects of temperature on Day 9 (linear contrast with Bonferroni correction; $Z = -2.406$, $p = 0.048$) and Day 10 ($Z = 2.319$, $p = 0.061$), but no difference between temperatures on Day 11. The directionality of the difference in animal protein content between temperature treatments changed across days.

I can describe how OA affects metabolism by comparing how the temperature coefficient (Q_{10}) of these reactions changes under different CO_2 levels. For larval-specific O_2 consumption, Q_{10} values ranged from 1.26 to 3.89 (Table 4). When O_2 consumption was normalized with protein content, Q_{10} values remained < 2 except for larvae released on Day

Figure 5. Protein concentrations of *P. damicornis* larvae following 6-hour exposures to combinations of pCO_2 and temperature. Mean ± SE concentrations of total holobiont protein for larvae used to measure rates of oxygen consumption (n = 6) (A) and total animal protein for larvae used to measure rates of citrate synthase activity (n = 3) (B). Total holobiont protein was higher at Ambient-pCO_2 and on Days 10 and 11. Total animal protein at 30.6°C (vs. 27.8°C) was higher on Day 10 but lower on Day 11. Refer to Tables 2 and 3 for statistical details. Symbols are offset to improve clarity: Ambient-pCO_2 at 450 µatm (circles), High-pCO_2 at 950 µatm (triangles), 27.8°C (blue), and 30.6°C (red).

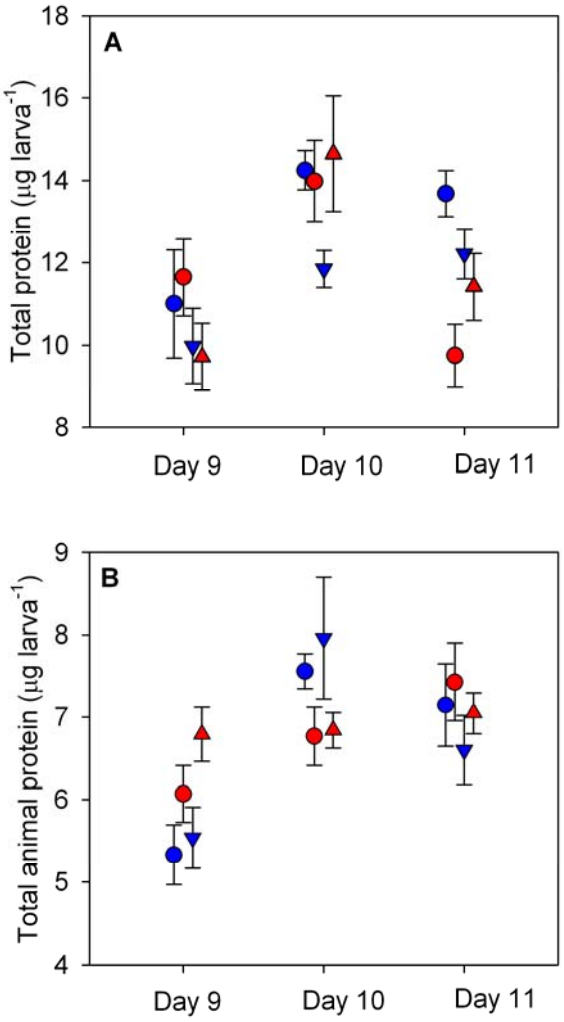

Table 4. Q_{10} values for rates of O_2 consumption and citrate synthase activity of *P. damicornis* larvae incubated for six hours in seawater at different temperature and CO_2 levels.

Dependent variable	Batch of Larvae	Q_{10} at Ambient-CO_2	Q_{10} at High-CO_2	Delta Q_{10}
Larval-specific O_2 consumption	Day 9	2.38	3.37	0.98
	Day 10	1.26	2.59	1.33
	Day 11	3.89	2.83	-1.06
Protein-specific O_2 consumption	Day 9	1.98	1.52	-0.45
	Day 10	1.37	1.10	-0.26
	Day 11	3.70	3.81	0.11
Larval-specific CS activity	Day 9	1.39	1.80	0.41
	Day 10	1.07	0.82	-0.25
	Day 11	0.44	0.97	0.52
Protein-specific CS activity	Day 9	0.95	0.74	-0.21
	Day 10	1.51	1.59	0.08
	Day 11	0.38	0.75	0.36

11. Regardless of standardization, Q_{10} varied among lunar days. On some days, High-pCO_2 increased the thermal sensitivities of oxygen consumption rates; on others, it depressed their temperature dependencies (Table 4). For CS activity, larval-specific Q_{10}s ranged from 0.44 to 1.80 (Table 4). Protein-specific Q_{10}s fell under 1.0 except for larvae released on Day 11. Again, Q_{10} values as well as the directional effect of pCO_2 on Q_{10} varied among days (Table 4).

Natural variability in pH and temperature proximal to the natal reef

Data for the present-day environmental exposures for coral larvae released on a Moorea fringing reef were measured using a SeaFET sensor near the coral collection site. Two key observations were made: (1) pH varied with a diel pattern, and (2) the delta pH (maxima minus minima) was 0.110 pH units. Throughout the 50-day deployment (data from 36 days shown here), pH and temperature fluctuated consistently through time with both parameters oscillating on a diel cycle with minima and maxima reached once every 24 hours (Fig. 6). pH values between 8.019 and 8.129 were recorded, with a mean value of 8.075 (Table 5). With regard to the nature of the diel pattern, pH maxima occurred on average around 06:14 UTC (20:14 local time), almost two hours after sunset, and pH minima occurred on average around 20:59 UTC (10:59 local time), almost five hours after sunrise. Temperature oscillated on a 24-hour period between 27.04°C and 28.62°C, averaging 27.73°C (Fig. 6A; Table 5). Daily minima and maxima occurred at approximately 14:00 and 02:00 UTC (04:00 and 16:00 local time), respectively. Fluctuations in pH lagged behind those in temperature by 4-7 hours. Temperature fluctuated according to the photoperiod with

Figure 6. Time series of temperature and pH at a fringing reef in Moorea, French Polynesia. During the month prior to larval release, environmental temperature (A) and pH (C) oscillated on a 24-hour period. A three-day window, March 13-15, 2011, corresponds to ambient temperature (B) and pH (D) conditions adjacent to the natal reef of the larvae used in manipulative experiments on those days. Temperatures represent averages from duplicate thermisters, processed by a one-hour low-pass filter. pH data from a SeaFET sensor were processed by a one-hour low-pass filter.

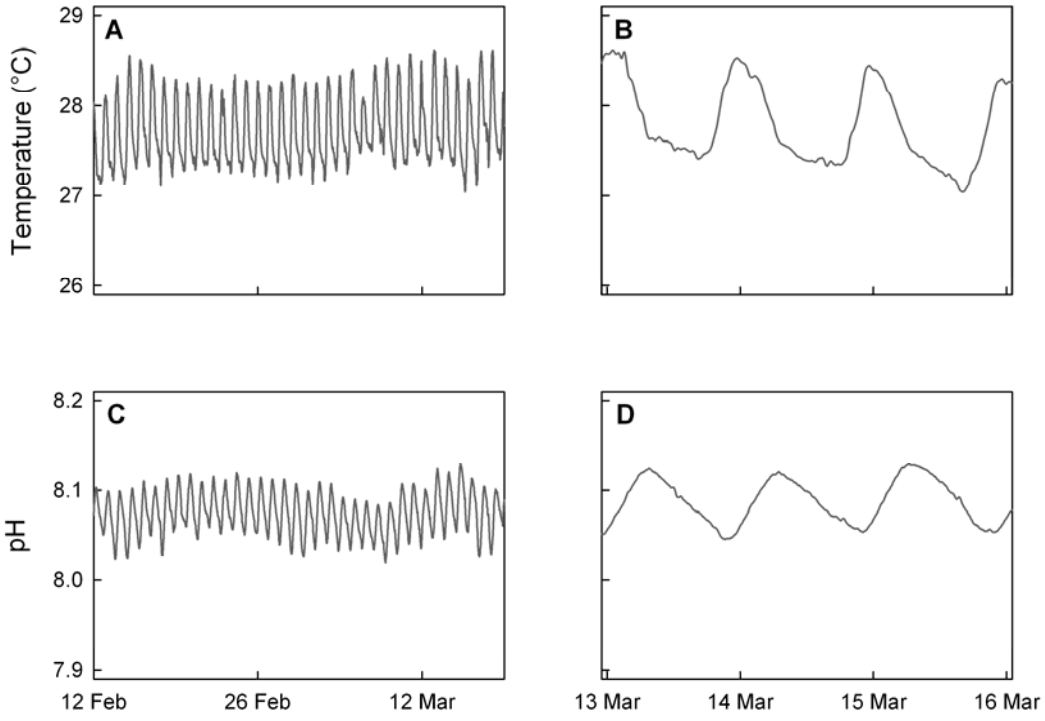

Table 5. Summary of oceanographic conditions on a fringing reef in Moorea, French Polynesia from February 12 – March 19, 2011 (UTC).

Summary Statistics	Temperature (ºC)	pH	Ω_{arag}	Ω_{calc}	pCO_2 (µatm)
n	25841	5169	5169	5169	5169
Mean	27.73	8.075	4.02	6.05	374
SD	0.38	0.023	0.16	0.23	25
Range	1.58	0.110	0.70	1.05	118
Max	28.62	8.129	4.38	6.59	437
Min	27.04	8.019	3.68	5.54	319
25%	27.42	8.058	3.90	5.87	354
75%	28.05	8.093	4.15	6.24	392

Temperatures were recorded by duplicate thermisters. pH (in total scale) was recorded by a SeaFET. Salinity and A_T were measured from a discrete seawater sample collected on February 24, 2011: S = 35.1; A_T = 2370.16.

coldest temperatures occurring two hours before dawn and warmest temperatures occurring two hours before sunset.

Discussion

To assess metabolic plasticity during early dispersal of *Pocillopora damicornis* larvae, I performed laboratory experiments whose treatment conditions were determined based on environmental extremes recorded at the collection site. These microcosm experiments tested effects of future projected ocean conditions. As indicators of performance under conditions of OA and warming, I used oxygen consumption and citrate synthase activity. The results indicate that *P. damicornis* larvae differ in their sensitivity to environmental change with respect to the day their cohort was released from adult colonies.

Metabolic status under multiple stressors

In general, high pCO_2 did not increase, but decreased, the demands of aerobic metabolism in *P. damicornis* larvae (Fig. 3A). Specifically, for the early release larvae (Days 9 and 10), changes in O_2 consumption were smaller, while on Day 11, larvae exhibited more distinct signs of metabolic depression under high pCO_2, high temperature conditions. With a small sample size of 6, the differences could be due to random variation in the size of individuals in the treatments (an estimated 24% chance from power analysis; Faul et al., 2007). In contrast to the results obtained for pCO_2 levels, temperature had a more consistent effect on larval oxygen consumption across days (Fig. 3A). Higher respiration rates at 30.6°C were expected, as body temperature (*i.e.* ambient temperature for coral larvae) and whole-

organism metabolic rate are highly correlated (Gillooly et al., 2001) via the kinetics of biochemical reactions. Despite the increased demand for energy that concurrent elevated temperature and pCO_2 likely imposed, the effects of these stressors - a direct effect on molecular kinetics and an increased cost of maintenance within larval energy budgets - were in general additive, with temperature having a consistently larger effect on aerobic metabolism.

High pCO_2 in the marine environment likely increases the maintenance costs of acid-base homeostasis, the intracellular ion balance required for protein folding and pH-sensitive physiological processes. Near-equivalent oxygen consumption rates under different pCO_2 conditions suggest that peak-release larvae may be able to use existing pools of ion pumps to conserve acid-base homeostasis under acute stress (Hand, 1991; Pörtner and Reipschlager, 1996; Guppy and Withers, 1999). However, as suggested by the results of this study, late-release larvae may not have the capacity to buffer against the physiological demands of a simultaneously warm and acidic environment, minimizing energy requirements as a result to reduce rates of ATP synthesis. Low metabolic rates in response to OA and hypercapnia have been recorded for several taxa including sipunculid worms (Pörtner et al., 1998), adult and juvenile bivalves (Michaelidis et al., 2005), jumbo squid (Rosa and Seibel, 2008), tropical fish (Munday et al., 2009), and brooded and non-brooded coral larvae (Albright and Langdon, 2011; Nakamura et al., 2011). Other groups, such as snails and teleost fish, appear to be resilient to elevated pCO_2 conditions (Bibby et al., 2007; Melzner et al., 2009a, 2009b). Overall, metabolic depression in response to anthropogenic ocean change could have severe consequences for these late-release larvae. If it affects their abilities to navigate the water column, then larval dispersal, settlement success, and fitness may be impaired.

While larval-specific oxygen consumption values recorded here fall within the range published for *P. damicornis* larvae (*e.g.* Richmond, 1987; Gaither and Rowan, 2010; Cumbo et al., 2013a, 2013b; Putnam et al., 2013), other studies on *P. damicornis* larvae have reported different results for responses to elevated pCO_2 and temperature levels. In March 2010 and 2012 with a population of *P. damicornis* in Taiwan, Cumbo *et al.* (2013a) found that for larvae released on four consecutive days, day x temperature and day x pCO_2 x temperature had significant effects on respiration per larva. The main effect of CO_2 on oxygen consumption was non-significant to negative, while elevated temperature stimulated aerobic metabolism. In contrast, a study with this same population conducted at the same time found no effect of pCO_2 and a negative effect of temperature on larval respiration (Putnam et al., 2013). Following longer exposure times (1-5 days), Cumbo *et al.* (2013b) found that temperature, but not pCO_2, affected mass-specific oxygen consumption in *P. damicornis* larvae from Taiwan. Interestingly, in that study, decreased oxygen consumption rates were observed in HTHC treatments for larvae at 5 days of incubation but not before. These studies differ from ours in terms of pCO_2 exposures used, length of exposures, and biogeographic locations of coral collection (Table 6). Additionally, these studies did not document in high frequency the current environmental conditions at the collection site of their study organisms, so the interpretation of their results without knowledge of the relationship between experimental and environmental conditions is challenging. Consequently, direct comparisons of the datasets are difficult. Considering the studies together, however, highlights important differences between the larvae from corals in Moorea (which appear to be more sensitive to pCO_2) and those from a genetically distinct Taiwan population (Forsman et al., 2013) that experiences significantly different seawater

Table 6. Summary of studies investigating the effects of temperature and pCO_2 on larval rates of oxygen consumption for *P. damicornis* larvae.

Study	Location	Species, Reproductive mode	Day of release	Treatment conditions	Length of exposure	O_2 consumption (nmol O_2 $larva^{-1}$ min^{-1})	Effect of pCO_2	Effect of T	Effect of Day	Interaction(s)
Cumbo *et al.* (2013a)	Taiwan	*Pocillopora damicornis*, brooder	Near peak-release (4 days)	25, 29°C; 400, 750 µatm pCO_2	1 d	0.068-0.262	Mostly NS, but few -	Mostly +	Yes	TxDay, CO_2xTxDay
Cumbo *et al.* (2013b)	Taiwan	*P. damicornis*, brooder	Peak-release only (1 day)	24, 31°C; 488, 851 µatm pCO_2†	1-5 d	0.077-0.188†	NS	+	N/A	T x Incubation time
Putnam *et al.* (2013)	Taiwan	*P. damicornis*, brooder	Near peak-release (1 day)	24, 29°C 415, 635 µatm pCO_2	9 d	0.035-0.129	NS	-	N/A	NS
This study	Moorea, French Polynesia	*P. damicornis*, brooder	Peak-release and after (3 days)	28, 30°C 450, 950 µatm pCO_2	0.25 d	0.083-0.139	-	+	Yes	NS
Nakamura *et al.* (2011)	Sesoko Island, Okinawa Island, Japan	*Acropora digitifera*, BS	N/A	26°C; 350, 1400, 2500 µatm pCO_2	3, 7 d	0.002-0.005	NS, -	N/A	N/A	N/A
Albright and Langdon (2011)	Summerland Key, Florida, USA	*Porites astreoides*, BS	N/A	26°C; 380, 560, 800 µatm pCO_2	1-2 d	0.015-0.033	-	N/A	N/A	N/A

carbonate chemistry (EB Rivest, unpublished data).

While larval-specific metabolism given as a rate per individual imparts function at the organismal level, normalization to protein accounts for variation in mass between larvae. The effect of pCO_2 disappeared when oxygen consumption rates were standardized by total protein content (Fig. 3B). Lower protein content of larvae incubated at High-pCO_2, due to slower growth or down-regulation of thermotolerance pathways, could have removed the larval-specific effect of pCO_2. Other factors could generate these respiration rates. Even if planulae contained similar amounts of total protein between treatments, differences in the enzyme composition of the protein pools could have led to the observed differences in performance. Similarly, differences in holobiont cell number, and differences in *Symbiodinium* density could have contributed to the differences between larval-specific and mass-specific results.

In this study, CS, a rate-limiting enzyme in the Krebs cycle, was used as a biochemical indicator for changes in metabolic function, notably mitochondrial density (Moyes, 2003). This approach is commonly used to assess the impacts of environmental parameters and ontogeny on the metabolism of marine organisms (***e.g.*** Kiessling et al., 1991; Gattuso et al., 1993; Lesser et al., 1994; Thuesen and Childress, 1994; Marsh et al., 1999; Moran and Manahan, 2004; Weiss et al., 2012). I used this enzyme assay to examine the effects of OA and temperature on the oxidative capacity of *P. damicornis* larvae. While O_2 consumption was measured for the entire larva, oxidative capacity was measured for the animal compartment only.

Temperature and pCO_2 did not dramatically affect larval- and protein-specific CS activity, though CS activity became suppressed at high temperature across days, particularly

for late-release larvae (Fig. 4A,B). These data contrast those for O_2 consumption, which generally show elevated rates of aerobic metabolism at higher temperatures and depressed rates at high pCO_2. While the O_2 consumption measurements represent the average respiration rate across the 6-hour exposure period, CS activity was a snapshot of oxidative capacity at the end of the incubation (t = 6 hours). The O_2 consumption measurements likely captured the peak in respiration rates while larvae were actively swimming but smoothed any variation due to developmental changes. Though all individuals used remained in the larval stage throughout the exposure, high temperatures do decrease time to metamorphosis in brooded coral larvae (*e.g.* Edmunds et al., 2001). As a result, subtle developmental and behavioral changes as larvae progressed towards metamorphosed polyps could have generated the lower rates of CS activity found in larvae incubated at 30.6°C (Lemos et al., 2003; Okubo et al., 2008; Weiss et al., 2012). However, our interpretation is limited because the oxidative capacity of *Symbiodinium* within the larvae was not assessed. High densities of mitochondria in the *Symbiodinium* fraction at 30.6°C could have caused the observed differences between O_2 consumption and CS activities. CS activities measured were lower than those published for adult coral (0.0007-0.041 units mg protein^{-1}; Gattuso et al., 1993; Lesser et al., 1994), whose processes specific to particular life history stages like calcification may demand higher respiration rates. Lower densities of mitochondria during larval development as well as lower surface area to volume ratios may contribute to the differences in CS activity between life history stages of coral (*e.g.* Childress and Somero, 1990; Chu and Ovsianicokoulikowsky, 1994; Marsh et al., 1999).

CS is an excellent proxy for the short-term metabolic responses of coral larvae because it correlates well with oxidative capacity required to satisfy routine and maximal

energy demands (*e.g.* Moyes, 2003; Weibel and Hoppeler, 2005). As measured by CS activity, larval oxidative capacity did not increase in response to elevated temperature or pCO_2. Thus, increased demands for respiration during the short experimental exposures were likely met by an increase in the energy production of the existing pool of mitochondria through metabolic regulation of enzymes rather than *de novo* synthesis of new enzymes. Furthermore, the lack of increase in oxidative capacity at elevated temperatures despite greater flux of aerobic machinery suggests that *P. damicornis* larvae may be unable to tolerate additional stresses like OA on their energy budget. Energy demands to maintain homeostasis under higher pCO_2 (>1000 μatm) may approach or surpass the ceiling of oxidative capacity, triggering metabolic suppression. However, following longer exposures (days to weeks), the sustained increase in energy demand imposed by acidity and warming may elicit mitochondrial biosynthesis as a compensatory response.

In this study, Q_{10} values for larval-specific rates of O_2 consumption generally fell within the common range for chemical reaction rates (2-3; *e.g.* Hochachka and Somero, 2002). Notably, aerobic respiration in other brooded coral larvae (*Porites astreoides*) had Q_{10} values close to 2 (Edmunds et al., 2001). Indicated by $Q_{10} < 2$, protein-specific metabolic rates were less sensitive to changes in temperature for larvae released on Day 9 and 10. For larvae released on Day 11, protein-specific O_2 consumption rates were hypersensitive to temperature change, as shown by $Q_{10} > 3$. Oxidative capacity (*i.e.* maximum activity of CS) on all days was temperature-independent or had negative temperature dependence, with $Q_{10} < 2$ and often 1. These low Q_{10} values indicate immediate temperature compensation; many poikilotherms exhibit compensation to acute fluctuations in temperature over a portion of their natural environmental temperature range (Hazel and Prosser, 1974). The Q_{10} patterns

shown here indicate that specific components of the metabolic machinery are less sensitive to changes in temperature, but this toxicity or metabolic compensation to environmental stress is not detectable at the whole-organism level following acute exposures to elevated pCO_2 and temperature.

Rates of O_2 consumption and CS activity of *P. damicornis* larvae are affected by pCO_2, but not consistently, as shown by the change in sign of ΔQ_{10} between days (Table 4). For some cohorts of larvae, an increase in pCO_2 enhanced the sensitivity of reaction rates to increases in temperature, while for other cohorts, an increase in pCO_2 decreased the sensitivity of reaction rates to increases in temperature. The general absence of dramatic changes in Q_{10} as pCO_2 increased indicates resistance or compensation to OA that is not revealed by biological responses of O_2 consumption and CS activity. In general, larvae seem to be able to preserve a homeostatic level of energy metabolism under the treatment conditions, though not through the metrics that we quantified. Still, high CO_2 levels may reduce performance of coral larvae, especially at the edges of their thermal envelope where larvae may be spending more of their energy metabolism on maintenance rather than growth or development (Pörtner, 2010). Variable compressions or shifts in thermal tolerance windows of *P. damicornis* larvae between days could explain the variation in Q_{10} values reported here (Pörtner, 2010). Elevated pCO_2 could compress the thermal envelope of coral larvae, resulting in lower maximum reaction rates and a narrower range of functional capacity. Alternatively, elevated pCO_2 could shift the thermal envelope to a lower range of temperatures, decreasing the temperature for optimum functional performance.

Variation in physiological plasticity among larval cohorts

My results indicate that there are differences in larval sensitivity to environmental change between three cohorts that were released from adult colonies at different times. This work, along with similar studies, reveals that larvae released on different days throughout the spawning period respond differently to changes in seawater temperature and acidity (*e.g.* Putnam et al., 2010). Larvae of *P. damicornis* and other brooding corals are known to differ by size, *Symbiodinium* density, and photophysiology throughout the spawning period (Edmunds et al., 2001; Isomura and Nishihira, 2001; Putnam et al., 2010; Cumbo et al., 2012; EB Rivest, unpublished data). As larvae are stacked within coral polyps during pre-release development (Stoddart and Black, 1985), variation in microenvironment by tissue depth may promote these physiological differences (Kuhl et al., 1995; Jimenez et al., 2008). Depending on development time within the maternal coral polyp, larvae may have different endowments of maternal *Symbiodinium* and lipid that consequently affect physiological performance. Variation in larval traits could also be a function of genotype. Due to low release numbers, ratios of genotypes within the larval pool were not consistent between days; however, our observations still reflect variation in biological response at the population level. Additionally, differences in larval physiology could be related to days in captivity, which was not possible to distinguish from day of release in this experiment. Variation in traits that affect physiological performance may be a product of natural selection – the range of phenotypes represented within larvae released monthly could confer selective advantage under different environmental conditions. Some phenotypes may favor retention of larvae on the natal reef, with physiology optimized for local conditions. Other phenotypes may favor longer

dispersals through open-ocean ecosystems with different abiotic pH and temperature regimes.

Natural variation of environmental pH and temperature

In order to elucidate the range of environmental conditions of the water mass bathing the fringing reef where *P. damicornis* adults were collected, I measured the variability of pH and temperature on the natal coral reef in Moorea. Data were recorded as close to the site where the adult coral colonies were collected as was possible. The conditions experienced by the adult coral collected within 100 m of the sensor location may have varied (*e.g.* Guadayol et al., 2014), but our environmental data likely represent the conditions experienced by freshly-released larvae in the plankton. In February-March 2011, the average pCO_2 on the study site (374 μatm) was similar to the global atmospheric average for the year (390 μatm, Conway and Tans, NOAA/ESRL [www.esrl.noaa.gov/gmd/ccgg/trends]). Additionally, current oscillations of pCO_2 at this site are within projected open-ocean averages for the middle of this century (IPCC, 2013). The pH and temperature time series recorded during this study confirm that the average values for our experimental treatments of pCO_2 and temperature were approximations of present-day reef conditions as well as extremes not yet observed within the seawater surrounding the fringing reef at the study site.

A key observation within the data was a 24-hour oscillation of pH (Fig. 6C,D). Larvae released from sunset to sunrise experience the nightly decrease in pH during the first part of their larval duration. The timing of the pH oscillation supports a hypothesis that within 1 m of the fringing reef at this location, biological processes (respiration and photosynthesis) are driving the 24-hour pattern in the surrounding seawater. This oscillation

may have been larger at the 1-2m collection depth of the adult corals used in this study. The slopes of the daily ascent and descent of pH are slightly different in absolute value and do not reflect a simple turning on and off of the balance between photosynthesis and respiration with the photoperiod. Particularly, the onset of the photosynthesis signal is delayed 5 hours after sunrise, perhaps due to calm weather reducing mixing at this time of day or lower physiological rates at the pH minima.

Despite measurable daily fluctuations in seawater chemistry, aragonite saturation states remained suitable for coral calcification, where calcium carbonate readily precipitates and does not erode ($\Omega_{arag} > 3.5$; Guinotte et al., 2003). pCO_2 fluctuated between 319 and 437 µatm with an average of 374 µatm (Table 5). At this site, changes in A_T are most likely due to freshwater influence following precipitation runoff from land. After a rain event, salinity at this site can decline up to 1 ppt, while A_T can fall by 50 µmol kg SW^{-1} (EB Rivest, unpublished data). Variations in salinity and A_T alter the calculated pCO_2 by approximately 5-10 µatm for the range of pH recorded at this site. Similarly, uncertainties for Ω_{arag} and Ω_{calc} are ~0.06 and ~0.04, respectively. Despite the uncertainties in the descriptive statistics shown in Table 5, the diel oscillation in pH remained distinct.

While fluctuations of temperature and pH are common in coral reefs and other habitats (*e.g.* Hofmann et al., 2011), variability in environmental carbonate chemistry recorded at the Moorea site differs slightly from conditions at other coral reefs (Ohde and van Woesik, 1999; Jan and Chen, 2009; Gagliano et al., 2010; Price et al., 2012). Compared with SeaFET pH time series data from protected reef terraces in the Northern Line islands (Price et al., 2012), pH on the Moorea fringing reef had similar amplitudes but a higher mean value (8.075 vs. 7.958–7.981). Oceanographic features, seawater retention times, and

differences in community composition may be responsible for these differences. These and other studies reporting the variability of nearshore pH and *in situ* biological responses are becoming more common (*e.g.* Yates and Halley, 2006; Yates et al., 2007; Hall-Spencer et al., 2008; Wootton et al., 2008; Chierici and Fransson, 2009; Gagliano et al., 2010; Price et al., 2012; Wootton and Pfister, 2012) and are refining our understanding of natural variability of pH and carbonate chemistry which has historically come from open-ocean measurements (*e.g.* WOCE, http://woce.nodc.noaa.gov/wdiu; BATS, http://www.bios.edu/research/bats.html; HOTS, http://hahana.soest.hawaii.edu/hot/hot_jgofs.html).

Implications for the future of coral reefs

The over-arching outcome of this study suggests that only a portion of larvae produced monthly exhibited physiological phenotypes suited for tolerating projected end-of-the-century levels of high temperature and low pH for the surface ocean. Furthermore, biochemical limits for increasing oxidative capacity to satisfy elevated energy demands in a warming, acidifying ocean (*i.e.* rates of enzyme activity and mitochondrial synthesis) may ultimately override the advantages offered by current phenotypes, barring acclimation and/or adaptation. If larvae cannot tolerate elevated temperatures and pCO_2 levels by up-regulating mitochondria biosynthesis to fuel stress response pathways, their demands for ATP synthesis may soon surpass the capacity of their aerobic machinery. These measured acute responses can inform a larger picture: given longer exposures to ocean warming, acidity, and other concurrent stressors, even over multiple generations, do corals have the potential to acclimate to changing carbonate chemistries, thereby avoiding a narrowing of their thermal tolerance

windows? Population-specific functional traits, such as the ones quantified here, can predict shifts in species' ranges and phenologies in response to global climate change (Buckley and Kingsolver, 2012).

Comparisons between coral populations on reefs with different carbonate chemistry conditions (*e.g.* Moorea, French Polynesia and Nanwan Bay, Taiwan) may provide clues as to how physiological plasticity can be shaped by environmental variability and whether local adaptation to temperature and pH regimes buffers sensitivities to OA and rising temperature. Local adaptation in coral dinoflagellate endosymbionts has already been documented, and thermotolerant *Symbiodinium* groups may be able to enhance the tolerance and fitness of their coral host (Oliver and Palumbi, 2011; Howells et al., 2012). Furthermore, on a global scale, there is a high degree of spatial variability in the intensity of multiple stressors for coral reefs (Maina et al., 2011; Karnauskas and Cohen, 2012). Acclimatization or local adaptation along this gradient of stress may maintain populations with suitable phenotypes for future ocean conditions. Estimates of physiological plasticity as well as contextual frameworks for variability of environmental conditions present potentially robust tools for marine conservation, allowing us to predict the influence of anthropogenic stressors on larval fitness, dispersal, and recruitment success and to manage local populations within a global context.

III. Effects of ocean acidification and elevated temperature on the oxidative state and ionic balance of larvae of the coral *Pocillopora damicornis*

Introduction

Corals and their free-swimming larvae will likely respond to changing environmental conditions, specifically ocean acidification (OA) and warming, in a variety of ways, including adaptation (Kelly and Hofmann, 2012; Munday et al., 2013; Sunday et al., 2014), and acclimatization or physiological plasticity (Godbold and Calosi, 2013; Palumbi et al., 2014). Although many studies have examined physiological processes such as calcification and primary production in response to predicted future ocean conditions (*e.g.* Anthony et al., 2008; Reynaud et al., 2003), other aspects of coral physiology, such as oxidative state and ionic balance, have not been explored but will likely be affected by OA and warming. With experiments described in this chapter, my aim was to assess the ability of coral planulae to tolerate OA and warming through the use of pathways involved in oxidative state and ionic balance.

From a mechanistic perspective, OA and warming may compromise cellular functional integrity by generating oxidative stress and changing redox potentials (reviewed in Kültz, 2005). Oxidative stress is caused by reactive oxygen species (ROS), which include hydrogen peroxide (H_2O_2), hydroxyl radicals ($OH^{\cdot -}$) and superoxide radicals ($O_2^{\cdot -}$), and singlet oxygen ($^1O_2$). ROS are generated in mitochondria during aerobic cellular metabolism throughout the coral holobiont and also by photosynthesis in the *Symbiodinium* within coral tissue (Dykens and Shick, 1982; Dykens et al., 1992; Lesser, 1996, 1997; Nii and Muscatine, 1997; Downs et al., 2000, 2002). *Symbiodinium* photosystem II is the likely source of ROS

(Jones et al., 1998; Downs et al., 2000; Weis, 2008). Oxidative stress has been documented in corals in response to elevated temperature (Lesser, 1997), and OA may exacerbate this stress when the two environmental stressors, high pCO_2 and high temperature, co-occur.

Free radical formation and changes in cellular redox potential activate the cellular stress response (CSR), which senses and repairs stress-induced damage by (1) repairing and stabilizing macromolecules, (2) modulating pathways of energy metabolism, (3) arresting cellular growth and proliferation, (4) regulating transcription of stress response genes, and (5) regulating apoptosis (reviewed in Kültz, 2005). A critical facet of the CSR in all cells is a system of antioxidant enzymes and compounds that scavenges free radicals while minimizing and repairing oxidative damage. Antioxidants are substances that, at low concentrations, impede or avert oxidation of a substrate (Halliwell and Gutteridge, 1999). Antioxidant capacity of the CSR depends on the expressed proteome and can be controlled through mRNA synthesis and processing and through post-translational modification of proteins. Two important antioxidant enzymes are catalase and glutathione reductase. Catalase dismutates H_2O_2 to O_2 and H_2O. Because catalase has a high turnover rate, conditions that affect protein turnover rates, such as osmotic and heat stresses, will decrease the enzyme's activity, making the organism vulnerable to oxidative stress (Asada and Takahashi, 1987; Cadenas, 1989; Hertwig et al., 1992; Fridovich, 1998; Halliwell and Gutteridge, 1999). Secondly, glutathione reductase is crucial for maintaining the reducing environment of cells. It regenerates a universal free radical scavenger, glutathione (GSH), by reducing the oxidized form (GSSG). GSH prevents damage to cells by reacting with $^1O_2$, $O_2\cdot^-$, and $OH\cdot^-$ and by breaking free radical chain reactions (Halliwell and Gutteridge, 1999). There are other non-protein antioxidants, such as α-tocopheral and ascorbic acid (reviewed by Lesser, 2006).

Together, both enzyme and non-enzyme antioxidants generate a cell's total antioxidant potential, which is defined as its net reducing ability (Benzie and Strain, 1996). Antioxidant potential of *P. damicornis* from Kaneohe Bay, Hawai'i peaked at 28°C; as temperature increased to 31°C, antioxidant potential decreased, a sign of weakening defense (Griffin and Bhagooli, 2004). Therefore, to assess the ability of coral planulae to maintain their oxidative state under conditions of environmental stress, I measured total antioxidant potential and catalase activity.

In addition to their effects on the oxidative state of the larvae of *P. damicornis*, OA and elevated ocean temperature may increase the costs of maintaining ionic gradients across cellular membranes. Na^+/K^+-ATPase, a transmembrane protein present in all animals, establishes gradients of Na^+ and K^+. These ionic gradients maintain cellular resting membrane potential and osmotic equilibria in addition to sustaining transmembrane electrochemistry necessary for transport of other molecules by Na^+-coupled cotransporters (Crane, 1977; Blanco and Mercer, 1998). Adult marine invertebrate tissues and cells expend 30-70% of their metabolic resources for maintaining Na^+ and K^+ gradients, making this one of the most energetically demanding physiological processes (detected via ouabain-sensitive respiration rates; Baker and Connelly, 1966; Lucu and Pavicic, 1995; Lannig et al., 2010). Na^+/K^+-ATPase is under fine transcriptional control; changes in its abundance and activity could have dramatic consequences for energy budgets, potentially causing reallocation of resources from other processes such as growth and reproduction. In marine teleost fish, Na^+/K^+-ATPase activity increased during acclimation to hypercapnic conditions (Deigweiher et al., 2008; Melzner et al., 2009a). Similarly, after adult oysters (*Crassostrea gigas*) were exposed to elevated temperatures and long-term high pCO_2 conditions, total cellular oxygen

demand and Na^+/K^+-ATPase activity increased in parallel, suggesting that energy demands for metabolism and its ion regulatory component are elevated under these conditions (Lannig et al., 2010). However, several marine invertebrates suffer from metabolic depression under hypercapnia (reviewed by Guppy and Withers, 1999), perhaps due to their inability to compensate a low extracellular fluid pH (Pörtner et al., 1998; Michaelidis et al., 2005). My previous work with the larvae of *P. damicornis* suggests that signs of metabolic depression at High-pCO_2 (Chapter 2) indicate that larvae may be less able to defend their oxidative state and ionic balance under OA. In particular, this is the case for larvae released late in the spawning period.

In this chapter, I aimed to extend my research on the responses of the metabolism of coral larvae to future ocean conditions to examine the physiological plasticity of processes that help to maintain homeostasis in coral cells. Methods by which corals can use their existing physiological repertoire to tolerate changing environmental conditions may provide insight into their potential for acclimatization and longer-term persistence as OA and warming continue (Hofmann and Todgham, 2010; Evans and Hofmann, 2012). I explored several physiological processes that are likely to be affected by OA and elevated temperature. Using exposures of pCO_2 and temperature, I measured the responses of *P. damicornis* larvae from a reef in Taiwan. First, I assessed the effects of pCO_2 and temperature on oxidative stress of coral larvae, using total antioxidant potential and catalase activity as indicators of physiological stress response. Second, I measured two forms of activity of an enzyme that is central to maintaining homeostatic acid-base balance within cells, Na^+/K^+-ATPase. The experiments addressed the prediction that OA and elevated temperature will increase oxidative stress in coral larvae and that the larvae will increase the maintenance of their ionic

balance under these future ocean conditions. I hypothesized that total antioxidant potential, catalase activity, and Na^+/K^+-ATPase activity would differ between high pCO_2, high temperature versus ambient conditions as well as between cohorts of larvae. Results for the assays used in this chapter were mixed: I was able to collect data for total antioxidant potential and one measure of Na^+/K^+-ATPase activity but was not able to collect activity for catalase activity or ouabain-sensitive Na^+/K^+-ATPase activity. Therefore, the comprehensive presentation of experiments in this chapter includes a description of the methodological challenges in this more biochemical component of my thesis.

Materials and Methods

To understand how the oxidative state and acid-base physiology of *Pocillopora damicornis* respond to increased ocean acidity and temperature, I incubated larvae in warmed seawater enriched with elevated pCO_2 after which the activities of antioxidant and acid-base regulatory enzymes were measured.

Collection of coral larvae

P. damicornis larvae were obtained from adult colonies collected in collaboration with the National Museum of Marine Biology and Aquarium (NMMBA) in Pingtung, Taiwan. On July 26, 2011, eight adult *P. damicornis* colonies were collected from a fringing reef at 5 m depth in Hobihu, Taiwan (21°57'5.92"N, 120°45'1.01"E). Colonies of *P. damicornis* were maintained in flow-through aquaria with indirect sunlight and coarsely filtered seawater (~29.6°C, ~33 psu, up to 781 μmol photons m^2 s^{-1}) at NMMBA until they

released planula larvae synchronous with the lunar cycle from July 31 – August 8, 2011. In Taiwan, larval release for *P. damicornis* occurs every month after nightfall on lunar days 2 through 9, with the greatest abundance of larvae released on lunar day 6 (Fig. 7; Fan et al., 2002). The larvae were collected on 100 μm mesh in the outflow of the tanks containing the adults. At dawn each day, all larvae released from each coral were counted. Equal numbers of larvae from each colony were pooled and randomly assigned to experimental treatments. Data presented here are from experiments conducted with cohorts of larvae released on August 2 ("Early"), August 3 ("Peak"), August 4 ("Middle"), and August 5 ("Late").

Experimental incubations

Two pCO_2 levels (450 μatm CO_2 and 800 μatm CO_2) and two temperature treatments (27.5 and 30.5°C) were prescribed. The pCO_2 treatments represent current atmospheric conditions and a pCO_2 level projected for the atmosphere by the year 2100 under a business-as-usual scenario (IPCC, 2013). The temperature treatments represent average annual sea surface temperature near the site where adult *P. damicornis* were collected (T-Y Fan, unpubl.) and an elevated temperature predicted for the surface ocean by 2100 (IPCC, 2013). These abiotic conditions were combined to create four experimental treatments: ambient temperature-ambient pCO_2 (ATAC), ambient temperature-high pCO_2 (ATHC), high temperature-ambient pCO_2 (HTAC), and high temperature-high pCO_2 (HTHC). Seawater of desired pCO_2 levels was created by bubbling gas mixtures of the desired CO_2 levels directly into experimental aquaria. The control treatment, Ambient-pCO_2, was

Figure 7. Release of *Pocillopora damicornis* larvae in August 2011. Larvae were released from July 31 (Lunar day 1) to August 8 (Lunar day 9). Larval release increased following the new moon and then decreased after Lunar day 6. Larvae used for this study were released on August 3-5 (Lunar days 4-6). Numbers of larvae released per colony (n = 8 colonies) are described by bar segments of different colors.

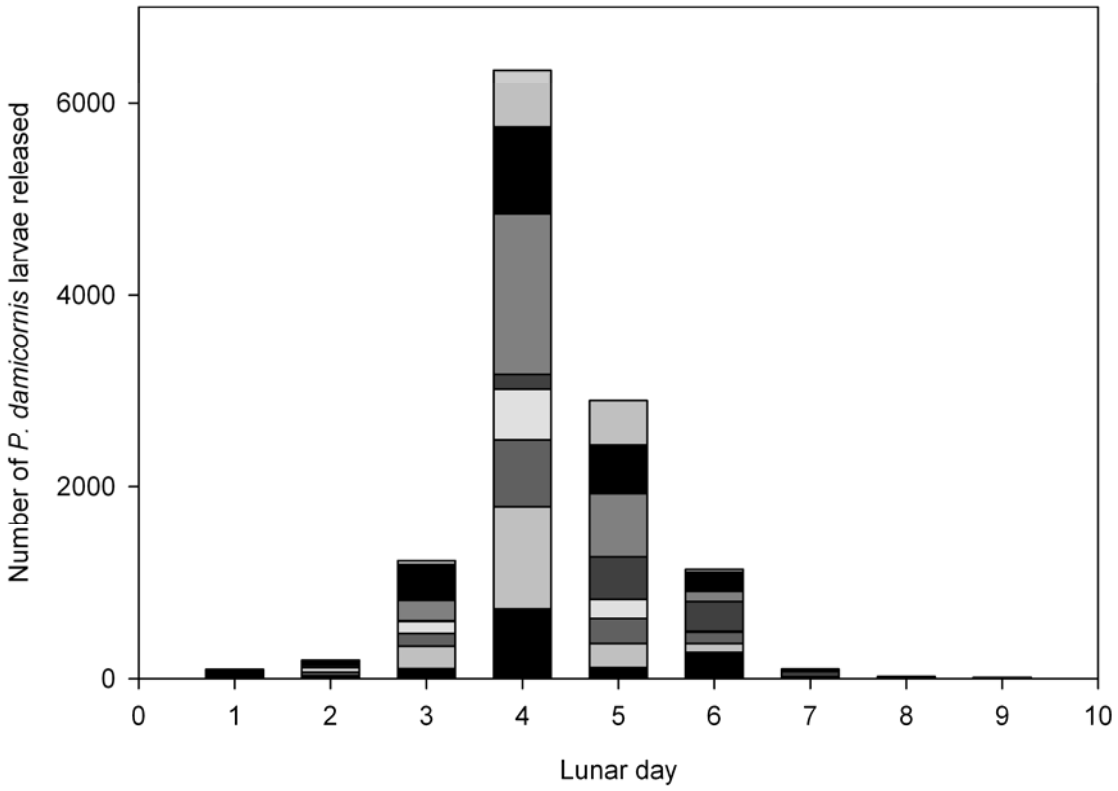

generated using compressed atmospheric air. The High-pCO_2 treatment gas mixture was generated through controlled blending of pure CO_2 and atmospheric air in a mixing chamber using high-precision needle valves and a solenoid (Model A-352, Qubit Systems). An Infra-Red Gas Analyzer (S151, Qubit Systems) continuously sampled the gas mixture from the chamber and provided dynamic feedback, adjusting the timing of the solonoid to maintain a consistent pCO_2 level in the gas mixture. Each treatment gas (Ambient- and High-pCO_2) was then bubbled into experimental aquaria continuously throughout the experimental time period.

Eight 150 L experimental aquaria were used, two for each treatment combination of pCO_2 and temperature. The aquaria were filled with seawater filtered to 1 μm. About 20% of the seawater was exchanged daily around 18:00 h; the seawater was equilibrated to treatment levels by the start of the next incubation of larvae. To maintain equilibration of the gas treatment, each aquarium was continuously mixed using a circulating pump (Rio 1110). Temperature was controlled in each tank by Aquacontrollers (Neptune Systems) that turned on and off individual aquarium heaters (300W, Taikong Corp.) and chillers (Aquatek AC11) to maintain set-point temperatures. Metal halide (Phillips 150 W 10,000k) and fluorescent bulbs (Phillips 39W T5 460 nm) above each aquarium provided photosynthetically active radiation throughout the exposures (258 ± 21 μmol photons m^2 s^{-1}).

To verify and monitor the carbonate chemistry parameters of the experimental treatments, chemistry of the seawater in the aquaria was analyzed daily. pH, temperature, salinity, and total alkalinity of seawater in each aquarium were measured during the incubations. Seawater temperature was measured using a certified digital thermometer (meter 15-077-8, probe 15-077-7, Thermo Fisher Scientific Inc., Waltham, MA, USA). Seawater

salinities were measured throughout the experimental exposures using conductivity meter (340i, WTW GmbH, Wilheim, Germany). pH was measured using a spectrophotometric method with indicator dye (SOP 3b, Dickson et al., 2007). Total alkalinity (A_T) was measured following (SOP 6b, Dickson et al., 2007) using an automatic titrator (DL50 with DG101-SC pH probe, Mettler Toledo LLC, Toledo, OH, USA). Titrations were performed using certified acid titrant (~0.1M HCl, 0.6M NaCl; A. Dickson Laboratory, Scripps Institute of Oceanography), and A_T was calculated following Dickson *et al.* (2007). Whenever titrations were run, analyzed certified reference materials from A. Dickson laboratory were titrated to confirm the precision and accuracy of the procedure; these reference titrations were accurate within 10 μmol kg^{-1} (0.1-0.4% error). pH at 25°C, A_T, temperature, and salinity were used to calculate the pH and pCO_2 of the treatments using CO2calc (Robbins et al., 2010), with CO_2 constants K1, K2 from Mehrbach *et al.* (1973) refit by Dickson and Millero (1987).

To determine the effects of OA and warming on oxidative stress and ion balance in *P. damicornis* larvae, planulae were exposed to combinations of pCO_2 and temperature levels for 6 hours. Larvae were incubated at a density of 1 larva mL^{-1}in 50 mL Falcon tubes, modified with windows of 100 μm mesh. There were 2-3 replicate tubes of larvae in each aquarium. Incubations were staggered by 40 minutes each day, with tank order randomized, to allow for expedient preservation of larvae at the end of the 6-hour period. Batches of larvae were flash-frozen in liquid N_2 and stored at -80°C for enzyme assays. On August 3 and 5, larvae were preserved for analyses of total antioxidant potential (3 tubes $aquarium^{-1}$ x 30 larvae) and symbiont density (1 x 5 larvae). On August 3 only, larvae were preserved for analyses of catalase activity (2 x 55 larvae). On August 2 and 4, larvae were preserved for

analyses of ouabain-sensitive Na^+/K^+-ATPase activity (2 x 30 larvae), K^+-dependent pNPPase activity (2 x 25 larvae), and symbiont density (1 x 5 larvae).

Total antioxidant potential

A measure of the larvae's ROS-reducing power, total antioxidant potential was assessed using a ferric reducing/antioxidant potential (FRAP) assay. The antioxidants in the sample reduce a ferric-tripyridyltrizine (Fe^{III}-TPTZ) complex, forming colored ferrous-tripyridyltrizine (Fe^{II}-TPTZ) (Benzie and Strain, 1996, 1999; Prior and Cao, 1999). Thus, the antioxidant level can be easily measured using a spectrophotometer. The working reagent for the FRAP analysis (following Griffin and Bhagooli, 2004) contained 300 mM acetate buffer (pH 3.6), 10 mM 2,4,6-tripyridyl-s-triazine (TPTZ) and 20 mM $FeCl_3 \cdot 6H_2O$ in a 10:1:1 ratio and was prepared and heated to 37°C right before use. A microplate spectrophotometer was used to measure absorbance at 600 nm of 150 µL of working reagent per well of a 96-well microtiter plate, which served as the background standard. Batches of 30 larvae were homogenized in 400 µL Tris-HCl buffer (pH 7.5). The homogenates were centrifuged at 10,000 rpm for 10 minutes at 4°C to remove cellular debris, and the pellet was discarded. A portion of each homogenate was saved for quantification of total protein content, and a protease inhibitor was then added to each homogenate (Sigma-Aldrich #P8340). A dilution series of Fe^{II} ($FeSO_4 \cdot 7H_2O$) was prepared (25-1000 µM). For each standard dilution and sample homogenate, 20 µL was added to three wells in the plate, already containing the working reagent for the FRAP analysis. The plate was then incubated at 37°C for 6-8 minutes before the absorbance was measured again at 600 nm. Changes in absorbance (absorbance after 8 minutes minus the initial reading) were compared to that of the standard

run simultaneously to calculate the FRAP value for each experimental sample. FRAP values were normalized per larva and by the total protein of the homogenate.

Catalase activity

Activity of the enzyme catalase was measured following Ross *et al.* (2010). Batches of 55 frozen larvae were homogenized in 150 µL 50 mM potassium phosphate buffer (pH 7.0) containing Triton X-100 using hand-held glass homogenizers on ice. A stock solution of 0.36% H_2O_2 was prepared using 10 mM potassium phosphate buffer (pH 7.0). Two thousand µL H_2O_2 solution and 100 µL coral protein extract were combined in a 3 mL cuvette and incubated at room temperature for 30 seconds. The absorbance of the solution was then read at 240 nm using a UV/VIS spectrophotometer. Aliquots of the homogenate in buffer were saved for quantifying total protein. Catalase activity was reported as specific activity (unit/mg total protein) where one unit would decompose 1.0 µmol H_2O_2 per minute at pH 7.0 at 25°C.

Catalase activity was also measured using the Amplex® Red Catalase assay kit (Molecular Probes #A22180). Larvae were homogenized in 100 µM phosphate buffer with 10% PVP-40 and 1% Triton X-100. After a brief centrifugation to pellet cellular debris, the diluted homogenates were pipetted into triplicate wells of a 96-well plate. Simultaneously, a dilution series of a catalase enzyme standard was prepared (0-5000 mU/mL) and pipetted into the plate. 40 µM H_2O_2 was added to each well and the plate was incubated for 30 min at room temperature in the dark. 100 µM Amplex® Red reagent containing 0.4 U/mL HRP was added to each well and the fluorescence of the reactions were measured in a microplate reader using an excitation wavelength of 544 nm and an emission wavelength of 590 nm.

The plate was read every 10 minutes for 1 hour at 37°C. Aliquots of the homogenate in buffer were saved for quantifying total protein. Catalase activity was reported as specific activity (unit/mg total protein) where one unit would decompose 1.0 μmol H_2O_2 per minute at pH 7.0 at 25°C.

Na^+/K^+-ATPase activity

Total Na^+/K^+-ATPase activity was measured as the ouabain-sensitive rate of release of inorganic phosphate in the presence of ATP (Esmann, 1988). Ouabain is a cardioactive steroid that binds directly to the enzyme in a 1:1 ratio and directly inhibits enzyme activity (*e.g.* Robinson and Flashner, 1979). Batches of 30 larvae were homogenized via sonication 300 mM sucrose, 1 mM EDTA, 30 mM Tris, pH 7.4 (Tang et al., 2010). An aliquot of each homogenate was preserved for quantification of total protein. To uncover any vesicle-concealed or latent activity of Na^+/K^+-ATPase, alamethicin was then added to each homogenate (15 μg alamethicin mg total $protein^{-1}$) and the solutions were incubated at 28°C (physiological temperature) for 20 minutes (Leong and Manahan, 1997). In two tubes, the homogenate was combined with a reaction mixture containing a final concentration of 100 mM imidazole, 125 mM NaCl, 75 mM KCl, 7.5 mM $MgCl_2$, 1 mM ATP, pH 7.6. To one tube, ouabain was added to a final concentration of 1 mM; to the other, water was added. Ouabain is an inhibitor of Na^+/K^+-ATPase activity, so total activity was defined as the difference between the amount of inorganic phosphates liberated in the absence and presence of ouabain in the reaction mixture. The reactions were incubated at 28°C (physiological temperature) for 30 minutes and then the reactions were stopped by placing the samples at -20°C for 10 minutes. To visualize the amount of inorganic phosphate generated, a color

reagent (7.6 g/L ammonium molybdate, 0.09M sulphuric acid, 1% Tween-20) was added to all reactions. After 3 minutes on ice, the absorbance of the reactions was measured at 405 nm in a 96-well plate on a plate reader. To convert absorbance to moles of inorganic phosphate, a dilution series of NaH_2PO_4 was run simultaneously (0-600 μM inorganic phosphate).

The K^+-dependent *p*-nitrophenyl phosphatase (pNPPase) activity of Na^+/K^+-ATPase was measured as the K^+-dependent hydrolysis of phosphoric anhydrides (*e.g.* pNPP) by Na^+/K^+-ATPase in the absence of Na^+ (Esmann, 1988). pNPPase activity was measured spectrophotometrically according to Esmann (1988) as modified by preliminary tests to determine optimal reaction conditions specific to *P. damicornis* larvae. First, the amount of homogenate added to the reaction was optimized by performing the assay with a range of total protein concentrations (0.015-0.29 mg protein in the reaction). While enzyme activity was detected for all protein concentrations, ~0.2 mg protein reaction^{-1} was used for all following assays. Next, I determined whether enzyme activity was affected by alamethicin (0-500 μg mg total protein^{-1}) and sodium deoxycholate (0-4 mg mg total protein^{-1}), chemicals that permeabilize membranes uncover any concealed or latent activity (Leong and Manahan, 1997). pNPPase activity was inhibited by sodium deoxycholate, but it was greatest under 50 μg mg total protein^{-1}. Next, I performed the assay under a range of buffer pH values (6.5, 7.0, 7.8, 8, 8.6, 9) and found that catalysis of pNPPase was optimized at pH 6.5. However, because this is likely not a common intracellular pH for coral cells (Kuhl et al., 1995; Venn et al., 2009), I used pH 7.0 for all subsequent assays. Finally, incubation time was optimized to ensure a linear reaction rate of pNPPase; I tested 5, 10, 15, 20, 25, 30, 40, 50, and 60 minutes and found that reaction rates were linear from 15 to 40 minutes. As a conservative approach, I selected 25 minutes for the assay incubation time.

Upon conclusion of the preliminary tests, experimental samples were analyzed as follows. Batches of 25 larvae were homogenized on ice via sonication in 150 mM histidine, pH 7.0, with a protein concentration of 0.5 mg mL^{-1}. An aliquot of each homogenate was preserved for quantification of total protein. The homogenate was combined with alamethicin (50 μg mg total $protein^{-1}$) and was incubated at 28°C (physiological temperature) for 20 minutes. Then, the homogenate was added to a reaction mixture containing a final concentration of 30 mM histidine (pH 8.0), 150 mM KCl, 20 mM $MgCl_2$, 2.5 mM EGTA, 10 mM pNPP. A duplicate reaction for each homogenate was prepared with the same reagent concentrations except with 150 mM NaCl substituted for the 150 mM KCl. As Na^+ inhibits the pNPPase activity (Esmann, 1988), K^+-dependent phosphatase activity of Na^+/K^+-ATPase was defined as the difference between the amount of *p*-nitrophenol produced in the absence and presence of Na^+ in the reaction mixture. The reactions proceeded at 28°C (physiological temperature) for 25 minutes before they were terminated by an addition of ice-cold 55% trichloroacetic acid and a 10-minute incubation on ice. Following a centrifugation, reaction supernatants were brought to room temperature and then combined with 500 mM Tris base. At the high pH caused by the presence of Tris base, *p*-nitrophenol, the product of the pNPPase reaction, is a yellow color; the intensity of color, and therefore, the enzyme activity, was measured via absorbance of the reactions at 410 nm. For technical replication, the reaction was performed twice per sample. Absorbance was used to calculate specific enzyme activity using the following equation:

$$\upsilon = \frac{r_A}{l \times \varepsilon_B \times \upsilon_B} \times \frac{V_{reaction}}{V_{sample} \times \rho}$$

where:

υ Specific activity of the enzyme is expressed as units per mg protein. One unit is one μmol *p*-nitrophenol produced per minute.

r_A Rate of absorbance change [min^{-1}].

= ($A_{410, KCl} - A_{410, NaCl}$) divided by incubation time in min

l Optical path length

= 1 cm

ε_B Extinction coefficient of B (*p*-nitrophenol) at 410 nm and 28°C

= 18.1 mM^{-1} cm^{-1} (Skou and Esmann, 1979)

υ_B Stoichiometric number of B (*p*-nitrophenol) in the reaction

= 1

$V_{reaction}$ Volume of the reaction

= 3100 μL

V_{sample} Volume of sample homogenate added to the reaction

= ~120 μL

ρ Mass concentrate of density of biological material in the sample, V_{sample}

= protein concentration of sample homogenate in mg total protein μL^{-1}

Quantification of total protein

Total protein of assay homogenates was assessed using the Bradford assay (Bradford, 1976). Larvae were homogenized in ice-cold water using sonication. Total protein was precipitated using trichloroacetic acid, re-dissolved using 1 M NaOH, neutralized using 1.68 M HCl before addition of Bradford dye concentrate (Bio-Rad Laboratories Inc., Hercules, CA, USA). Absorbance of samples at 595 nm was measured in a plate reader following an incubation of 20 minutes at room temperature. Total protein was calculated using a standard curve of known concentrations of bovine serum albumin (Bio-Rad Laboratories Inc., Hercules, CA, USA). Total protein values were used to normalize all enzyme assay data.

Assessment of symbiont density

To determine density of *Symbiodinium* cells in coral larvae, a batch of 5 larvae from each aquarium was homogenized in de-ionized water using a pestle. *Symbiodinium* cells in six 10 μL aliquots of homogenate were counted using a haemocytometer and a compound light microscope. Coefficients of variation between replicate counts were less than 10%, suggesting that any differences in symbiont density greater than 10% are not expected to be from chance alone or from variability in the analysis.

Statistical analyses

All data were analyzed using R version 3.0.1 (R Core Team 2013). In all cases,

statistical assumptions of normality and homogeneity of variance were tested using quantile-quantile (Q-Q) plots and Levene's test and were met, sometimes following a power-based transformation of the response variable. Effects on physical conditions and biological response variables were estimated using linear mixed-effect models (nlme package in R; Pinheiro and Bates, 2000). To compare physical conditions between treatments, pCO_2 and temperature treatments were fixed factors. Total antioxidant potential and pNPPase activity of Na^+/K^+-ATPase were standardized by larvae, by total protein, and by symbiont density. To compare normalized total antioxidant potential, pNPPase activity, total protein, and symbiont density between treatments, pCO_2 ("pCO_2"), temperature ("T"), and day of release ("Day") were fixed factors. For all of these comparisons, to account for random variation among all possible aquaria, "tank" was considered a random factor in all statistical analyses. Model selection was performed incrementally following Burnham and Anderson (2002): at each iteration, the simpler model was chosen if the model AIC value did not increase by 2 or more and if there was not a significant difference in the model log likelihood ratio. To determine which factors in models were significant, a type III sum of squares was conducted on selected models fit using maximum likelihood (Zuur et al., 2009; Crawley, 2013). When significant differences were detected among treatments, orthogonal contrasts were performed as post-hoc analyses using the multcomp package in R (Hothorn et al., 2008). Tukey's HSD was used for models without significant interactions between terms. When significant interactions were present, post-hoc analyses were performed using general linear hypothesis tests with Bonferroni corrections for multiple comparisons (abbreviated GLHT).

Results

To assess aspects of physiological plasticity of *Pocillopora damicornis* planulae associated with homeostatic maintenance of oxidative state and intracellular pH, I performed laboratory microcosm experiments where larvae were exposed to levels of pCO_2 and temperature, I was able to maintain fairly stable conditions with physical conditions in each treatment group remaining within expected ranges (Table 7). For example, temperature varied significantly between, but not within, temperature treatments (Ambient-T vs. High-T; type III sum of squares, $X^2 = 2370.5$, $p < 0.001$). Salinity did not vary significantly by temperature, pCO_2 or their interaction (type III sum of squares). A_T varied significantly by temperature (type III sum of squares; $X^2 = 8.936$, $p = 0.003$), with higher A_T at High-T than at Ambient-T (Tukey's HSD; $z = 2.875$, $p = 0.004$). pH and pCO_2 varied significantly between, but not within, pCO_2 treatments (Ambient-pCO_2 vs. High-pCO_2; type III sum of squares, pH: $X^2 = 1352.2$, $p < 0.001$; pCO_2: $X^2 = 1997.5$, $p < 0.001$).

Total antioxidant potential (FRAP) was quantified to assess the net response of the planula holobiont to potential oxidative stress imposed by high pCO_2 and high temperature. FRAP varied between 8.98 μM $larva^{-1}$ (Peak ATAC) to 19.73 μM $larva^{-1}$ (Late HTHC). Larval FRAP was significantly affected by pCO_2, but not by T, Day or any interactive effects (Table 8). Planulae had higher total antioxidant potential at High-pCO_2 than at Ambient-pCO_2 (Fig. 8; Tukey's HSD; $z = 0.494$, $p = 0.005$). When FRAP was normalized to total protein, only the effect of Day was significant (Table 8). Total antioxidant potential was greater for Peak larvae than for Late larvae (Fig. 8; Tukey's HSD; $z = 1.925$, $p = 0.054$). When FRAP was normalized to symbiont density within the planulae, significant effects included pCO_2xTxDay, pCO_2xDay, and Day (Table 8). However, post-hoc analyses

Table 7. Summary of physical conditions in aquaria for experiments conducted on August 3-5, 2011. Data are presented as mean ± SE. For all parameters, $n = 10$.

Treatment	Temperature (°C)	Salinity (psu)	pH	A_T (µmol kg^{-1})	pCO_2 (µatm)
ATAC	27.60 ± 0.04	33.09 ± 0.05	7.985 ± 0.002	2179 ± 7	451 ± 4
HTAC	30.65 ± 0.05	33.07 ± 0.11	7.990 ± 0.006	2186 ± 7	445 ± 8
ATHC	27.61 ± 0.03	33.13 ± 0.06	7.739 ± 0.004	2193 ± 3	877 ± 8
HTHC	30.50 ± 0.03	32.98 ± 0.08	7.752 ± 0.005	2205 ± 6	859 ± 10

Table 8. Analysis of total antioxidant potential (FRAP) for *P. damicornis* larvae among treatments, standardized to number of larvae (µM larva^{-1}), total protein content (µM µg protein^{-1}), and symbiont density (µM 10^3 *Symbiodinium* cells^{-1}). Comparisons were made using a type III sum of squares with pCO_2, temperature (T) and day of release (Day) as fixed effects. Interaction terms that were removed from the model are not shown here.

Dependent variable	Effect	X^2	Degrees of Freedom	*p*
Larval-specific FRAP	pCO_2	8.824	1	**0.003**
	T	0.646	1	0.421
	Day	2.064	1	0.151
Protein-specific FRAP	pCO_2	0.002	1	0.967
	T	0.003	1	0.955
	Day	3.981	1	**0.046**
Symbiont-specific FRAP	pCO_2	0.139	1	0.071
	T	0.145	1	0.704
	Day	43.464	1	**<0.001**
	pCO_2xT	0.711	1	0.399
	pCO_2xDay	7.826	1	**0.005**
	TxDay	0.617	1	0.432
	pCO_2xTxDay	8.736	1	**0.003**
Total protein (µg larva^{-1})	pCO_2	6.389	1	**0.012**
	T	0.450	1	0.502
	Day	8.421	1	**0.004**
Symbiont density (x10^3 cells larva^{-1})	pCO_2	<0.001	1	0.994
	T	0.042	1	0.838
	Day	37.108	1	**<0.001**

Figure 8. Total antioxidant potential of *P. damicornis* larvae following 6-hour exposures to combinations of pCO_2 and temperature. Mean ± SE (n = 6) ferric reducing/antioxidant potential (FRAP), total holobiont protein levels and symbiont density for larvae released on days Peak and Late. FRAP values are normalized per larva, per protein, and per symbiont density. Experimental treatments: Ambient-T, Ambient-pCO_2 (ATAC), High-T, Ambient-pCO_2 (HTAC), Ambient-T, High-pCO_2 (ATHC), High-T, High-pCO_2 (HTHC).

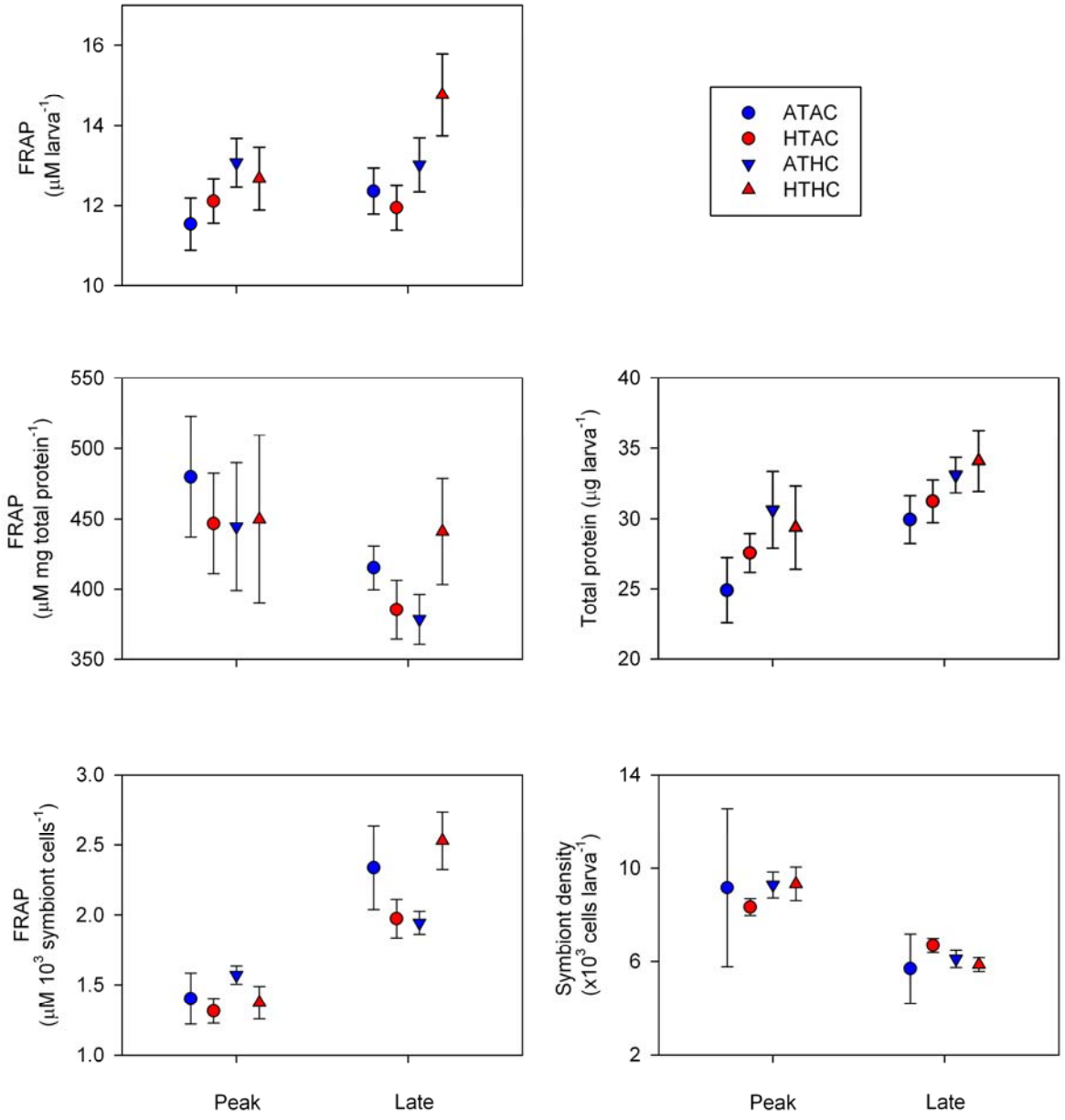

using linear contrasts with Bonferroni corrections showed insignificant differences between groups. As a general trend, planulae on day Peak had lower FRAP values and had similar responses between treatments; planulae on day Late had higher FRAP values in general and at ATAC and HTHC. Total holobiont protein varied significantly by pCO_2 and Day (Table 8). Planulae contained more total protein at High-pCO_2 than at Ambient-pCO_2 (Fig. 8; Tukey's HSD; $z = 2.033$, $p = 0.042$). Late larvae contained more total protein than Peak larvae (Fig. 8; Tukey's HSD; $z = -2.841$, $p = 0.005$). Finally, symbiont density varied significantly by Day but not by pCO_2 or T (Table 8). Peak larvae had significantly greater symbiont density than Late larvae (Fig. 8; Tukey's HSD; $z = 5.698$, $p < 0.001$).

Catalase, one component of a cell's antioxidant defenses, neutralizes H_2O_2. The first assay performed using 0.036% H_2O_2 in potassium phosphate buffer did not yield a decrease in absorbance at 240 nm as expected, if H_2O_2 was being consumed by the enzyme in the reaction. I tried increasing the concentration of total protein in the reaction, thereby increasing the potential abundance of catalase enzyme. I tried increasing the reaction time in case the decrease in absorbance was progressing very slowly. I tried the assay with brand new H_2O_2, which can degrade easily once opened. None of these adjustments yielded a detectable signal of catalase activity. It is also possible that catalase is vulnerable to heat during sonication, so I could try homogenizing with a pestle in a dry ice/ethanol bath in the future. Based on my communication with Dr. Cliff Ross who published a study using this assay with coral tissue, I decided to try a Molecular Probes kit to enhance my signal to noise ratio. Unlike the H_2O_2-based assay, the kit came with purified catalase enzyme so a standard curve and positive control were performed with each run of the assay. The standard curves worked well. I performed the assay with a range of total protein and the results were unusual.

I expected absorbance to decrease as the concentration of catalase (based on total protein) increased but I measured the opposite trend. I tried detecting the signal of the assay using absorbance and fluorescence, but I got the same result. What I noticed was that reactions with high concentrations of total protein were more opaque in color, likely due to the abundance of lipids in the tissue homogenate. I tried a variety of centrifugations to remove particulates, detergents to enhance the signal, and dilutions of the homogenate to reduce opacity, but I could not increase my signal to noise ratio. Also, there could be photosynthetic pigments in the homogenate that are absorbing or fluorescing at the detection wavelength(s), thus obscuring the signal of the enzyme activity. However, since others have succeeded in using this kit to quantify catalase activity in symbiotic coral tissue, I suspect that the pigments may not be the source of the problem. I was unable to successfully measure catalase activity in the experimental samples of *P. damicornis* larvae.

The ouabain-sensitive rate of Na^+/K^+-ATPase was quantified to estimate the total activity of this enzyme. First, I used an assay technique modified from (Esmann, 1988; Leong and Manahan, 1997). I was able to detect ATPase activity but no ouabain-sensitive activity. I tried increasing the amount of homogenate added to the reaction as well as the concentration of ouabain in the reaction, but neither attempt yielded ouabain-sensitive enzyme activity. At NMMBA in Taiwan, I then formed a collaboration with Dr. Wario Tang, who has developed an assay to measure ouabain-sensitive Na^+/K^+-ATPase activity in fish. He ran his assay with some of my coral larvae and succeeded in detecting an ouabain-sensitive activity. However, when I performed the assay based on his written protocol, I was not successful. It is possible that his written protocol does not exactly reflect how he performed the assay with my samples. His protocol was also missing some details such as what

homogenization buffer should be used. Preliminary tests that I conducted showed that the absorbance values of the assay depend on the homogenization buffer used. Also, I determined that the standard curve should be prepared in the homogenization buffer to ensure comparable absorbance values between the standards and the experimental samples. Again, in this assay, I had problems with the opacity of the samples. It looked like a precipitate formed in the wells of the 96-well plate where the reaction took place, which likely elevated the absorbance readings. A series of centrifugation steps or a different chemical detection system may improve the signal to noise ratio. In the end, I was unable to successfully measure ouabain-sensitive Na^+/K^+-ATPase activity in my experimental samples of *P. damicornis* larvae.

K^+-dependent *p*-nitrophenyl phosphatase (pNPPase) activity was quantified, as it represents a partial reaction of Na^+/K^+-ATPase (Glynn and Karlish, 1975; Schwartz et al., 1975; Robinson and Flashner, 1979). pNPPase activity varied between 56.7 (Early ATAC) and 115.5 pmol pNPPase min^{-1} $larva^{-1}$ (Middle HTHC). When normalized per larva and per total protein, pNPPase activity varied significantly by Day but not by pCO_2 or T (Table 9). In both cases, Middle larvae had significantly more pNPP than Early larvae (Fig. 9; Tukey's HSD; per larva: $z = 2.224$, $p = 0.026$; per protein: $z = 2.364$, $p = 0.018$). When pNPPase activity was expressed with respect to *Symbiodinium* density, pCO_2xTxDay was significant (Table 9). However, post-hoc analyses did not reveal any significant differences (GLHT). Total holobiont protein was only significantly affected by pCO_2 (Table 9) but post-hoc analyses did not confirm this difference. Finally, symbiont density did not vary significantly any effect or interaction (Table 9).

Table 9. Analysis of K^+-dependent *p*-nitrophenyl phosphatase (pNPPase) activity of Na^+/K^+-ATPase for *P. damicornis* larvae among treatments, standardized to number of larvae (units $larva^{-1}$), total protein content (units mg $protein^{-1}$), and symbiont density (units 10^3 *Symbiodinium* $cells^{-1}$). Comparisons were made using type III sum of squares with pCO_2, temperature (T), and day of release (Day) as fixed effects. Interaction terms that were removed from the model are not shown here.

Dependent variable	Effect	X^2	Degrees of Freedom	*p*
Larval-specific pNPPase activity	pCO_2	0.857	1	0.355
	T	0.295	1	0.587
	Day	5.162	1	**0.023**
Protein-specific pNPPase activity	pCO_2	0.733	1	0.392
	T	0.357	1	0.550
	Day	5.574	1	**0.018**
Symbiont-specific pNPPase activity	pCO_2	0.026	1	0.872
	T	0.678	1	0.410
	Day	0.506	1	0.477
	pCO_2xT	1.707	1	0.191
	pCO_2xDay	9.964	1	**0.002**
	TxDay	1.256	1	0.262
	pCO_2xTxDay	10.797	1	**0.001**
Total protein ($\mu g\ larva^{-1}$)	pCO_2	3.803	1	**0.051**
	T	2.159	1	0.142
	Day	0.898	1	0.343
Symbiont density ($x10^3$ cells $larva^{-1}$)	pCO_2	0.788	1	0.375
	T	1.385	1	0.239
	Day	<0.001	1	0.995
	pCO_2xT	3.562	1	**0.059**
	pCO_2xDay	2.203	1	0.138
	TxDay	0.186	1	0.667
	pCO_2xTxDay	2.254	1	0.112

Figure 9. pNPPase activity in *P. damicornis* larvae following 6-hour exposures to combinations of pCO_2 and temperature. Mean ± SE (n = 4) pNPPase activity, total holobiont protein levels, and symbiont density for larvae released on days Early and Middle. Enzyme activities are normalized per larva, per protein, and per symbiont density. Experimental treatments: Ambient-T, Ambient-pCO_2 (ATAC), High-T, Ambient-pCO_2 (HTAC), Ambient-T, High-pCO_2 (ATHC), High-T, High-pCO_2 (HTHC).

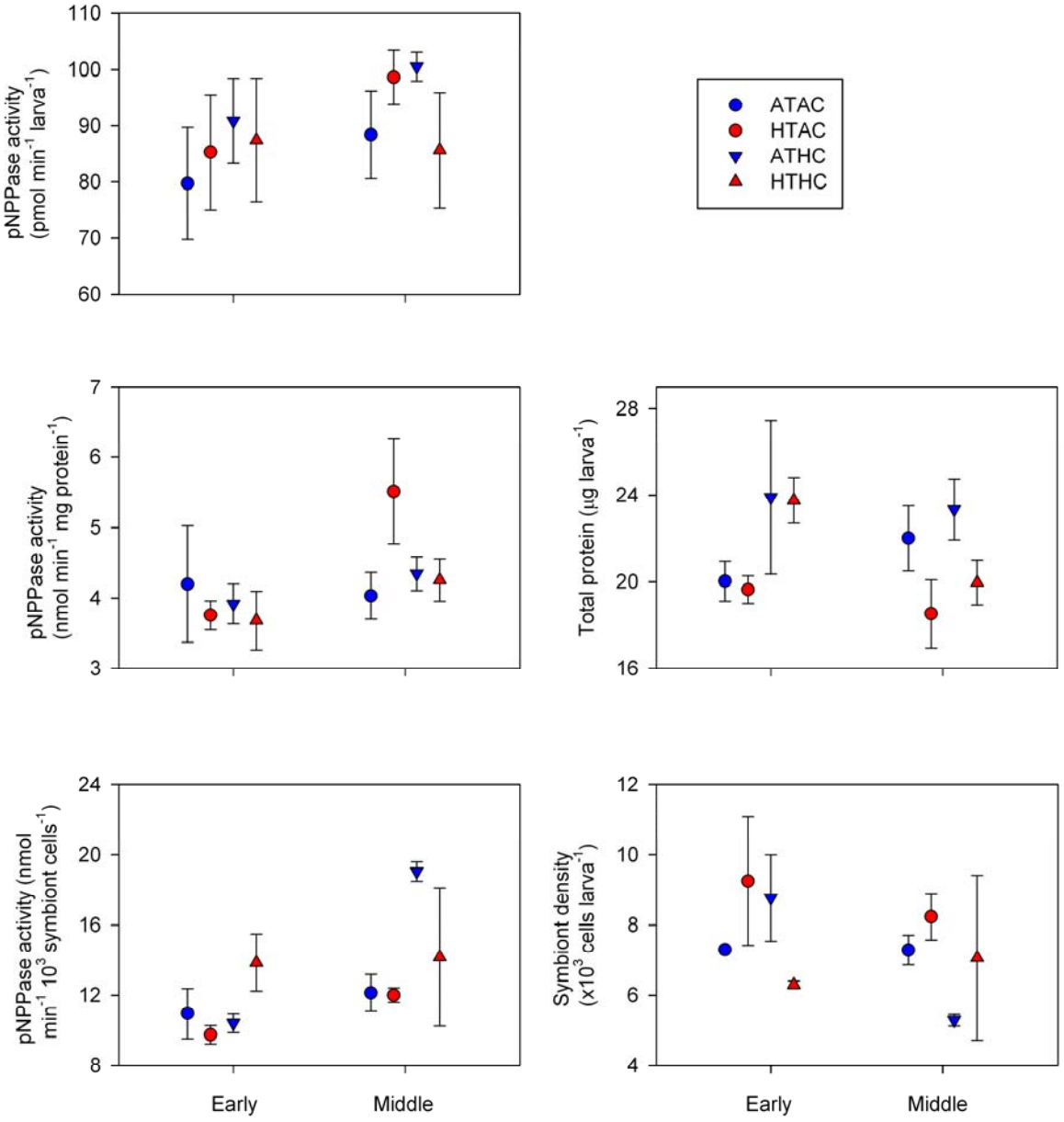

Discussion

To assess aspects of physiological plasticity of *Pocillopora damicornis* planulae associated with homeostatic maintenance of oxidative state and intracellular pH, I performed laboratory microcosm experiments where larvae were exposed to levels of pCO_2 and temperature before being analyzed for two biochemical indicators. To measure performance under conditions of OA and warming, I used (1) total antioxidant potential as a proxy for oxidative stress (FRAP), and (2) Na^+/K^+-ATPase activity as a proxy for acid-base regulation. My results indicated that future ocean conditions, particularly OA, could cause oxidative stress in *P. damicornis* larvae. The data also suggested that any hypercapnia was not compensated by a significant increase in activity of Na^+/K^+-ATPase.

Oxidative stress

Within 6 hours of release and exposure to elevated pCO_2, *P. damicornis* larvae ramped up their total antioxidant potential in response to increases in oxidative stress from high pCO_2. While I was unable to quantify changes in particular components of larval stress response to oxidative stress, the increase in total antioxidant potential likely comprised both enzyme and non-enzyme antioxidants. A concurrent increase in total protein at High-pCO_2 suggests that larvae may have produced more antioxidant enzymes, such as catalase or glutathione reductase, as part of their cellular stress response. From work done in mammalian cells, signal transduction, transcription, and translation can be completed within a few hours of exposures to a signal (Hargrove et al., 1991). Indeed, an increase in antioxidant enzyme activity following ≤ 6-hour heat stress has been observed in other coral species (Yakovleva et al., 2004; Olsen et al., 2013).

Corals, like many marine invertebrates without a buffered internal fluid (*i.e.* blood, haemolymph), have relatively poor abilities to regulate pH in intracellular spaces. Corals can elevate extracellular pH at the site of calcification across a range of seawater pH levels, but intracellular pH levels are not simultaneously elevated (Venn et al., 2011; McCulloch et al., 2012). As a result, ocean acidification may cause hypercapnia within coral tissue, resulting in oxidative stress. There are several proposed mechanisms by which OA can trigger an increase in production of ROS, leading to oxidative stress. First, mitochondria are the primary producers of ROS in animal cells, and malfunction of these organelles can lead to ROS production (reviewed by Murphy, 2009). The electron transport chain pumps protons across the inner membrane of the mitochondria, driven by energy released during the transfer of electrons to oxygen molecules. During this electron transport, electron leaks at complexes I and III can lead to single-electron reduction of oxygen, forming superoxide $O_2{\cdot}^-$. Superoxide production is very sensitive to the pH gradient across the inner membrane of mitochondria (Lambert and Brand, 2004), which could be disturbed during OA-induced hypercapnia. Secondly, an increase in intracellular pCO_2 can also increase the production of carbonate radicals, as CO_2 readily reacts with peroxynitrite ($ONOO^-$; Dean, 2010). Third, decreased intracellular pH favors several ROS-producing redox reactions, including the forward reaction of the Fenton reaction, where ferrous iron is oxidized by H_2O_2, generating the more potent ROS, ·OH (reviewed by Dean, 2010). Evidence of oxidative stress as a result of high pCO_2 was presented by Tomanek *et al.* (2011), who explored the effects of ocean acidification on the proteome of the eastern oyster *Crassostrea gigas*. They found that oysters, which live in estuaries with seasonal and diurnal increases in ambient pCO_2, experience oxidative stress in response to exposure to high-pCO_2, up-regulating proteins

associated with antioxidant defense. Oxidative stress in corals can occur not only via these mitochondria-based responses to OA, but also due to ROS production by *Symbiodinium* endosymbionts. Heat and light cause damage to the photosynthetic machinery, causing the production of ROS (Weis, 2008). Since electron transport plays an important role in photosynthesis, this is additional evidence that electron transport will likely contribute to ROS production during intracellular acidosis. Kaniewska *et al.* (2012) found that high-pCO_2 caused changes in gene expression of the coral, *Acropora millepora*, that suggested responses of oxidative stress and metabolic suppression.

Surprisingly, total antioxidant potential did not increase with exposure temperature. Other studies with corals have shown increased oxidative stress in response to warming (Lesser, 1997; Downs et al., 2002; Yakovleva et al., 2004; Ross et al., 2012; Olsen et al., 2013). Interestingly, a previous study with *P. damicornis* found that antioxidant potential increased with temperature but then decreased after a threshold temperature was reached. 30.5°C, the elevated temperature used in this study, may not have been high enough to cause significant production of ROS within coral larvae. Or, the larvae may have been able to use their constituent pool of antioxidants to neutralize ROS produced during the experimental exposure. Alternatively, it is possible that 30.5°C was above the threshold for the study population of *P. damicornis* and an antioxidant defense was no longer possible (Griffin and Bhagooli, 2004).

Interpreting larval-specific total antioxidant potential is useful for comparing to results of other studies that present physiological responses at the level of the whole organism. However, total antioxidant potential likely scales with larval size, as larger larvae with more mitochondria are likely to produce more ROS. When differences in size of larvae

between treatments were controlled for by normalizing FRAP with total protein content, the significant effect of pCO_2 on total antioxidant potential disappeared. This was expected since FRAP and total protein were correlated with respect to pCO_2. However, total antioxidant potential varied significantly based on which day the larvae were released, with greater antioxidant potential in Peak larvae than in Late larvae. If Peak larvae contained these elevated FRAP levels upon release, their innate high antioxidant potential may have been sufficient to accommodate any stress due to ROS during the exposures, as levels of total antioxidant potential were equivalent across treatments (Fig. 8). The lower levels of FRAP in Late larvae may not have been enough to neutralize ROS at HTHC, necessitating an increase in antioxidant production under this condition (Fig. 8).

In addition to abiotic inducers of oxidative stress such as OA, corals also have an endogenous source in the form of the metabolic activity of their endosymbionts. This process has been studied extensively, and it has been demonstrated that *Symbiodinium* can contribute to oxidative stress experienced within coral animal cells (Dykens and Shick, 1982; Dykens et al., 1992; Lesser, 1996, 1997; Nii and Muscatine, 1997; Downs et al., 2000, 2002). Therefore, symbiont density within the *P. damicornis* larvae in my experiments may have affected the total ROS produced during the laboratory exposures.

Mechanistically, exposure to elevated temperature and intense light cause *Symbiodinium* to produce more ROS, accompanied by reduced photosynthetic efficiency (Lesser, 1996; Weis, 2008). ROS can overwhelm antioxidant defense systems within the symbiont cells and diffuse into host cells (Tchernov et al., 2004; Lesser, 2006), where they can damage host DNA, protein, and lipids (Lesser and Farrell, 2004; Richier et al., 2006). In this study, Peak larvae may have been more vulnerable to oxidative stress during the

experimental exposures because they contained more symbionts than the Late larvae. However, FRAP per larva did not differ between cohorts, suggesting that even with their higher symbiont density, Peak larvae did not elevate their antioxidant potential overall. In fact, when normalized by symbiont density, FRAP activity per symbiont cell was lower in Peak larvae than in Late larvae. For Late larvae, across equivalent symbiont densities, total antioxidant potential, and therefore oxidative stress, was greatest under multi-stressor versus single stress scenarios. This unique response to experimental exposures in Late larvae confirms the results of Chapter 2, that Late larvae are particularly vulnerable to OA and warming.

Acid-base physiology

Regardless of normalization procedure, the K^+-dependent pNPPase activity of Na^+/K^+-ATPase did not differ significantly as a function of pCO_2 or temperature exposure. It is possible that the existing pool of Na^+/K^+-ATPase was sufficient for accommodating any increased maintenance of intracellular homeostasis. Conversely, the exposure time may not have been long enough to detect an increase in synthesis of this enzyme in response to High-T, High-pCO_2 conditions. For *Acropora millepora*, 28 days of exposure to high-pCO_2 conditions caused changes in abundance of membrane transporters, including an up-regulation of Na+/K+ transporters (Kaniewska et al., 2012). Passive ion gradient transporters were up-regulated while ATP-dependent active ion transporters were down-regulated. This may be the case in our study, where the pNPPase activity of Na^+/K^+-ATPase activity, an ATP-consuming enzyme, did not increase in response to high pCO_2. In order to save energy,

especially if metabolic suppression also occurs under these OA conditions, passive ion transporters may be up-regulated in an effort to maintain pH homeostasis.

The acid-base balance of corals is likely to be particularly sensitive to OA because corals cannot buffer the seawater surrounding their tissue. In contrast, fish are able to counteract OA-induced hypercapnia through extracellular bicarbonate accumulation in extracellular compartments, like blood or haemolymph (Pörtner, 2008). Without these extracellular compartments and respiratory pigments, corals rely on favorable diffusion gradients for gas exchange. As a result, as pCO_2 increases in the surrounding water, it will readily diffuse into the coral ectoderm, resulting in a lower intracellular pH. For example, in isolated host cells from *P. damicornis*, intracellular pH declined only 15 minutes after exposure to high extracellular pCO_2 (Gibbin et al., 2014). Other marine invertebrates with similar vulnerabilities in regulation of acid-base balance are not able to compensate the extracellular acidosis and metabolic suppression ensues (Pörtner et al., 1998; Michaelidis et al., 2005). Conversely, teleost fish can almost immediately compensate extracellular acidosis with no effect of their metabolic rate (Pörtner, 2008).

Symbiodinium may play an important role in ionic balance within host coral cells. After acidosis of the cytoplasm following exposure to high extracellular pCO_2, symbiotic host cells of *P. damicornis* were able to achieve full recovery of cytoplasm pH, likely due to the work of membrane ion transporters (Gibbin et al., 2014). However, this recovery was dependent on the photosynthetic activity of the symbionts. Non-symbiotic or photosynthetically-compromised coral cells were not able to recover intracellular pH following acidosis (Gibbin et al., 2014). In this study, symbiont density did not differ significantly between larvae exposed to experimental treatments or between larvae released

on different days. This pattern was likely due to large variability in symbiont density in certain treatments. The pattern of pNPPase activity per symbiont density in Figure 9 resembles a mirror image of the pattern of symbiont density, suggesting that symbiont density affected the larval rates of pNPPase activity. Therefore, as a general trend, with respect to their ability to recover cytoplasm pH via their symbionts, ***P. damicornis*** larvae exhibited elevated rates of pNPPase activity at High-pCO_2, High-T conditions. Increased regulation of acid-base balance may be amplified when both stressors are combined, as High-T causes a collapse of the host-*Symbiodinium* symbiosis and therefore larvae will rely more on host cell machinery to recover intracellular pH (Gibbin et al., 2014). Therefore, OA could increase maintenance costs for acid-base homeostasis in ***P. damicornis*** larvae through the up-regulation of Na^+/K^+-ATPase.

Variation in physiological response between larval cohorts

This study supports the findings of Chapter 2 that innate physiology may differ between cohorts of larvae that are released at different times and, further, that these differences can mediate sensitivity to environmental change. As observed for rates of oxygen consumption in Chapter 2, FRAP and K^+-dependent pNPPase activity of Na^+/K^+-ATPase both varied significantly by day of release of larvae. The differential responses of total antioxidant potential to conditions of OA and warming may have been mediated by innate differences between cohorts (see Chapter 4, but also Edmunds et al., 2001; Isomura and Nishihira, 2001; Putnam et al., 2010; Cumbo et al., 2012). The variation in larval traits described by these studies may be due to different developmental conditions based on the location of the larvae within the vertical depth of the polyp (Kuhl et al., 1995; Jimenez et al.,

2008) or spatially throughout the colony in relation to gradients of light, flow, nutrients, and dissolved gases. Also, time in captivity may play a role, as the adult corals were held continuously in husbandry aquaria during the larval release. Natural variation in traits that affect physiological performance may be a bet-hedging strategy, where corals produce offspring with a range of phenotypes that are each suited to different environmental conditions. This strategy may allow corals to maximize the success of a portion of their offspring upon release. This study may allow us to predict if the existing variation in larval phenotypes contain traits advantageous for tolerating future ocean conditions.

Conclusion

In this study, I found that *P. damicornis* larvae increased their total antioxidant potential in response to oxidative stress under exposures to high pCO_2, but not elevated temperature. In addition, OA-induced hypercapnia resulted in an increase in activity of Na^+/K^+-ATPase, but only for rates normalized to symbiont density. The innate antioxidant and ion balance physiology of these larvae varied based on the day the larvae were released from the parent. An increase in antioxidant potential as part of a larger cellular stress response would be energetically costly and would need to be accommodated by an increase in overall metabolic rate or a shift in the allocation of the larval energy budget. Similarly, acid-base regulation can compose a significant portion of energy budgets (Baker and Connelly, 1966; Lucu and Pavicic, 1995; Lannig et al., 2010). The activity of Na^+/K^+-ATPase was elevated under High-T, High-pCO_2 in order to counteract the decrease in intracellular pH that was not compensated by photosynthetic activities of *Symbiodinium*. The change in enzyme activity indicates the high vulnerability of corals to perturbation in

intracellular pH during OA. The correlation between pNPPase activity and symbiont density emphasizes this vulnerability; bleaching in corals in response to environmental stress may reduce their ability to regulate intracellular pH. In response to environmental stress due to OA and warming, the cellular stress response of coral larvae may be engaged, causing an increase in antioxidant defense, and this holistic response may include an up-regulation in acid-base regulation with respect to symbiont density. The break-down of host-*Symbiodinium* symbiosis at High-pCO_2 due to oxidative stress may cause reduced buffering of intracellular pH and then metabolic depression, which has been observed in larvae and recruits of scleractinian corals under high-pCO_2 conditions (Cumbo et al., 2013a; Edmunds et al., 2013; Rivest and Hofmann, 2014). These results highlight the overall complex response of *P. damicornis* larvae to future OA and warming. The heterogeneity introduced by differences between larval cohorts as well as differences in symbiont abundance and photophysiology within larvae may foster a suite of larval physiological phenotypes where some larvae may succeed in a future ocean.

IV. Effects of high pCO_2 and temperature on lipid use and physiological condition of larvae of *Pocillopora damicornis*

Introduction

The health and persistence of the incredibly diverse coral reef ecosystem depends on the successful recruitment of larvae of the reef-building foundational organisms, scleractinian corals. This input of the next generation rejuvenates degraded reef communities via new settlers and supports standing genetic variation through the addition of new genotypes (Amar et al., 2007). Due to the energy requirements and sometimes limited physiological capacity of dispersing early life stages, larvae are especially vulnerable to changing environmental conditions (Pechenik, 1999; Byrne, 2011). Understanding the resilience of early life history stages is a research priority in light of co-occurring environmental changes such as ocean acidification (OA) and warming that threaten tropical coral reefs (*e.g.* Anthony et al. 2011, Pandolfi et al. 2011). In this chapter, I examined how planula larvae of the coral *Pocillopora damicornis* respond to laboratory-simulated conditions of OA and warming through shifts in composition of cellular lipids that are ecologically significant biomolecules. My studies also examined the role of maternal investment, day of release during planulation, and biogeographic location in mediating the response of coral planulae to scenarios of future anthropogenic change in coral reef environments (Hoegh-Guldberg et al., 2007; IPCC, 2013).

OA may have deleterious effects on various biological processes of young marine invertebrates. For coral larvae, fertilization success, recruitment, and survival can be suppressed under elevated pCO_2 scenarios (Albright et al., 2010; Suwa et al., 2010; Albright and Langdon, 2011; Cumbo et al., 2013a, 2013b; Rivest and Hofmann, 2014). Larvae of

some broadcast-spawning and brooding corals experience metabolic suppression at high pCO_2 (Albright and Langdon, 2011; Nakamura et al., 2011) while other species are more tolerant (Chua et al., 2013). Recent studies on larvae from a population of *P. damicornis* in Taiwan have found variable responses of metabolism to elevated temperatures and a lack of response to elevated pCO_2 (Cumbo et al., 2013a, 2013b; Putnam et al., 2013).

While evidence of the physiological effects of OA and warming accumulates, the question remains: how will changes in larval physiology under future ocean change affect coral populations through shifts in dispersal distance and recruitment success? The answer may lie in the energy stores of coral larvae. Two classes of lipid serve the majority of the energetic demands of lecithotrophic larvae: triacylglycerols and wax esters. Triacylglycerols can be quickly hydrolyzed for immediate energy needs and are the first lipid class to be consumed during larval development or during periods of starvation (Lee et al., 1971, 2006b; Moran and Manahan, 2003, 2004; Sewell, 2005). Wax esters have a slower turnover rate, so they serve as long-term energy deposits for larvae. In addition, they play an important role in dispersal of coral larvae, governing buoyancy (Nevenzel, 1970; Lee et al., 1971, 2006b; Arai et al., 1993; Villinski et al., 2002) and entraining larvae in surface currents (Willis and Oliver, 1990; Wellington and Fitt, 2003). If triglyceride stores are consumed, larvae will utilize wax esters, but their vertical position in the water column will change as a result, with potentially negative consequences for dispersal. Other types of lipids have important physiological functions: phospholipids maintain the structure for biological membranes, and other lipids serve as hormones and antioxidants in coral physiology.

For larvae of brooding corals, another important source of energy comes from the symbiotic dinoflagellate *Symbiodinium*, which is vertically transmitted to larvae prior to

release. The *Symbiodinium* dinoflagellates living in coral tissue can translocate ~15% of their fixed carbon to the planulae (Richmond, 1981). The endosymbionts satisfy a significant portion of larval energy budgets; without photosynthates, the larvae are forced to consume their lipid and protein stores at faster rates, with possible negative consequences for dispersal and recruitment (Ben-David-Zaslow and Benayahu, 2000; Alamaru et al., 2009; Harii et al., 2010). In particular, wax ester consumption increases when endosymbiont metabolites are not available (Harii et al., 2010); thus, buoyancy of the larvae may be significantly impacted following degeneration of the symbiosis. Maintaining a healthy relationship with *Symbiodinium* may allow zooxanthellate coral larvae to extend larval duration and competency periods.

OA and elevated temperature may perturb larval energetics by challenging the symbiotic relationship as well as host physiology. Temperature stress can decrease the ratio of photosynthesis to respiration in coral larvae (*Porites astreiodes*, Edmunds et al., 2001). As temperature increases, less energy is provided by the *Symbiodinium* to meet elevated demands. This decoupling of the symbiosis could be worsened by the addition of OA, which could lower the thermotolerance ceiling of coral larvae. Additionally, OA could increase energetic demands by eliciting cellular stress response, oxidative defense, and ion-balance pathways. Without sufficient metabolite input from *Symbiodinium* under future ocean conditions, lecithotrophic coral larvae may rely more heavily on their lipid stores to fuel their dispersal and recruitment. Less stored energy and decreased buoyancy can increase mortality, shorten larval durations, and cause premature metamorphosis (Edmunds et al., 2001), with negative consequences for suitable habitat selection, recruitment success, restoration of damaged populations and region-wide connectivity. If larval energy stores are reduced

enough, settlement and metamorphosis may not be possible (Lucas et al., 1979; Kempf, 1981). Thus, an understanding of the biochemical and physiological energetics of coral larvae as they relate to lipid content and composition is essential in order to predict how OA and warming will affect development, dispersal potential, and recruitment.

Mechanistically, the effects of OA and elevated temperature on the energy metabolism of coral larvae may be mediated by innate differences in larval physiology based on the day the larvae were released. Developing larvae may experience different microenvironments (dissolved gas, oxygen, light, etc.) that promote the physiological differences observed, as a function of tissue depth as larvae are stacked within coral polyps (Kuhl et al., 1995; Jimenez et al., 2008) as well as the position of the polyp within the colony. Regardless of the mechanism, larvae of *P. damicornis* and other brooding corals can differ in size, *Symbiodinium* density, and photophysiology across the spawning period (Edmunds et al., 2001; Isomura and Nishihira, 2001; Putnam et al., 2010; Cumbo et al., 2012; Rivest and Hofmann, 2014; E Rivest, unpublished data). Differences between cohorts of larvae released on adjacent days, like those used in this study may be more subtle, but the innate differences between cohorts may translate into the between-cohort differences in response to OA and elevated temperature observed previously (Putnam et al., 2010; Rivest and Hofmann, 2014).

Local environmental conditions may shape the responses of resident corals to future environmental changes. Adaptation to fluctuations of pH and temperature may grant coral populations more or less tolerance of future changes in these parameters. The phenomenon of local adaptation is particularly likely over a sufficient spatial scale where environmental conditions differ consistently and where gene flow is low (Kawecki and Ebert, 2004;

Alleaume-Benharira et al., 2006; Kelly and Hofmann, 2012), and in this context, local adaptation to temperature has been well studied (Conover, 1998; Sanford and Kelly, 2011). But we are just beginning to be able to examine this phenomenon for seawater pH, due to our recent ability to acquire long-term, high-frequency data using autonomous sensors (Martz et al., 2010; Hofmann et al., 2011, 2013; Lunden, Rivest et al., in review). If coral populations are locally adapted to their environmental regime, corals living in a naturally more acidic environment may have developed physiological tools for maintaining normal function in low-pH seawater, as has been shown for elevated temperature (Oliver and Palumbi, 2011).

The data analyses presented in this chapter serve different perspectives. I expressed lipid utilization and biochemical composition per larva, per μg total protein, and per symbiont density. These modes of normalization reveal different patterns in the data, and here I clarify when and why each mode is favored. Firstly, traits expressed per larva reveal patterns of physiology at the level of the whole organism. In the context of ecology and for interspecies comparisons, this normalization mode is favored as the patterns refer to the properties of the specific individuals assessed and may reveal absolute thresholds in biological properties. Secondly, physiological and biological processes often scale to the size of the organism. And if size varies between the individuals studied, normalizing quantified traits by size, in this case via total protein, improves the signal-to-noise ratio in the data by removing variation attributed to body size. This mode of normalization would allow you to decipher patterns independent of the specific individuals under study and to apply the derived relationship to other members of the population based on their size. Lastly, I normalized traits by symbiont density in order to account for variation in the signal-to-noise ratio associated with photosynthetic activities of *Symbiodinium* in the coral larvae. Since

Symbiodinium are involved in synthesizing lipid stores, normalizing to symbiont density reveals lipid consumption rates independent of the potential for new lipid synthesis.

Part A: The role of larval release day in the response of coral larvae to OA and warming

In this study, I explored the effects of OA and temperature on larval physiology, using lipid utilization and biochemical composition as indices of performance of these early life stages. To do so, I performed CO_2 manipulation experiments in the laboratory with *P. damicornis* larvae collected in Moorea, French Polynesia. To help provide context for the pCO_2 levels used in the experimental design, I deployed autonomous pH and temperature sensors on the natal fringing reef (described in Chapter 6). Here, I aimed to investigate the capacity of present-day coral genotypes, in terms of their physiological plasticity, to tolerate future conditions of OA and warming. Specifically, I asked: (1) how are lipid composition and physiological condition of *P. damicornis* larvae affected by combinations of pCO_2 and temperature levels?, and (2) do the effects of OA and warming on larval energetics differ between cohorts of larvae, based on day of release? For this study, I measured lipid composition of larvae both upon release and after exposure to experimental conditions in order to assess how OA and warming might alter larval performance and dispersal.

Part B: The role of biogeography and environmental history in the response of coral larvae to OA and warming

In this study, I expanded the assessment of the effects of OA and temperature on lipid utilization and biochemical composition to inquire about the effects of biogeography and environmental history on performance of these early life stages. To do so, I combined the

results of the previous study with data collected during similar CO_2 manipulation experiments with *P. damicornis* larvae collected in Taiwan. The laboratory results were coupled with environmental data using autonomous pH and temperature sensors deployed in both locations (see Chapter 6). For this study, lipid composition and biological traits of larvae were measured both upon release and after exposure to experimental conditions in order to assess how OA and warming might alter larval performance and dispersal.

Part A: The role of larval release day in the response of coral larvae to OA and warming

Materials and methods

Collection of coral larvae

To obtain coral larvae, adult corals were brought to the laboratory, and larvae were captured upon their release. Specimens of adult *Pocillopora damicornis* were collected from a fringing reef (17°28'49.08S, 149°47'56.04W) on Moorea, French Polynesia; eight colonies of *P. damicornis* were collected on the new moon in February 2012, from a depth of ~1-3 m. Colonies were maintained in individual aquaria that received indirect natural sunlight and coarsely filtered seawater (T ~ 29°C). Larvae were collected from adult colonies following their lunar pattern of reproduction (Fan et al., 2006). Larval release reached a peak in cohort size around 7 days after the new moon, followed by a decline (Fig. 10). Overnight, larvae were captured in 100 μm mesh-lined cups that received the outflow of each aquarium. Daily

Figure 10. Release of *Pocillopora damicornis* larvae in (A) Moorea, French Polynesia and in (B) Taiwan. Larval release increased following the new moon and then decreased after lunar day 6. Numbers of larvae released per colony (n = 8 colonies) are described by bar segments of different colors.

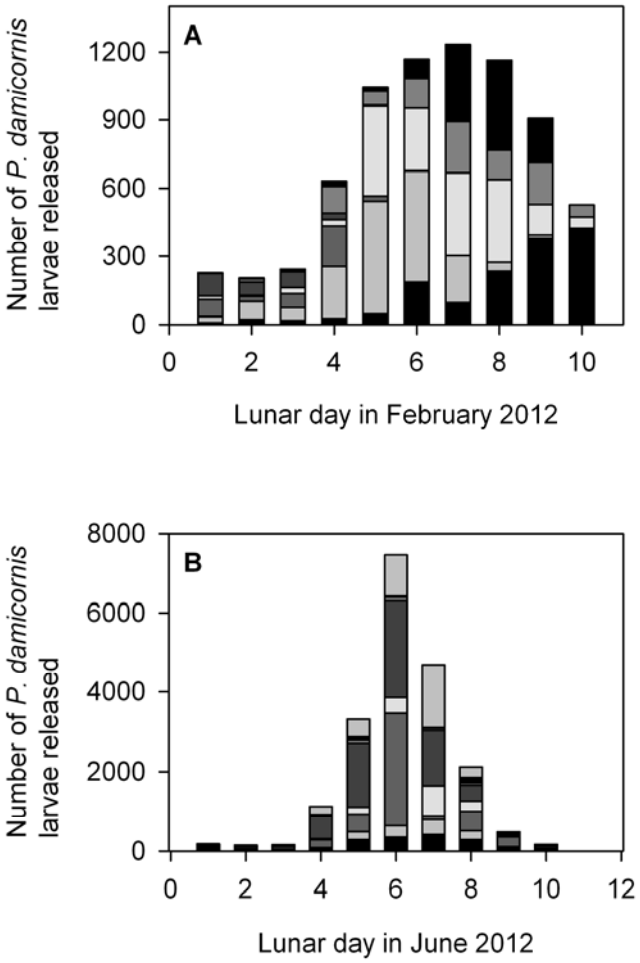

at dawn, larvae from each colony were collected, counted, and pooled. The small numbers of larvae released from some colonies required the use of all larvae released, resulting in unequal genotype ratios in the pool. On each day, larvae from this pool were immediately photographed and preserved to quantify larval quality and lipid metrics (see below) that represented the condition of freshly-released larvae. The remaining larvae in the pool were then randomly assigned to experimental treatments. Data presented here were collected before and after manipulative experiments were conducted with cohorts of larvae released on adjacent days: February 28 (Lunar day 7, "Peak"), February 29 (Lunar day 8, "Middle"), and March 1 (Lunar day 9, "Late").

Experimental incubations

In preparation for the experimental incubations, the daily pool of released larvae was divided among 8 tanks containing 4 treatment combinations of pCO_2 and temperature. Larvae were incubated in 2 400 mL containers per aquarium at a density of ~0.15-0.25 larva mL^{-1}; these containers had 100 μm mesh sides and a PAR-transparent lid, and they were anchored in place within the aquarium to ensure that PAR exposure was replicated across tanks (Fig. 11). Larvae were incubated for 24 hours under experimental conditions. Due to the time needed to photograph and preserve larvae post-incubation, incubations were staggered by one hour per aquarium, with the order randomized daily. At the end of each incubation, larvae within tanks were pooled, and 10 larvae were randomly selected for size measurements (n = 20 per treatment). The remaining larvae were aliquoted and frozen at -80°C for downstream analyses of lipid classes (3 tubes per aquarium x 25 larvae), total protein content (2 x 5 larvae), and symbiont density (2 x 5 larvae). Therefore, for

Figure 11. Experimental set-up for larval incubations in Moorea (A) and Taiwan (B). Containers (400 mL) were modified with 100 µm mesh windows on 5 sides. The lid contained a plastic film that is PAR-transparent. The containers were centered under aquarium lights using zip-tie corrals to ensure replicate irradiance across tanks.

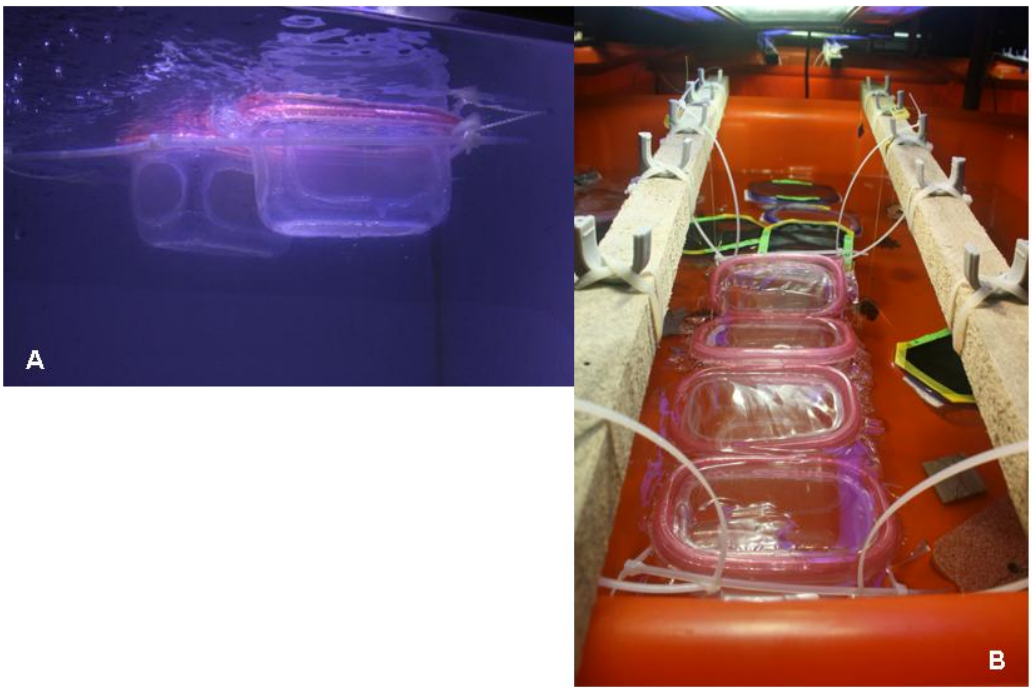

comparisons between treatments, $n = 6$ for lipid classes, 4 for total protein, and 4 for symbiont density.

For the experimental incubations, two CO_2 treatments were prescribed. Ambient-pCO_2 was ~450 µatm CO_2, and High-pCO_2 was ~1000 µatm CO_2. The control treatment approximates current environmental conditions for the adult coral (verified by environmental data), while the high treatment represents a level of dissolved pCO_2 expected by the year 2100 under a business-as-usual scenario (IPCC, 2013). pCO_2 levels were combined with two experimental temperatures. Ambient-T and High-T treatments were 28°C and 31°C, respectively. The control temperatures approximate the multi-year average temperature for the fringing reefs close to the collection sites for adult *P. damicornis* (Leichter, 2014). The elevated temperatures represent an average surface ocean temperature by year 2100 as predicted by global temperature projections (IPCC, 2013). The four treatments created by this experimental set-up are defined as ambient temperature-ambient pCO_2 (ATAC), ambient temperature-high pCO_2 (ATHC), high temperature-ambient pCO_2 (HTAC), and high temperature-high pCO_2 (HTHC).

Experimental pCO_2 treatments were created using a gas mixing system at the MCR LTER facility at the University of California, Berkeley Richard B. Gump South Pacific Research Station with two aquaria for each treatment combination of pCO_2 and temperature (previously described in Edmunds et al., 2012). Aquaria were illuminated on a 13hr:11hr light:dark cycle (Sol LED Module, Aquaillumination, 75W, Ames, IA, USA); light was provided from 5:30 to 18:30 including a 4-hour ramping period at the beginning and end of each light cycle. At full intensity, larvae experienced approximately 1800 ± 140 µmol photons m^{-2} s^{-1} of photosynthetically active radiation. Light levels were measured just below

the seawater surface during the experiment using a 4π quantum sensor (LI-193, Li-Cor Inc., Lincoln, NE, USA) and a Li-Cor LI-1400 meter (Li-Cor Inc., Lincoln, NE, USA).

To verify and monitor the physical parameters of the OA x temperature treatments, the carbonate chemistry (pH, salinity, and total alkalinity) and the temperature of the seawater in the aquaria was analyzed daily during the incubations.

Seawater temperature was measured throughout the experimental exposures (~10 times) using a certified digital thermometer (meter 15-077-8, probe 15-077-7, Thermo Fisher Scientific Inc., Waltham, MA, USA). Seawater salinities were measured using a conductivity meter (YSI 3100, YSI Inc., Yellow Springs, OH, USA). Seawater pH was measured using a spectrophotometric method with indicator dye, *m*-cresol purple (SOP 6b, Dickson et al., 2007). Total alkalinity (A_T) was measured using an automated, closed-cell potentiometric titration (SOP 3b, Dickson et al., 2007) using an automatic titrator (T50 with DG115-SC pH probe, Mettler Toledo, LLC., Toledo, OH, USA). Titrations were performed using certified acid titrant (~0.1M HCl, 0.6M NaCl; A. Dickson Laboratory, Scripps Institute of Oceanography), and A_T was calculated following Dickson *et al.* (2007). For each day of the experiment, analyzed certified reference materials from A. Dickson Laboratory were titrated to confirm the precision and accuracy of the process; these reference titrations were accurate within 10 μmol kg^{-1}. pH at 25°C, A_T, temperature, and salinity were used to calculate the pH and pCO_2 of the treatments using CO2calc (Robbins et al., 2010), with CO_2 constants K1, K2 from (Mehrbach et al., 1973) refit by (Dickson and Millero, 1987) and pH expressed on the total scale (mol kg-SW^{-1}).

Assessment of physiological condition of larvae

To assess quality of incubated larvae, size, density of *Symbiodinium*, and total protein were quantified. Larval size was determined via image analysis using ImageJ (Rasband, 1997). Larvae were photographed using a dissecting microscope fitted with a camera (objective 5, Western Scientific Company Inc., Valencia, CA, USA; Q-color 3 camera with QCapture suite software, Olympus American Inc., Center Valley, PA, USA). A stage micrometer was photographed under these settings and was used to calibrate all image analyses. In practice, circumferences of the larvae were traced to calculate larval area in μm^2, and maximum larval length was measured.

Total protein was quantified as the water soluble protein of the cell contents, using the Bradford assay (Bradford, 1976). Frozen larvae were homogenized in ice-cold 0.2 μm-filtered water using a sonicator. For all larval homogenates, total protein was precipitated using trichloroacetic acid, re-dissolved using 1 M NaOH, and neutralized using 1.68 M HCl before the addition of Bradford dye concentrate (Bio-Rad Laboratories Inc., Hercules, CA, USA). Absorbance at 595 nm was measured following an incubation of 20 minutes at room temperature. Total protein was calculated with a standard curve made using known concentrations of bovine serum albumin (Bio-Rad Laboratories Inc., Hercules, CA, USA).

To determine symbiont density, batches of 5 larvae were homogenized in de-ionized water using a pestle. *Symbiodinium* cells in six 10 μL aliquots of homogenate were counted using a haemocytometer and a compound light microscope. Coefficients of variation between replicate counts were less than 10%, suggesting that any differences in symbiont density greater than 10% are not expected to be from chance alone or from variability in the analysis.

Characterization of cellular lipids

For these analyses, lipid composition was used as a biochemical index in two general categories: the content of (1) energy-storage lipids (WE and TAG) and (2) structural lipids (PL). Wax esters (WE) contribute to long-term energy storage and larval buoyancy (Nevenzel, 1970; Lee et al., 1971, 2006b; Arai et al., 1993; Villinski et al., 2002), and triacylglycerol (TAG) is a readily-used source of cellular energy. Phospholipids (PL) in larvae served as a proxy for cell number because of their structural role within cell membranes. Aliquots of 25 larvae were homogenized in 1x phosphate-buffered saline (PBS) using glass beads (Sigma-Aldrich Corp., St. Louis, MO, USA) and a bead-beater (Biospec Products, Inc., Bartlesville, OK, USA). Three 5-minute rounds of homogenization at 30 repetitions per second were spaced with flash-freezing of sample tubes in liquid nitrogen. At this point, an aliquot of homogenate was removed and analyzed for total protein content using the BCA assay (Pierce Biotechnology Inc., Rockford, IL, USA; Smith et al., 1985). The BCA assay was used because the chemicals in the homogenization buffer interfered with the color formation process in the Bradford assay. Total protein concentrations were used to normalize lipid extracts for down-stream analysis.

Lipid was extracted from the remaining homogenate following Bligh and Dyer (1959), modified by Luo (2008). Because it is easy to lose a portion of the experimental sample during the lipid extraction process, an exogenous spike or internal standard was used to quantify the efficient of lipid extraction for each sample (Parrish, 1987). 149 μg ketone (1-hexadecanone, Sigma-Aldrich Corp., St. Louis, MO, USA) was added to remaining raw homogenate as the internal standard (Delmas et al., 1984; Parrish and Ackman, 1985; Parrish, 1987). Briefly, homogenate, chloroform, methanol, and acidic saline were

sequentially added to and mixed in glass test tubes for final volumetric ratios of 0.8:2:2:1, respectively. Between each addition, tubes were vortexed vigorously for 10 seconds and then allowed to stand for 10 minutes at room temperature. The chloroform layer was transferred to a new test tube, where it was washed again in a final volumetric ratio 2:2:1.8, chloroform: methanol: acidic saline. The chloroform layer containing extracted lipids was transferred into a pre-weighed brown glass autosampler vial. The chloroform was evaporated at 37°C under inert gas (nitrogen). Total lipid was calculated by subtracting weights of empty, clean vials from weights of vials containing dried lipid. Vials with dried lipid were stored under inert gas at -80°C until further analysis. All solvents used in the extraction procedure were HPLC-grade.

Lipid classes of wax ester (WE), triacylglycerol (TAG), and phospholipid (PL) were separated and quantified using an Iatroscan MK-5 thin layer chromatography-flame ionization detection (TLC-FID) analyzer (Iatron Laboratories, Inc., Tokyo, Japan). Lipid extracts were reconstituted in 100 μL chloroform; 1 μL of this solution was spotted at the origin of a Chromarod® (S-III; Iatron Laboratories, Inc., Tokyo, Japan) using a Drummond Digital Microdispenser with Drummond Precision Glass Bores (Drummond Scientific Co., Broomall, PA, USA). The same 10 rods were used to process all samples and standards described here. Three separate samples were processed on each run of the frame, with 3 technical replicates per extract; the remaining rod was used as a blank. To separate target lipid classes from total lipid, a two-step solvent system was used. Once dry, each frame of 10 rods was fully developed (25 min) in hexane:ethyl ether: acetic acid (99:1:0.05, v:v:v). The rods were dried at 100°C for 4 min. Then, each frame of rods was fully developed (25 min) in hexane:ethyl ether:acetic acid (85:15:0.1, v:v:v). The rods were dried at 100°C for 4 min.

This solvent system is a modification from Rodrigues *et al.* (2008). The entire length of the rods was scanned by the Iatroscan under 1200 mL min^{-1} O_2 and 160 mL min^{-1} H_2. Data were collected using LabView software (National Instruments, Austin, TX, USA).

To determine the quantity of lipid classes in each sample, a standard curve generated from mixtures of known lipid standards was run on the frame of Chromarods® at the beginning and end of sample analysis. The standard curve consisted of: 0.06-1.96 μg μL^{-1} hydrocarbon (5-α-cholestane), 0.06-5.89 μg μL^{-1} wax ester (palmitic acid palmityl ester), 0.12-1.98 μg μL^{-1} ketone (1-hexadecanone), 0.06-3.93 μg μL^{-1} triacylglycerol (tripalmitin), 0.06-3.93 μg μL^{-1} free fatty acid (stearic acid), 0.06-3.93 μg μL^{-1} sterol (stigmastanol), and 0.06-5.89 μg μL^{-1} phospholipid (L-α-phosphatidylcholine). Standard curves of lipid concentration vs. peak area were used to calculate concentrations of lipid classes in resuspended sample extracts. The internal standard was used to adjust these values to account for extraction efficiency. Amounts of lipid classes were then normalized to number of larva, total protein, and symbiont density.

Statistical analyses of biological data

All data were analyzed using R version 3.0.1 (R Core Team 2013). In all cases, statistical assumptions of normality and homogeneity of variance were met based on Q-Q plots and Levene's test, often following a power-based transformation of the response variable. Effects on physical conditions were estimated using linear mixed-effect models (nlme package in R; Pinheiro and Bates, 2000) as described below. To compare physical conditions between treatments, pCO_2 and temperature treatments were fixed factors, and tank was a random factor. For initial conditions of larvae, absolute values of lipid and quality

metrics were analyzed for effects of day of release of larvae ("Day") using a one-way ANOVA. For post-incubation conditions of larvae, absolute values of lipid and quality metrics measured at the end of the 24-hour exposures were analyzed as described below. Because initial conditions of larvae often varied between days, changes in response variables with respect to starting levels may more accurately represent the effects of OA and warming on larval physiology. Mean starting condition levels were subtracted from post-incubation levels, henceforth referred to as Δ, "delta". Therefore, a negative ΔWE per larva represents a net consumption of WE per larva during the 24-hr incubation. Differences in wax ester (WE), triacylglycerol (TAG), and phospholipid (PL) quantities were standardized by larva, by total protein, and by symbiont density.

With pCO_2 ("pCO_2"), temperature ("T"), and day of release ("Day") as fixed factors, effects on standardized lipid quantities and standardized measures of larval quality were estimated using linear mixed-effect models (nlme package in R; Pinheiro and Bates, 2000). To account for random variation among all possible aquaria, "tank" was considered a random factor in all statistical analyses. Model selection was performed incrementally following Burnham and Anderson (2002): at each iteration, the simpler model was chosen if the model AIC value did not increase by 2 or more and if there was not a significant difference in the model log likelihood ratio. To determine which factors in models were significant, a type III sum of squares was conducted on selected models fit using maximum likelihood (Zuur et al., 2009; Crawley, 2013). When significant differences were detected among treatments, orthogonal contrasts were performed as post-hoc analyses using the multcomp package in R (Hothorn et al., 2008). Tukey's HSD was used for models without significant interactions between terms. When significant interactions were present, post-hoc analyses were

performed using general linear hypothesis tests with Bonferroni corrections for multiple comparisons (abbreviated GLHT).

Environmental data collection

pH and temperature time series were generated on a fringing reef in Moorea, French Polynesia approximately 33 m from the collecting location of adult *P. damicornis* parents. Refer to Chapter 6 for more details.

Results

Condition of P. damicornis *larvae immediately after release*

To detect possible variation in maternal provisioning of *P. damicornis* planulae, I measured a series of traits of freshly-released larvae as a function of the day they were released from their parent. I assessed whether lipid composition and physiological condition varied between different days of release – the three cohorts of larvae that were collected and analyzed are henceforth called Peak, Middle or Late.

As a general pattern, I found that initial condition of larvae did not differ significantly as a function of day of release. Initial WE varied significantly by Day when expressed as a function of symbiont density, but not when standardized per larva or per protein (Table 10). When expressed per µg total protein, initial TAG varied significantly by Day; however, groups were not different for TAG per larva or per symbiont density (Table 10). TAG per

Table 10. Analysis of newly-released *P. damicornis* larvae among days of larval release, standardized per larva (µg larva^{-1}), per protein (µg µg total protein^{-1}), and per symbiont density (µg cell^{-1}), unless otherwise noted. Comparisons were made using a one-way ANOVA with day of release (Day) as a fixed effect. Test-statistic F, degrees of freedom (df) and p-values (*p*) are reported.

Response variable	F	df	*p*
WE per larva	1.041	2, 6	0.409
WE per total protein	0.496	2, 6	0.632
WE per symbiont density	4.714	2, 6	**0.059**
TAG per larva	0.984	2, 6	0.427
TAG per protein	11.855	2, 6	**0.008**
TAG per symbiont density	1.155	2, 6	0.376
PL per larva	1.517	2, 6	0.293
PL per protein	4.485	2, 6	**0.064**
PL per symbiont density	1.654	2, 6	0.268
TL per larva	0.322	2, 5	0.739
TL per protein	0.695	2, 5	0.542
TL per symbiont density	2.089	2, 5	0.219
TP per larva	1.513	2, 3	0.351
TP per symbiont density	3.526	2, 3	0.163
Symbiont density (cells larva^{-1})	0.072	2, 3	0.932
Larval area (µm^2)	5.533	2, 27	**0.010**
Larval length (µm)	7.379	2, 27	**0.003**

protein was significantly greater on days Peak and Middle than on day Late (Tukey's HSD, Table 11; Fig. 12). Initial PL levels did not vary significantly by Day, for all three expressions of lipid concentrations (Table 10).

Regardless of standardization method, initial levels of TL, TP, and symbiont density did not vary significantly by Day (Table 10). Larval area and length did respond significantly to Day (Table 10). Initial area was significantly greater on day Middle than on day Peak (Tukey's HSD, Table 11; Fig. 12). Larval length was significantly greater on day Middle than on days Peak and Late (Tukey's HSD, Table 11; Fig. 12).

Physiological responses of larvae in response to pCO_2 and temperature

In order to assess the response of coral larvae to different levels of temperature and pCO_2, lipid composition and quality of *P. damicornis* planulae were measured following 24-hour incubations in combinations of pCO_2 and temperature conditions (Table 12). During the lab experiments, temperature varied significantly by T (Table 13). Salinity was significantly higher at High-T and total alkalinity did not vary by temperature or pCO_2 (Table 13). pH and pCO_2 of seawater varied significantly by pCO_2 and T treatments, with greater values under Ambient conditions (Table 13).

In terms of biomolecules that provide long-term energy storage and confer buoyancy, the post-incubation abundance of wax esters (WE) was significantly affected by pCO_2xTxDay, pCO_2xDay, and Day (Table 14). Post-hoc comparisons did not reveal any significant differences between temperature or pCO_2 treatments on different days (GLHT, Table 15). When WE levels were standardized by total protein content, pCO_2xTxDay, TxDay, and Day were significant. For Middle larvae, WE per protein was greater at

Table 11. Post-hoc analyses for significant effects on lipid content and physiological conditions of newly-released *P. damicornis* larvae among days of larval release. Post-hoc tests were either Tukey's HSD or general linear hypothesis tests with Bonferroni corrections for multiple comparisons (GLHT). Test statistic z and p-values (*p*) are reported for each comparison.

Post-hoc test	Biological response	Significant effect	Comparison	z	*p*	Summary description
Tukey's HSD	Initial WE per symbiont density	Day	Peak vs. Middle	0.054	0.998	Peak = Middle < Late
			Peak vs. Late	2.686	0.081	
			Middle vs. Late	2.632	0.086	
Tukey's HSD	Initial TAG per protein	Day	Peak vs. Middle	0.444	0.899	Peak = Middle > Late
			Peak vs. Late	4.422	**0.010**	
			Middle vs. Late	3.977	**0.017**	
Tukey's HSD	Initial larval area	Day	Peak vs. Middle	3.308	**0.007**	Peak ≤ Middle = Late
			Peak vs. Late	1.348	0.382	
			Middle vs. Late	1.96	0.142	
Tukey's HSD	Initial larval length	Day	Peak vs. Middle	3.609	**0.003**	Middle > Peak = Late
			Peak vs. Late	0.665	0.786	
			Middle vs. Late	2.944	**0.018**	

Figure 12. Traits describing the status of newly-released *P. damicornis* larvae. Mean ± SE (n = 3) quantities of biochemical composition (A) and size (B) of larvae released on days Peak, Middle, and Late. Traits are standardized per larva (µg lava^{-1}), per protein (µg µg total protein^{-1}), and per symbiont density ([µg symbiont cell^{-1}]x10^{-3}) unless otherwise noted. Means with the same lowercase letter are not significant different ($p > 0.05$). Refer to Tables 10 and 11 for statistical details.

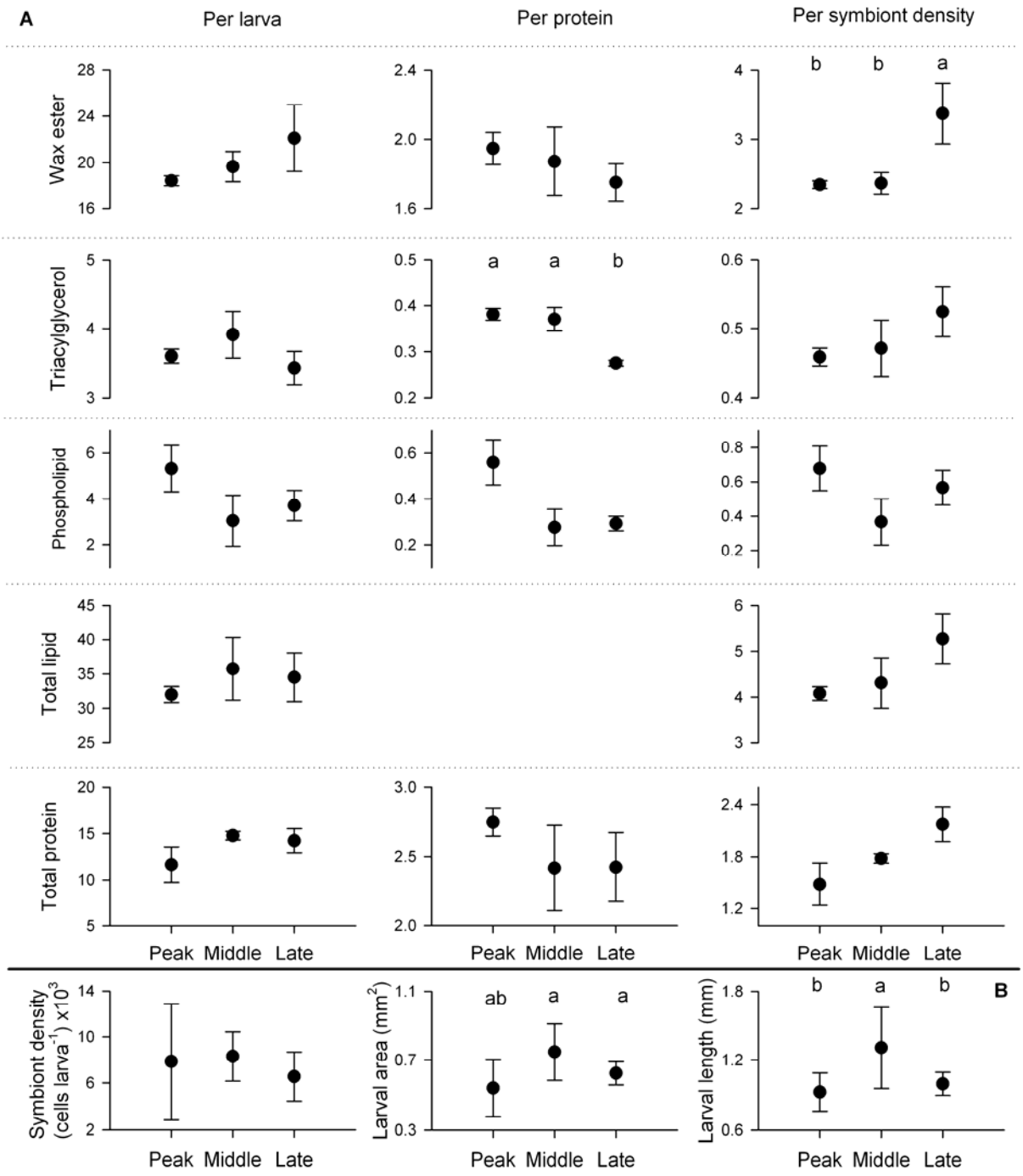

Table 12. Summary of physical conditions in experimental aquaria used in Moorea, French Polynesia and in Taiwan. Data are presented as mean ± SE. For all parameters, *n* = 3.

Site	Treatment	Temperature (°C)	Salinity (psu)	pH_{total}	A_T (µmol kg^{-1})	pCO_2 (µatm)
Moorea	ATAC	27.99 ± 0.10	35.82 ± 0.02	8.004 ± 0.003	2362 ± 1	459 ± 4
	HTAC	30.57 ± 0.11	35.85 ± 0.02	7.970 ± 0.007	2363 ± 1	496 ± 9
	ATHC	28.12 ± 0.18	35.83 ± 0.02	7.719 ± 0.008	2364 ± 1	1002 ± 22
	HTHC	30.77 ± 0.20	35.88 ± 0.02	7.692 ± 0.012	2368 ± 2	1068 ± 33
Taiwan	ATAC	27.75 ± 0.18	30.61 ± 0.18	7.971 ± 0.007	2234 ± 4	494 ± 9
	HTAC	30.53 ± 0.05	30.63 ± 0.23	7.978 ± 0.005	2253 ± 6	487 ± 9
	ATHC	27.70 ± 0.20	30.26 ± 0.29	7.733 ± 0.006	2204 ± 15	923 ± 14
	HTHC	30.43 ± 0.04	30.93 ± 0.14	7.748 ± 0.004	2243 ± 6	900 ± 9

Table 13. Statistical comparison of sea water treatment conditions using type III sum of squares with pCO_2 and temperature (T) as fixed effects and Tukey's HSD. Interaction terms were removed from the model if the AIC value did not increase by 2 or more and if there was not a significant difference in the model log likelihood ratio; removed terms are not shown here. Comparisons were performed using type III sum of squares, with test statistic X^2, degrees of freedom (df) and p-values (*p*) reported. Post-hoc analyses were performed using Tukey's HSD with test statistic z and p-values (*p*) reported.

Site	Parameter	Effect	Type-III SS X^2	df	*p*	Tukey's HSD z	*p*
Moorea	Temperature	pCO_2	0.675	1	0.411		
		T	165.511	1	**<0.001**	10.170	**<0.001**
	Salinity	pCO_2	1.982	1	0.159		
		T	5.505	1	**0.019**	2.076	**0.038**
	pH_{total}	pCO_2	604.400	1	**<0.001**	19.440	**<0.001**
		T	7.010	1	**0.008**	2.093	**0.036**
	A_T	pCO_2	5.081	1	**0.024**	1.782	0.075
		T	3.284	1	0.070		
	pCO_2	pCO_2	813.377	1	**<0.001**	22.550	**<0.001**
		T	7.815	1	0.005	2.210	**0.027**
Taiwan	Temperature	pCO_2	0.360	1	0.549		
		T	465.129	1	**<0.001**	20.170	**<0.001**
	Salinity	pCO_2	0.007	1	0.932		
		T	2.010	1	0.156		
	pH_{total}	pCO_2	1960.400	1	**<0.001**	35.000	**<0.001**
		T	4.522	1	**0.033**	1.681	0.093
	A_T	pCO_2	2.732	1	0.098		
		T	5.920	1	**0.015**	1.924	**0.054**
	pCO_2	pCO_2	1880.415	1	**<0.001**	39.360	**<0.001**
		T	2.396	1	0.122		

Table 14. Analysis of absolute abundance of lipid classes (wax ester WE, triacylglycerol TAG, phospholipid PL) in *P. damicornis* larvae following a 24-hour exposure to seawater of controlled temperature and pCO_2. Lipid content was compared among treatments and days of release, standardized to per larva (μg $larva^{-1}$), per larval protein content (μg μg total $protein^{-1}$), and per symbiont density (μg $cell^{-1}$). Comparisons were made using type III sum of squares with pCO_2, temperature (T), and day of release (Day) as fixed effects. The final reduced model is shown, with test statistic X^2, degrees of freedom (df) and p-values (*p*) reported. Interaction terms were removed from the model if the AIC value did not increase by 2 or more and if there was not a significant difference in the model log likelihood ratio; removed terms are not shown here.

	Per larva			**Per protein**			**Per symbiont density**		
WE									
Effect	X^2	df	*p*	X^2	df	*p*	X^2	df	*p*
pCO_2	0.634	1	0.426	1.247	1	0.264	7.445	1	**0.006**
Temp	1.156	1	0.282	0.225	1	0.636	10.259	1	**0.001**
Day	23.37	2	**<0.001**	20.212	2	**<0.001**	84.974	2	**<0.001**
pCO_2xT	0.130	1	0.719	0.472	1	0.492			
pCO_2xDay	6.086	2	**0.048**	4.946	2	0.084	13.617	2	**0.001**
TxDay	4.735	2	0.094	8.155	2	**0.017**			
pCO_2xTxDay	8.570	2	**0.013**	7.151	2	**0.028**			
TAG									
Effect	X^2	df	*p*	X^2	df	*p*	X^2	df	*p*
pCO_2	2.081	1	0.149	1.054	1	0.305	2.764	1	0.096
Temp	1.114	1	0.291	12.599	1	**<0.001**	23.642	1	**<0.001**
Day	31.949	2	**<0.001**	3.406	2	0.182	9.773	2	**0.008**
pCO_2xT	5.647	1	**0.017**						
pCO_2xDay							12.870	2	**0.002**
TxDay							11.719	2	**0.003**
pCO_2xTxDay									
PL									
Effect	X^2	df	*p*	X^2	df	*p*	X^2	df	*p*
pCO_2	2.109	1	0.146	0.757	1	0.384	8.857	1	**0.003**
Temp	0.938	1	0.333	0.982	1	0.322	1.959	1	0.162
Day	16.715	2	**<0.001**	40.937	2	**<0.001**	17.033	2	**<0.001**
pCO_2xT									
pCO_2xDay							10.252	2	**0.006**
TxDay									
pCO_2xTxDay									

Table 15. Post-hoc analyses for significant effects of treatment and day of release on absolute abundance of lipid classes (wax ester WE, triacylglycerol TAG, phospholipid PL) in *P. damicornis* larvae, standardized to per larva (µg larva^{-1}), per larval protein content (µg µg total protein^{-1}), and per symbiont density (µg cell^{-1}). Post-hoc tests were either Tukey's HSD or general linear hypothesis tests with Bonferroni corrections for multiple comparisons (GLHT). Test statistic z and p-values (*p*) are reported for each comparison.

Post-hoc test	Biological response	Significant effect	Comparison	z	*p*	Summary description
GLHT	WE per larva	pCO_2xTxDay	Peak: Ambient-T vs. High-T	0.483	1.000	N/A
			Peak: Ambient-pCO_2 vs. High-pCO_2	0.502	1.000	
			Middle: Ambient-T vs. High-T	1.193	1.000	
			Middle: Ambient-pCO_2 vs. High-pCO_2	1.615	0.638	
			Late: Ambient-T vs. High-T	1.075	1.000	
			Late: Ambient-pCO_2 vs. High-pCO_2	0.796	1.000	
GLHT	WE per protein	pCO_2xTxDay	Peak: Ambient-T vs. High-T	2.450	0.086	Middle: High-T > Ambient-T
			Peak: Ambient-pCO_2 vs. High-pCO_2	0.032	1.000	
			Middle: Ambient-T vs. High-T	3.307	0.006	
			Middle: Ambient-pCO_2 vs. High-pCO_2	1.940	0.315	
			Late: Ambient-T vs. High-T	0.474	1.000	
			Late: Ambient-pCO_2 vs. High-pCO_2	1.117	1.000	
GLHT	WE per symbiont density	pCO_2xDay	Peak: Ambient-pCO_2 vs. High-pCO_2	0.284	1.000	Late: Ambient-pCO_2 > High-pCO_2
			Middle: Ambient-pCO_2 vs. High-pCO_2	2.256	0.096	
			Late: Ambient-pCO_2 vs. High-pCO_2	2.497	**0.050**	
		T	Ambient-T vs. High-T	2.688	**0.029**	Ambient-T < High-T
GLHT	TAG per larva	pCO_2xT	ATAC vs. HTAC	1.011	1.000	N/A
			ATHC vs. HTHC	2.207	0.137	
		Day	Peak vs. Middle	4.718	**<0.001**	Peak < Middle = Late
			Peak vs. Late	4.654	**<0.001**	
			Middle vs. Late	0.064	1.000	
Tukey's HSD	TAG per protein	T	Ambient-T vs. High-T	2.806	**0.005**	Ambient-T < High-T
GLHT	TAG per symbiont density	pCO_2xDay	Peak: Ambient-pCO_2 vs. High-pCO_2	0.618	1.000	Late: Ambient-T < High-T
			Middle: Ambient-pCO_2 vs. High-pCO_2	2.542	0.066	
			Late: Ambient-pCO_2 vs. High-pCO_2	1.442	0.895	
			Peak: Ambient-T vs. High-T	0.770	1.000	
			Middle: Ambient-T vs. High-T	1.106	1.000	
			Late: Ambient-T vs. High-T	4.218	**<0.001**	
Tukey's HSD	PL per larva	Day	Peak vs. Middle	3.926	**<0.001**	Peak > Middle = Late
			Peak vs. Late	2.285	**0.058**	
			Middle vs. Late	1.642	0.228	
Tukey's HSD	PL per protein	Day	Peak vs. Middle	1.010	0.571	Peak > Middle = Late
			Peak vs. Late	4.768	**<0.001**	
			Middle vs. Late	5.778	**<0.001**	
GLHT	PL per symbiont density	pCO_2xDay	Peak: Ambient-pCO_2 vs. High-pCO_2	0.606	1.000	Late: Ambient-pCO_2 > High-pCO_2
			Middle: Ambient-pCO_2 vs. High-pCO_2	1.134	0.770	
			Late: Ambient-pCO_2 vs. High-pCO_2	2.828	**0.014**	

High-T than at Ambient-T (GLHT, Table 15; Fig. 13). WE per symbiont density was significantly affected by pCO_2, T, and pCO_2xDay (Table 14). Larvae exposed to Ambient-T contained less WE per symbiont density than larvae exposed to High-T (GLHT, Table 15; Fig. 13).

Changes in abundance of wax esters (WE) ranged from -12.851 μg $larva^{-1}$ (Middle HTHC; 65% depletion of initial levels) to +5.066 μg $larva^{-1}$ (Late ATAC; 23% increase from initial levels); significant effects included pCO_2xTxDay, pCO_2xDay and Day (Table 16). Post-hoc comparisons did not reveal any significant differences between temperature or pCO_2 treatments on different days (GLHT, Table 17; Fig. 14). For WE content standardized by total protein, significant effects included pCO_2xTxDay, TxDay, and Day (Table 16). Middle larvae consumed less WE under High-T than under Ambient-T (GLHT, Table 17; Fig. 14). When WE content was standardized by symbiont abundance, effects of pCO_2xDay, pCO_2, T, and Day were significant (Table 16). For Peak larvae, ΔWE did not differ in response to pCO_2. Conversely, Late larvae consumed more WE at High-pCO_2 (GLHT, Table 17; Fig. 14). Also, larvae consumed significantly more WE per symbiont density at Ambient-T than at High-T (GLHT, Table 17; Fig. 14).

Under various conditions of pCO_2 and temperature, the abundance of a biomolecule that confers a rapid source of energy, post-incubation levels of triacylglycerol (TAG) were significantly affected by pCO_2xT and Day (Table 14). Peak larvae contained significantly less TAG per larva than did Middle and Late larvae (GLHT, Table 15; Fig. 13). When TAG was standardized by protein content, only T was significant (Table 14). TAG per protein was higher for larvae incubated at High-T (Tukey's HSD, Table 15; Fig. 13). Per symbiont

Figure 13. Lipid composition of *P. damicornis* larvae following 24-hour exposures to combinations of pCO_2 and temperature. Mean ± SE (n = 6) changes in abundance of wax ester (WE), triacylglycerol (TAG) and phospholipid (PL) classes for larvae released on days Peak, Middle, and Late. Lipid quantities are standardized per larva (µg $lava^{-1}$), per protein (µg µg $total\ protein^{-1}$), and per symbiont density ([µg $symbiont\ cell^{-1}$]x10^{-3}). Experimental treatments: Ambient-T, Ambient-pCO_2 (ATAC), High-T, Ambient-pCO_2 (HTAC), Ambient-T, High-pCO_2 (ATHC), High-T, High-pCO_2 (HTHC). Refer to Tables 14 and 15 for statistical details.

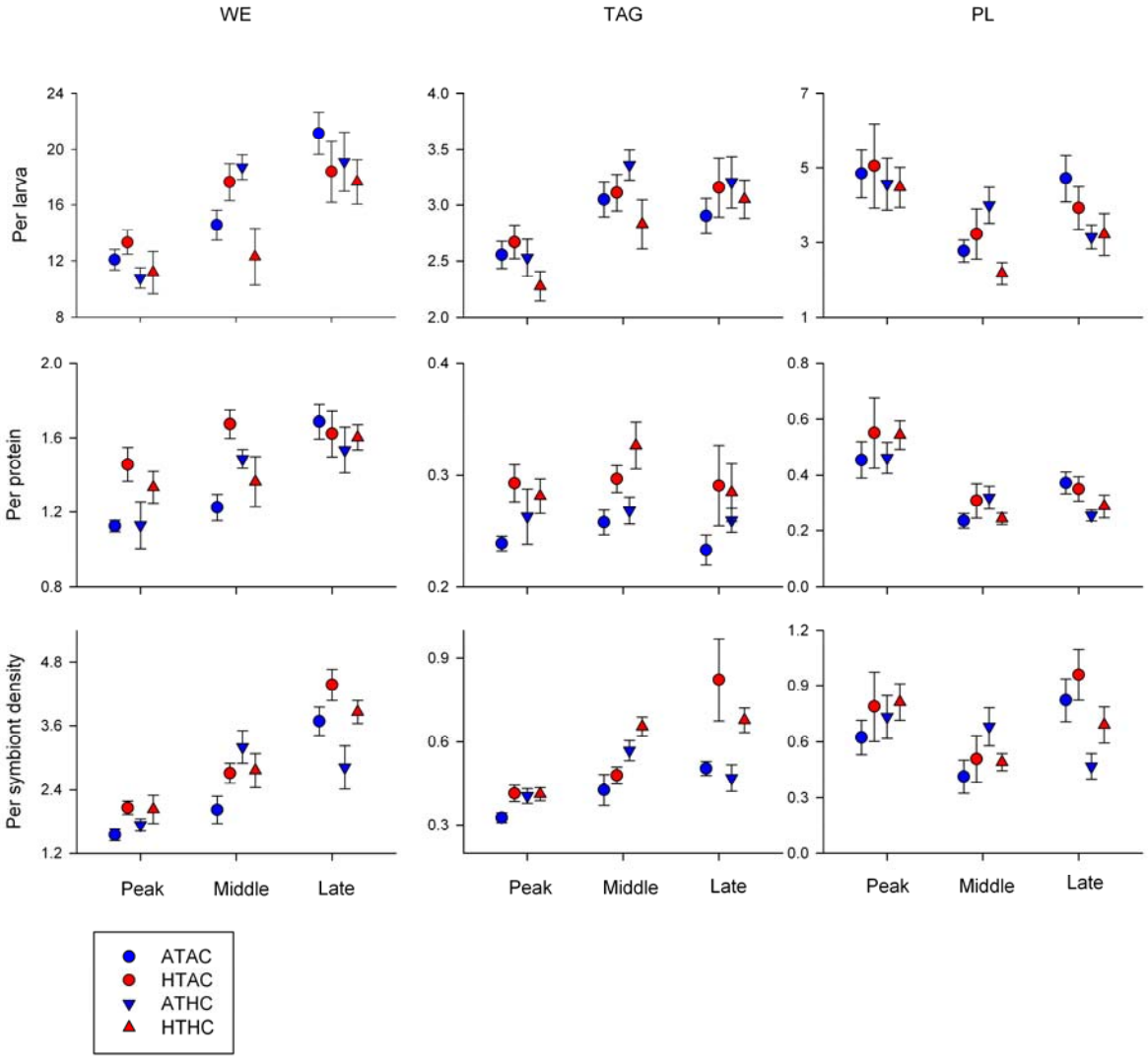

Table 16. Analysis of changes in abundance of lipid classes (wax ester WE, triacylglycerol TAG, phospholipid PL) in *P. damicornis* larvae among treatments and days of release, standardized to per larva (µg larva^{-1}), per larval protein content (µg µg total protein^{-1}), and per symbiont density (µg cell^{-1}). Comparisons were made using type III sum of squares with pCO_2, temperature (T), and day of release (Day) as fixed effects. The final reduced model is shown, with test statistic X^2, degrees of freedom (df) and p-values (*p*) reported. Interaction terms were removed from the model if the AIC value did not increase by 2 or more and if there was not a significant difference in the model log likelihood ratio; removed terms are not shown here.

	Per larva			**Per protein**			**Per symbiont density**		
ΔWE									
Effect	X^2	df	*p*	X^2	df	*p*	X^2	df	*p*
pCO_2	0.634	1	0.426	1.247	1	0.264	7.445	1	**0.006**
Temp	1.156	1	0.282	0.225	1	0.635	10.259	1	**0.001**
Day	8.459	2	**0.015**	35.452	2	**<0.001**	22.823	2	**<0.001**
pCO_2xT	0.130	1	0.719	0.472	1	0.492			
pCO_2xDay	6.086	2	**0.048**	4.946	2	0.084	13.617	2	**0.001**
TxDay	4.735	2	**0.094**	8.155	2	**0.017**			
pCO_2xTxDay	8.670	2	**0.013**	7.151	2	**0.028**			
ΔTAG									
Effect	X^2	df	*p*	X^2	df	*p*	X^2	df	*p*
pCO_2	2.081	1	0.149	1.054	1	0.384	2.764	1	0.869
Temp	1.114	1	0.291	12.599	1	0.323	23.642	1	0.096
Day	40.696	2	**<0.001**	76.505	2	0.097	4.023	2	**<0.001**
pCO_2xT	5.647	1	**0.018**						
pCO_2xDay							12.870	2	**0.002**
TxDay							11.719	2	**0.003**
pCO_2xTxDay									
ΔPL									
Effect	X^2	df	*p*	X^2	df	*p*	X^2	df	*p*
pCO_2	2.109	1	0.147	0.757	1	0.384	8.857	1	**0.003**
Temp	0.938	1	0.333	0.982	1	0.322	1.959	1	0.162
Day	2.815	2	0.245	4.677	2	0.097	8.895	2	**0.012**
pCO_2xT									
pCO_2xDay							10.252	2	**0.006**
TxDay									
pCO_2xTxDay									

Table 17. Post-hoc analyses for significant effects of treatment and day of release on changes in abundance of lipid classes (wax ester WE, triacylglycerol TAG, phospholipid PL) in *P. damicornis* larvae among treatments and days of release, standardized to per larva (µg larva^{-1}), per larval protein content (µg µg total protein^{-1}), and per symbiont density (µg cell^{-1}). Post-hoc tests were either Tukey's HSD or general linear hypothesis tests with Bonferroni corrections for multiple comparisons (GLHT). Test statistic z and p-values (*p*) are reported for each comparison.

Post-hoc test	Biological response	Significant effect	Comparison	z	*p*	Summary description
GLHT	ΔWE per larva	pCO_2xTxDay	Peak: Ambient-T vs. High-T	0.483	1.000	N/A
			Peak: Ambient-pCO_2 vs. High-pCO_2	0.502	1.000	
			Middle: Ambient-T vs. High-T	1.193	1.000	
			Middle: Ambient-pCO_2 vs. High-pCO_2	1.615	0.638	
			Late: Ambient-T vs. High-T	1.075	1.000	
			Late: Ambient-pCO_2 vs. High-pCO_2	0.796	1.000	
GLHT	ΔWE per protein	pCO_2xTxDay	Peak: Ambient-T vs. High-T	2.450	0.086	Middle: High-T > Ambient-T
			Peak: Ambient-pCO_2 vs. High-pCO_2	0.032	1.000	
			Middle: Ambient-T vs. High-T	3.307	**0.006**	
			Middle: Ambient-pCO_2 vs. High-pCO_2	1.940	0.315	
			Late: Ambient-T vs. High-T	0.474	1.000	
			Late: Ambient-pCO_2 vs. High-pCO_2	1.117	1.000	
GLHT	ΔWE per symbiont density	pCO_2xDay	Peak: Ambient-pCO_2 vs. High-pCO_2	0.028	1.000	Late: Ambient-pCO_2 > High-pCO_2
			Middle: Ambient-pCO_2 vs. High-pCO_2	2.256	0.096	
			Late: Ambient-pCO_2 vs. High-pCO_2	2.497	**0.050**	
		T	Ambient-T vs. High-T	2.688	**0.029**	Ambient-T < High-T
GLHT	ΔTAG per larva	pCO_2xT	ATAC vs. ATHC	1.381	0.836	N/A
			HTAC vs. HTHC	1.837	0.331	
		Day	Peak vs. Middle	2.189	0.143	Peak = Middle < Late
			Peak vs. Late	6.033	**<0.001**	
			Middle vs. Late	3.843	**0.001**	
Tukey's HSD	ΔTAG per protein	T	Ambient-T vs. High-T	2.806	**0.005**	Ambient-T < High-T
		Day	Peak vs. Middle	2.340	**0.051**	Peak = Middle < Late
			Peak vs. Late	8.345	**<0.001**	
			Middle vs. Late	6.005	**<0.001**	
GLHT	ΔTAG per symbiont density	pCO_2xDay	Peak: Ambient-pCO_2 vs. High-pCO_2	0.618	1.000	Late: Ambient-T < High-T
			Middle: Ambient-pCO_2 vs. High-pCO_2	2.542	0.066	
			Late: Ambient-pCO_2 vs. High-pCO_2	1.442	0.895	
			Peak: Ambient-T vs. High-T	0.770	1.000	
			Middle: Ambient-T vs. High-T	1.106	1.000	
			Late: Ambient-T vs. High-T	4.218	**<0.001**	
GLHT	ΔPL per symbiont density	pCO_2xDay	Peak: Ambient-pCO_2 vs. High-pCO_2	0.606	1.000	Late: Ambient-pCO_2 > High-pCO_2
			Middle: Ambient-pCO_2 vs. High-pCO_2	1.134	0.770	
			Late: Ambient-pCO_2 vs. High-pCO_2	2.828	**0.014**	

Figure 14. Changes in lipid composition of *P. damicornis* larvae over 24-hour exposures to combinations of pCO_2 and temperature. Mean ± SE (n = 6) changes in abundance of wax ester (WE), triacylglycerol (TAG) and phospholipid (PL) classes for larvae released on days Peak, Middle, and Late. Negative Δ values indicate net consumption over the experimental exposure. Positive Δ values indicate net production over 24 hours. Lipid quantities are standardized per larva (µg lava^{-1}), per protein (µg µg total protein^{-1}), and per symbiont density ([µg symbiont cell^{-1}]x10^{-3}). Experimental treatments: Ambient-T, Ambient-pCO_2 (ATAC), High-T, Ambient-pCO_2 (HTAC), Ambient-T, High-pCO_2 (ATHC), High-T, High-pCO_2 (HTHC). Refer to Tables 16 and 17 for statistical details.

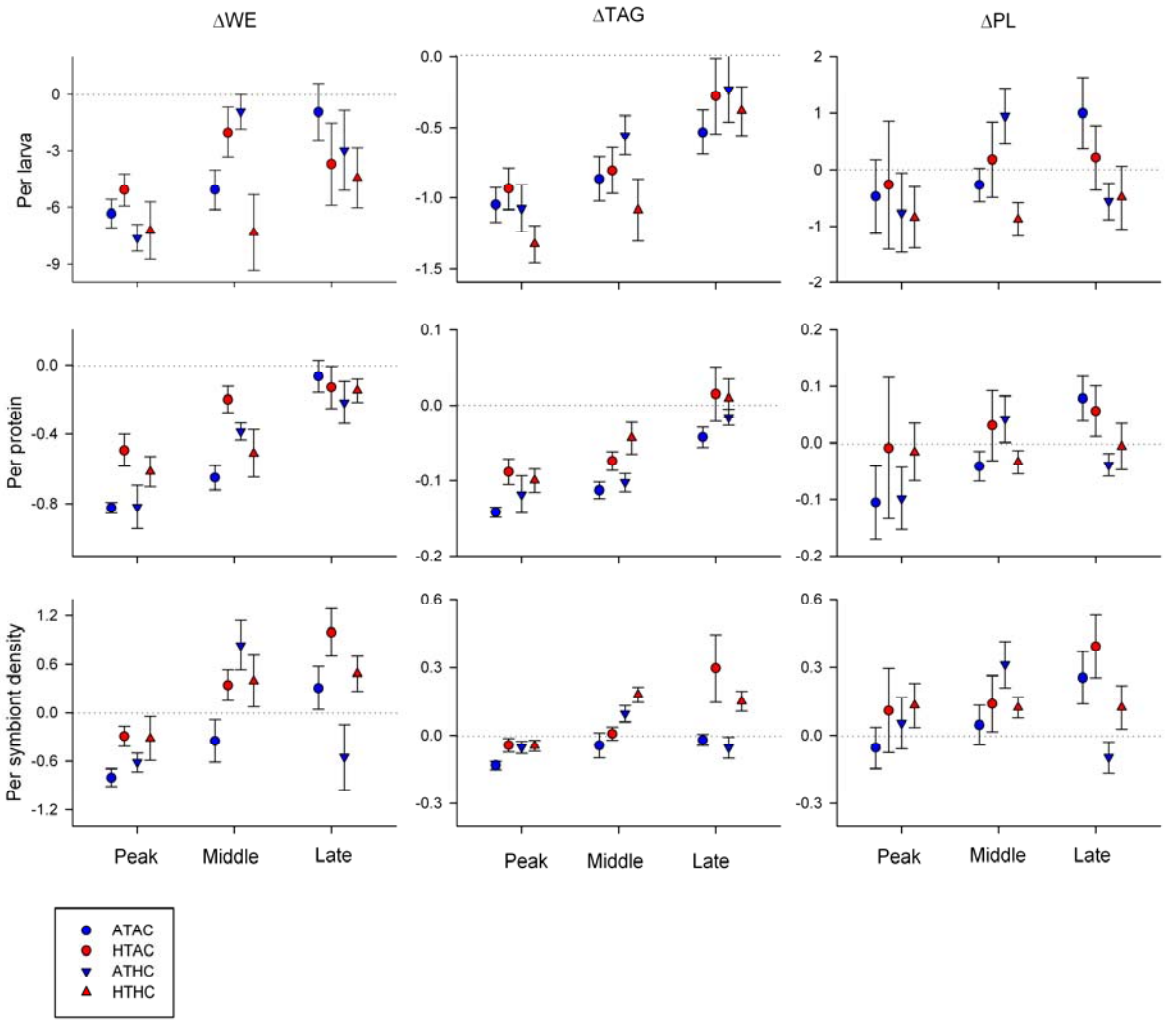

density, TAG varied by pCO_2xDay, TxDay, T, and Day (Table 14). For Late larvae, TAG was significantly greater at High-T than at Ambient-T (GLHT, Table 15; Fig. 13).

Changes in TAG varied between -1.800 μg $larva^{-1}$ (Peak HTHC; 50% depletion of initial levels) and +0.768 μg $larva^{-1}$ (Late HTAC; 22% increase from initial levels); effects of CO_2xT and Day were significant (Table 16). However, post-hoc comparisons of ΔTAG between pCO_2 treatments by temperature level were not significantly different (GLHT). Peak and Middle larvae consumed significantly more TAG than Late larvae (GLHT, Table 17; Fig. 14). Protein-standardized ΔTAG levels differed significantly by T and Day, but not pCO_2 and with no significant interactions between effects (Table 16). Larvae consumed less TAG at High-T than at Ambient-T (Tukey's HSD, Table 17; Fig. 14). Peak and Middle larvae consumed significantly more TAG than Late larvae (Tukey's HSD, Table 17; Fig. 14). Significant effects included TxDay, pCO_2xDay, and Day for ΔTAG per larval symbiont abundance (Table 16). Temperature had a significant effect on ΔTAG on Late larvae, with more TAG production at High-T (GLHT, Table 17; Fig. 14).

Phospholipids (PL) served as a rough indicator of cell number and important structural molecules. Post-incubation levels of PL per larva and per protein were significantly affected by Day (Table 14). Peak larvae contained more post-incubation PL than Middle and Late larvae (Tukey's HSD, Table 15; Fig. 13). When standardized by symbiont density, PL varied significantly by pCO_2xDay, pCO_2 and Day (Table 14). Late larvae contained more PL per symbiont density at Ambient-pCO_2 than at High-pCO_2 (GLHT, Table 15; Fig. 13).

Changes in abundance of PL ranged from -4.004 μg $larva^{-1}$ (Peak HTAC; 75% depletion) to +3.465 μg $larva^{-1}$ (Middle HTAC; >100% increase). For ΔPL expressed per larva and per protein, no effects or their interactions explained a significant amount of the

variation (Table 16). However, for ΔPL per symbiont density, effects of pCO_2xDay, pCO_2, and Day were significant (Table 16). Late larvae produced significantly more PL at Ambient-CO_2 than at High-CO_2 (GLHT, Table 17; Fig. 14).

Changes in larval quality in response to different pCO_2 and temperature levels were measured in the form of total lipid (TL), total protein (TP), and symbiont density. At the end of the 24-hour exposures, TL was significantly affected by pCO_2xDay, T, and Day (Table 18). However post-hoc analyses did not reveal any significant differences (GLHT, Table 19; Fig. 15). When TL was normalized to protein content, only T was significant (Table 18). TL per protein was greater at Ambient-T than at High-T (Tukey's HSD, Table 19; Fig. 15). When normalized to symbiont density, TL was significantly affected by TxDay and T (Table 18), but post-hoc analyses did not reveal significant differences (GLHT, Table 19; Fig. 15). TP per larva was significantly affected by Day (Table 18), with Late larvae containing more TP than Peak or Middle larvae (Tukey's HSD, Table 19; Fig. 15). When normalized to symbiont density, TP varied significantly by pCO_2xDay, TxDay, T, and Day (Table 18). For Late larvae, TP was greater at High-T than at Ambient-T (GLHT, Table 10; Fig. 15). Symbiont density varied significantly by pCO_2xDay, pCO_2, and T (Table 18). Middle larvae contained more *Symbiodinium* at Ambient-pCO_2 than at High-pCO_2 (GLHT, Table 19; Fig. 15). In general, symbiont density was higher at Ambient-T than at High-T (GLHT, Table 19; Fig. 15). Larval area was significantly affected by Day (Table 18), with larger area in Late larvae than in Peak or Middle larvae (Tukey's HSD, Table 19; Fig. 15). Larval length varied by pCO_2 only (Table 18). Length was greater at High-pCO_2 than at Ambient-pCO_2 (Tukey's HSD, Table 19; Fig. 15).

Table 18. Analysis of absolute values of indices of physiological condition in *P. damicornis* larvae following a 24-hour exposure to seawater of controlled temperature and pCO_2. Physiological condition was compared among treatments and days of release, standardized to per larva (μg $larva^{-1}$), per larval protein content (μg μg total $protein^{-1}$), and per symbiont density (μg $cell^{-1}$), unless otherwise noted. Indices include total lipid (TL), total protein (TP), symbiont density, and larval size. Comparisons were made using type III sum of squares with pCO_2, temperature (Temp), and day of release (Day) as fixed effects. The final reduced model is shown, with test statistic X^2, degrees of freedom (df) and p-values (*p*) reported. Interaction terms were removed from the model if the AIC value did not increase by 2 or more and if there was not a significant difference in the model log likelihood ratio; removed terms are not shown here.

	Per larva			**Per protein**			**Per symbiont density**		
TL									
Effect	X^2	df	*p*	X^2	df	*p*	X^2	df	*p*
pCO_2	3.774	1	0.052	0.101	1	0.750	0.138	1	0.710
Temp	7.874	1	**0.005**	4.875	1	**0.027**	7.185	1	**0.007**
Day	7.751	2	**0.021**	4.313	2	0.116	5.449	2	0.066
pCO_2xT									
pCO_2xDay	7.549	2	**0.023**						
TxDay							9.820	2	**0.007**
pCO_2xTxDay									
TP									
Effect	X^2	df	*p*				X^2	df	*p*
pCO_2	0.331	1	0.565				3.374	1	0.066
Temp	3.139	1	0.076				16.995	1	**<0.001**
Day	69.156	2	**<0.001**				25.669	2	**<0.001**
pCO_2xT									
pCO_2xDay							14.055	2	**0.001**
TxDay							7.947	2	**0.019**
pCO_2xTxDay									

	Symbiont per larva (μg $cell^{-1}$)			**Larval area (mm^2)**			**Larval length (mm)**		
Effect	X^2	df	*p*	X^2	df	*p*	X^2	df	*p*
pCO_2	0.913	1	0.339	1.196	1	0.274	5.385	1	**0.020**
Temp	11.543	1	**0.001**	2.841	1	0.092	3.336	1	0.068
Day	10.921	2	**0.004**	25.415	2	**<0.001**	5.427	2	0.066
pCO_2xT									
pCO_2xDay	7.1415	2	**0.028**						
TxDay									
pCO_2xTxDay									

Table 19. Post-hoc analyses for significant effects of treatment and day of release on absolute values of indices of physiological condition in *P. damicornis* larvae. Values were standardized to per larva (μg larva^{-1}), per larval protein content (μg μg total protein^{-1}), and per symbiont density (μg cell^{-1}), unless otherwise noted. Indices include total lipid (TL), total protein (TP), symbiont density, and larval size. Post-hoc tests were either Tukey's HSD or general linear hypothesis tests with Bonferroni corrections for multiple comparisons (GLHT). Test statistic z and p-values (*p*) are reported for each comparison.

Post-hoc test	Biological response	Significant effect	Comparison	z	*p*	Summary description
Tukey's HSD	TL per larva	pCO_2xDay	Peak: Ambient-pCO_2 vs. High-pCO_2	0.350	1.000	N/A
			Middle: Ambient-pCO_2 vs. High-pCO_2	1.719	0.343	
			Late: Ambient-pCO_2 vs. High-pCO_2	1.774	0.304	
		T	Ambient-T vs. High-T	2.260	0.095	
Tukey's HSD	TL per protein	T	Ambient-T vs. High-T	2.108	**0.035**	Ambient-T > High-T
Tukey's HSD	TL per symbiont density	TxDay	Peak: Ambient-T vs. High-T	0.525	1.000	N/A
			Middle: Ambient-T vs. High-T	0.710	1.000	
			Late: Ambient-T vs. High-T	2.348	**0.057**	
Tukey's HSD	TP per larva	Day	Peak vs. Middle	0.735	0.743	Peak < Middle = Late
			Peak vs. Late	7.252	**<0.001**	
			Middle vs. Late	6.517	**<0.001**	
GLHT	TP per symbiont density	TxDay	Peak: Ambient-T vs. High-T	1.122	1.000	Late: Ambient-T < High-T
			Middle: Ambient-T vs. High-T	0.801	1.000	
			Late: Ambient-T vs. High-T	3.502	**0.003**	
		pCO_2xDay	Peak: Ambient-pCO_2 vs. High-pCO_2	1.293	1.000	N/A
			Middle: Ambient-pCO_2 vs. High-pCO_2	2.200	0.167	
			Late: Ambient-pCO_2 vs. High-pCO_2	1.560	0.712	
GLHT	Symbiont density	pCO_2xDay	Peak: Ambient-pCO_2 vs. High-pCO_2	1.609	0.431	Middle: High-pCO_2 < Ambient-pCO_2
			Middle: Ambient-pCO_2 vs. High-pCO_2	2.483	**0.052**	
			Late: Ambient-pCO_2 vs. High-pCO_2	0.883	1.000	
		T	Ambient-T vs. High-T	3.140	**0.007**	Ambient-T > High-T
Tukey's HSD	Larval area	Day	Peak vs. Middle	1.993	0.130	Peak = Middle < Late
			Peak vs. Late	4.952	**<0.001**	
			Middle vs. Late	2.993	**0.008**	
Tukey's HSD	Larval length	pCO_2	Ambient-pCO_2 vs. High-pCO_2	2.296	**0.022**	Ambient-pCO_2 > High-pCO_2

Figure 15. Larval quality traits for *P. damicornis* larvae following 24-hour exposures to pCO_2 and temperature. Mean ± SE (n = 3) changes in larval composition and size for larvae released on days Peak, Middle, and Late. Quality traits are standardized per larva (µg lava^{-1}), per protein (µg µg total protein^{-1}), and per symbiont density ([µg symbiont cell^{-1}]x10^{-3}) unless otherwise noted. Experimental treatments: Ambient-T, Ambient-pCO_2 (ATAC), High-T, Ambient-pCO_2 (HTAC), Ambient-T, High-pCO_2 (ATHC), High-T, High-pCO_2 (HTHC). Refer to Tables 18 and 19 for statistical details.

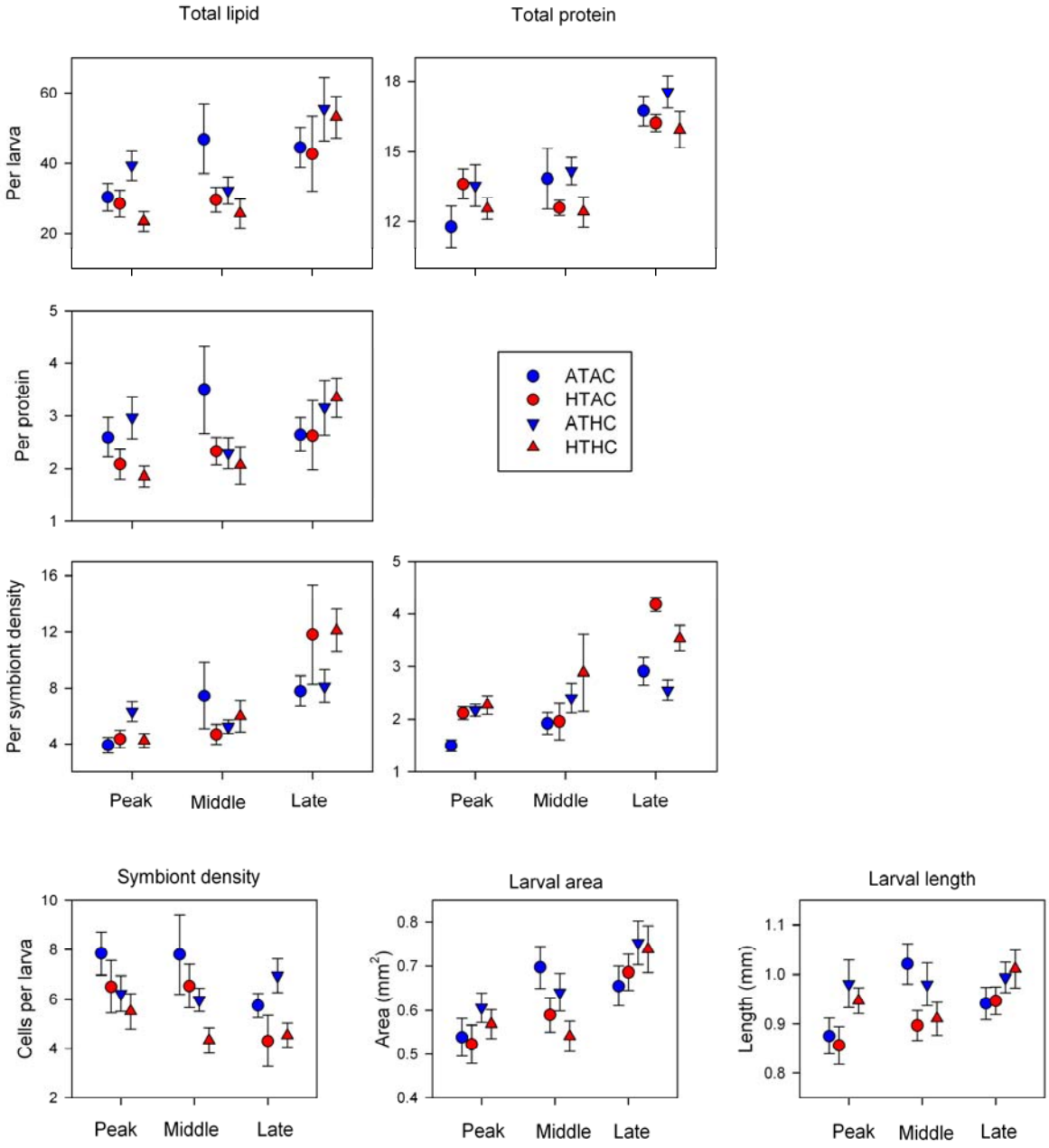

Per larva, ΔTL varied between -23.236 μg larva^{-1} (Middle HTHC; 65% depletion) and +57.021 μg larva^{-1} (Late ATHC; >100% increase). Regardless of the standardization method, ΔTL varied significantly by Temp and Day (Table 20). In each case, larvae incubated at High-T consumed more TL than at Ambient-T (Tukey's HSD, Table 21; Fig. 16). For each expression of ΔTL, Late larvae produced significantly more TL over 24 hours than other cohorts (Tukey's HSD, Table 21; Fig. 16).

ΔTP per larva ranged from -4.503 μg larva^{-1} (Middle ATAC; 30% depletion) to +4.885 μg larva^{-1} (Late ATHC; 34% increase); only the effect of Day was significant (Table 20). Larval ΔTP were significantly more negative for Middle larvae than Peak and Late larvae (Tukey's HSD, Table 21; Fig. 16). When standardized by larval symbiont density, significant effects included pCO_2xTxDay and pCO_2xDay (Table 20). However, post-hoc comparisons did not reveal any significant differences between temperature or pCO_2 treatments on different days (GLHT, Table 21; Fig. 16).

Per larva, changes in symbiont abundance ranged from -4697.22 cells larva^{-1} (Middle ATAC; 57% decrease from initial levels) to +2394.44 cells larva^{-1} (Late ATHC; 37% increase from initial levels). Model effects of pCO_2xDay and T were significant (Table 20). Multiple comparisons revealed that only for Middle larvae did symbiont abundance per larva change significantly with pCO_2 (GLHT, Table 21; Fig. 16). Symbiont density decreased significantly with temperature (GLHT, Table 21; Fig. 16). Larval area varied significantly by Day only (Table 20). Middle larvae became significantly smaller in area than other cohorts (Tukey's HSD, Table 21; Fig. 16). Changes in larval length ranged from -722.14 μm (Middle ATHC; 55% reduction) to +784.81 μm (Peak ATHC; 85% increase); significant effects included CO_2 and Day (Table 20). Larval length decreased more at High-pCO_2 than at

Table 20. Analysis of changes in indices of physiological condition in *P. damicornis* larvae among treatments and days of release, standardized to per larva (µg larva^{-1}), per larval protein content (µg µg total protein^{-1}), and per symbiont density (µg cell^{-1}), unless otherwise noted. Indices include total lipid (TL), total protein (TP), symbiont density, larval size. Comparisons were made using type III sum of squares with pCO_2, temperature (Temp), and day of release (Day) as fixed effects. The final reduced model is shown, with test statistic X^2, degrees of freedom (df) and p-values (*p*) reported. Interaction terms were removed from the model if the AIC value did not increase by 2 or more and if there was not a significant difference in the model log likelihood ratio; removed terms are not shown here.

	Per larva			**Per protein**			**Per symbiont density**		
ΔTL									
Effect	X^2	df	*p*	X^2	df	*p*	X^2	df	*p*
pCO_2	0.001	1	0.975	0.187	1	0.666	0.001	1	0.975
Temp	5.427	1	**0.020**	4.069	1	**0.044**	5.427	1	**0.020**
Day	30.828	2	**<0.001**	14.438	2	**<0.001**	11.897	2	**0.003**
pCO_2xT									
pCO_2xDay									
TxDay									
pCO_2xTxDay									
ΔTP									
Effect	X^2	df	*p*				X^2	df	*p*
pCO_2	0.331	1	0.565				0.070	1	0.792
Temp	3.139	1	0.077				0.788	1	0.375
Day	65.951	2	**<0.001**				0.307	2	0.858
pCO_2xT							0.269	1	0.604
pCO_2xDay							7.219	2	**0.027**
TxDay							1.883	2	0.390
pCO_2xTxDay							5.933	2	**0.052**
	Δ Symbiont per larva (µg cell^{-1})			**Δ Larval area (mm^2)**			**Δ Larval length (mm)**		
Effect	X^2	df	*p*	X^2	df	*p*	X^2	df	*p*
pCO_2	0.913	1	0.339	1.196	1	0.274	5.385	1	**0.020**
Temp	11.543	1	**0.001**	2.841	1	0.092	3.336	1	0.068
Day	1.277	2	0.528	53.661	2	**<0.001**	239.428	2	**<0.001**
pCO_2xT									
pCO_2xDay	7.142	2	**0.028**						
TxDay									
pCO_2xTxDay									

Table 21. Post-hoc analyses for significant effects of changes in indices of physiological condition in *P. damicornis* larvae among treatments and days of release, standardized to per larva (µg larva^{-1}), per larval protein content (µg µg total protein^{-1}), and per symbiont density (µg cell^{-1}), unless otherwise noted. Indices include total lipid (TL), total protein (TP), symbiont density, larval size. Post-hoc tests were either Tukey's HSD or general linear hypothesis tests with Bonferroni corrections for multiple comparisons (GLHT). Test statistic z and p-values (*p*) are reported for each comparison.

Post-hoc test	Biological response	Significant effect	Comparison	z	*p*	Summary description
Tukey's HSD	ΔTL per larva	T	Ambient-T vs. High-T	1.984	**0.047**	Ambient-T > High-T
		Day	Peak vs. Middle	0.017	1.000	Peak = Middle < Late
			Peak vs. Late	4.713	**<0.001**	
			Middle vs. Late	4.743	**<0.001**	
Tukey's HSD	ΔTL per protein	T	Ambient-T vs. High-T	1.937	**0.053**	Ambient-T > High-T
		Day	Peak vs. Middle	1.713	0.200	Peak = Middle < Late
			Peak vs. Late	3.648	**0.001**	
			Middle vs. Late	2.036	0.104	
Tukey's HSD	ΔTL per symbiont density	T	Ambient-T vs. High-T	1.984	**0.047**	Ambient-T > High-T
		Day	Peak vs. Middle	0.452	0.893	Peak = Middle < Late
			Peak vs. Late	3.113	**0.005**	
			Middle vs. Late	2.709	**0.019**	
Tukey's HSD	ΔTP per larva	T	Ambient-T vs. High-T	1.523	0.128	N/A
		Day	Peak vs. Middle	-5.361	**<0.001**	Middle < Peak = Late
			Peak vs. Late	2.221	0.068	
			Middle vs. Late	7.582	**<0.001**	
GLHT	ΔTP per symbiont density	pCO_2xTxDay	Peak: Ambient-T vs. High-T	1.200	1.000	N/A
			Peak: Ambient-pCO_2 vs. High-pCO_2	1.988	0.281	
			Middle: Ambient-T vs. High-T	2.311	0.125	
			Middle: Ambient-pCO_2 vs. High-pCO_2	0.925	1.000	
			Late: Ambient-T vs. High-T	0.888	1.000	
			Late: Ambient-pCO_2 vs. High-pCO_2	0.264	1.000	
GLHT	Symbiont density	pCO_2xDay	Peak: Ambient-pCO_2 vs. High-pCO_2	1.601	0.431	Middle: High-pCO_2 >
			Middle: Ambient-pCO_2 vs. High-pCO_2	2.483	**0.052**	Ambient-pCO_2
			Late: Ambient-pCO_2 vs. High-pCO_2	0.883	1.000	
		T	Ambient-T vs. High-T	3.140	**0.007**	Ambient-T > High-T
Tukey's HSD	Larval area	Day	Peak vs. Middle	4.962	**<0.001**	Middle < Peak = Late
			Peak vs. Late	2.133	0.083	
			Middle vs. Late	7.065	**<0.001**	
Tukey's HSD	Larval length	pCO_2	Ambient-pCO_2 vs. High-pCO_2	2.296	**0.022**	Ambient-pCO_2 > High-pCO_2
		T	Ambient-T vs. High-T	1.807	0.071	N/A
		Day	Peak vs. Middle	13.540	**<0.001**	Middle < Peak = Late
			Peak vs. Late	0.500	0.871	
			Middle vs. Late	13.000	**<0.001**	

Figure 16. Changes in larval quality traits for *P. damicornis* larvae over 24-hour exposures to pCO_2 and temperature. Mean ± SE (n = 6) changes in larval composition and size for larvae released on days Peak, Middle, and Late. Negative Δ values indicate net consumption over the experimental exposure. Positive Δ values indicate net production over 24 hours. Quality traits are standardized per larva (µg $lava^{-1}$), per protein (µg µg $total\ protein^{-1}$), and per symbiont density ([µg $symbiont\ cell^{-1}$]x10^{-3}) unless otherwise noted. Experimental treatments: Ambient-T, Ambient-pCO_2 (ATAC), High-T, Ambient-pCO_2 (HTAC), Ambient-T, High-pCO_2 (ATHC), High-T, High-pCO_2 (HTHC). Refer to Tables 20 and 21 for statistical details.

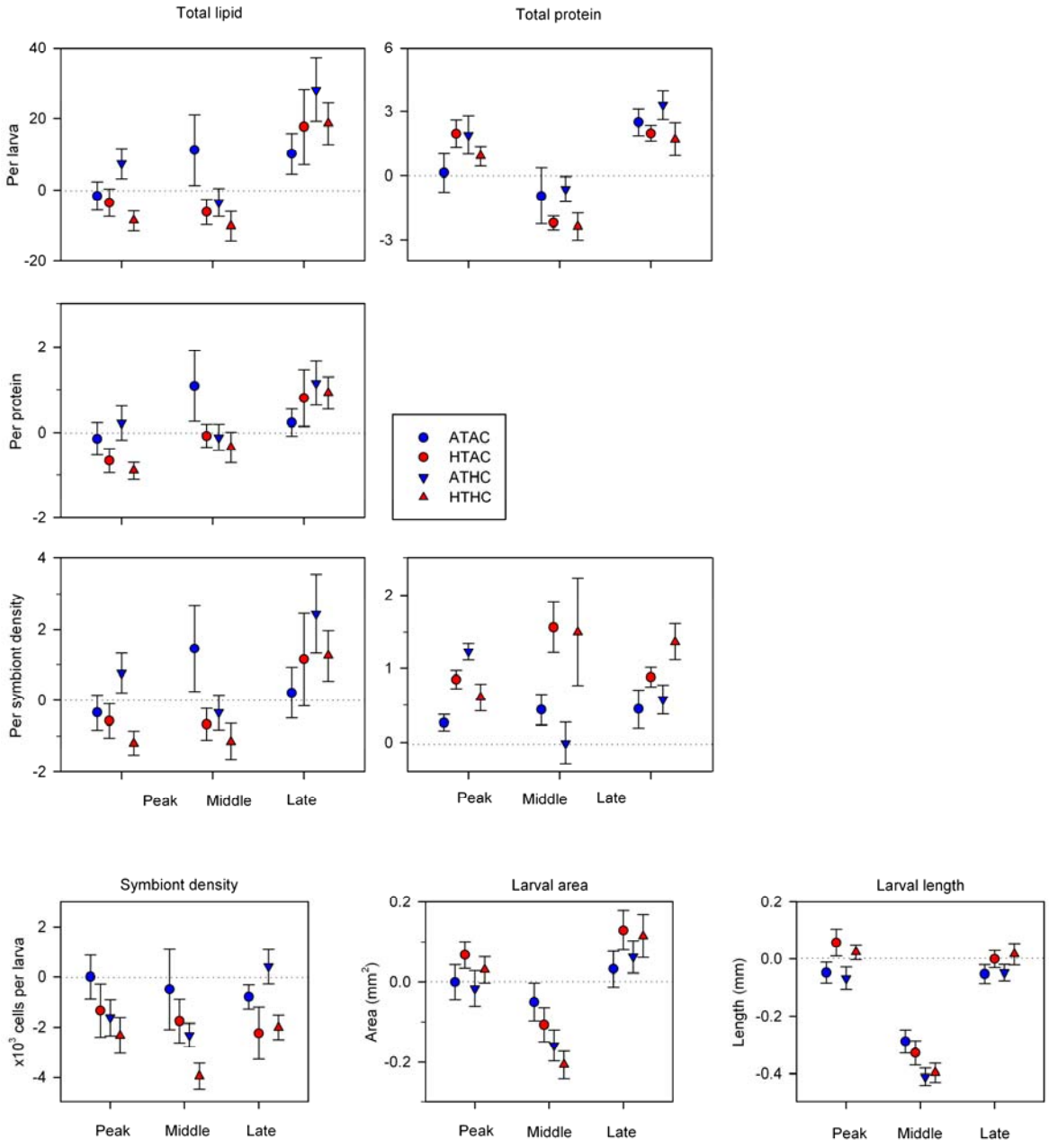

Ambient-pCO_2 (Tukey's HSD, Table 21; Fig. 16). Middle larvae became significantly smaller in length than other cohorts (Tukey's HSD, Table 21; Fig. 16).

Discussion

The objective of this study was to test the hypothesis that lipids have important physiological and ecological roles in larvae of stony corals, providing long-term energy storage as well as buoyancy for dispersal. I sought to examine this connection between physiology and ecology in the light of environmental change. An experimental approach was taken where larvae were exposed to varying conditions of pCO_2 and temperature in the laboratory, and changes in lipid content and physiological condition were measured. My results demonstrate that *P. damicornis* larvae utilized lipid stores differently in response to experimental manipulations that mimicked OA and warming. If these changes in lipid significantly affect the buoyancy of larvae and the length of time they can remain competent as planuale, future ocean conditions may have consequences for their dispersal potential. However, the day the larvae are released often has a dominant influence on lipid utilization and physiological condition of the planulae.

Observations on maternal investment in P. damicornis *larvae*

Larvae released from *P. damicornis* colonies were similar in biochemical composition regardless of day of release. In general, maternal investment did not differ significantly between broods of larvae in terms of endowment of energy storage lipids, TL, and TP. In addition, symbiont density did not vary between consecutive cohorts. As a result,

broods released on each of three days had similar potential to meet energy demands, as ecological units. However, Late larvae contained elevated levels of WE with respect to symbiont density and lower levels of TAG with respect to protein content. These Late larvae may have fewer energy stores to meet immediate stochastic energy demands following release due to their lack of liquid energy assets (*i.e.* TAG). Instead, their energy metabolism may be more influenced by the rate limits of carbon-fixation and translocation by symbionts and by energy conversion from long-term storage molecules (WE).

Although PL levels did not differ between cohorts, larval size did vary. Middle larvae were larger in area and length than those released on other days. In general, pocilloporid larvae of larger size can have longer lifespans than smaller larvae (Isomura and Nishihira, 2001), which may give them greater dispersal potential (Marshall and Keough, 2003). Dispersal could be advantageous for increasing the likelihood that the larvae will find a suitable or new habitat for settlement, but dispersal may also take larvae away from the hospitable environment of their parents (Strathmann, 1974; Morgan, 1995; Pechenik, 1999; Marshall and Keough, 2003). Additionally, large larvae may better escape predation by small planktivores, but a longer dispersal means that they have a higher risk of encountering predators (Morgan, 1995). The mechanistic connection between larval size and long dispersal time for lecithotrophic (non-feeding) larvae, as in those of *P. damicornis*, is that larger size implies greater stores of energy in the form of lipids, protein, and symbionts. In this case, Middle larvae did have slightly higher levels of TAG, TL, and TP, though not significantly different from larvae released on other days. However, their size may disguise the limitations of their physiological abilities to produce and use energy (*e.g.* metabolic rate, *Symbiodinium*

physiology), and therefore larval size may not always be a good indicator of dispersal potential.

This study supports previous findings that maternal provisioning of *P. damicornis* planulae varies across the entire release period while planulae released close to the Peak day are very similarly endowed in terms of biochemical content (Putnam et al., 2010; Cumbo et al., 2012). In other brooding species, such as a Caribbean coral *Porites astreoides*, larvae released later during a reproduction event have higher concentrations of *Symbiodinium* and higher potential for autotrophy (Edmunds et al., 2001). Here, variation in investments between adults and variation in proportions of the larval pool represented by each parent may overshadow subtle changes in maternal provisioning between adjacent release days.

Responses of larval energy metabolism and fitness-related traits to changes in pCO_2 and temperature

In brooded larvae, like *P. damicornis*, the WE quantified at the beginning of the experiment was provided by the parent. Once in the plankton, changes in WE abundance represent a balance of the energy metabolism of the larvae and the carbon fixation activities of its symbionts. Carbon translocated to the coral animal tissue is stored as lipids (Patton et al., 1977; Patton and Burris, 1983; Battey and Patton, 1984). *P. damicornis* larvae consumed more than 25% of their WE during the first 24 hours of their pelagic duration. This rate does not reflect any translocated carbon that was consumed as well. In general, this consumption rate declined as the spawning period progressed. Additionally, the energy metabolism of these larvae became slightly more sensitive to abiotic stress as the reproductive window closed. Over the three days of the experiment, the interaction of pCO_2 and T on WE

consumption changed such that Peak larvae consumed more WE under High-pCO_2 but Late larvae consumed more under both High-pCO_2 and High-T (Fig. 14). Under these High-pCO_2 conditions, larvae contained lower WE content after 24 hours (Fig. 13). Also, for Peak and Middle larvae, under Ambient-pCO_2 conditions, WE consumption was often less at High-T than at Ambient-T, suggesting that symbiont performance at elevated temperature can perhaps fuel a greater portion of physiological maintenance. However, for Late larvae, this relationship was reversed, where WE consumption rates were greater, and therefore final WE density was lower, for single-stressor and multi-stressor treatments than in the control. Shifts in WE consumption due to temperature and pCO_2 were not heavily influenced by the variation attributed to larval size, as controlling for differences in larval size, using holobiont TP, did not dramatically alter these relationships.

The *Symbiodinium* in *P. damicornis* larvae help satisfy the energetic demands of dispersal (Arai et al., 1993; Lee et al., 2006b; Harii et al., 2010); indeed aposymbiotic coral larvae (*Goniastrea retiformis*, *Pocillopora damicornis*, *Montiopora digitata*) consume about twice as much WE during their first week than do symbiotic larvae (Harii et al., 2010; Figueiredo et al., 2012). Because *Symbiodinium* fix carbon and provide the means by which larvae can replenish their lipid reserves or avoid consumption of maternally-derived lipids, *Symbiodinium* abundance with respect to changes in WE in larvae provides important insight into how vulnerable the larvae are to future demands on their energy budget. When ΔWE was normalized to symbiont density, WE consumption rates were still significantly different between treatment groups, suggesting that host respiration and not *Symbiodinium* abundance alone may drive patterns of WE consumption in *P. damicornis* larvae. Based on my measurements of oxygen consumption of *P. damicornis* larvae to laboratory exposures to

pCO_2 and temperature, I estimated the amount of WE required to fuel aerobic respiration during the various treatment exposures. In Chapter 2, I measured 0.07-0.15 nmol O_2 consumed $larva^{-1}$ min^{-1}. Based on the oxy-joule coefficient for lipid (19.63 J mL O_2 $consumed^{-1}$; Davies, 1991) and the energy equivalent for wax ester (42 kJ g $wax\ ester^{-1}$; Davies, 1991), and assuming constant rates of respiration during the exposures, larvae would need to consume 1.16-2.49 μg WE over the 24-hour incubation. In this study, I measured rates of WE depletion of up to 9 μg WE $larva^{-1}$ consumed within 24 hours. However, once symbiont density was controlled for, WE depletion was ≤ 1 μg within 24 hours. The remaining fuel for respiration likely came from symbiont photosynthetic activities as well as other lipid classes. In general, larvae lost *Symbiodinium* cells when High-CO_2 and High-T were imposed, and in these treatments, symbiont-normalized WE consumption was less. If symbiont abundance did not affect WE consumption at all, patterns of symbiont-specific ΔWE would have been similar to those of ΔWE per larva. For Peak larvae, treatment effects on ΔWE were greater than those caused by symbiont abundance itself, and larvae in all treatments exhibited net consumption of WE when controlling for variation in symbiont abundance. For Middle and Late larvae, loss of symbionts likely resulted in the net increase in WE in most treatments, but differential performance of remaining symbionts may also have played a role. For example, in Late larvae, High-pCO_2 caused more WE consumption, but the positive effect of High-T on symbionts may have counteracted the costs of pCO_2 tolerance, resulting in net WE increase at High-pCO_2, High-T. Also, in adult *Montipora capitata*, recovery of lipid levels following a bleaching event were coincident with increases in gross photosynthesis (Rodrigues and Grottoli, 2007). While a previous study with *P. damicornis* larvae in Taiwan found no change in photophysiology in response to elevated T

and pCO_2 after 9 days (Putnam et al., 2013), any initial effects of treatment occurring within the first 24 hours may have been masked by a general increase in symbiont density over the long exposure duration (*e.g.* Cumbo et al., 2013b). The observed patterns in larvae released on days Middle and Late could also be explained by metabolic depression in the animal component of the larvae, which has been observed in response to High-pCO_2 for this Moorea population (Rivest and Hofmann, 2014).

Combining the results of all three comparisons of ΔWE, both temperature and pCO_2 have effects on WE consumption in *P. damicornis* larvae, and these effects were mediated by the influence of day of release. For Peak larvae and larvae in High-T, High-pCO_2 treatments, greater consumption and lower final densities of WE in general may translate to greater mortality or faster settlement rates in these groups (*e.g.* Harii et al., 2010). The ΔWE per larva roughly translates to a loss of 20-50% of their buoyancy (WE density: 0.86 g WE L^{-1}, Phleger, 1998; WE buoyancy: +0.165 g buoyancy mL WE^{-1}, Sargent, 1976), which will likely affect dispersal potential of Peak larvae and larvae in High-T, High-pCO_2 treatments. Finally, while coral lipid content, especially WE and TAG, is known to decrease in response to thermal bleaching (Stimson, 1987; Fitt et al., 2000; Oku et al., 2003; Grottoli et al., 2004), our study provides preliminary evidence that symbiont performance may play an important role in mediating the negative effects of exposures to single or multiple stressors.

TAG levels were less sensitive to the effects of pCO_2 and T. However, because turnover rates of this lipid class are more rapid, it is possible that equivalent consumption rates represent different rates of turnover of TAG pools. Even so, larvae under HTHC may have had greater energy demands, consuming TAG beyond turnover in control rates, particularly for Peak and Middle larvae. With respect to changes in symbiont density,

changes in symbiont abundance had an effect on changes in TAG, perhaps more so than the experimental treatments. Again, High-pCO_2 was energetically costly to tolerate, with Peak larvae consuming TAG beyond the effect of symbiont abundance. Together with the observed changes in WE, Peak larvae are likely utilizing both WE and TAG pools to fuel responses to High-pCO_2 conditions while larvae released later in the spawning period consume less.

TAG is important for energy metabolism of coral larvae due to its likely double role as storage of saturated fatty acids (energy) and as a reservoir of poly-unsaturated fatty acids, which are used to build structural lipids and in metabolic pathways (Napolitano et al., 1988; Lee et al., 2006b). In other marine invertebrate larvae, TAG is essential fuel for major developmental changes, including metamorphosis (Holland and Walker, 1975; Gallager et al., 1986; Moran and Manahan, 2003). Because *P. damicornis* larvae can settle within hours of their release, TAG may be especially important as a rapid energy source. Consequently, larvae at HTHC may settle more quickly as they deplete TAG most rapidly (Fig. 14) and contain lower densities of TAG after 24 hours (Fig. 4); under these conditions, larval dispersal may be limited.

Phospholipids are important for the structural function of coral larvae as well as for formation of cell membranes (Lee et al., 1971, 2006b). PL content of *P. damicornis* larvae remained unchanged over 24 hours in the different temperature and pCO_2 treatments. Harii et al. (2007) found that PL did not vary over 30 days for *Acropora tenuis* planulae maintained in culture. However, changes in symbiont abundance within larvae could cause significant variation in PL content; loss of *Symbiodinium* during the exposure would remove their contribution to larval holobiont PL. Once variation in symbiont density was controlled for, *P.*

damicornis larvae exhibited an increase in PL at Ambient-pCO_2 vs. High-pCO_2, most noticeable for Late larvae. Lower PL at High-pCO_2 could be explained by metabolic suppression; if larvae lowered their metabolic rates in response to OA, physiological processes involved with structural changes associated with development and preparation for settlement would likely be slowed or stopped altogether (***e.g.*** Michaelidis et al., 2005).

Traits of planulae related to size and growth also changed in response to elevated temperature and pCO_2. For larvae of species like *P. damicornis* that are brooded and lecithotrophic, or non-feeding, potential for growth during planula dispersal comes from the contribution of their symbionts to their energy metabolism. Although this contribution can satisfy their metabolic needs, TL commonly declines during dispersal (Richmond, 1987; Harii et al., 2002, 2010). While less is known about whether coral larval size also changes during dispersal, size of temperate marine invertebrate larvae usually decreases during their planktonic duration (Kempf and Hadfield, 1985; Emlet, 1986; Highsmith and Emlet, 1986). Smaller larval size at time of metamorphosis and settlement could be due to delayed metamorphosis or an increase in energy expenditure during dispersal; regardless of the reason, small larval size can have carryover effects into later stages, resulting in lower settlement specificity, lower post-settlement survival and growth, and older age at first reproduction (Knight-Jones, 1953; Sebens, 1983; Emlet, 1986; Woollacott et al., 1989; Miller, 1993; Stevens et al., 1999; Olive et al., 2000; Marshall et al., 2003). Therefore, larger larval size at time of metamorphosis and settlement may have a fitness advantage (Sinervo, 1990; Stearns, 1992; Williams, 1994; Bernardo, 1996). Larval energy metabolism during dispersal may have fitness consequences through depletion in total lipid and protein that may ultimately affect size and mortality.

Because larval area did not change significantly with respect to pCO_2 and T, I can conclude that larval size was unaffected by the treatments imposed. Larvae size (volume) may not be a plastic trait in *Pocillopora damicornis* (Harii et al., 2010). However, larvae remained long and skinny, even elongating, under High-T, while larvae at Ambient-T became shorter and more circular. The morphological change in larvae at Ambient-T may indicate partial metamorphosis prior to settlement, which is common in scleractinian planulae (Fadlallah, 1983). Metamorphosis in *P. damicornis* larvae at High-T may be delayed due to stress caused by elevated temperature and low pH (Bassim and Sammarco, 2003; Randall and Szmant, 2009a, 2009b; Albright et al., 2010; Albright and Langdon, 2011; Kenkel et al., 2011a; Nakamura et al., 2011). However, absolute lengths of larvae at the end of the exposures were similar across all treatments and cohorts (Fig. 15). Additionally, TL decreased under High-T, likely a combined result of slightly greater depletion of WE, TAG, and PL. This depletion of energetic resources under higher metabolic rates (Rivest and Hofmann, 2014) and a loss of ability to acquire more energy as seen here by loss of symbionts may contribute to the potential relative delay in development observed. Furthermore, this lipid depletion may be related to the increase in TP per symbiont density at High-T, suggesting an up-regulation of stress response pathways in the coral animal. Symbiont density, a fitness trait related to potential for growth, decreased at High-T, with an additive effect of High-pCO_2 on this bleaching depending on the day of release. These results contrast with a study conducted in Taiwan that showed no differences in absolute values of total protein or symbiont density of *P. damicornis* in response to temperature and pCO_2 (Cumbo et al., 2013b). In summary, temperature and pCO_2 influenced different portions of

traits that affect the fitness of *P. damicornis* larvae and can act additively to reduce overall fitness.

The role of day of larval release in energy metabolism

Effects of Day and its interactions with other independent variables explained most of the variation among groups of larvae exposed to the four treatments. For changes in energy-related lipid classes, lipid consumption declined as the spawning period progressed, such that Late larvae consumed the least amount of lipid and contained the most lipid at the end of 24 hours. These changes occurred without a large shift in the amount of structural lipids present. ΔTL, ΔTP, and larval size were also sensitive to Day. Patterns of ΔTP reflected those of larval size, with negative change in response to treatments on day Middle and a general increase in absolute size as the spawning period progressed. Interestingly, changes in symbiont density did not vary significantly by Day, indicating that the sensitivities of *Symbiodinium* to the experimental treatments may be equivalent and that differences in response to High-pCO_2 and High-T were perhaps due to the coral animal.

This study along with previous work supports the idea that larvae released from adult colonies at different times exhibit different sensitivities to elevated temperature and pCO_2 (Cumbo et al., 2013a; Rivest and Hofmann, 2014). Specifically, Late larvae showed the least change in energy-related lipids overall. These Late larvae can have naturally lower respiration rates that are depressed further under High-pCO_2 conditions, with respect to Peak larvae (Rivest and Hofmann, 2014). The naturally lower metabolic rate of Late larvae can account for their miniscule consumption of energy-related lipids. Already sluggish in metabolism, they may be limited in the physiological response they can launch to combat the

hypothesized stress associated with elevated temperature and pCO_2, such as repair of heat-damaged molecules (*e.g.* Black et al., 1995) and increased maintenance of acid-base homeostasis (*e.g.* Deigweiher et al., 2008; Portner, 2008). However, the maternal effects discussed earlier may have a larger influence on the physiological traits exhibited by *P. damicornis* larvae than their response to the temperature and pH of the surrounding seawater.

A sinking ship?

Ocean acidification and warming have great potential to affect the dispersal and recruitment of *P. damicornis* planulae, as suggested here by changes in lipid utilization and physiological condition under elevated pCO_2 and temperature. In particular, patterns of WE utilization suggest that the metabolic costs of tolerating projected future ocean conditions will be greatest under multiple stressor scenarios. Increased rates of utilization of energy-storage lipids may cause planulae to reach the energetic threshold for metamorphosis and settlement more quickly. Maintaining normal function in a future ocean may therefore result in shorter dispersal distances, or if suitable habitat cannot be found or competency cannot be achieved, individuals may terminate as planulae. Beyond larval energetics, the physiological responses of *P. damicornis* planulae to OA and warming have indirect ecological consequences. Depletion of WE stores to fuel metabolism also deplete larval buoyancy (Nevenzel, 1970; Lee et al., 1971, 2006b; Arai et al., 1993; Villinski et al., 2002). Based on different physiologies between cohorts of planulae, Peak-release planulae, the largest cohort in terms of numbers of larvae produced, will experience the greatest changes in buoyancy. Lower buoyancy will remove larvae more quickly from surface currents and will increase their chance of interaction with benthic substrate, contributing to the likelihood of shorter

dispersal distances. In this way, my results highlight how OA and warming may affect future population dynamics of a reef-building coral, through the role of lipids as sources of energy and buoyancy for planula dispersal.

Part B: The role of biogeography and environmental history in the response of coral larvae to OA and warming

Materials and methods

Collection of coral larvae

Larvae were collected from adult colonies following the lunar pattern of reproduction of *P. damicornis* (Fig. 10; Fan *et al.* 2006). Specifically, on the new moon in February and three days prior to the new moon in June 2012, eight colonies of *P. damicornis* were collected from respective fringing reef sites at ~1-3 m depth. Larvae in Moorea were collected as described previously (this chapter, Part A, p. 102). At the National Museum of Marine Biology and Aquarium (NMMBA) in Taiwan, each colony was maintained in an aquarium with indirect natural sunlight and a slow flow of coarsely filtered seawater. Overnight, larvae were captured in 100 μm mesh-lined cups that received the outflow of each aquarium. Daily at dawn, larvae from each colony were collected, counted, and pooled. These counts were performed daily so that the peak in the predicted release curve of the colonies was identified (*e.g.* Cumbo et al., 2013a; Rivest and Hofmann, 2014) and that these "peak" larvae could be used for the experiment. In Moorea, all larvae released were used in the experiments, resulting in unequal genotype ratios. In Taiwan, equal numbers of larvae from each colony were contributed to this pool. Larvae from this pool were immediately photographed and preserved to quantify larval quality and lipid metrics (see below) that represented the condition of freshly-released larvae. The remaining larvae in the pool were then randomly assigned to experimental treatments. Data presented here were collected

before and after manipulative experiments were conducted with larvae collected on the peak day of release, February 28, 2012 in Moorea and June 25, 2012 in Taiwan.

Experimental incubations

In preparation for the experimental incubations, larvae were divided among 8 tanks containing 4 treatment combinations of pCO_2 and temperature. Larvae were incubated in 2 400 mL containers per aquarium at ~0.15-0.25 larva mL^{-1}. These containers had 100 μm mesh sides and a PAR-transparent lid and were anchored in place within the aquarium to ensure that PAR exposure was replicated across tanks (Fig. 11). Larvae were incubated for 24 hours under experimental conditions. Due to the time needed to photograph and preserve larvae post-incubation, incubations were staggered by one hour per aquarium, with the order randomized. At the end of each incubation, larvae within tanks were pooled, and 10 larvae were randomly selected for size measurements (n = 20 per treatment). The remaining larvae were frozen at -80°C in aliquots for downstream analyses of lipid classes (3 x 25 larvae), total protein content (2 x 5 larvae), and symbiont density (2 x 5 larvae). Therefore, for comparisons between treatments, n = 6 for lipid classes, n = 4 for total protein, and n = 4 for symbiont density.

In laboratories at both sites, two pCO_2 treatments were prescribed. In Moorea, Ambient-pCO_2 was ~450 μatm CO_2 and High-pCO_2 was ~1000 μatm CO_2; in Taiwan, Ambient-pCO_2 was ~500 μatm CO_2) and High-pCO_2 was ~900 μatm CO_2. The low treatment approximated current environmental conditions of the water mass bathing the fringing reef where the adult corals were collected (confirmed by environmental data). The high treatment represents a level of dissolved pCO_2 expected by the year 2100 under a business-as-usual

scenario (IPCC, 2013). pCO_2 levels were combined with two experimental temperatures. In Moorea, the ambient and high temperature treatments were 28°C and 31°C, respectively; in Taiwan the ambient and high temperature treatments were 27.5°C and 30.5°C, respectively. The control temperatures approximated the multi-year average temperature for the fringing reefs close to the collection sites for adult *P. damicornis* (Leichter, 2014; T-Y Fan, unpubl. data). The elevated temperatures represent an average surface ocean temperature by year 2100 as predicted by global temperature projections (IPCC, 2013). The experimental temperatures differed between sites in order to mimic present-day seawater temperatures: Taiwan had a lower mean seawater temperature than Moorea during the experiments (Chapter 6). The four treatments created by this experimental set-up are defined as ambient temperature-ambient pCO_2 (ATAC), ambient temperature-high pCO_2 (ATHC), high temperature-ambient pCO_2 (HTAC), and high temperature-high pCO_2 (HTHC).

In Moorea, larval exposures were conducted as described previously (this chapter, Part A, p. 104). In Taiwan, treatments were created as described in Cumbo *et al.* (2013a) at the National Museum of Marine Biology and Aquarium coral husbandry facility, with two aquaria for each treatment combination of pCO_2 and temperature. Atmospheric air was bubbled directly into 50 µm-filtered seawater in experimental aquaria to generate the Ambient-pCO_2 treatment. A controlled gas mixture of atmospheric air and CO_2 was bubbled into aquaria to create the high-pCO_2 treatment. The closed-circuit treatment aquaria contained 30 L of 1-µm filtered seawater, 15% of which was changed daily. Temperature was controlled for each tank individually using heaters (100W, Taikong Corp., Changjhih, Taiwan), chillers (Aquatech Ac11), and aquarium pumps (Rio 1110). Metal halide lamps illuminated the aquaria on a 12:12 hr light:dark cycle, providing average intensity of

photosynthetically active radiation of 241 ± 16 μmol photons m^{-2} s^{-1}, starting at 7:00 daily. Light levels were measured just below the seawater surface during the experiment using a cosine-corrected 4π quantum sensor (LI-193; Li-Cor Inc., Lincoln, NE, USA) and a LI-250A meter (Li-Cor Inc., Lincoln, NE, USA).

To verify and monitor the physical parameters of the OA x temperature treatments, the chemistry of the seawater in the aquaria was analyzed during the experiment. pH, temperature, salinity, and total alkalinity of seawater in each aquarium were measured during the incubations. These analyses were conducted as previously described (this chapter, Part A, p. 107). In Taiwan, the following equipment was used: certified digital thermometer (meter 15-077-8, probe 15-077-7, Thermo Fisher Scientific Inc., Waltham, MA, USA), conductivity meter (340i, WTW GmbH, Weilheim, Germany), automatic titrator (DL50 with DG101-SC pH probe, Mettler Toledo, LLC., Toledo, OH, USA).

Analyses of larval quality

To assess quality of incubated larvae, size, density of *Symbiodinium*, and total protein were quantified as described previously (this chapter, Part A, p. 108). In Taiwan, larvae were photographed using a compound light microscope (Zeiss Axiostar Plus, Zeiss, Thornwood, NY, USA) fitted with a camera (Nikon CoolPix 4500 4.0 megapixel, Nikon Corp., Melville, NY, USA). Larval area and maximum larval length were measured. To quantify total protein, the Bradford assay was used (Bradford, 1976; Jaeckle and Manahan, 1989b).

Aliquots of 25 larvae were homogenized and extracted as previously described (this chapter, Part A, p. 109; Bligh and Dyer, 1959; Luo, 2008). A portion of the raw homogenate was analyzed for total protein content using the BCA assay (Pierce Biotechnology Inc.,

Rockford, IL, USA; Smith et al., 1985). Total protein concentrations were used to normalize lipid extracts for down-stream analysis. Ketone was not used as an internal standard for the Taiwan analyses as it could not be obtained at that location. Total lipid values were obtained from lipid extracts dried under inert gas.

Lipid classes of wax ester (WE), triacylglycerol (TAG), and phospholipid (PL) were quantified using two chromatography-based techniques. For larvae sampled in Moorea, a thin layer chromatography-flame ionization detection (TLC-FID) analyzer was used (Iatroscan MK-5, Iatron Laboratories, Inc., Tokyo, Japan). Refer to Part A, p. 110 for more information. For larvae sampled in Taiwan, these lipid classes were separated and quantified using thin layer chromatography (TLC) on silica gel plates. Lipid extracts were normalized to protein content of the original homogenate through resuspension in chloroform:methanol (2:1, v/v). Lipid extracts were applied at the origin of a TLC silica gel plate (60G, F254, Merck KGaA, Germany) in the volume corresponding to 20 μg total protein (3 technical replicates per extract). A standard curve was spotted on four lanes on each plate: 5-60 μg wax ester (palmityl palmitate, Sigma Aldrich), 5-35 μg triacylglycerol (mixture MDT12-1KT, Sigma-Aldrich Corp., St. Louis, MO, USA). Once dry, the plates were developed halfway in chloroform:ethanol:water:triethylamine (35:35:7:35, v/v). After a 10-minute drying period, the plates were then developed fully in hexane. After a 10-minute drying period, the plates were developed fully in hexane:diethyl ether: acetic acid (70:30:1). Dried plates were stained for 2 hours in a solution of 20% methanol containing 0.03% Coumassie Blue and 0.5% acetic acid. After destaining overnight in 20% methanol, the plates were dried and then photographed using a document scanner. Densitometry was performed using ImageJ

(Rasband, 1997) to calculate the standard curve and the quantities of lipid classes in experimental samples.

Phospholipids (PL) were quantified from extracts using a spectrophotometric assay for phosphorus determination (modified from Rouser et al., 1970). Lipid extracts (in chloroform) from homogenate volume equivalent to 50 μg total protein were placed in test tubes (n = 3 per extract), and the solvent was completely evaporated under Argon gas at 37°C. A standard curve was generated using 1 mM KH_2PO_4 in water; 0- 50 nmol were used. To all tubes, 140 μL 70% perchloric acid, which were then covered and heated at 180°C for 1 hour. In order, water (500 μL), 1.25% ammonium molybdate (200 μL) and 10% ascorbic acid (100 μL) were added, and tubes were mixed. All tubes were heated for 5 minutes at 100°C while covered. The released inorganic phosphate reacted with the ammonium molybdate to generate a blue color. Tube contents were pipetted in triplicate into a 96-well plate; absorbance was measured at 820 nm using a Synergy H4 (BioTek Instruments Inc., Winooski, VT, USA) plate reader. The standard curve was used to calculate the amount of phosphorus in each sample (nmol), which is equivalent to the amount of phospholipid (nmol). For comparisons to larval phospholipid quantities measured in Moorea, nmoles of phospholipid was converted to μg using the molar mass of L-α-phosphatidylcholine, the standard used for Taiwan samples.

Statistical analyses of biological data

All data were analyzed using R version 3.0.1 (R Core Team 2013). Statistical assumptions of normality and homogeneity of variance were met based on Q-Q plots and Levene's test, sometimes following a natural log or inverse transformation of the response

variable. Effects on physical conditions were estimated using linear mixed-effect models as described previously (this chapter, Part A, p. 111; nlme package in R; Pinheiro and Bates, 2000). To compare physical conditions between treatments, pCO_2 and temperature treatments were fixed factors, and tank was a random factor. For initial conditions of larvae, absolute values of lipid and quality metrics were analyzed for effect of Site using a one-way ANOVA. To describe how lipid levels and traits of physiological condition changed over 24 hours, mean pre-incubation levels were subtracted from post-incubation levels, henceforth referred to as Δ, "delta". Therefore, a negative ΔWE per larva represents a net consumption of WE per larva during the 24-hr incubation. ΔWE, ΔTAG, and ΔPL quantities were standardized by larva, by total protein, and by symbiont density. Linear mixed-effect models (nlme package in R; Pinheiro and Bates, 2000) were used to estimate effects on standardized response variables, with pCO_2, temperature, and site as fixed factors and aquarium ("tank") as a random factor. Model selection was performed as previously described (this chapter, Part A, p. 108), following (Burnham and Anderson, 2002). To determine which factors in models were significant, a type III sum of squares was conducted on selected models fit using maximum likelihood (Zuur et al., 2009; Crawley, 2013). Post-hoc analyses were performed as described previously (this chapter, Part A, p. 111; Hothorn et al., 2008).

Environmental data collection

pH and temperature time series were generated on fringing reefs in Moorea, French Polynesia and in Taiwan, within 33 m from the collecting locations of adult *P. damicornis* parents. Refer to Chapter 6 for more details.

Results

Condition of P. damicornis *larvae immediately after release*

To assess variation in maternal endowment of *P. damicornis* larvae, I measured traits of newly-released individuals and tested whether they differed based on the site of the population – Moorea or Taiwan. Lipid composition was assessed as the content of energy-storage (WE and TAG) and structural (PL) lipids. General traits of TL, TP, symbiont density, larval area, and larval length were also measured. Overall, initial condition of larvae differed between biogeographic locations.

Larvae in Moorea contained on average 32.00 μg total lipid per larva^{-1}, composed of 58% WE, 11% TAG, and 17% PL. The total protein fraction of these larvae was less, a mean of 11.65 μg larva^{-1}. Larvae in Taiwan contained on average 20.47 μg total lipid per larva^{-1}, composed of 39% WE, 18% TAG, and 6% PL. The total protein fraction of these larvae was larger than that of total lipid, a mean of 22.37 μg larva^{-1}. Average *Symbiodinium* density was 7850 cells larva^{-1} in Moorea and 9008 cells larva^{-1} in Taiwan.

Initial WE per larva varied significantly with Site when normalized to number of larvae and to symbiont density, but not when normalized to total protein (Table 22). Larvae in Moorea contained significantly greater initial larval WE levels than in Taiwan (Tukey's HSD, Table 23; Fig. 17). Regardless of the normalization procedure, initial TAG varied significantly by Site (Table 22). Larvae in Moorea had significantly less TAG per larva, per total protein, and per symbiont density than those in Taiwan (Tukey's HSD, Table 23; Fig. 17). Larval PL was significantly affected by Site across all types of normalization (Table 22). Consistently, PL per larva was significantly greater in Moorea than in Taiwan (Tukey's HSD, Table 23; Fig. 17).

Table 22. Analysis of newly-released *P. damicornis* larvae among sites, standardized per larva (µg larva^{-1}), per protein (µg µg total protein^{-1}), and per symbiont density (µg cell^{-1}), unless otherwise noted. Comparisons were made using a one-way ANOVA, with biogeographic site (Site) as a fixed effect. Test statistic F, degrees of freedom (df) and p-values (*p*) are reported.

Response variable	F	df	*p*
WE per larva	68.651	1, 4	**0.001**
WE per total protein	3.266	1, 4	0.145
WE per symbiont density	131.13	1, 4	**<0.001**
TAG per larva	22.115	1, 4	**0.009**
TAG per protein	41.383	1, 4	**0.003**
TAG per symbiont density	9.021	1, 4	**0.040**
PL per larva	73.749	1, 4	**0.001**
PL per protein	15.434	1, 4	**0.017**
PL per symbiont density	104.114	1, 4	**0.001**
TL per larva	22.250	1, 4	**0.009**
TL per protein	173.760	1, 4	**<0.001**
TL per symbiont density	41.206	1, 4	**0.003**
TP per larva	3.518	1, 2	0.202
TP per symbiont density	1.602	1, 2	0.333
Symbiont density (cells larva^{-1})	0.040	1, 2	0.861
Larval area (µm^2)	18.492	1, 18	**<0.001**
Larval length (µm)	33.836	1, 18	**<0.001**

Table 23. Post-hoc analyses (Tukey's HSD) for significant differences in lipid content and physiological conditions of newly-released *P. damicornis* larvae among sites. Test statistic z and p-values (*p*) are reported for each comparison.

Biological response	Significant effect	z	*p*	Summary description
Initial WE per larva	Site	6.430	**0.003**	Moorea > Taiwan
Initial WE per symbiont density	Site	11.450	**<0.001**	Moorea > Taiwan
Initial TAG per larva	Site	4.703	**0.009**	Moorea < Taiwan
Initial TAG per protein	Site	6.430	**0.003**	Moorea < Taiwan
Initial TAG per symbiont density	Site	3.004	**0.040**	Moorea < Taiwan
Initial PL per larva	Site	8.588	**0.001**	Moorea > Taiwan
Initial PL per protein	Site	3.929	**0.017**	Moorea > Taiwan
Initial PL per symbiont density	Site	10.200	**0.001**	Moorea > Taiwan
Initial TL per larva	Site	4.717	**0.009**	Moorea > Taiwan
Initial TL per protein	Site	13.180	**<0.001**	Moorea > Taiwan
Initial TL per symbiont density	Site	6.419	**0.003**	Moorea > Taiwan
Initial larval area	Site	4.300	**<0.001**	Moorea < Taiwan
Initial larval length	Site	5.817	**<0.001**	Moorea < Taiwan

Figure 17. Traits describing the status of newly-released *P. damicornis* larvae in two locations. Mean ± SE (n = 3) quantities of biochemical composition (left) and size (right) of larvae released in Moorea, French Polynesia and in Taiwan. Traits are standardized per larva (µg lava^{-1}), per protein (µg µg total protein^{-1}), and per symbiont density ([µg symbiont cell^{-1}]x10^{-3}) unless otherwise noted. Means with the same lowercase letter are not significant different (p > 0.05). Refer to Tables 22 and 23 for statistical details.

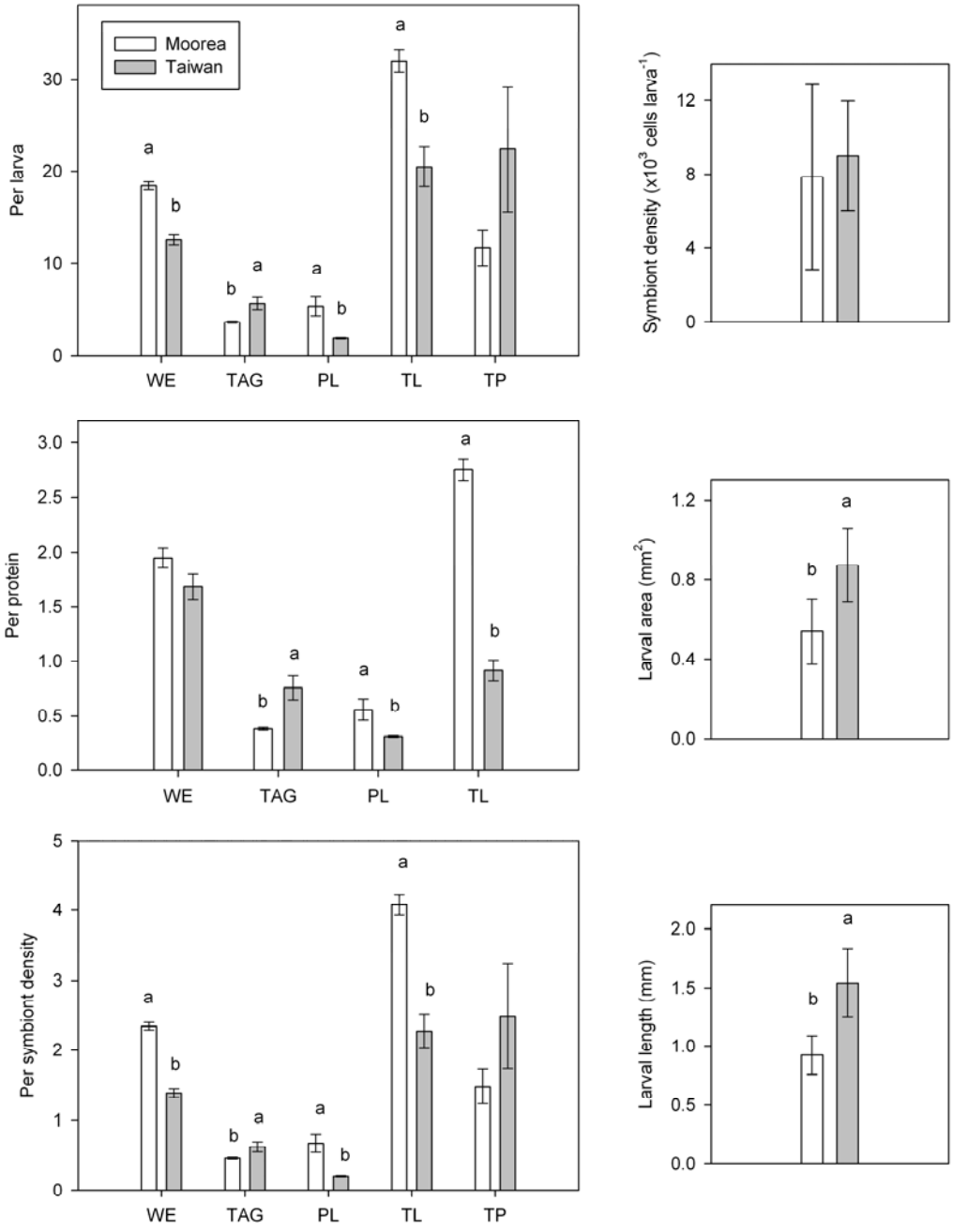

Regardless of standardization method, initial levels of total lipid varied significantly by Site (Table 22); levels in Moorea were greater than those in Taiwan (Tukey's HSD, Table 2; Fig. 17). Neither total protein nor symbiont density differed by Site (Table 22). Larval area and length varied significantly by Site (Table 13), with larger larvae released in Taiwan (Tukey's HSD, Table 23; Fig. 17).

Responses of lipid composition and quality of larvae to pCO_2 and temperature

At two sites and on several days during the monthly larval release, I measured the effects of OA and warming on lipid composition and quality of *P. damicornis* larvae, following a 24-hour exposure to treatment conditions. Because initial biological metrics of larvae often differed by day of release and site, I compared the change in these metrics over the first 24 hours of larval duration between pCO_2 exposures, temperature exposures, day of release and site.

In order to assess the response of coral larvae to different levels of temperature and pCO_2, larvae were incubated under laboratory conditions where temperature and seawater chemistry were controlled (Table 12). Temperature varied significantly by T but not within each temperature level (Table 13). Salinity and total alkalinity did not vary significantly by pCO_2 or T treatment (Table 13). pH and pCO_2 both varied significantly by pCO_2 treatment (Table 13).

Post-incubation levels of wax ester (WE) varied significantly by Site when normalized per larva and per protein (Table 24). Larvae from Taiwan contained more WE post incubation than larvae in Moorea (Tukey's HSD, Table 25; Fig. 18). WE per symbiont density varied significantly by TxSite and Site (Table 24). In Taiwan, larvae contained more

Table 24. Analysis of absolute abundance of lipid classes (wax ester WE, triacylglycerol TAG, phospholipid PL) in *P. damicornis* larvae following a 24-hour exposure to seawater of controlled temperature and pCO_2. Lipid content was compared among treatments and days of release, standardized to per larva (μg $larva^{-1}$), per larval protein content (μg μg total $protein^{-1}$), and per symbiont density (μg $cell^{-1}$). Comparisons were made using type III sum of squares with pCO_2, temperature (T), and biogeographic location (Site) as fixed effects. The final reduced model is shown, with test statistic X^2, degrees of freedom (df) and p-values (*p*) reported. Interaction terms were removed from the model if the AIC value did not increase by 2 or more and if there was not a significant difference in the model log likelihood ratio; removed terms are not shown here.

	Per larva			**Per protein**			**Per symbiont density**		
WE									
Effect	X^2	df	*p*	X^2	df	*p*	X^2	df	*p*
pCO_2	2.930	1	0.087	3.290	1	0.070	0.192	1	0.661
T	0.947	1	0.330	0.133	1	0.715	2.773	1	0.096
Site	5.258	1	**<0.001**	8.685	1	**<0.001**	17.696	1	**<0.001**
pCO_2xT									
pCO_2xSite									
TxSite							18.987	1	**<0.001**
pCO_2xTxSite									
TAG									
Effect	X^2	df	*p*	X^2	df	*p*	X^2	df	*p*
pCO_2	0.938	1	0.334	0.234	1	0.629	10.799	1	**0.001**
T	0.009	1	0.926	0.236	1	0.627	11.398	1	**0.001**
Site	277.742	1	**<0.001**	114.753	1	**<0.001**	180.244	1	**<0.001**
pCO_2xT	6.710	1	**0.010**				7.283	1	**0.007**
pCO_2xSite									
TxSite				8.333	1	**0.004**	24.106	1	**<0.001**
pCO_2xTxSite									
PL									
Effect	X^2	df	*p*	X^2	df	*p*	X^2	df	*p*
pCO_2	0.094	1	0.759	0.2337	1	0.629	1.431	1	0.232
T	0.072	1	0.789	0.2362	1	0.627	2.095	1	0.148
Site	61.172	1	**<0.001**	114.7527	1	**<0.001**	17.264	1	**<0.001**
pCO_2xT									
pCO_2xSite									
TxSite				8.333	1	**0.004**	3.906	1	**0.048**
pCO_2xTxSite									

Table 25. Post-hoc analyses for significant effects of treatment and site on absolute abundance of lipid classes (wax ester WE, triacylglycerol TAG, phospholipid PL) in *P. damicornis* larvae, standardized to per larva (µg larva^{-1}), per larval protein content (µg µg total protein^{-1}), and per symbiont density (µg cell^{-1}). Post-hoc tests were either Tukey's HSD or general linear hypothesis tests with Bonferroni corrections for multiple comparisons (GLHT). Test statistic z and p-values (*p*) are reported for each comparison.

Post-hoc test	Biological response	Significant effect	Comparison	z	*p*	Summary description
Tukey's HSD	WE per larva	pCO_2	Ambient-pCO_2 vs High-pCO_2	1.986	**0.047**	Moorea < Taiwan
Tukey's HSD	WE per protein	Site	Moorea vs. Taiwan	2.552	**0.011**	Moorea < Taiwan
GLHT	WE per symbiont density	TxSite	Moorea: Ambient-T vs. High-T	1.381	0.335	Taiwan: Ambient-T > High-T
			Taiwan: Ambient-T vs. High-T	3.729	**<0.001**	
GLHT	TAG per larva	pCO_2xT	ATAC vs. ATHC	0.917	1.000	HTAC > HTHC
			HTAC vs. HTHC	2.551	**0.032**	
		Site	Moorea vs. Taiwan	15.774	**<0.001**	Moorea < Taiwan
Tukey's HSD	TAG per protein	TxSite	Moorea: Ambient-T vs. High-T	0.403	1.000	Taiwan: Ambient-T > High-T
			Taiwan: Ambient-T vs. High-T	2.982	**<0.001**	
GLHT	TAG per symbiont density	pCO_2xSite	ATAC vs. ATHC	3.853	**0.017**	ATAC < ATHC
			HTAC vs. HTHC	0.460	1.000	Moorea: Ambient-T < High-T
			Moorea: Ambient-T vs. High-T	2.931	**0.014**	
			Taiwan: Ambient-T vs. High-T	1.991	0.186	
Tukey's HSD	PL per larva	Site	Moorea vs. Taiwan	7.488	**<0.001**	Moorea > Taiwan
Tukey's HSD	PL per protein	Site	Moorea vs. Taiwan	5.665	**<0.001**	Moorea > Taiwan
GLHT	PL per symbiont density	TxSite	Moorea: Ambient-T vs. High-T	1.370	0.341	N/A
			Taiwan: Ambient-T vs. High-T	1.276	0.404	

Figure 18. Lipid composition of *P. damicornis* larvae following 24-hour exposures to combinations of pCO_2 and temperature. Mean ± SE (n = 6) changes in abundance of wax ester (WE), triacylglycerol (TAG) and phospholipid (PL) classes for larvae released in Moorea, French Polynesia and Taiwan. Lipid quantities are standardized per larva (µg $lava^{-1}$), per protein (µg µg $total\ protein^{-1}$), and per symbiont density ([µg $symbiont\ cell^{-1}$]x10^{-3}). Experimental treatments: Ambient-T, Ambient-pCO_2 (ATAC), High-T, Ambient-pCO_2 (HTAC), Ambient-T, High-pCO_2 (ATHC), High-T, High-pCO_2 (HTHC). Refer to Tables 24 and 25 for statistical details.

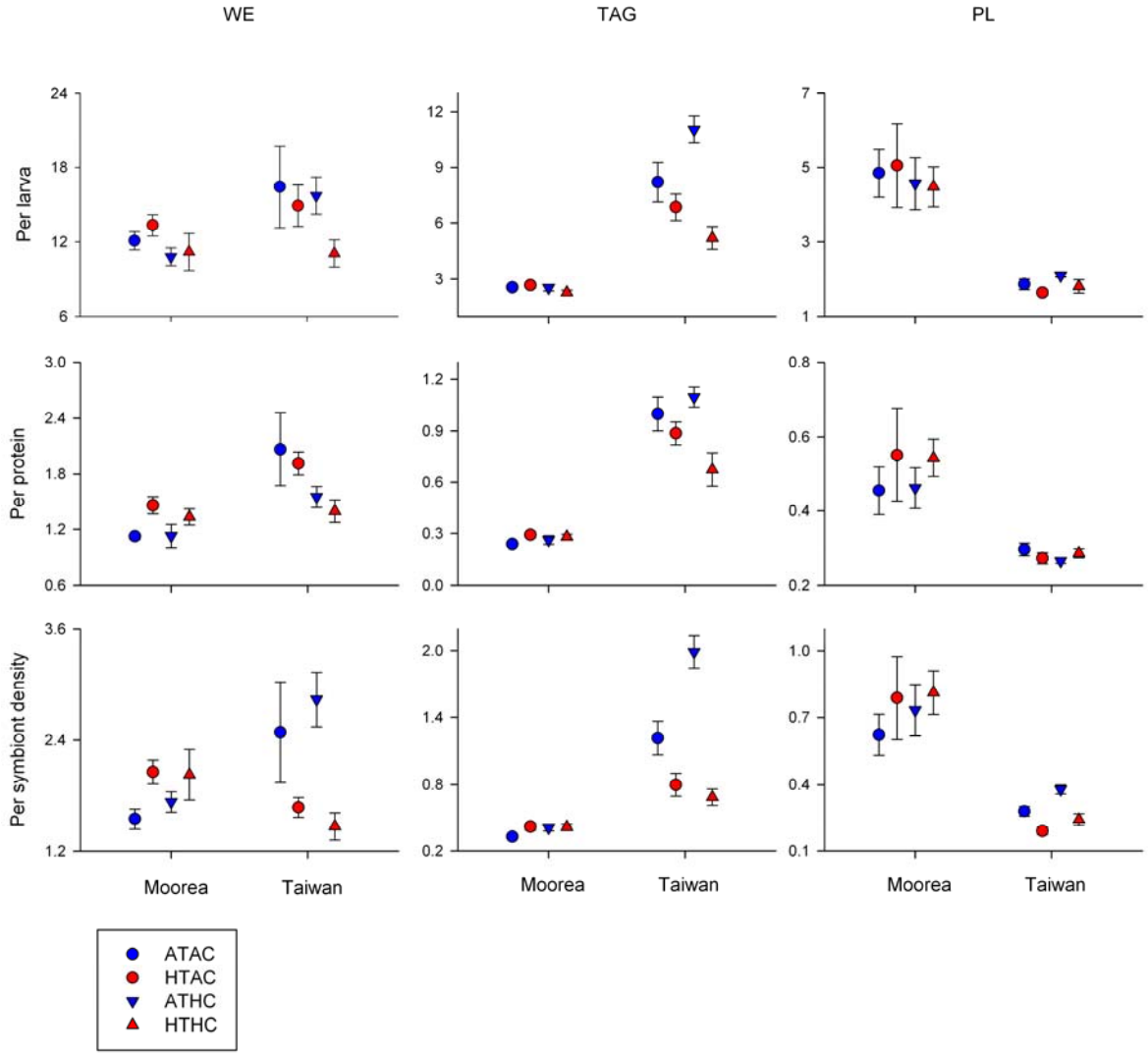

WE at Ambient-T than at High-T, but this difference was not significant in Moorea (GLHT, Table 25; Fig. 18).

Per larva, ΔWE ranged from -11.468 μg $larva^{-1}$ (MCR HTHC; 62% depletion of initial levels) to +17.640 μg $larva^{-1}$ (TWN ATAC; >100% increase from initial levels). When normalized by number of larva and by protein content, ΔWE varied significantly only by Site (Table 26). Larvae consumed more WE in Moorea than in Taiwan (Tukey's HSD, Table 27; Fig. 19). When WE content was standardized by symbiont abundance, effects of TxSite and Site were significant (Table 26). Post-hoc analyses revealed significant differences between temperature levels in Taiwan (GLHT, Table 27; Fig. 19) but not in Moorea (GLHT, Table 27; Fig. 19). In Taiwan, WE levels increased more with respect to symbiont density at Ambient-T than at High-T.

Triacylglycerol (TAG) content of larvae was quantified to inform how this easily-used source of energy is consumed under conditions of elevated pCO_2 and temperature. pCO_2xT and Site significantly affected post-incubation levels of TAG per larva (Table 24). At High-T, larvae contained more TAG at Ambient-pCO_2 vs. High-pCO_2 (GLHT, Table 25; Fig. 18). Larvae also contained more TAG in Taiwan than in Moorea (GLHT, Table 25; Fig. 18). When normalized to protein content, TAG varied by TxSite and Site (Table 24). In Taiwan, larvae had greater TAG content at Ambient-T than at High-T (GLHT, Table 25; Fig. 18). For TAG per symbiont density, significant effects included pCO_2xT and TxSite (Table 24). At Ambient-T, larvae contained more TAG at High-pCO_2 than at Ambient-pCO_2 (GLHT, Table 25; Fig. 18). In Moorea, larvae contained more TAG at High-T than at Ambient-T (GLHT, Table 25; Fig. 18).

Table 26. Analysis of changes in abundance of lipid classes (wax ester WE, triacylglycerol TAG, phospholipid PL) in *P. damicornis* larvae among treatments and sites, standardized to per larva (µg larva^{-1}), per larval protein content (µg µg total protein^{-1}), and per symbiont density (µg cell^{-1}). Comparisons were made using type III sum of squares with pCO_2, temperature (T), and biogeographic location (Site) as fixed effects. The final reduced model is shown, with test statistic X^2, degrees of freedom (df) and p-values (*p*) reported. Interaction terms were removed from the model if the AIC value did not increase by 2 or more and if there was not a significant difference in the model log likelihood ratio; removed terms are not shown here.

	Per larva			**Per protein**			**Per symbiont density**		
ΔWE									
Effect	X^2	df	*p*	X^2	df	*p*	X^2	df	*p*
pCO_2	2.930	1	0.087	2.830	1	0.093	0.192	1	0.661
T	0.947	1	0.330	0.015	1	0.902	2.773	1	0.096
Site	53.857	1	**<0.001**	13.124	1	**<0.001**	66.332	1	**<0.001**
pCO_2xT									
pCO_2xSite									
TxSite							18.987	1	**<0.001**
pCO_2xTxSite									
ΔTAG									
Effect	X^2	df	*p*	X^2	df	*p*	X^2	df	*p*
pCO_2	0.136	1	0.712	0.692	1	0.406	3.469	1	0.063
T	0.946	1	0.331	9.4075	1	**0.002**	0.915	1	0.339
Site	2.113	1	0.146	34.547	1	**<0.001**	4.069	1	**0.044**
pCO_2xT	2.048	1	0.152						
pCO_2xSite	0.128	1	0.720				3.904	1	**0.048**
TxSite	0.007	1	0.933						
pCO_2xTxSite	3.792	1	**0.052**						
ΔPL									
Effect	X^2	df	*p*	X^2	df	*p*	X^2	df	*p*
pCO_2	1.179	1	0.278	0.008	1	0.927	0.001	1	0.972
T	0.798	1	0.372	1.378	1	0.241	2.273	1	0.132
Site	1.282	1	0.258	0.695	1	0.405	0.042	1	0.838
pCO_2xT									
pCO_2xSite									
TxSite									
pCO_2xTxSite									

Table 27. Post-hoc analyses for significant effects of changes in abundance of lipid classes (wax ester WE, triacylglycerol TAG, phospholipid PL) in *P. damicornis* larvae among treatments and sites, standardized to per larva (µg larva^{-1}), per larval protein content (µg µg total protein^{-1}), and per symbiont density (µg cell^{-1}). Post-hoc tests were either Tukey's HSD or general linear hypothesis tests with Bonferroni corrections for multiple comparisons (GLHT). For Tukey's HSD tests, t-statistics are reported; for GLHT, z-statistics are reported. Test statistic z and p-values (*p*) are reported for each comparison.

Post-hoc test	Biological response	Significant effect	Comparison	z	*p*	Summary description
Tukey's HSD	ΔWE per larva	Site	Moorea vs. Taiwan	6.355	**<0.001**	Moorea < Taiwan
		pCO_2	Ambient-pCO_2 vs. High-pCO_2	1.482	0.138	Ambient-pCO_2 < High-pCO_2
Tukey's HSD	ΔWE per protein	Site	Moorea vs. Taiwan	3.137	**0.002**	Moorea < Taiwan
GLHT	ΔWE per symbiont density	TxSite	Moorea: Ambient-T vs. High-T	1.381	0.335	Taiwan: Ambient-T
			Taiwan: Ambient-T vs. High-T	3.729	**<0.001**	> High-T
GLHT	ΔTAG per larva	pCO_2xTxSite	Moorea: Ambient-T vs. High-T	0.972	1.000	N/A
			Moorea: Ambient-pCO_2 vs. High-pCO_2	0.369	1.000	
			Taiwan: Ambient-T vs. High-T	0.810	1.000	
			Taiwan: Ambient-pCO_2 vs. High-pCO_2	0.137	1.000	
Tukey's HSD	ΔTAG per protein	T	Ambient-T vs. High-T	2.934	**0.003**	Ambient-T > High-T
		Site	Moorea vs. Taiwan	5.620	**<0.001**	Moorea < Taiwan
GLHT	ΔTAG per symbiont density	pCO_2xSite	Moorea: Ambient-pCO_2 vs. High-pCO_2	1.763	0.156	N/A
			Taiwan: Ambient-pCO_2 vs. High-pCO_2	0.882	0.756	

Figure 19. Changes in lipid composition of *P. damicornis* larvae over 24-hour exposures to combinations of pCO_2 and temperature. Mean ± SE (n = 6) changes in abundance of wax ester (WE), triacylglycerol (TAG) and phospholipid (PL) classes for larvae released in Moorea, French Polynesia and Taiwan. Negative Δ values indicate net consumption over the experimental exposure. Positive Δ values indicate net production over 24 hours. Lipid quantities are standardized per larva (µg $lava^{-1}$), per protein (µg µg $total\ protein^{-1}$), and per symbiont density ([µg $symbiont\ cell^{-1}$]x10^{-3}). Experimental treatments: Ambient-T, Ambient-pCO_2 (ATAC), High-T, Ambient-pCO_2 (HTAC), Ambient-T, High-pCO_2 (ATHC), High-T, High-pCO_2 (HTHC). Refer to Tables 26 and 27 for statistical details.

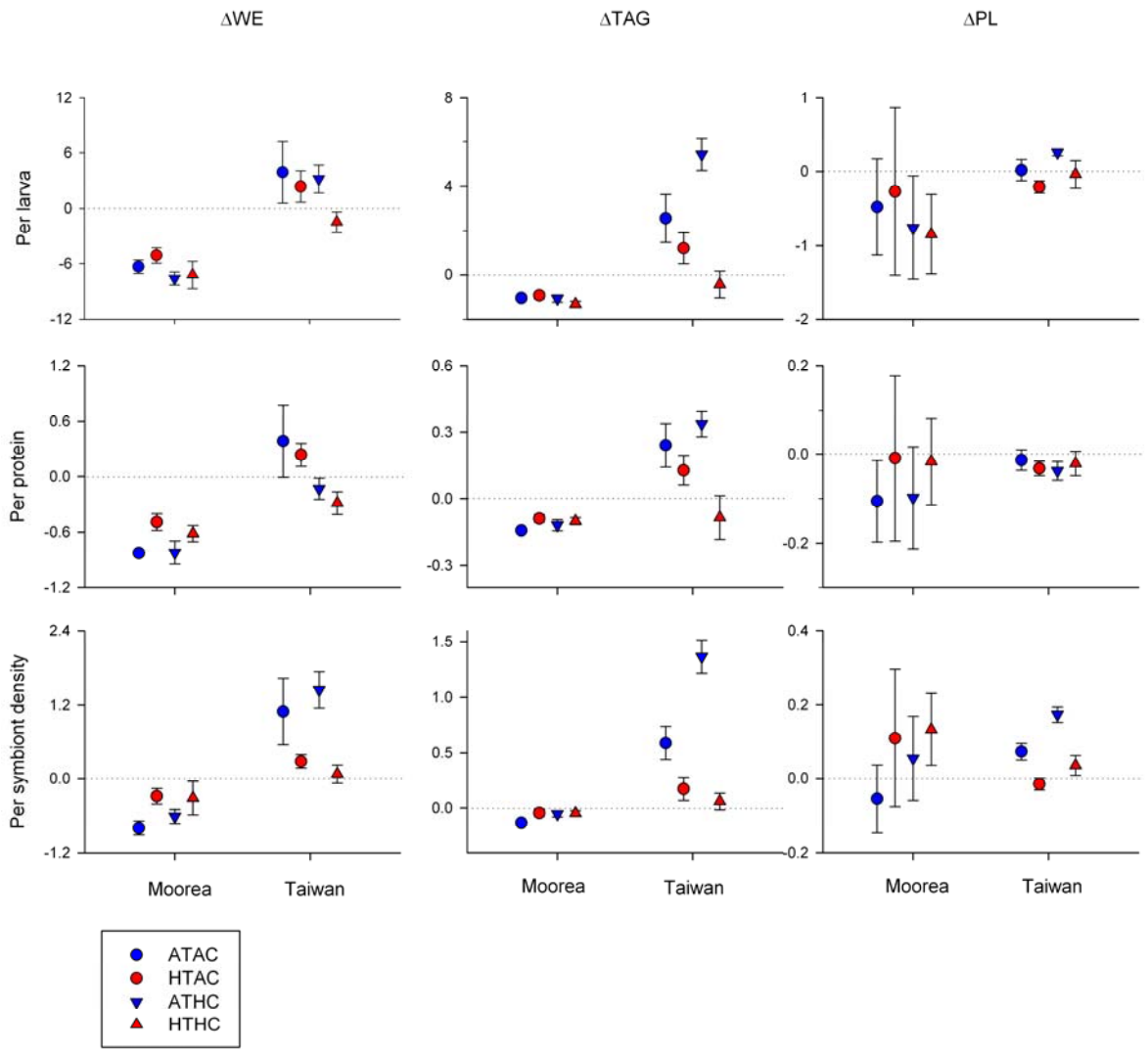

ΔTAG per larvae varied between -2.383 μg $larva^{-1}$ (TWN HTHC; 42% depletion of initial levels) and +7.574 μg $larva^{-1}$ (TWN ATHC; >100% increase from initial levels); the effect of pCO_2xTxSite was significant (Table 26), but post-hoc comparisons of ΔTAG between groups were not significantly different (GLHT, Table 27). Protein-standardized ΔTAG levels differed significantly by T and Site (Table 26). ΔTAG was more positive at Ambient-T vs. High-T (Tukey's HSD, Table 27; Fig. 19). Larvae consumed TAG more in Moorea than in Taiwan (Tukey's HSD, Table 27; Fig. 19). Significant effects included pCO_2xSite and Site for ΔTAG per larval symbiont abundance (Table 26), though post-hoc analyses did not reveal any significant differences between pCO_2 levels at each site (GLHT, Table 27; Fig. 19).

Phospholipids (PL) in larvae were quantified as a proxy for holobiont cell number because of their structural role within cell membranes. Following the 24-hour exposures, PL per larva and per protein varied significantly by Site (Table 24), with more PL in larvae from Moorea than from Taiwan (Tukey's HSD, Table 25; Fig. 18). When normalized to symbiont density, PL levels varied significantly by TxSite and Site (Table 24), but post-hoc analyses did not reveal significant differences (GLHT, Table 25; Fig. 18). ΔPL per larva ranged from -4.004 μg $larva^{-1}$ (MCR HTAC; 75% depletion) to +2.990 μg $larva^{-1}$ (MCR HTAC; 56% increase). Regardless of the normalization procedure, ΔPL did not differ significantly by any effect tested (Table 26).

Changes in larval quality in response to different pCO_2 and temperature levels were measured in the form of total lipid (TL), total protein (TP), and symbiont density. Following

the 24-hour incubations, TL varied significantly by effects including pCO_2xT and Site (Table 28). At Ambient-T, larvae contained more TL at High-pCO_2 than at Ambient-pCO_2 (GLHT, Table 29; Fig. 20). Larvae in Moorea had higher TL content than larvae in Taiwan (GLHT, Table 29; Fig. 20). When normalized to protein content, TL varied by TxSite, T, and Site (Table 28). Larvae contained more TL at Ambient-T in Moorea, but not in Taiwan (GLHT, Table 29; Fig. 20). Significant effects on TL per symbiont density included pCO_2xT and Site (Table 28). TL content was greater at ATAC than at ATHC (GLHT, Table 29; Fig. 20). Larvae in Moorea contained more TL per symbiont density than larvae in Taiwan (GLHT, Table 29; Fig. 20).

Per larva, ΔTL varied between -18.222 μg $larva^{-1}$ (MCR HTAC; 57% depletion) and +21.653 μg $larva^{-1}$ (MCR ATHC; 68% increase); pCO_2xT and pCO_2 were significant effects (Table 30). ΔTL per larva increased with pCO_2 significantly at ambient temperature (GLHT, Table 31; Fig. 21) but did not change at High-T (GLHT, Table 31; Fig. 21). Effects of TxSite and Site caused significant changes in ΔTL when standardized by total protein (Table 30). Protein-specific ΔPL was significantly greater for larvae from Moorea when exposed to High-T vs. Ambient-T (GLHT, Table 31; Fig. 21); however, this difference was not significant for larvae from Taiwan (GLHT, Table 31; Fig. 21). When standardized to larval symbiont density, ΔTL varied significantly by effects including pCO_2xT and Site. At Ambient-T, ΔTL normalized to symbiont density was significantly greater at High-pCO_2 than at Ambient-pCO_2 (GLHT, Table 31; Fig. 21); at High-T, the difference was not significant (GLHT, Table 31; Fig. 21). ΔTL per symbiont density was significantly greater for larva from Moorea than Taiwan (GLHT, Table 31; Fig. 21).

Post-incubation TP per larva varied by Site (Table 28), with more TP present in

Table 28. Analysis of absolute values of indices of physiological condition in *P. damicornis* larvae following a 24-hour exposure to seawater of controlled temperature and pCO_2. Physiological condition was compared among treatments and sites, standardized to per larva (μg $larva^{-1}$), per larval protein content (μg μg total $protein^{-1}$), and per symbiont density (μg $cell^{-1}$), unless otherwise noted. Indices include total lipid (TL), total protein (TP), symbiont density, and larval size. Comparisons were made using type III sum of squares with pCO_2, temperature (T), and biogeographic site (Site) as fixed effects. The final reduced model is shown, with test statistic X^2, degrees of freedom (df) and p-values (*p*) reported. Interaction terms were removed from the model if the AIC value did not increase by 2 or more and if there was not a significant difference in the model log likelihood ratio; removed terms are not shown here.

	Per larva			**Per protein**			**Per symbiont density**		
TL									
Effect	X^2	df	*p*	X^2	df	*p*	X^2	df	*p*
pCO_2	12.374	1	**<0.001**	0.7031	1	0.402	22.636	1	**<0.001**
T	0.005	1	0.945	10.793	1	**0.001**	0.022	1	0.882
Site	14.547	1	**<0.001**	45.958	1	**<0.001**	11.381	1	**0.001**
pCO_2xT	9.644	1	**0.002**				10.503	1	**0.001**
pCO_2xSite									
TxSite				4.187	1	**0.041**			
pCO_2xTxSite									
TP									
Effect	X^2	df	*p*				X^2	df	*p*
pCO_2	<0.001	1	0.999				6.353	1	**0.012**
T	0.504	1	0.478				1.817	1	0.178
Site	50.554	1	**<0.001**				55.133	1	**<0.001**
pCO_2xT									
pCO_2xSite									
TxSite							18.430	1	**<0.001**
pCO_2xTxSite									

	Symbiont per larva (μg $cell^{-1}$)			**Larval area (mm^2)**			**Larval length (mm)**		
Effect	X^2	df	*p*	X^2	df	*p*	X^2	df	*p*
pCO_2	4.730	1	0.030	1.944	1	0.163	5.645	1	**0.018**
T	1.585	1	0.208	2.305	1	0.129	3.981	1	**0.046**
Site	1.140	1	0.286	47.491	1	**<0.001**	87.055	1	**<0.001**
pCO_2xT									
pCO_2xSite									
TxSite	7.188	1	**0.007**						
pCO_2xTxSite									

Table 29. Post-hoc analyses for significant effects of treatment and site on absolute values of indices of physiological condition in *P. damicornis* larvae. Values were standardized to per larva (μg larva^{-1}), per larval protein content (μg μg total protein^{-1}), and per symbiont density (μg cell^{-1}). Indices include total lipid (TL), total protein (TP), symbiont density, and larval size. Post-hoc tests were either Tukey's HSD or general linear hypothesis tests with Bonferroni corrections for multiple comparisons (GLHT). Test statistic z and p-values (*p*) are reported for each comparison.

Post-hoc test	Biological response	Significant effect	Comparison	z	*p*	Summary description
GLHT	TL per larva	pCO_2xT	ATAC vs. ATHC	3.090	**0.006**	ATAC < ATHC
			HTAC vs. HTHC	0.833	1.000	Moorea > Taiwan
		Site	Moorea vs. Taiwan	3.364	**0.002**	
GLHT	TL per protein	TxSite	Moorea: Ambient-T vs. High-T	2.686	**0.015**	Moorea: Ambient-T > High-T
			Taiwan: Ambient-T vs. High-T	0.256	1.000	
GLHT	TL per symbiont density	pCO_2xT	ATAC vs. ATHC	3.923	**<0.001**	ATAC < ATHC
			HTAC vs. HTHC	0.049	1.000	Moorea > Taiwan
		Site	Moorea vs. Taiwan	2.837	**0.014**	
Tukey's HSD	TP per larva	Site	Moorea vs. Taiwan	6.312	**<0.001**	Moorea < Taiwan
GLHT	TP per protein	TxSite	Moorea: Ambient-T vs. High-T	1.130	0.517	Taiwan: Ambient-T > High-T
			Taiwan: Ambient-T vs. High-T	3.960	**<0.001**	
GLHT	TP per symbiont density	TxSite	Moorea: Ambient-T vs. High-T	1.156	0.743	N/A
			Taiwan: Ambient-T vs. High-T	2.326	0.060	
		pCO_2	Ambient-pCO_2 vs. High-pCO_2	1.998	0.137	
Tukey's HSD	Larval area	Site	Moorea vs. Taiwan	6.804	**<0.001**	Moorea < Taiwan
Tukey's HSD	Larval length	Site	Moorea vs. Taiwan	8.841	**<0.001**	Moorea < Taiwan
		pCO_2	Ambient-pCO_2 vs. High-pCO_2	2.251	**0.024**	Ambient-pCO_2 > High-pCO_2
		T	Ambient-T vs. High-T	1.890	**0.059**	

Figure 20. Larval quality traits for *P. damicornis* larvae following 24-hour exposures to pCO_2 and temperature. Mean ± SE (n = 6) changes in larval composition and size for larvae released in Moorea, French Polynesia and Taiwan. Quality traits are standardized per larva (µg $lava^{-1}$), per protein (µg µg $total\ protein^{-1}$), and per symbiont density ([µg $symbiont\ cell^{-1}$]x10^{-3}) unless otherwise noted. Experimental treatments: Ambient-T, Ambient-pCO_2 (ATAC), High-T, Ambient-pCO_2 (HTAC), Ambient-T, High-pCO_2 (ATHC), High-T, High-pCO_2 (HTHC). Refer to Tables 28 and 29 for statistical details.

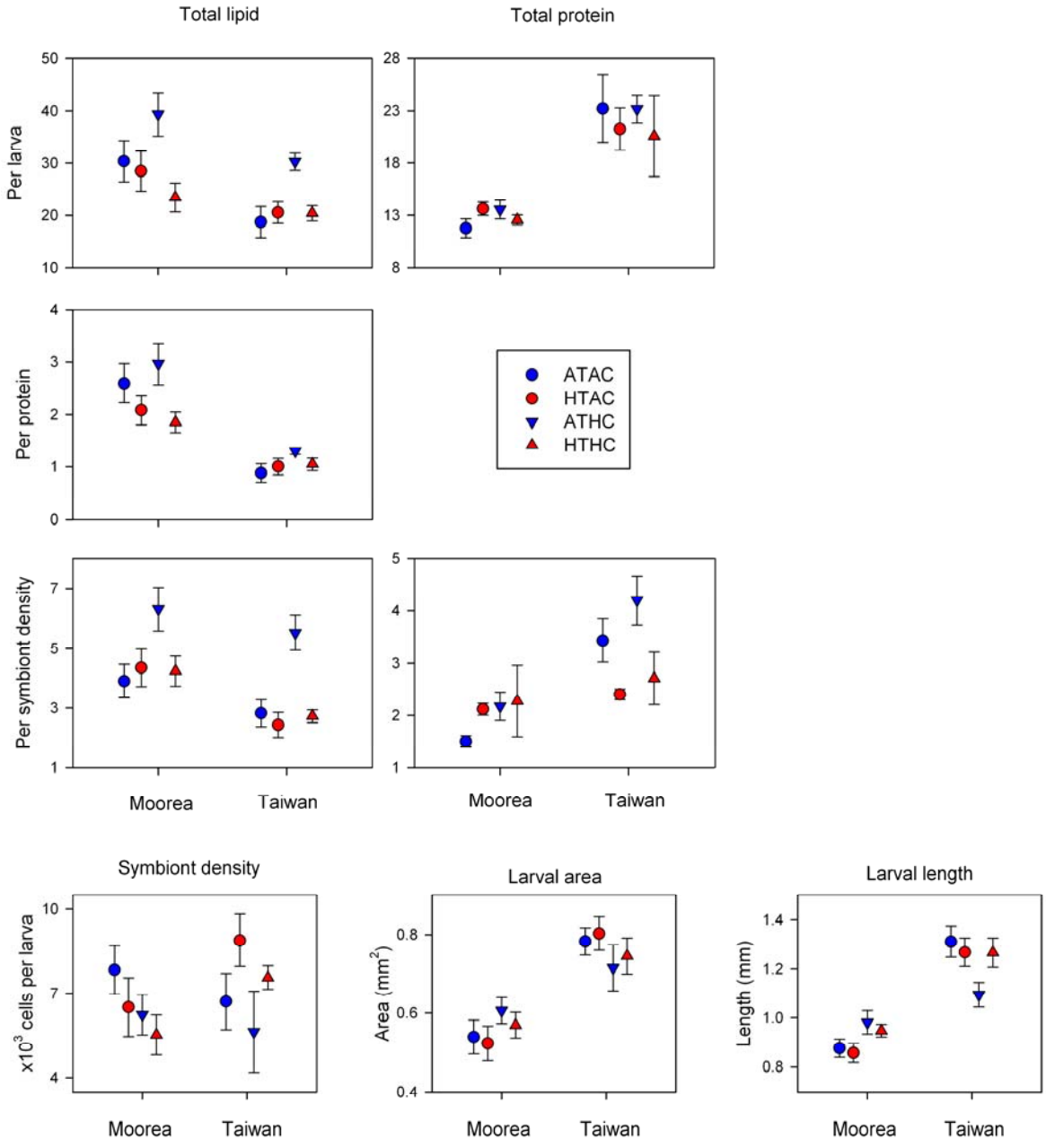

Table 30. Analysis of changes in indices of physiological condition in *P. damicornis* larvae among treatments and sites, standardized to per larva (µg larva^{-1}), per larval protein content (µg µg total protein^{-1}), and per symbiont density (µg cell^{-1}), unless otherwise noted. Indices include total lipid (TL), total protein (TP), symbiont density, larval size. Comparisons were made using type III sum of squares with pCO_2, temperature (T), and biogeographic site (Site) as fixed effects. The final reduced model is shown, with test statistic X^2, degrees of freedom (df) and p-values (*p*) reported. Interaction terms were removed from the model if the AIC value did not increase by 2 or more and if there was not a significant difference in the model log likelihood ratio; removed terms are not shown here.

	Per larva			**Per protein**			**Per symbiont density**		
ΔTL									
Effect	X^2	df	*p*	X^2	df	*p*	X^2	df	*p*
pCO_2	12.374	1	**<0.001**	0.703	1	0.402	12.374	1	**<0.001**
T	0.005	1	0.945	10.795	1	**0.001**	0.005	1	0.945
Site	3.036	1	0.081	0.432	1	0.511	10.647	1	**0.001**
pCO_2xT	9.644	1	**0.002**				9.644	1	**0.002**
pCO_2xSite									
TxSite				4.188	1	**0.041**			
pCO_2xTxSite									
ΔTP									
Effect	X^2	df	*p*				X^2	df	*p*
pCO_2	0.011	1	0.917				1.171	1	0.279
T	0.433	1	0.511				0.020	1	0.888
Site	1.951	1	0.162				2.976	1	**0.085**
pCO_2xT									
pCO_2xSite									
TxSite									
pCO_2xTxSite									

	Δ Symbiont per larva (µg cell^{-1})			**Δ Larval area (mm^2)**			**Δ Larval length (mm)**		
Effect	X^2	df	*p*	X^2	df	*p*	X^2	df	*p*
pCO_2	1.171	1	0.279	1.693	1	0.193	4.114	1	**0.043**
T	0.020	1	0.888	2.013	1	0.156	0.888	1	0.346
Site	2.976	1	**0.085**	20.136	1	**<0.001**	4.298	1	**0.038**
pCO_2xT									
pCO_2xSite									
TxSite									
pCO_2xTxSite									

Table 31. Post-hoc analyses for significant effects of changes in indices of physiological condition in *P. damicornis* larvae among treatments and sites, standardized to per larva (µg larva^{-1}), per larval protein content (µg µg total protein^{-1}), and per symbiont density (µg cell^{-1}). Indices include total lipid (TL), total protein (TP), symbiont density, and larval size. Post-hoc tests were either Tukey's HSD or general linear hypothesis tests with Bonferroni corrections for multiple comparisons (GLHT). Test statistic z and p-values (*p*) are reported for each comparison.

Post-hoc test	Biological response	Significant effect	Comparison	z	*p*	Summary description
GLHT	ΔTL per larva	pCO_2xT	ATAC vs. ATHC	3.090	**0.004**	ATAC > ATHC
			HTAC vs. HTHC	0.833	0.809	
GLHT	ΔTL per protein	TxSite	Moorea: Ambient-T vs. High-T	2.686	**0.015**	Moorea: Ambient-T > High-T
			Taiwan: Ambient-T vs. High-T	0.256	1.000	
GLHT	ΔTL per symbiont density	pCO_2xT	ATAC vs. ATHC	3.090	**0.004**	ATAC > ATHC
			HTAC vs. HTHC	0.833	0.809	Moorea < Taiwan
		Site	Moorea vs. Taiwan	2.886	**0.002**	
Tukey's HSD	Larval area	Site	Moorea vs. Taiwan	4.430	**<0.001**	Moorea > Taiwan
Tukey's HSD	Larval length	Site	Moorea vs. Taiwan	2.047	**0.041**	Moorea > Taiwan
		pCO_2	Ambient-pCO_2 vs. High-pCO_2	2.003	**0.045**	Ambient-pCO_2 < High-pCO_2

Figure 21. Changes in larval quality traits for *P. damicornis* larvae following 24-hour exposures to pCO_2 and temperature. Mean ± SE (n = 6) changes in larval composition and size for larvae released in Moorea, French Polynesia and Taiwan. Negative Δ values indicate net consumption over the experimental exposure. Positive Δ values indicate net production over 24 hours. Quality traits are standardized per larva (µg $lava^{-1}$), per protein (µg µg total $protein^{-1}$), and per symbiont density ([µg $symbiont\ cell^{-1}$]x10^{-3}) unless otherwise noted. Experimental treatments: Ambient-T, Ambient-pCO_2 (ATAC), High-T, Ambient-pCO_2 (HTAC), Ambient-T, High-pCO_2 (ATHC), High-T, High-pCO_2 (HTHC). Refer to Tables 30 and 31 for statistical details.

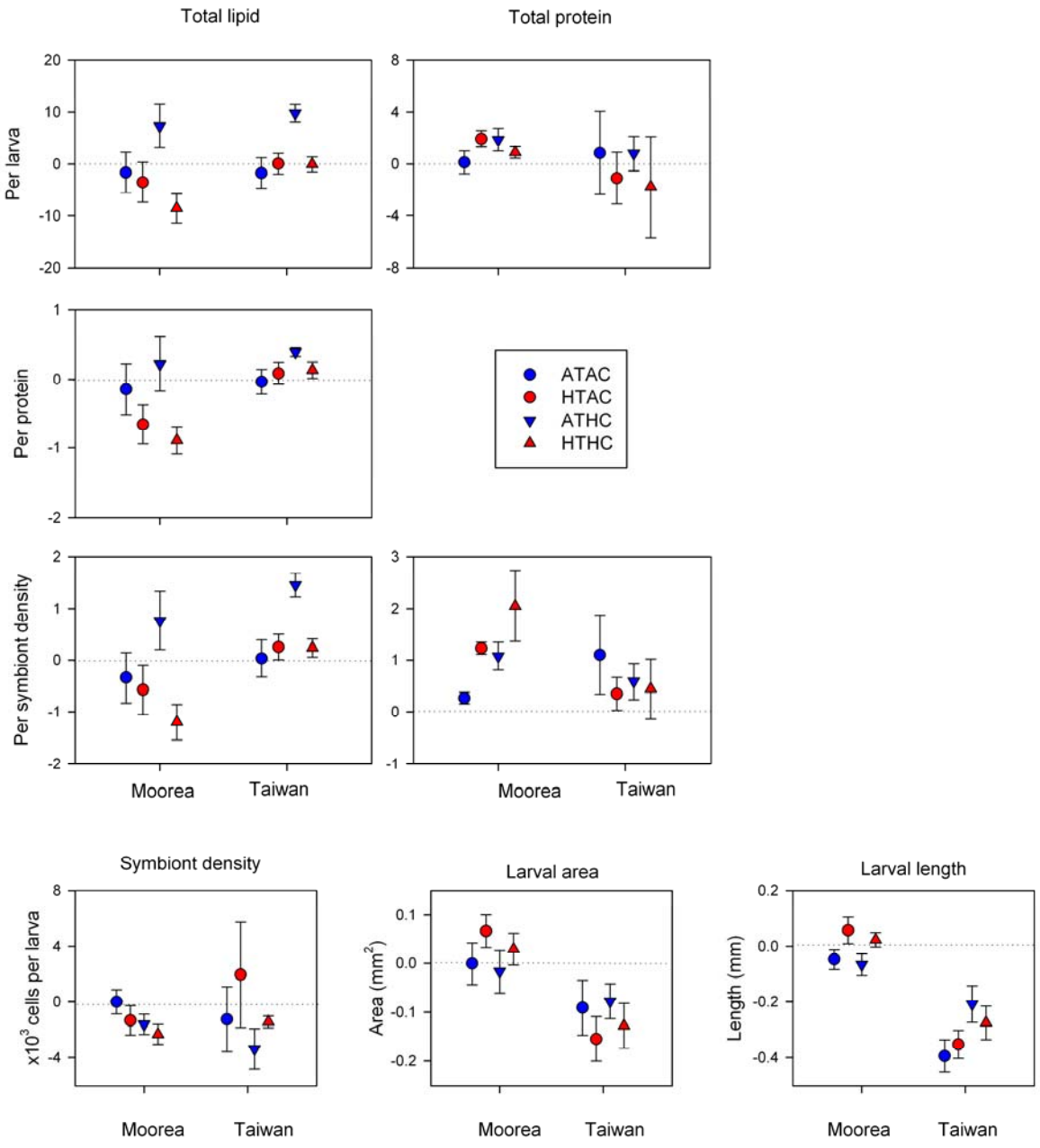

larvae from Taiwan than from Moorea (Tukey's HSD, Table 29; Fig. 20). Significant effects for TP per symbiont density included TxSite and pCO_2 (Table 28). In Taiwan, larvae contained more TP at Ambient-T than at High-T, but this difference was not significant in Moorea (GLHT, Table 29; Fig. 20). Symbiont density varied significantly by TxSite and pCO_2 (Table 28), but post-hoc analyses did not reveal any significant differences (GLHT, Table 29; Fig. 20). Larval area was significantly affected by Site (Table 28), with larger larvae in Taiwan (Tukey's HSD, Table 29; Fig. 20). pCO_2, T, and Site significantly affected larval length (Table 28). Longer larvae were found at High-pCO_2, at Ambient-T, and in Taiwan, respectively (Tukey's HSD, Table 29; Fig. 20).

ΔTP per larva ranged from -7.425 μg $larva^{-1}$ (TWN HTHC; 56% depletion) to +7.529 μg $larva^{-1}$ (TWN ATAC; 34% increase). When normalized to number of larvae and to symbiont density, total protein content of larvae did not vary significantly by pCO_2, Temp or Site (Table 30). Per larva, changes in symbiont abundance ranged from -6614.05 cells $larva^{-1}$ (TWN ATAC; 73% decrease) to +8558.33 cells $larva^{-1}$ (TWN HTAC; 95% increase). However, symbiont density did not vary significantly by any of the effects tested (Table 30). Changes in larval area varied between 69% growth (TWN ATAC) and 64% decrease (TWN HTAC). Only the effect of Site explained a significant amount of variation in this parameter (Table 30), with significantly more growth in larval area in Taiwan than in Moorea (Tukey's HSD, Table 31; Fig. 21). Changes in larval length ranged from -863.92 μm (TWN ATAC) to +784.81 μm (MCR ATHC); significant effects included pCO_2 and Site (Table 30). Larvae became significantly shorter in length in Taiwan vs. Moorea (Tukey's HSD, Table 31; Fig. 21) and at Ambient-pCO_2 vs. High-pCO_2 (Tukey's HSD, Table 31; Fig. 21).

Discussion

This study enhances the ability to predict the effects of OA and warming on the successful dispersal and recruitment of *P. damicornis* larvae by comparing populations across the species' biogeographic range. To assess the physiological responses of *P. damicornis* larvae to these co-occurring environmental stressors, I conducted laboratory experiments and measured lipid utilization and physiological condition of larvae. This comparison between coral populations in Moorea and Taiwan along with data on recent environmental history provides insight as to which of the populations is closer to its tolerance limits, tested using the physiological responses described here, and the role that environmental variability of pH and temperature may play in defining those limits.

Variation in maternal investment of P. damicornis *larvae*

Measurements of biochemical and biological traits of newly-released *P. damicornis* larvae provide critical contextual information about the physiological condition of freshly-released larvae and help us draw a link between maternal endowment and larval performance. In general, newly-released larvae differed in their biochemical composition, but not symbiont density, based on their site of origin. *P. damicornis* larvae in Moorea received more TL, WE, and PL; these lipid-rich individuals may have greater dispersal potential than their counterparts in Taiwan, as WE plays a large role in the energy storage and buoyancy of coral larvae (Nevenzel, 1970; Lee et al., 1971, 2006b; Arai et al., 1993; Villinski et al., 2002). This greater dispersal potential may account for genetic similarity between populations of *P. damicornis* around the island of Moorea, but these larvae likely do not successfully recruit to other islands in French Polynesia (Adjeroud et al., 2013).

Elsewhere, brooded *P. damicornis* larvae also commonly disperse several kilometers away from the natal reef, though local retention is observed (Torda et al., 2013). Additionally, the concentration of energy in long-term storage (WE) vs. short-term storage (TAG) indicates that in order to mount a physiological response to environmental changes, such as OA, the larvae will likely need to mobilize part of their WE pool, sacrificing their buoyancy in the process. Larvae from corals of the Taiwan population contained more TAG and TP upon release. Maternal investment may prime these larvae for more immediate response to rapidly changing environmental conditions (see Chapter 6, Figs. 25, 27), but with fewer long-term lipid stores, their dispersal distance may be diminished. With equal symbiont densities upon release, larvae of the two populations had similar potential to produce new energy, in the form of fixed carbon, assuming they contained the same clade of *Symbiodinium* with similar photophysiology. Additionally, the clades of *Symbiodinium* may have differed between sites, likely appropriate for the local environmental conditions of each location. In southern Taiwan, Chen et al. (2004) found that *P. damicornis* harbors clades C_1 and C_2 that are typically more thermally sensitive. In Moorea, the predominant hosted clade is D (Putnam et al., 2012), which is considered the most stress-tolerant clade (*e.g.* Stat and Gates, 2011), but *P. damicornis* in Moorea can also host clades A and C.

Larval size correlated with TP, not TL or PL, and was greater in larvae from Taiwan. In a study from a single population in Japan, large *P. damicornis* larvae can survive for a longer period of time in the plankton than small larvae (Isomura and Nishihira, 2001) and can therefore potentially disperse farther; however the authors did not examine whether planula size was correlated with lipid or protein content. A longer dispersal period may allow planulae to discover preferred or novel habitats for settlement, but at the cost of

extended predation risk and removal from the favorable parental habitat (Strathmann, 1974; Morgan, 1995; Pechenik, 1999; Marshall and Keough, 2003). In my study, while larvae from Taiwan may be larger in size, they may have a shorter dispersal distance due to smaller stores of long-term energy biomolecules (WE).

Responses of larval lipid consumption and physiological condition to changes in pCO_2 and temperature

Brooded planulae, like *P. damicornis*, rely on parentally-derived lipids as well as translocated carbon from their endosymbionts to fuel their dispersal. Changes in lipid content of planulae therefore represent the balance between demands of holobiont metabolism and the carbon translocation by the *Symbiodinium.* When lipid utilization was quantified in *P. damicornis* planulae over 24 hours under experimental conditions, a range of responses across treatments and biogeographic sites was observed. In some cases, planulae depleted up to half of their energy-storage lipids while other planulae more than doubled their deposits of these lipids. Based on my measurements of aerobic metabolism of *P. damicornis* larvae from Moorea in Chapter 2, Peak larvae consumed ~0.08-0.13 nmol O_2 $larva^{-1}$ min^{-1}. Assuming constant rates of respiration over a 24-hour period and similar values for larvae from Taiwan, larvae would need to consume 1.33-2.16 µg WE over the 24-hour incubation (Davies, 1991). Larvae in this study consumed ≤ 1 µg WE per symbiont density, but photosynthetic activities and consumption of TAG may have accounted for the remaining energy burned during respiration. The net production of WE and TAG during experimental exposures was likely due to the photosynthetic activities of their *Symbiodinium*. Given the ecological significance that energy-storage lipids play in the

successful dispersal of these lecithotrophic larvae (Richmond, 1987; Arai et al., 1993; Harii et al., 2002, 2007; Wellington and Fitt, 2003; Alamaru et al., 2009), the point when larvae stop accumulating lipid and start depleting lipid stores may be a useful indicator of stressful environmental conditions.

Wax esters (WE) are particularly important for larval dispersal, as they confer buoyancy to planulae (Nevenzel, 1970; Lee et al., 1971, 2006b; Arai et al., 1993; Villinski et al., 2002). Because the larvae rely on cilia for swimming, their buoyancy may play an important role in where they can easily remain in the water column. Positive buoyancy will keep them closer to the surface where higher irradiance and stronger currents usually occur. A longer dispersal distance would be possible in this case if the currents transport planulae to more distant reefs. Less buoyancy may bring planulae closer to the reef, closer to predators and closer to settlement cues. Surviving larvae may recruit to the benthos more quickly. For Peak planulae used in this study, pCO_2 and temperature often did not have a significant effect on utilization of WE. However, in general, planulae consumed more WE under HTHC (Fig. 10). In Taiwan, the co-occurrence of OA and warming created a negative balance in planula energy metabolism, causing net consumption of WE at HTHC while there was net production of this energy-storage lipid under all other conditions. An interesting trend, temperature seemed to have an opposite effect on WE utilization depending on the location. In Moorea, planulae consumed slightly more WE at Ambient-T, while in Taiwan, planulae produced slightly more WE. Metabolic rates of planulae increase with temperature (Cumbo et al., 2013a; Rivest and Hofmann, 2014), so utilization of lipids, from stores or from photosynthesis, would also be expected to rise. However, in Moorea, planulae at High-T consumed less WE than at Ambient-T. Increased primary productivity of *Symbiodinium* at

High-T or increased rates of translocation may explain this pattern, as *P. damicornis* in Moorea tend to host a more thermotolerant *Symbiodinium* clade (Stat and Gates, 2011; Putnam et al., 2012) than *P. damicornis* in Taiwan (Chen et al., 2004). Putnam *et al*. (2013) observed no change in the photophysiology of *P. damicornis* planulae in response to elevated pCO_2 and temperature; however, rates of translocation of fixed carbon can increase in response to low pH and elevated temperature (Loram et al., 2007; Tremblay et al., 2013). Translocated carbon could be used to satisfy immediate energy demands than oxidizing already-stored WE (Harii et al., 2010).

The utilization of WE may occur when demand for energy surpasses the pool of triacylglycerol (TAG) (Lee, 1974; Patton et al., 1975; Sargent et al., 1977). Patterns of TAG consumption were similar to those for WE. In general, TAG was consumed in all treatments in Moorea; TAG provides short-term energy storage in the form of saturated fatty acids as well as storage of poly-unsaturated fatty acids, building blocks of structural lipids (Napolitano et al., 1988; Lee et al., 2006b). In Moorea, the energetic demands of early dispersal surpassed the combined resources of TAG synthesis and translocated fixed carbon, perhaps due to smaller initial TAG stores for larvae from Moorea (Fig. 17). The smaller pool of TAG is partially maintained as WE is oxidized (Patton and Benson, 1975; Bauermeister and Sargent, 1979). In Taiwan, planulae produced TAG in general, except at HTHC where net consumption occurred. While most of these relationships were not significant, the patterns indicate that *P. damicornis* planulae are launching a physiological response to OA and warming, fueled by the utilization of WE and TAG. As a result, planulae may have fewer resources for performing the developmental changes associated with metamorphosis and settlement (Holland and Walker, 1975; Gallager et al., 1986; Moran and Manahan,

2003), particularly for larvae in Taiwan that depleted WE and TAG stores under HTHC only.

Our measurements of utilization of energy-storage lipids represent the net activity of the planula holobiont (animal + symbiont). However, the abundance of *Symbiodinium* within the planulae could affect the patterns observed. The symbiont cells themselves contain lipid that contributes to the measured amount for the holobiont (*e.g.* Harland et al., 1991). Additionally, the photosynthetic activities of the *Symbiodinium* as well as their translocation rates of glycerol and lipid bodies containing WE and TAG potentially change the amount of fixed carbon received by the host (*e.g.* Muscatine, 1967; Trench, 1971; Muscatine and Porter, 1977; Luo et al., 2009; Gordon and Leggat, 2010; Chen et al., 2012; Tremblay et al., 2013) and therefore the amount of lipid available. When ΔWE and ΔTAG were standardized by symbiont abundance, patterns of lipid utilization did not differ for planulae released in Moorea; in this case, the physical presence of symbionts does not influence the response of lipid utilization. However, enhanced productivity of *Symbiodinium* at High-T may have supplemented use of existing lipid stores, as discussed above. In Taiwan, loss of symbiont abundance at High-CO_2 (Fig. 21) contributed to changing levels of WE and TAG per larva (Figs. 18, 19). However, consumption of these energy-storage lipids remained greatest at HTHC. These results highlight the important roles, both direct and indirect, that *Symbiodinium* plays in the overall lipid content of *P. damicornis* planulae.

Traits of size and growth were not significantly affected by elevated pCO_2 and temperature, in general. For temperature marine invertebrate larvae, size usually decreases over the course of dispersal (Kempf and Hadfield, 1985; Emlet, 1986; Highsmith and Emlet, 1986). Planula size in *P. damicornis* may not be sensitive to OA and warming due to the

contribution of *Symbiodinium* to larval energy metabolism; this input of exogenous energy may even allow them to grow in size during dispersal, a possibility not available to aposymbiotic lecithotrophic (non-feeding) larvae. First, phospholipid levels were assessed as a proxy for cell number, due to the structural role of this lipid class (Lee et al., 1971, 2006b). As shown before (this chapter, Part A), PL did not change significantly in response to pCO_2, temperature, and site. Changes in symbiont density were similar across all sites but when ΔPL was normalized by symbiont density, PL content of planulae in Taiwan increased under Ambient-T but not in High-T. The increased costs of thermotolerance at elevated temperature may slow growth rates. Similarly, larval area and length did not differ by pCO_2 and temperature, though there was a significant effect of site. However, in Taiwan, larval size complemented ΔPL, with greater decrease in larval area observed at High-T. If this trend of reduced planula PL and size over the first 24 hours of dispersal continues throughout the larval stage, it may carry over to reduce the stringency of habitat selection for settlement, increase post-settlement survival and growth, and increase the age of first reproduction (Knight-Jones, 1953; Sebens, 1983; Emlet, 1986; Woollacott et al., 1989; Miller, 1993; Stevens et al., 1999; Olive et al., 2000; Marshall et al., 2003). However, even though larval size decreased over the 24-hour exposures in Taiwan, absolute larval size still remained larger than larvae in Moorea (Fig. 20). While smaller planula size at the beginning of settlement would be a fitness disadvantage (Sinervo, 1990; Stearns, 1992; Williams, 1994; Bernardo, 1996), this may not be the case for planulae from Taiwan, which maintained their symbiont density, TL, and TP at High-T, despite the decrease in larval size.

My results complement those of previous studies with *P. damicornis* and other coral species. Larval physiology is thought to vary across the release period of reproduction

(Edmunds et al., 2001; Putnam et al., 2010; Cumbo et al., 2013a; Rivest and Hofmann, 2014), and Peak larvae may be more tolerant of elevated pCO_2 and temperature than planulae released on other days (Rivest and Hofmann, 2014). Within their first hours-days of dispersal, coral larvae respond to elevated temperature through changes in size, symbiont density, rates of development, time to metamorphosis, gene expression, and rates of respiration (Edmunds et al., 2005; Nozawa and Harrison, 2007; Rodriguez-Lanetty et al., 2009; Heyward and Negri, 2010; Rivest and Hofmann, 2014). The observed responses of coral larvae to elevated pCO_2 have been more diverse. Conditions of OA are known to reduce larval respiration rates (Albright and Langdon, 2011; Rivest and Hofmann, 2014) but other species, populations, or larval cohorts are not affected by high pCO_2 (Cumbo et al., 2013a, 2013b; Putnam et al., 2013; Rivest and Hofmann, 2014). Low pH reduces larval metamorphosis and settlement for some species (Albright et al., 2010; Albright and Langdon, 2011; Nakamura et al., 2011) but not for others (Albright et al., 2008; Anlauf et al., 2011; Chua et al., 2013). While the energetic costs of tolerating high pCO_2 may delay metamorphosis and settlement, it is also important to note that changes in the cues produced by the algal community on the settlement surface may contribute to the responses observed in these experiments (*e.g.* Albright and Langdon, 2011).

The role of environmental history and geographic site in the physiology of planulae

I compared the responses of *P. damicornis* planulae between two sites across their biogeographic range. The study sites in Moorea and Taiwan had different regimes of temperature and pH (Chapter 6) that have presumably persisted over the recent history of the study populations. Corals in Moorea experienced, on average, warmer temperatures with a

narrower range of values than corals in Taiwan. On the other hand, corals in Taiwan experienced lower mean pH and a greater range of pH values. In both sites, autonomous sensors deployed on natal fringing reefs (described in Chapter 6) confirmed that the Ambient treatment conditions were observed within the water mass bathing the fringing reef during the experiment. The High treatment conditions were not observed during this time.

Overlaid on the between-site differences in environmental conditions are the genetic differences between *P. damicornis* populations. Firstly, high levels of phenotypic plasticity make *P. damicornis* difficult to distinguish between other species in its genus, and it is possible that the individuals used in the experiments were different, cryptic species. Although recent developments in morphological and molecular systematics have re-organized and fine-tuned the taxonomy of the *Pocillopora* genus, the cumulative body of work confirms that *P. damicornis* is present from the Great Barrier Reef, to Taiwan, to Hawaii (Schmidt-Roach et al., 2014). Additionally, there are several haplotypes of *P. damicornis* found in Moorea that have not been found in Taiwan (Forsman et al., 2013). The genetic diversity between sites may indicate the possibility of local adaptation to environmental conditions.

While my results cannot inform the potential of the study populations in Moorea and Taiwan to adapt or acclimatize to future environmental change, they shed light on the possibility that the physiological plasticity of *P. damicornis* planulae to tolerate future ocean conditions may be influenced by the environmental conditions to which its population is adapted or acclimatized (Kelly and Hofmann, 2012). In general, my results confirm expectations based on a local adaptation scenario: planulae from Moorea should perform better than those from Taiwan under High-T, and planulae from Taiwan should perform

better than those from Moorea under High-pCO_2. I found that larvae from Taiwan were sensitive to High-T, producing fewer energy-storage lipids in this scenario. In Moorea, planulae at High-T consumed less lipid, suggesting that their demands for stored energy were diminished, perhaps due to increased carbon translocation from their symbionts. Planulae in Taiwan responded positively and negatively to High-pCO_2, often producing the most lipid at ATHC. However, the presence of High-T enhanced their sensitivity to OA. For planulae in Moorea, High-pCO_2 did not produce the same effects; consumption of lipid was consistent across temperature levels. Additionally, corals in the study sites with different environments produced larvae with different characteristics, which may play a role in the different physiological responses observed. Larger sized larvae were produced in Taiwan but larvae with more long-term energy stores were produced in Moorea. Notably, planulae in Taiwan increased their stores of WE and TAG in general over the first 24 hours of their dispersal with interactive effects among stressors whereas planulae from Moorea consumed energy-storage lipids in all cases with additive effects of stressors.

Conclusion

Comparisons of physiological responses of *P. damicornis* larvae to OA and warming between sites across the species' biogeographic range improve our understanding of the possible future success of this species. An overarching outcome of this study is that site-specific aspects of planula physiology provide the framework within which manifest the consequences of environmental stress. For example, ΔWE in larvae from Taiwan was more positive than in larvae from Moorea, across all experimental treatments. Because larvae from Moorea are endowed with more total lipid and WE upon release, they may be able to

accommodate depletion of these stores without sacrificing their dispersal potential or the energy reserves required to complete metamorphosis and settlement. While there is still much to learn about the interplay of environmental history and population genetics, the variety of physiological responses maintained within *P. damicornis* may enhance the overall persistence of this species in the light of global climate change.

V. Transcriptomic responses of the larvae of *Pocillopora damicornis* to ocean acidification and warming

Introduction

Many of the core physiological responses to ocean acidification and elevated temperature will likely be subtle and potentially undetectable at the organismal to biochemical levels (*i.e.* through measures of lipid use and oxygen consumption). While physiological pathways can be regulated in a variety of ways, modulation of gene expression is a swift and resilient mechanism for responding to changes in the environment. The use of sensitive molecular approaches, such as gene expression studies, provides a powerful avenue for exploring the entire spectrum of impacts of anthropogenic change in the ocean, not just the ones easily observed from outside the black box of the organism. Exploring responses to a changing environment at the level of the transcriptome yields valuable information about the potential for physiological plasticity and thus tolerance (*e.g.* Hofmann et al., 2008; Todgham and Hofmann, 2009; Whitehead et al., 2010), mechanisms driving the response, and current physiological thresholds. Importantly, these transcriptomic techniques reveal how the organism is regulating its response to a changing environment before this response manifests at the whole organism level. Additionally, responsive genes can be adopted as targets for detecting stress response to provide better feedback information for making predictions about the future of ocean ecosystems.

Genomic resources for corals have been limited in the past, but the advent of next-generation high-throughput sequencing (*e.g.* RNASeq) has made studies of coral transcriptomes more approachable. In the last two years, more data and transcriptomes on

scleractinian corals and related cnidarians have emerged. Additionally, RNASeq and the accompanying bioinformatics tools have allowed transcriptomic studies to include symbiotic life history stages, allowing for better parsing of coral and symbiont gene expression (*e.g.* Shinzato et al., 2014). Two reference transcriptomes have been generated for adult *Pocillopora damicornis* (Traylor-Knowles et al., 2011; Vidal-Dupiol et al., 2013). Vidal-Dupiol *et al.* (2013) showed an up-regulation of genes related to calcification and energy metabolism in response to low-pH conditions. For other corals, reference transcriptomes for aposymbiotic *Acropora millepora* larval and recruits have revealed pathways sensitive to heat and high-pCO_2 exposure (Meyer et al., 2011; Moya et al., 2012). Annotated transcriptomes of symbiotic *Favia* and *Porites australiensis* coral adults are now available (Mehr et al., 2013; Shinzato et al., 2014). Additionally, RNASeq of *Acropora hyacinthus* and *Symbiodinium* has enabled the comparisons of gene expression profiles in response to temperature stress and between symbiont clades (Barshis et al., 2013, 2014; Palumbi et al., 2014). A recently assembled transcriptome of sea fan *Gorgonia ventalina* has been used to elucidate immune response pathways (Burge et al., 2013).

In this chapter, I explored the response of coral larvae to future conditions of OA and warming at the level of the transcriptome. This is the first study I am aware of that examines gene expression in symbiotic coral larvae in response to projected ocean conditions. I assessed broad patterns in the transcriptome in response to laboratory exposures of pCO_2 and temperature. Using next-generation high-throughput RNA sequencing (RNASeq), I generated a *de novo* transcriptome assembly and quantified differentially expressed genes (DE genes) between pCO_2 and temperature levels. I complemented these molecular data with measurements of larval physiological condition, in this case, total protein,

Symbiodinium density, and size. The study described in this chapter was conducted on my study population in Moorea, French Polynesia.

Materials and Methods

Collection of coral larvae

To obtain coral larvae, adult corals were brought to the laboratory, and larvae were captured upon their release. Specimens of adult *Pocillopora damicornis* were collected from two fringing reefs on Moorea, French Polynesia; eight colonies of *P. damicornis* were collected on the new moon in January 2012, from a depth of ~1-3 m. Colonies were maintained in individual aquaria that received indirect natural sunlight and coarsely filtered seawater (T ~ 29°C). Larvae were collected from adult colonies following their lunar pattern of reproduction (Fan et al., 2006). Larval release reached a peak in cohort size around 8 days after the new moon, followed by a decline. Overnight, larvae were captured in 100 μm mesh-lined cups that received the outflow of each aquarium. Daily at dawn, larvae from each colony were collected and counted in order to identify the day with the peak release of larvae. On the peak day, all larvae released were counted and pooled. The small numbers of larvae released from some colonies required the use of all larvae released, resulting in unequal genotype ratios in the pool. Larvae from this pool were immediately photographed and preserved to quantify larval quality metrics and gene expression (see below) that represented the condition of freshly-released larvae. The remaining larvae in the pool were then randomly assigned to experimental treatments. Data presented here were collected before and after manipulative experiments were conducted with the cohort of larvae released on January 30 (Lunar day 8, "Peak").

Experimental incubations

Larvae were divided among 8 tanks containing 4 treatment conditions and were incubated for 24 hours. Two pCO_2 levels (475 and 1045 μatm pCO_2) and two temperature levels (28 and 31°C) were used. Refer to Chapter 4 Part A for details on how the treatments were created and how the incubations were performed (p. 101). The four treatments created by this experimental set-up are defined as ambient temperature-ambient pCO_2 (ATAC), ambient temperature-high pCO_2 (ATHC), high temperature-ambient pCO_2 (HTAC), and high temperature-high pCO_2 (HTHC). To verify and monitor the physical parameters of the OA x temperature treatments, the carbonate chemistry (pH, salinity, and total alkalinity) and the temperature of the seawater in the aquaria was analyzed daily during the incubations (see Chapter 4 p. 103). At the end of each incubation, larvae within tanks were pooled, and 10 larvae were randomly selected for size measurements (n = 20 per treatment). The remaining larvae were aliquoted and frozen at -80°C for downstream analyses of gene expression (2 x 25 larvae), total protein content (2 x 5 larvae), and symbiont density (2 x 5 larvae). Therefore, for comparisons between treatments, n = 4 for gene expression, total protein, and symbiont density.

Larval quality metrics

Larval size, protein content, and *Symbiodinium* density were measured as described in Chapter 4 (p. 108).

Statistical analyses for physical conditions and larval quality

All data were analyzed using R version 3.0.1 (R Core Team 2013). In all cases,

statistical assumptions of normality and homogeneity of variance were tested using quantile-quantile (Q-Q) plots and Levene's test and were met. Effects on physical conditions and larval quality variables were estimated using linear mixed-effect models (nlme package in R; Pinheiro and Bates, 2000) with pCO_2 and temperature treatments as fixed factors and "tank" as a random factor. Refer to Chapter 4 (p. 112) for descriptions of model selection, determination of significant factors, and post-hoc analyses.

RNA extraction

For RNA extraction, aliquots of 25 *P. damicornis* larvae were homogenized in 0.5 mL TRIzol® (Thermo Fisher Scientific, Inc., Waltham, MA USA) using glass beads (Sigma-Aldrich Corp., St. Louis, MO, USA) and a bead-beater (Biospec Products, Inc., Bartlesville, OK, USA). Homogenates were brought to a total volume of 2 mL TRIzol® and split into two microcentrifuge tubes. Proceeding with one half of the homogenate, 200 µL chloroform was added to each tube. The samples were shaken vigorously, and the solutions were incubated at RT for 5 minutes. Then, the samples were centrifuged at 12,000xg for 15 min at 4°C to separate the aqueous and organic layers. The aqueous phase containing RNA was carefully removed and transferred to a new 1.5 mL microcentrifuge tube. 250 µL isopropanol and 250 µL high salt buffer (0.8 M sodium citrate, 1.2 M sodium chloride) were added to each tube, and RNA precipitated for 10 minute at RT. The samples were centrifuged at 12,000xg for 10 min at 4°C and the supernatant was discarded. The RNA pellet was washed with 1 mL 75% ethanol followed by a centrifugation at 7600xg for 5 min at 4°C. The ethanol supernatant was discarded and the pellet was allowed to dry for several minutes. RNA pellets were dissolved in 100 µL DEPC-treated water and heated for 10 min

at 55°C. The concentration and quality of RNA in the purified solution was quantified using a NanoDrop spectrophotometer (Thermo Fisher Scientific, Inc., Waltham, MA USA). Concentrations ranged from 62.9-138.0 ng RNA/μL. The 260/280 values were slightly greater than 2, the generally accepted ratio for "pure" RNA. The 260/230 values were higher than the common range for "pure" nucleic acid (1.8-2.2). These deviations from expected values likely indicated the presence of protein or other contaminants that absorb strongly at 260 nm, common for marine organisms.

To improve the quality of the RNA extracts, a Qiagen RNeasy® MinElute® Cleanup Kit was used, following the kit's instructions for use of starting volumes ≤ 100 μL but with a final elution volume of 50 μL in DEPC-treated RNase-free water. After the clean-up, the extracts, now in half the volume of the original extract, contained 113.0-247.9 ng RNA/μL. The 260/280 and 260/230 values improved in general. To make a more precise assessment of RNA quality in the extracts before cDNA library construction, an Agilent RNA 6000 Pico Kit was used with a Bioanalyzer Agilent 2100 instrument (Agilent Technologies, Inc., Santa Clara, CA USA). Aliquots of the RNA extracts were diluted to 0.5-5.0 ng RNA/μL and RNA quality was assessed following the kit manual. The electropherograms showed clean, resolved peaks with no obvious signs of RNA degradation. Importantly, RNA quality was consistent across all extracts.

cDNA library preparation

cDNA libraries were prepared from at least 1 μg total RNA from each extract using a TruSeq RNA Sample Prep Kit v.2 (Illumina, Inc., San Diego, CA USA), following the kit's instructions. From the two tubes of larvae preserved from each aquarium, one was used to

prepare a library for paired-end RNA sequencing and the other was used to prepare a library for single-read RNA sequencing. First, poly-A containing mRNA molecules were purified using poly-T oligo-attached magnetic beads. The mRNA was then fragmented and primed for cDNA synthesis. The cleaned mRNA was reverse transcribed into first-strand cDNA using random primers. Then, the RNA templates were removed and a replacement cDNA strand was synthesized to generate double-strand cDNA. In this step, I used Qiagen Buffer EB instead of the kit's Resuspension Buffer (both should be 10 mM Tris-Cl pH 8.5). Next, the cDNA strands were repaired to have blunt ends and the 3' ends were adenlyated to prevent chimera formation during the next step. Then, a unique RNA Adapter Index was ligated to the cDNA fragments in each library. These adapters are used to index the data from the next-generation sequencing run, where libraries from multiple samples are mixed together on the same lane. Out of the pool of sequences generated, the indices are used to identify the original library for each sequence. Finally, the cDNA was enriched in a PCR step. Quality of cDNA libraries was assessed using NanoDrop analysis and gel electrophoresis, confirming the presence of cDNA and sufficient quality for sequencing. The libraries contained cDNA sequences of insert size ~260 bp.

Next-generation high-throughput sequencing: RNASeq

The concentration of cDNA in the libraries was adjusted to ~50 ng cDNA/μL, and 25 μL of each was sent to the UC Davis Genome Center DNA Technologies Core (http://dnatech.genomecenter.ucdavis.edu/) for high-throughput sequencing. The HiSeq 2500 Illumina sequencing platform was used, and 9 libraries were pooled in each of 2 lanes. One lane was used to generate 100 bp paired end reads, where each library insert was

sequenced from both ends. This type of sequencing is particularly useful for *de novo* transcriptome assembly because of the spatial relationship provided with each pair of reads. The second lane was used to generate 50 bp single reads, where each library insert was sequenced from one end.

Reference transcriptome assembly and annotation

I assembled a transcriptome *de novo* from 100-nucleotide paired-end short sequence reads (SSRs). Published reference transcriptomes for *P. damicornis* were made utilizing old sequencing technology with adults (Roche 454; Traylor-Knowles et al., 2011) or made with RNA from adult specimens that had not been exposed to low pH (Vidal-Dupiol et al., 2013). Therefore, the published transcriptomes for *P. damicornis* may not include transcripts or spliced transcripts that are only expressed in larvae and under low pH, high pCO_2 conditions. As a result, I chose to assemble *de novo* a reference transcriptome from my RNASeq reads and did not map my sequences to the published transcriptomes.

All analyses were performed using command line and the Knot computing cluster at the UCSB Center for Scientific Computing (http://csc.cnsi.ucsb.edu/clusters/knot). 187,925,419 paired-end short sequence reads (SSRs) and 157,325,043 short-read SSRs were generated. First, paired-end and single-read SSRs were trimmed to remove ends with Phred quality score < 20 and to remove any remaining adapter index sequences (Trim Galore!, Bioinformatics Group, Babraham Institute). The Trinity platform (Broad Institute, Hebrew University of Jerusalem) was used for *de novo* construction of the *P. damicornis* transcriptome from the 182,161,357 trimmed paired-end SSRs.

Differential gene expression analysis

To measure changes in gene expression associated with pCO_2, temperature, and the interaction of these environmental stressors, paired-end SSRs were mapped against the transcriptome, and the number of reads that aligned to each genomic locus was counted using the RSEM package (B. Li and C. Dewey, University of Wisconsin, WI, USA). To identify genes that were significantly differentially expressed among treatment conditions, the edgeR package in R was used (Robinson et al., 2010; McCarthy et al., 2012). The data were first normalized for RNA composition to minimize the log-fold changes between the samples for most genes and to scale the library size for each sample. This normalization prevented highly expressed genes unique to one sample from causing the remaining genes in that sample to appear relatively down-regulated. Additionally, this normalization controls for the dependent relationship between counts, the molar concentration of the transcripts, and the transcript lengths. Differential expression was determined using the generalized linear model likelihood ratio test in EdgeR, which is recommended for experiments with multiple factors. The false discovery rate for each comparison (transcript) was adjusted using the Benjamini-Hochberg method (Benjamini and Hochberg, 1995). Common dispersion was calculated to get an idea of the overall degree of inter-library variability in the data. The log-fold-changes were plotted across expression levels (average log-counts-per-million-reads), with DE genes highlighted. The biological CV, the coefficient of variation with which the true, unknown abundance of the genes varies between replicate samples, was also plotted across expression levels. To show the relationship of log-fold-changes between all samples, a multi-dimensional scaling plot was generated where distance in two-dimensional space correlated with the root-mean-square of the largest absolute log-

fold-changes between each pair of samples. As an alternative, hierarchical clustering was performed using the Ward method (hclust). In the plot, tighter clusters are displayed on the left.

Results

To assess how changes in the transcriptome might shape physiological plasticity in *Pocillopora damicornis* planulae in response to multiple abiotic factors, I performed laboratory microcosm experiments where larvae were exposed to variable levels of pCO_2 and temperature. I was able to maintain fairly stable conditions with physical conditions in each treatment group remaining within expected ranges (Table 32). For example, temperature varied significantly between and temperature treatments (Table 33), with higher temperature at High-T and at High-pCO_2 (Tukey's HSD). Salinity and total alkalinity did not vary significantly by temperature, pCO_2 or their interaction (Table 33). pH and pCO_2 varied significantly between, but not within, pCO_2 treatments (Table 33).

Changes in larval quality in response to different pCO_2 and temperature levels were measured in the form of total protein per larva, *Symbiodinium* density, larval length, and larval size. Larval total protein ranged from 9.07 μg $larva^{-1}$ at ATAC to 29.00 μg $larva^{-1}$ at HTAC (Fig. 22A). At the end of the 24-hour exposures, total protein did not differ significantly by pCO_2, temperature (T) or their interaction (Table 34). Varying between 6188 and 14,357 cells $larva^{-1}$, *Symbiodinium* density was also least at ATAC and greatest at HTAC (Fig. 22B). *Symbiodinium* density was significantly affected by T and pCO_2xT. However, post-hoc analyses did not confirm significant differences (Table 34). Larval area

Table 32. Summary of physical conditions in experimental aquaria. Data are presented as mean ± SE. For all parameters, $n = 4$.

Treatment	Temperature (°C)	Salinity (psu)	pH	A_T (µmol kg^{-1})	pCO_2 (µatm)
ATAC	28.40 ± 0.07	36.13 ± 0.08	7.988 ± 0.005	2356 ± 2	476 ± 7
HTAC	31.10 ± 0.21	36.28 ± 0.08	7.697 ± 0.004	2363 ± 5	477 ± 6
ATHC	27.93 ± 0.25	36.08 ± 0.03	7.981 ± 0.022	2352 ± 1	1059 ± 63
HTHC	30.73 ± 0.15	36.23 ± 0.08	7.705 ± 0.029	2359 ± 2	1030 ± 81

Table 33. Statistical comparison of sea water treatment conditions using type III sum of squares with pCO_2 and temperature (T) as fixed effects and Tukey's HSD. Interaction terms were removed from the model if the AIC value did not increase by 2 or more and if there was not a significant difference in the model log likelihood ratio; removed terms are not shown here. Comparisons were performed using type III sum of squares, with test statistic X^2, degrees of freedom (df) and p-values (*p*) reported. Post-hoc analyses were performed using Tukey's HSD with test statistic *z* and p-values (*p*) reported.

Parameter	Effect	Type-III SS X^2	df	*p*	Tukey's HSD z	*p*
Temperature	pCO_2	7.027	1	**0.008**	2.390	**0.017**
	T	294.225	1	**<0.001**	15.460	**<0.001**
Salinity	pCO_2	0.421	1	0.516		
	T	3.790	1	**0.052**	1.539	0.124
pH_{total}	pCO_2	296.850	1	**<0.001**	15.530	**<0.001**
	T	<0.001	1	0.976		
A_T	pCO_2	0.929	1	0.335		
	T	3.248	1	0.072		
pCO_2	pCO_2	160.235	1	**<0.001**	11.410	**<0.001**
	T	0.098	1	0.754		

Figure 22. Larval quality traits for *P. damicornis* larvae following 24-hour exposures to pCO_2 and temperature. Mean ± SE changes in larval composition (n = 4) and size (n = 20) for larvae. Experimental treatments: Ambient-T, Ambient-pCO_2 (ATAC), High-T, Ambient-pCO_2 (HTAC), Ambient-T, High-pCO_2 (ATHC), High-T, High-pCO_2 (HTHC). Refer to Table 34 for statistical details.

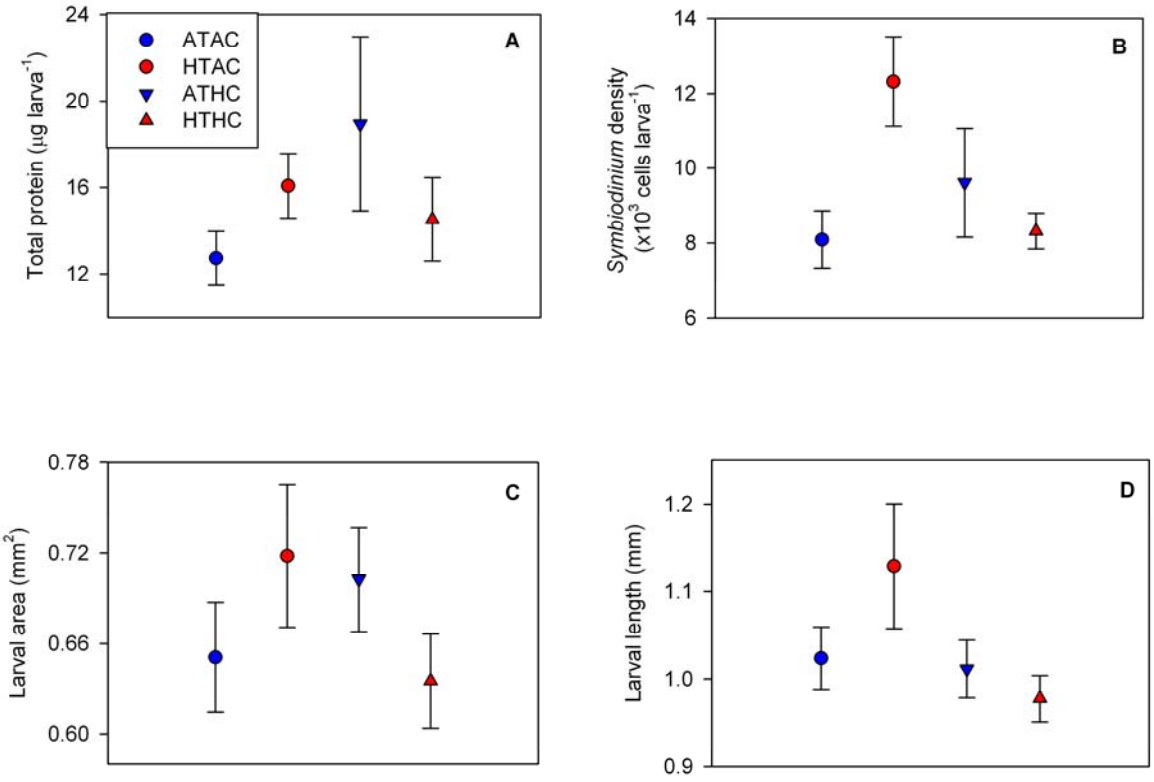

Table 34. Analysis of total protein content, *Symbiodinium* density, and size of *P. damicornis* larvae following a 24-hour exposure to seawater of controlled temperature and pCO_2. Lipid content was compared among treatments and days of release, standardized to per larva (μg $larva^{-1}$), per larval protein content (μg μg total $protein^{-1}$), and per symbiont density (μg $cell^{-1}$). Comparisons were made using type III sum of squares with pCO_2, temperature (T), and day of release (Day) as fixed effects. The final reduced model is shown, with test statistic X^2, degrees of freedom (df) and p-values (*p*) reported. Interaction terms were removed from the model if the AIC value did not increase by 2 or more and if there was not a significant difference in the model log likelihood ratio; removed terms are not shown here. Post-hoc tests were either Tukey's HSD or general linear hypothesis tests with Bonferroni corrections for multiple comparisons (GLHT). Test statistic z and p-values (*p*) are reported for each comparison.

Response variable	Effect	Type-III SS X^2	df	*p*	Post-hoc z	*p*
Total protein (μg $larva^{-1}$)	pCO_2	1.014	1	0.314		
	T	0.053	1	0.818		
Symbiont density (cells $larva^{-1}$)	pCO_2	0.680	1	0.410		
	T	5.248	1	**0.022**		
	pCO_2xT	5.081	1	**0.034**		
	ACAT vs. HCAT				0.825	**1.000**
	ACHT vs. HCHT				2.166	**0.121**
	ACAT vs. ACHT				2.291	0.088
	HCAT vs. HCHT				0.700	1.000
Larval area (mm^2)	pCO_2	0.522	1	0.470		
	T	1.965	1	0.161		
	pCO_2xT	2.718	1	0.099		
Larval length (mm)	pCO_2	4.026	1	**0.045**	0.539	0.590
	T	1.200	1	0.273		

did not differ significantly by pCO_2, T or their interaction. Larval length varied significantly by pCO_2, though post-hoc analyses did not confirm the significant difference (Table 34). Larvae had the smallest area and longest length at HTAC while having the biggest area at ATAC (Figs. 22C,D).

Assembly of the reference transcriptome

To quantify changes in gene expression between High-T, High-pCO_2 conditions and ambient conditions, I assembled a reference transcriptome *de novo* for ***P. damicornis*** larvae. The assembly yielded a transcriptome of 422.3 Mb with 379,263 contigs. The mean contig length was 1,114 bases, the N50 (the shortest sequence length such that 50% of the total sequence output is contained in sequences that are shorter) was 2,146 bases, and the GC content was 43.39%.

Differential gene expression

To determine the genes that there significantly up- or down-regulated in responses to exposure to experimental conditions, mapped counts were analyzed using the EdgeR R package. Counts were analyzed for 52,352 out of 244,527 transcripts based on the requirement of at least 7 counts per million summed across all samples. For the entire dataset, the dispersion was estimated to be 0.069, and the biological coefficient of variation (BCV) was 26% (Fig. 23A). These dispersion estimates are within the range expected for human data (BCV = 40%) and model organism data (BCV = 10%). Sequences grouped by experimental treatment did not cluster in MDS or hierarchical plots by pCO_2 or temperature level (Figs. 23B,C).

Figure 23. Attributes of the RNASeq dataset for *P. damicornis* larvae. A. Tag-specific dispersion estimates plotted as biological coefficient of variation (BCV) across the range of normalized transcript abundance (average log counts-per-million [CPM]). B. Relationships among samples based on multidimensional scaling of distances based on BCV. C. Hierarchical clustering of samples based on similarity. Samples are named by their experimental treatment. Experimental treatments: Ambient-T, Ambient-pCO_2 (ATAC), High-T, Ambient-pCO_2 (HTAC), Ambient-T, High-pCO_2 (ATHC), High-T, High-pCO_2 (HTHC).

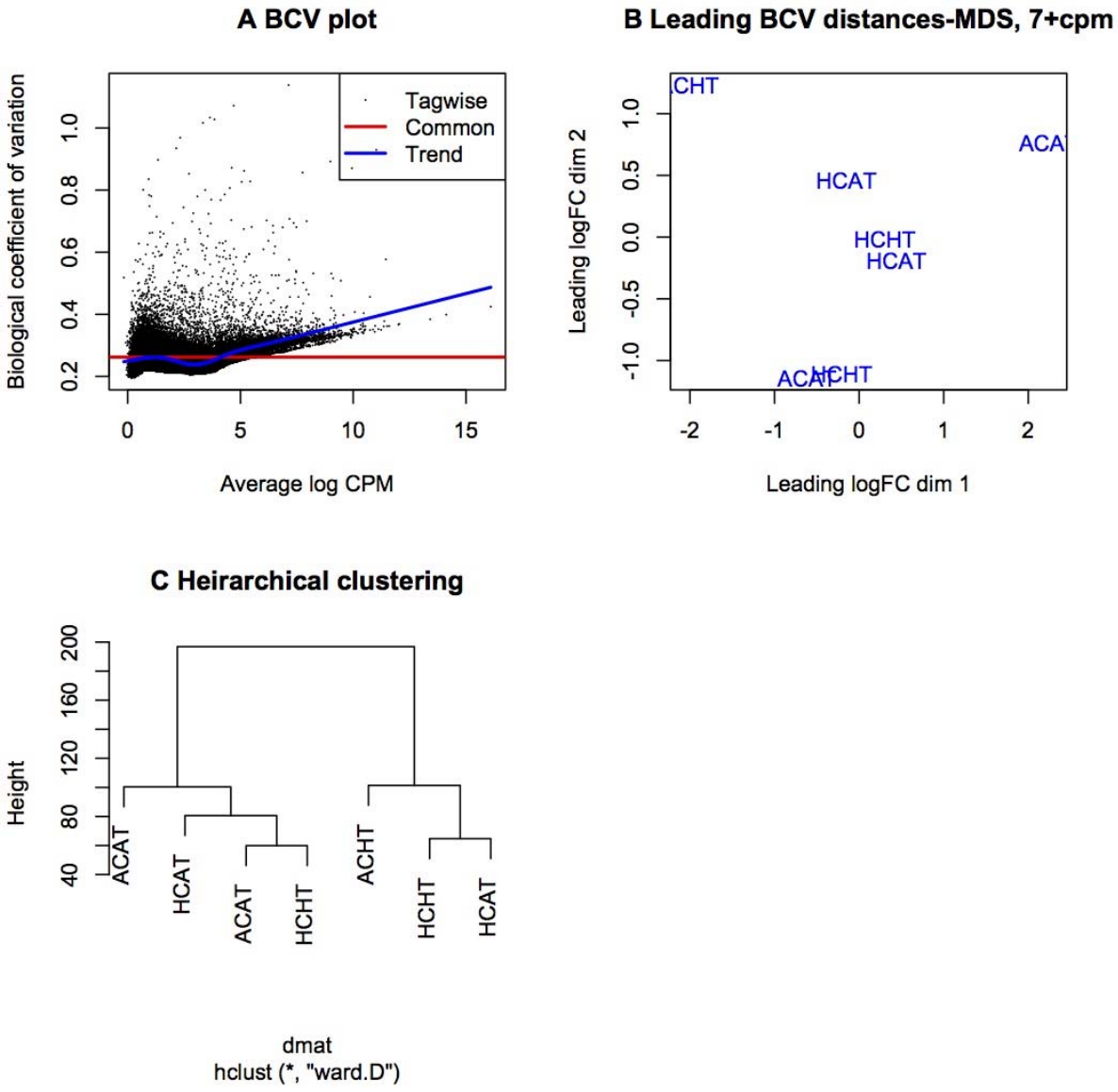

In response to 31°C, 1728 transcripts (3.3%) were down-regulated and 9 (<0.1%) were up-regulated (Fig. 24A). In response to 1045 µatm pCO_2, 269 transcripts (0.5%) were down-regulated and 1 transcript (<0.1%) was up-regulated (Fig. 24B). In response to 31°C and 1045 µatm pCO_2, 2 transcripts (<0.1%) were down-regulated and 1477 transcripts (2.8%) were up-regulated (Fig. 24C).

Discussion

I used an RNASeq approach to compare the transcriptome profiles of *P. damicornis* larvae exposed to combinations of pCO_2 and temperature levels. The small fraction of transcripts (<10%) that were differentially expressed in experimental conditions relative to the control indicated that a majority of the transcriptome was not altered in responses to the potential stressors, at least within the first 24 hours of exposure. It is possible that some DE genes were missed due to the coverage and depth of the sequencing and the counts-per-million threshold used in the EdgeR analysis. Changes in gene expression in response to high pCO_2 and high temperature were not reflected in larval quality traits, which were similar among all treatments.

Changes in gene expression in response to high temperature

Unexpectedly, the majority of DE genes in *P. damicornis* at High-T were down-regulated. It is unlikely that this is due to a loss of *Symbiodinium* cells within the larvae as symbiont densities were similar across all treatments (Fig. 22B). Gene expression in adults of some coral species is linked to their thermal habitat, with higher constitutive levels of

Figure 24. Differential gene expression between control samples and samples exposed to (A) High-T, (B) High-pCO_2, and (C) both stressors. Each dot represents a transcript. Red dots are transcripts with significant differential expression based on a false discovery rate of 0.05 (adjusted p-value). Blue lines represent ±2 and ±4 fold-change (FC) reference thresholds. The x-axis, average log counts-per-million (CPM) represents the normalized abundance of the transcript.

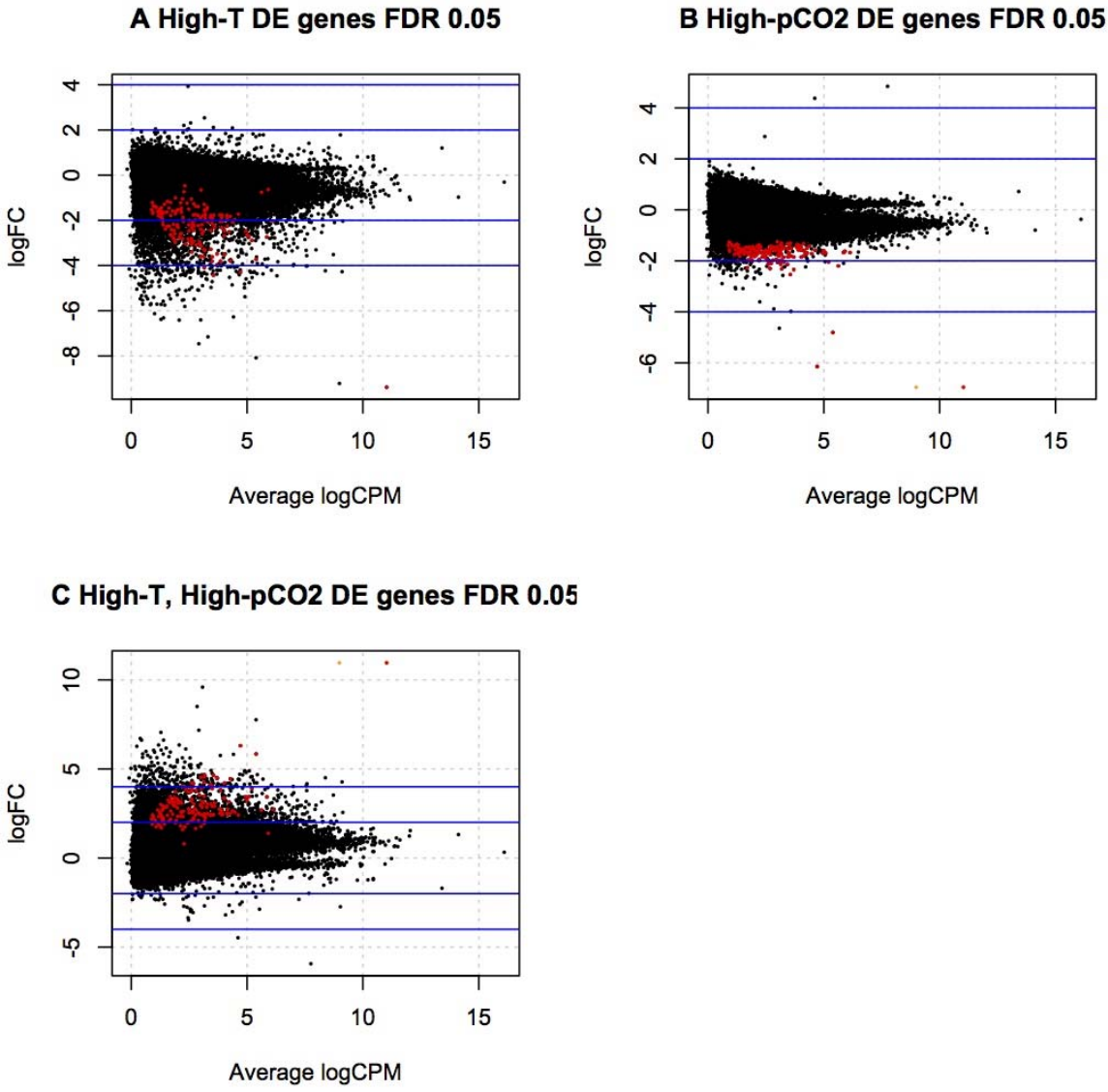

certain genes in thermally resilient corals (Barshis et al., 2013; Kenkel et al., 2013). Once heat stress is ongoing, these genes are less up-regulated due to their higher levels of constitutively produced proteins, such as those involved in heat shock response, antioxidant defense, apoptosis, and innate immunity (Barshis et al., 2013). It is possible that the larvae used in my experiment were from adults who were acclimatized to warmer seawater, such that induced expression at 31°C was minimal for genes that are normally immediately up-regulated under heat stress (*e.g.* heat shock proteins and antioxidant enzymes; Császár et al., 2009; DeSalvo et al., 2010, 2008; Kenkel et al., 2011; Seneca et al., 2010). These types of genes are involved in short-term acclimatization that confers similar levels of thermotolerance to corals as does long-term adaptation to higher seawater temperatures (Palumbi et al., 2014).

Additionally, it is possible that the down-regulation of genes in *P. damicornis* larvae in response to high temperature observed in my study indicates that the larvae were approaching the onset of bleaching. Vidal-Dupiol *et al.* (2009) identified two genes in *P. damicornis* whose expression was reduced dramatically during temperature stress prior to coral bleaching: *PdC-lectin*, whose encoded protein is involved in molecular host-symbiont communication and *Pdcyst-rich*, whose encoded protein is involved in biomineralization. The down-regulation of these genes foreshadowed the breakdown of symbiosis and calcification, respectively, related to coral bleaching.

Several RNASeq studies have examined transcriptomic responses of coral larvae to elevated temperature. In aposymbiotic larvae of the coral *Acropora millepora*, heat stress caused up-regulation of heat-shock proteins, ion transport, and metabolism (Meyer et al., 2011). In aposymbiotic larvae of *Acropora palmata*, genes related to metabolism and cell

development were down-regulated in response to high temperature while genes related to protein chaperoning, calcium signaling and macromolecular repair (Polato et al., 2013). Another important result was that transcriptomic patterns changed through time in *A. palmata* larvae (Polato et al., 2013), but it is necessary to note that this species has multiple discrete developmental larval stages while *P. damicornis* does not. The Acroporid larvae used by Polato and co-authors were maintained as aposymbiotic to simplify the analysis of gene expression data, but the transcriptomic profiles assessed may not reflect changes in holobiont gene expression when host and symbiont are interacting *in situ*. My results may differ from those previously published due to the added complexity of the host-symbiont relationship present in the *P. damicornis* larvae I used.

Changes in gene expression in response to high pCO_2

P. damicornis larvae did not compensate for the challenges high pCO_2 conditions imposed on physiology by up-regulating gene expression. Instead, the majority of their small number of DE genes (~3% of all transcripts) was down-regulated. Vidal-Dupiol *et al.* (2013) reported similar findings for *P. damicornis* adults: only a small portion of the *P. damicornis* transcriptome was sensitive to low-pH (pH 7.4) conditions. Of the DE genes, the down-regulated portion was associated with cellular metabolic processes (Vidal-Dupiol et al., 2013). However, the study also documented that a smaller portion of DE genes were up-regulated at pH 7.4, with ontologies related to calcification, heterotrophy, autotrophy, and photosynthesis. The absence of up-regulated genes in my experimental data set may reflect the fact that the calcification and heterotrophy are not engaged during the larval stage in *P. damicornis* life history. Additionally, the larvae in my experiment may have hosted a

different *Symbiodinium* clade that was less sensitive than the one(s) hosted in Vidal-Dupiol *et al.* (2013). With *Acropora millepora* adults, Kaniewska *et al.* (2012) found changes in gene expression in response to high pCO_2 consistent with metabolic suppression. Up-regulated genes coded for membrane transporters and proteins involved in the cytoskeleton. Changes in gene expression profiles from day 1 to day 28 of the exposure to high-pCO_2 suggest that a greater proportion of the transcriptome was affected over long-term vs. short-term pCO_2 stress (Kaniewska et al., 2012). Another study with *A. millepora*, but at the primary polyp stage (albeit aposymbiotic), found metabolic suppression and up-regulation of calcification-related pathways (Moya et al., 2012). These three studies are the only ones to date using RNASeq to examine the effects of ocean acidification on coral transcriptomes (Kaniewska et al., 2012; Moya et al., 2012; Vidal-Dupiol et al., 2013).

Similar results have been found in transcriptomic studies with sea urchin larvae. When *Strongylocentrotus purpuratus* urchin larvae were raised in acidic conditions, changes in gene expression suggested metabolic depression in response to ocean acidification as well as suppression of biomineralization, cellular stress response, acid/base and ion regulation, protein homeostasis, and apoptosis pathways (Todgham and Hofmann, 2009). A similar study with *Lytechinus pictus* larvae showed that under ocean acidification conditions, the expression of sea urchin genes involved in metabolism, protein synthesis, biomineralization, and the cellular defensome was suppressed; the expression of genes associated with acid/base and ion balance were also sensitive to acidic conditions (O'Donnell et al., 2010). Furthermore, ocean acidification hampered the induction of the heat shock response. Shown with larval sea urchins, expression levels of *hsp70* were lower under temperature stress when larvae had developed under high pCO_2 conditions (O'Donnell et al., 2009).

Synergistic effects of high temperature and high pCO_2

While DE genes were down-regulated under single-stressor scenarios, the combined effect of high temperature and high pCO_2 was up-regulation of most DE genes. The effects of neither stressor alone predicted the effects of the combined stressors. It is difficult to predict the identity of the *P. damicornis* DE genes at HTHC without a completed annotation. Additionally, there are no published transcriptomics studies which examine changes in gene expression in response to concurrent high pCO_2 and high temperature. However, the initial results presented here highlight the importance of examining the interactions of multiple environmental stressors. Because coral reefs are bombarded with local and global stressors, in order to appropriately manage coral reefs for the future, it is essential to know how exposure to one stressor may affect the outcome of another stressor.

Conclusion

Next-generation high-throughput sequencing represents a powerful approach to understand the complexity of expression-level responses to environmental stress. As wet lab and bioinformatics techniques continue to improve, the study of gene expression in corals is rapidly moving beyond an assessment of the behavior of a few genes to encompass comparisons of greater depth and breadth. Now, it is possible to sequence and parse holobiont transcriptomes. We are learning more about how gene expression profiles change through time during exposure to environmental stress. And we are beginning to better understand the different sensitivities of various life stages of coral to environmental stress.

The analysis of the *de novo* transcriptome assembly and the DE genes from this project is ongoing. I plan to annotate the assembly and the DE gene lists. I also intend to

blast my results to existing *Symbiodinium* genomic databases in an effort to partition the transcripts based on their origin, host or symbiont. Doing so will enable me to examine DE genes specific to each partner. These results will provide insight into the subtle controlled responses of *P. damicornis* larvae to high temperature and high pCO_2. The DE genes will infer mechanisms of physiological plasticity to projected environmental conditions and will generate hypotheses for downstream organismal-level phenotypic responses to abiotic stress.

VI. Comparison of oceanographic conditions between two sites across the biogeographic range of the coral *Pocillopora damicornis*

The data analysis for this chapter was performed in collaboration with Professor Tarik Gouhier (Northeastern University).

Introduction

As a final element in my thesis, I added a component of environmental context to complement my process-based studies in Chapter 4. Here, I deployed autonomous oceanographic sensors, including SeaFETs (Martz et al., 2010; Lunden, Rivest et al., in review), at my two study sites and qualitatively compared these field observations to laboratory experiments. The locations where I conducted this part of my dissertation spanned part of the reported biogeographic range of *Pocillopora damicornis* (Indian and Pacific oceans; Veron, 2000), and in addition to the oceanographic data, I compared the response of coral larvae to ocean acidification (OA) and warming between sites (Chapter 4, Part B). The oceanographic data not only provided context for the range of natural environmental exposures of the study populations used in laboratory experiments, but assessed whether pH and temperature variability differed between sites. Although the differences in physiology between study populations of *P. damicornis* in Moorea, French Polynesia and Taiwan could be due to genetic differences (*i.e.* different species or sub-species), the corals could be locally adapted or acclimatized to the environmental characteristics at each site. Local adaptation and acclimatization of heat tolerance in corals has been recently demonstrated for *Acropora hyacinthus* in American Samoa using gene expression and *Symbiodinium* clade ratios (Palumbi et al., 2014). Additionally, laboratory

acclimation to elevated temperatures can improve the responses of some corals to future temperature exposures (Edmunds, 2014).

Studies regarding the variability of pH and *in situ* biological response for coastal marine ecosystems are accumulating (*e.g.* Yates and Halley, 2006; Yates et al., 2007; Hall-Spencer et al., 2008; Wootton et al., 2008; Chierici and Fransson, 2009; Gagliano et al., 2010; Frieder et al., 2012; Guadayol et al., 2014). A few studies have linked natural variability of carbonate chemistry on coral reefs with community-level performance. Price *et al*. (2012) and Albright *et al.* (2013) have shown that *in situ* pH variability correlates with community succession and rates of net accretion and net production on coral reefs. Lower daily pH causes slower net accretion and results in greater relative abundance of non-calcifying benthic taxa (Price et al., 2012). Shaw *et al.* (2012) reported community calcification rates across a wide range of carbonate chemistry, predicting future declines in accretion under OA. More recently, several studies have paired these physical measurements with direct measurements of biological response of resident organisms to future ocean conditions (Yu et al., 2011; Shaw et al., 2012; Evans et al., 2013; Kelly et al., 2013; Padilla-Gamiño et al., 2013; Frieder, 2014; Hofmann et al., 2014). Yu *et al.* (2011) found that sea urchins in the Santa Barbara Channel experience high fluctuations of pH due to seasonal upwelling (about 8.2-7.7). When larvae from this population were raised under pH 7.7 and pH 7.5, they developed normally and showed similar morphological and growth responses. These results suggested that populations of sea urchins that naturally experience high variation of ambient pH may be more resilient to anthropogenic changes in acidity, though no comparison with a population of low-variability environmental pH was conducted.

Additionally, Kelly *et al.* (2013) found evidence for local adaptation to carbonate chemistry conditions in sea urchin populations on the Oregon coast.

As described in Chapter 4, I found that *P. damicornis* larvae from French Polynesia and Taiwan responded differently to laboratory exposures to pCO_2 and temperature levels. In this chapter, I tested the hypothesis that the study sites used are characterized by differing carbonate chemistry environments, which may have shaped their responses to environmental stress. The prediction is that coral may be locally acclimatized or adapted to the pH and temperature variation under which their populations have evolved, a process that is well known in terms of local adaptation to temperature in marine invertebrates (reviewed in Sanford and Kelly, 2011). Coral populations that have experienced high variability in pH or frequent pulses of low pH seawater, for example from upwelling, may have developed the physiological capacity to tolerate the global average low pH, high pCO_2 conditions predicted to occur by the end of this century. Physiological adaptation to historical environmental conditions has been shown with Sockeye salmon in British Colombia, Canada. Population-specific cardiorespiratory performance in these fish is optimized to the temperatures experienced during annual river migrations (Eliason et al., 2011). Similarly, though they are likely reproductively isolated, groups of coral at locations of differing pH conditions may have varying degrees of physiological plasticity reflecting the historical nature of their carbonate chemistry environment. I compared environmental conditions between fringing reef locations at Moorea, French Polynesia and Nanwan Bay, Taiwan. I predicted that pH and temperature would differ between reef locations because previous work has shown that Nanwan Bay experiences tidally-driven upwelling events (Lee et al., 1999), while the fringing reef in Moorea is more protected inside a lagoon. In addition, this geographic

comparison (Moorea-Taiwan) would likely include a difference in total alkalinity, perhaps by 100 μmol kg SW^{-1} (*e.g.* Lee et al., 2006).

Materials and Methods

Environmental data collection in Moorea

From January 20 to March 16, 2012, time series of pH, temperature, and depth were recorded for a fringing reef on the north shore of Moorea (17°28'49.08S, 149°47'56.04"W). For a description of the study site, refer to Chapter 1. pH was recorded continuously using an autonomous data logger based on a Honeywell Durafet® pH sensor, called a SeaFET (Martz et al., 2010). The SeaFET was deployed at 3.3 m depth and suspended approximately 0.6 m off the sandy bottom; the instrument measured pH voltage at 10-minute intervals, averaging data over 30-second periods. The deployment location was approximately 33 m from the collecting location of adult *P. damicornis* used in experiments described in Chapters 2, 4, and 5. Adjacent to the SeaFET were two thermisters (SBE 39, Sea-Bird Electronics, Bellevue, WA) and two HOBO® water level data loggers (U20, ONSET® Computer Corp., Bourne, MA), synchronized with the SeaFET to simultaneously record temperature and depth. SeaFET electrode surfaces and depth loggers were caged in copper mesh to deter fouling; cages were cleaned twice a month with a toothbrush when the sensor was idle between measurements.

Following deployment, the SeaFET electrodes were allowed to stabilize and then were calibrated using discrete seawater samples collected *in situ*, a method based on ISFET electrode characteristics (Martz et al., 2010; Lunden, Rivest et al., in review). On February

16, 2012, a SCUBA diver using a Niskin bottle collected a single calibration sample adjacent to the SeaFET concurrently with its voltage reading. Temperature of the seawater *in situ* was measured using an alcohol thermometer. The seawater sample was used to rinse and fill two 500 mL borosilicate glass bottles with minimal contact of seawater and atmospheric air. The bottles were sealed with gas-impermeable grease and a ground-glass stopper (Dickson et al., 2007). Analyses of carbonate chemistry were performed within 1-2 hours of sample collection

Environmental data collection in Taiwan

The study site in Taiwan is a fringing reef in Nanwan Bay, located at the southern tip of the island. For a description of the study site, refer to Chapter 1. From May 24 to July 12, 2012, time series of pH, temperature, salinity, and depth were recorded for a fringing reef in Nanwan Bay, Taiwan (21°56'20.10"N, 120°44'45.80"E). pH was recorded continuously using a SeaFET (Martz et al., 2010), which was deployed at ~4 m depth and suspended approximately 0.6 m off the sandy bottom. The instrument measured pH voltage at 6-minute intervals, averaging data over 30-second periods. Adjacent to the SeaFET were two conductivity/temperature sensors (SBE 37, Sea-Bird Electronics, Bellevue, WA) and two HOBO® water level data loggers (U20, ONSET® Computer Corp., Bourne, MA), synchronized with the SeaFET to simultaneously record conductivity, temperature, and depth. SeaFET electrode surfaces and depth loggers were caged in copper mesh to deter fouling; cages were cleaned twice a month with a toothbrush when the sensor was idle between measurements. The deployment location for the sensors was located within 33 m of

the collecting locations of adult *P. damicornis* used in experiments described in Chapters 3 and 4.

Following deployment, the electrodes in the SeaFET sensors were allowed to stabilize and then were calibrated using discrete seawater samples collected *in situ* (Lunden, Rivest et al., in review; Martz et al., 2010). On July 2, 2012, a SCUBA diver using a Niskin bottle collected a single calibration sample adjacent to the SeaFET in concurrence with its voltage reading. Temperature of the seawater *in situ* was measured using an alcohol thermometer. The seawater in the Niskin bottle was used to rinse and fill two 500 mL borosilicate glass bottles with minimal contact of seawater and atmospheric air. The bottles were sealed with gas-impermeable grease and a ground-glass stopper (Dickson et al., 2007). Analyses of carbonate chemistry were performed within 1-2 hours of sample collection

Seawater chemistry analyses of SeaFET calibration samples

pH, total alkalinity (A_T), and salinity from bottle samples were measured in four replicates within 1-2 hours of sample collection. Samples in Moorea were analyzed in collaboration with the Moorea Coral Reef Long Term Ecological Research facility at UC Berkeley's Richard B. Gump South Pacific Research Station. Samples in Taiwan were analyzed in collaboration with Dr. PJ Edmunds (CSUN) and Dr. T-Y Fan at the National Museum of Marine Biology and Aquarium.

Seawater salinity was measured using a conductivity meter (Moorea: YSI 3100, YSI Inc., Yellow Springs, OH, USA; Taiwan: 340i, WTW GmbH, Weilheim, Germany). Seawater pH was measured using a spectrophotometric method with indicator dye, *m*-cresol purple (SOP 6b, Dickson et al., 2007). Total alkalinity (A_T) was measured using an

automated, closed-cell potentiometric titration (SOP 3b, Dickson et al., 2007) using an automatic titrator (Moorea: T50 with DG115-SC pH probe, Mettler Toledo, LLC., Toledo, OH, USA; Taiwan: DL50 with DG101-SC pH probe, Mettler Toledo, LLC., Toledo, OH, USA). Titrations were performed using certified acid titrant (~0.1M HCl, 0.6M NaCl; A. Dickson Laboratory, Scripps Institute of Oceanography), and A_T was calculated following Dickson *et al.* (2007). Analyzed certified reference materials from A. Dickson Laboratory were titrated to confirm the precision and accuracy of the process; these reference titrations were accurate within 10 μmol kg SW^{-1} (0.1-0.3%).

pH measured at 25°C was converted to pH at environmental temperature using A_T, temperature, and salinity of the bottle samples via CO2calc (Robbins et al., 2010), with CO_2 constants K1, K2 from (Mehrbach et al., 1973) refit by (Dickson and Millero, 1987) and pH expressed on the total scale (mol kg-SW^{-1}). The calculated bottle pH at environmental temperature was then compared with the voltage recorded by the sensor at the time points of sample collection to determine the value E* for the Nernst equation. This equation was then used to calculate pH from raw sensor voltage for he entire time series (Martz et al., 2010). Salinity was also used to calculate pH from raw sensor voltage. In Moorea, the value measured from the bottle sample was assumed constant and used for the entire time series. In Taiwan, the salinity time series was used for this calculation.

After *in situ* pH was calculated, CO2CALC (Robbins et al., 2010) was used to estimate the remaining carbonate chemistry parameters, with CO_2 constants K1, K2 from (Mehrbach et al., 1973) refit by (Dickson and Millero, 1987) and pH expressed on the total scale (mol kg-SW^{-1}). For this calculation, A_T was assumed constant throughout the deployment; average A_T measured from the bottle samples was used. For the Moorea data

set, salinity was also assumed constant and the bottle sample average was used for CO2CALC calculations. For the Taiwan data set, the salinity time series was used for CO2CALC calculations. Assumptions of constant A_T and/or salinity during the 1-2 month deployments were necessary because these parameters could only be measured using discrete samples. The assumptions could introduce errors of ± 1 psu in salinity and ± 50 μmol kg SW^{-1} in A_T (Rivest and Hofmann, 2014).

Data analysis

Analyses were carried out using MatLab (v. 7.2.0; Mathworks, Inc.) and R (v. 3.0.1; R Core Team, 2013).

First, time series of pH, temperature, salinity, and depth were processed through a series of quality control procedures following Lunden, Rivest *et al.* (in review). Briefly, the time series were trimmed and cleaned to exclude erroneous values. Due to the fact that there was only one calibration sample per time series, drift in SeaFET pH due to biofouling or internal sensor drift was not identifiable. The time series pH, temperature, salinity, and depth were then processed using a one-hour low-pass filter.

To better understand the composition of variance in the time series of pH, temperature, salinity, and depth, wavelet analysis was performed. Wavelet analysis was chosen over traditional spectral analyses because wavelet analysis does not assume that the properties of the time series do not vary through time (Cazelles et al., 2008). While the time series used here are very short, even for ecological time scales, dynamics in pH and temperature likely change with larger climate oscillations so an assumption of stationary behavior is not appropriate. Another advantage of wavelet analysis is that it allows

characterization of how frequency content of a signal changes with time (Cazelles et al., 2008). I am particularly interested in this aspect of the analysis to examine changes in small-scale variation in pH and temperature. Variance in the time and frequency domains was decomposed, and instances of significantly high temporal variation were identified. Then, wavelet power was averaged across the frequency (*i.e.* period) or time domains. The resulting synthesis described global wavelet power or changes in variance by frequency and scale-averaged power or changes in variance over time.

To characterize differences in environmental variability between study sites in Moorea and Taiwan, I compared the mean and the variance of pH and temperature time series. Monte Carlo randomizations were performed, as the data violated the assumptions (*e.g.* normality) of more traditional parametric tests (Manly, 2006). Specifically, for each metric, the null hypothesis that the values from both sites came from a single statistical population characterized by the same mean and variance was tested. For each randomization, values from the statistical population were randomly assigned to each site and then the between-site difference in the metric of interest was computed (*e.g.* difference in mean or variance between sites). This generated a distribution of differences in the metric of interest under the null hypothesis. Then, the p-value was computed via a two-tailed test by determining the proportion of randomizations that yielded a difference in the metric of interest whose magnitude was greater than or equal to the one observed in the actual data. As with traditional parametric approaches, if the p-value generated via Monte Carlo randomizations is smaller than a predefined threshold (*i.e.* $\alpha = 0.05$), then the null hypotheses can be rejected, and the difference between sites in the metric of interest is significant at the alpha level. In addition to this analysis testing the difference in

environmental parameters across the distribution of pH, temperature, and depth values recorded, histograms were used to visualize the distribution of pH across percentiles. Monte Carlo randomizations were also performed to test the difference between environmental parameters of Moorea and Taiwan for each percentile. This analysis allows me to describe if differences between sites are consistent for commonly occurring values as well as rarely occurring values. Additionally, cross-spectral analyses (wavelet coherence) were performed to measure the time-resolved correlation between simultaneous time series of temperature and pH. Partial wavelet coherence was performed for pH, salinity, and temperature time series for Taiwan data sets.

Results

In Moorea and Taiwan, I used autonomous sensors to characterize the abiotic environment to which the resident corals were acclimatized, specifically to characterize the variability of pH and temperature. Use of the SeaFETs required the collection of discrete water samples for data calibration: the seawater chemistry for the bottle sample in Moorea was: pH_{total} = 8.026; salinity = 35.65 psu; A_T = 2353 μmol kg SW^{-1}. The seawater chemistry for the discrete bottle sample in Taiwan was: pH_{total} = 8.006, salinity = 33.43; A_T = 2181 μmol kg SW^{-1}. The dates of these collections were February 16, 2012 at the Moorea study site and July 2, 2012 at the Taiwan study site.

The two sites had distinctly different profiles of seawater characteristics as assessed using summary statistics (Table 35). Mean seawater pH, temperature, $\Omega_{aragonite}$, $\Omega_{calcite}$, and A_T were greater in Moorea than in Taiwan. However, mean pCO_2 was higher in Taiwan.

Table 35. Summary of oceanographic conditions at fringing reefs in Moorea, French Polynesia and Taiwan in 2012. pH (total scale) was measured by a SeaFET. Temperature was measured by duplicate thermistors in Moorea. Temperature and salinity were measured using a CT sensor in Taiwan. In Moorea, salinity was measured from a discrete water sample. A_T was measured from a discrete seawater sample at each site.

Site	Summary Statistics	Temperature (°C)	Salinity (psu)	pH	A_T (µmol kg SW^{-1})	Ω_{arag}	Ω_{calc}	pCO_2 (µatm)
Moorea	*n*	8001	1	8001	1	8001	8001	8001
	Mean	28.76	35.65	7.989	2353	3.57	5.35	473
	SD	0.61	NA	0.038	NA	0.26	0.38	53
	Range	3.26	NA	0.233	NA	1.39	2.09	344
	Maximum	30.63	NA	8.069	NA	4.10	6.13	718
	Minimum	27.34	NA	7.836	NA	2.70	4.05	373
	25%	28.32	NA	7.966	NA	3.53	5.30	431
	75%	29.18	NA	8.019	NA	3.40	5.10	503
Taiwan	*n*	11012	11012	11012	1	11012	11012	11012
	Mean	27.74	33.12	7.974	2181	3.03	4.57	467
	SD	1.40	0.35	0.0315	NA	0.21	0.31	42
	Range	10.47	4.52	0.255	NA	1.67	2.42	337
	Maximum	30.01	34.56	8.105	NA	3.97	5.97	655
	Minimum	19.54	30.04	7.850	NA	2.30	3.55	318
	25%	27.14	32.96	7.953	NA	2.97	4.35	437
	75%	28.70	33.34	7.996	NA	3.18	4.80	494

The extreme values and amplitude of fluctuations of abiotic factors were also different between the two sites. Temperature, $\Omega_{aragonite}$, and $\Omega_{calcite}$ reached higher maxima in Moorea, but lower minima in Taiwan, with 3x greater range of temperature in Taiwan. For seawater pH and pCO_2, the range was similar between sites, but Moorea had lower maxima and minima.

Dynamics of environmental pH

pH time series at both sites are characterized by strong and consistent daily fluctuations (Figs. 25A, B). A portion of the Moorea pH time series was removed because these data failed to meet quality control standards (Lunden, Rivest et al., in review). The plots of wavelet power (Figs. 25C, D) show areas delineated by black lines, which show variability or fluctuations in the signal that are significantly different than what would be expected from a null model. In these plots, the white line represents the cone of influence. Values inside the cone are reliable, and values outside the cone are less reliable because of edge effects in analysis of the finite time series. pH varied at different periods and the periodicity of the signal varied through time (Figs. 25C, D). Throughout the entire time series for both Moorea and Taiwan, high wavelet power was observed on a ~24-hour period, with some intermittent significant fluctuations occurring at lower periods (< 16 hours; Figs. 25C, D). In Moorea, the dark blue portion of the figure corresponds to the section of the pH time series that was excluded from the analysis. Integrating across time, the global power in Moorea was concentrated at the 24-hour and ~10-hour periods (Fig. 25E), more consistent and with higher magnitude than in Taiwan. Global wavelet power for seawater pH in Taiwan also contained a significant 24-hour period but with greater power at lower

Figure 25. Time series and wavelet power analyses of seawater pH. Time series plots of seawater pH collected on a fringing reef in (A) Moorea [MCR], French Polynesia and (B) Taiwan [TWN]. Wavelet power quantifies the changes of relative contribution of each period in the pH signal to the overall variance of the signal for time series collected in (C) Moorea and (D) Taiwan. High power is represented in warm colors and low power is represented in cold colors. Black contours designate regions of significantly high temporal variation. The white line represents the cone of influence – values outside of this region are less reliable due to edge effects in the analysis. (E) A comparison between sites wavelet power integrated over time. Wavelet power was also integrated over period to describe changes in total variance over time for MCR (F) and TWN (G).

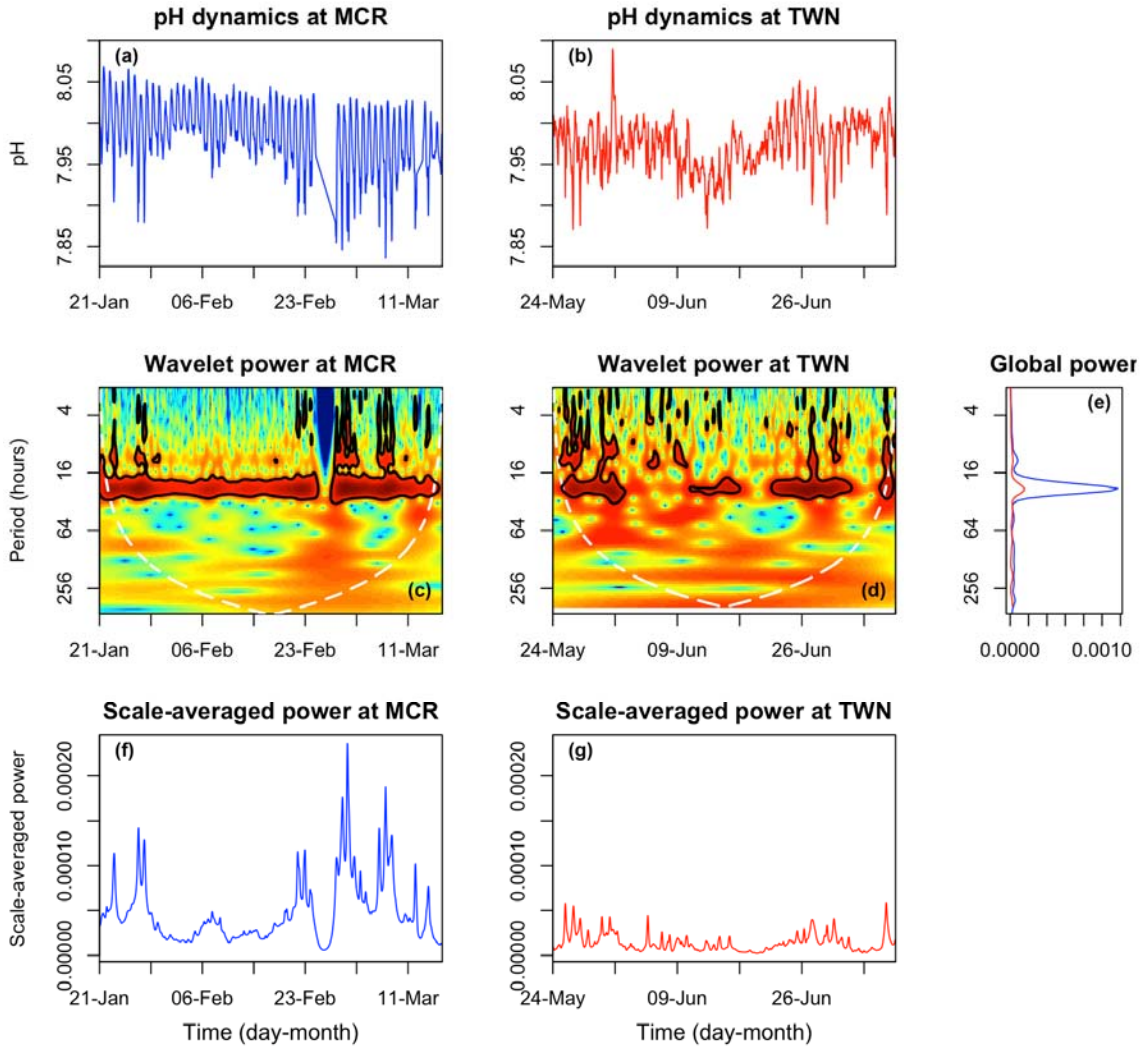

frequencies than in Moorea (Fig. 25E). When power was averaged over all periods, scale-averaged power was greater in Moorea than in Taiwan (Figs. 25F, G).

When considering the entire distribution of pH values, the Taiwan site spent more time at lower pH. When distributions of seawater pH were compared between Moorea and Taiwan, the Moorea time series contained more values of high seawater pH while the distribution in Taiwan was shifted lower, with more counts of lower seawater pH (Fig. 26A). Plotting the data as a distribution of pH over percentiles of the dataset, seawater pH in Moorea was greater than seawater pH in Taiwan for high percentiles but not low percentiles (Fig. 26B). Monte Carlo randomizations were used to test the difference between pH in Moorea and Taiwan for each percentile of the pH distributions. The observed differences in pH between sites at all but one quantile were statistically significant (Fig. 26C). The most rare pH values were significantly lower in Moorea than in Taiwan (Fig. 26C), as suggested by the summary statistics (Table 35). However, seawater pH was significantly lower in Taiwan for the majority of the distribution (Fig. 26C). The non-parametric Kolmogorov-Smirnov test confirmed that there is a significant difference in the overall distribution of pH values between the sites ($p < 0.001$). Overall, the observed differences in mean and variance of pH were more extreme than those expected if the differences were drawn from a single statistical population, based on 999 Monte Carlo randomizations ($p < 0.001$ for both).

Dynamics of environmental temperature

Temperature time series at both sites were characterized by strong daily fluctuations, with some larger period depressions in temperature in Taiwan (Figs. 27A, B). The plots of wavelet power show that temperature varied at different periods and the periodicity of the

Figure 26. Comparisons of seawater pH between Moorea [MCR] and Taiwan [TWN]. (A) Histogram of the frequency densities of pH values observed during the deployments. (B) Distributions of frequencies of pH values during the deployments. (C) Differences in pH (TWN – MCR) for each percentile of the distribution of seawater pH, tested whether different from zero using Monte Carlo randomizations.

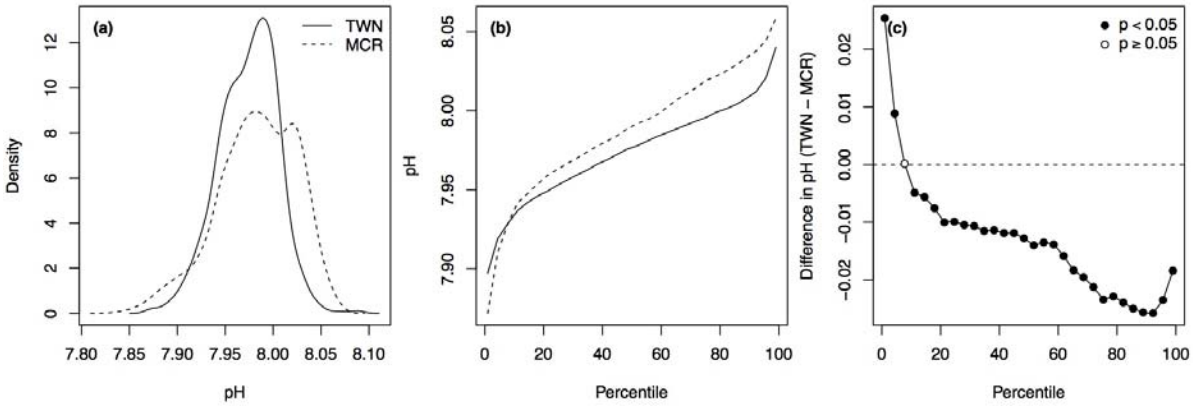

Figure 27. Time series and wavelet power analyses of seawater temperature. Time series plots of seawater temperature collected on a fringing reef in (A) Moorea [MCR], French Polynesia and (B) Taiwan [TWN]. Wavelet power quantifies the changes of relative contribution of each period in the pH signal to the overall variance of the signal for time series collected in (C) MCR and (D) TWN. See Figure 25 legend for details. (E) A comparison between sites wavelet power integrated over time. Wavelet power was also integrated over period to describe changes in total variance over time for MCR (F) and TWN (G).

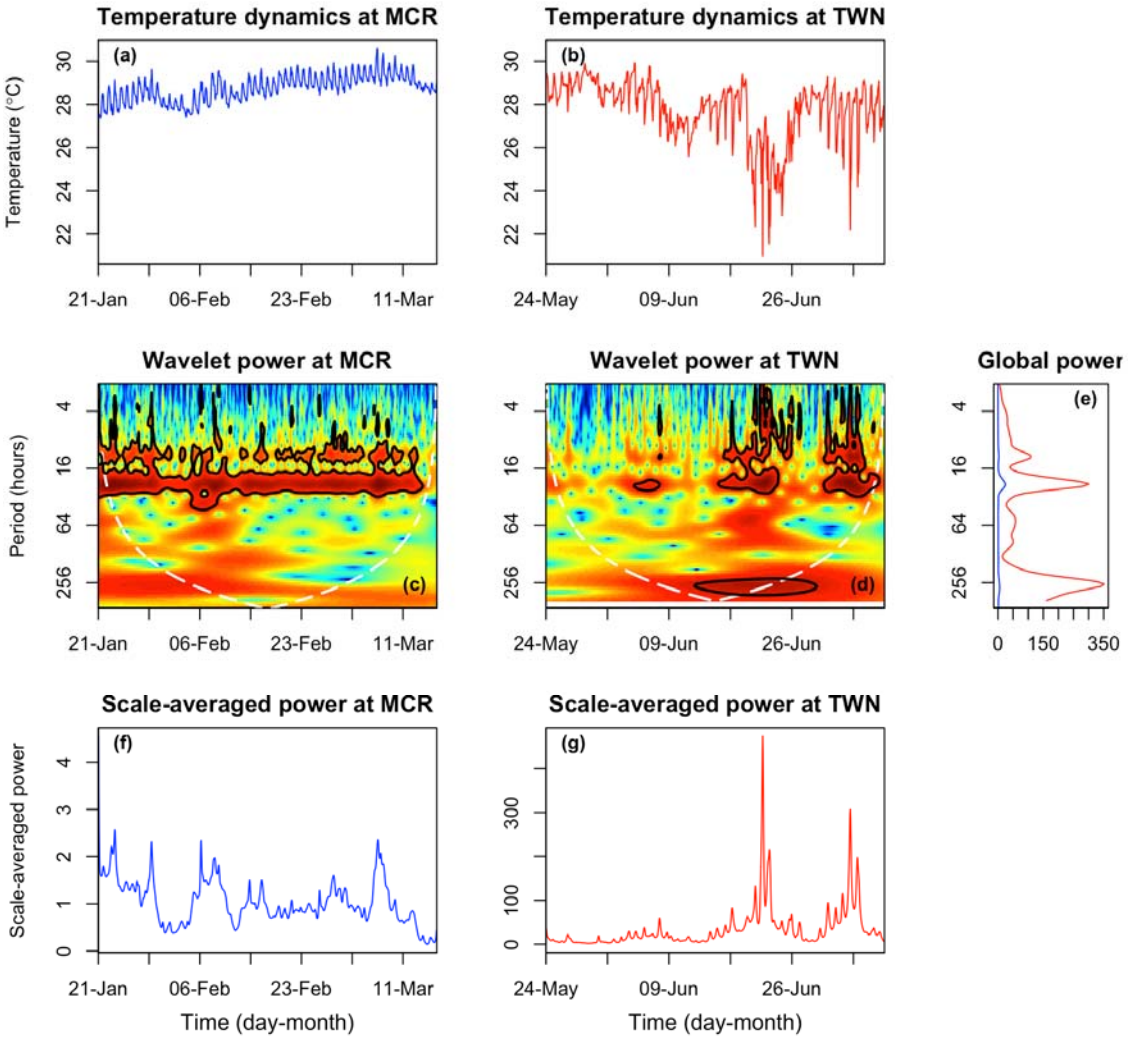

signal varied through time (Figs. 27C, D). Throughout the entire time series for Moorea, high wavelet power was observed on a ~24-hour period, with some intermittent significant fluctuations occurring at lower periods (< 16 hours; Fig. 27C). In Taiwan, wavelet power at the 24-hour period was not consistently high, only significant during the second half of the time series (Figure 27D). In these cases, lower periods were also significantly high in wavelet power. During the first portion of the time series, there were no periods of signal that were significantly different from the null model (Fig. 27D). The Taiwan dataset also contained a unique feature of strong power on a 2-week period (Fig. 27D). Integrating across time, the global power in Moorea was concentrated at the 24-hour period (Fig. 27E), with lower magnitude than in Taiwan. Global wavelet power for seawater temperature in Taiwan was consistently higher than in Moorea, with peaks at 12-, 24- and 256-hour periods (Fig. 27E). When power was averaged over all periods, scale-averaged power was greater in Taiwan than in Moorea (Figs. 27F, G).

Overall, the observed differences in mean and variance of temperature were significant between sites based on 999 Monte Carlo randomizations ($p < 0.001$ for both). When distributions of seawater temperature were compared between Moorea and Taiwan, the Moorea time series was concentrated around values of higher seawater temperature while the distribution in Taiwan had a tail with more counts of lower seawater temperature (Fig. 28A). Plotting the data as a distribution of temperature over percentiles of the dataset, seawater temperature in Moorea was greater than seawater temperature in Taiwan for all percentiles (Fig. 28B). Monte Carlo randomizations were used to test the difference between temperature in Moorea and Taiwan for each percentile of the temperature distributions. The

Figure 28. Comparison of seawater temperature between Moorea [MCR] and Taiwan [TWN]. (A) Histogram of the frequency densities of temperature values observed during the deployments. (B) Distributions of frequencies of temperature values during the deployments. (C) Differences in temperature (TWN – MCR) for each percentile of the distribution of seawater temperature, tested whether different from zero using Monte Carlo randomizations.

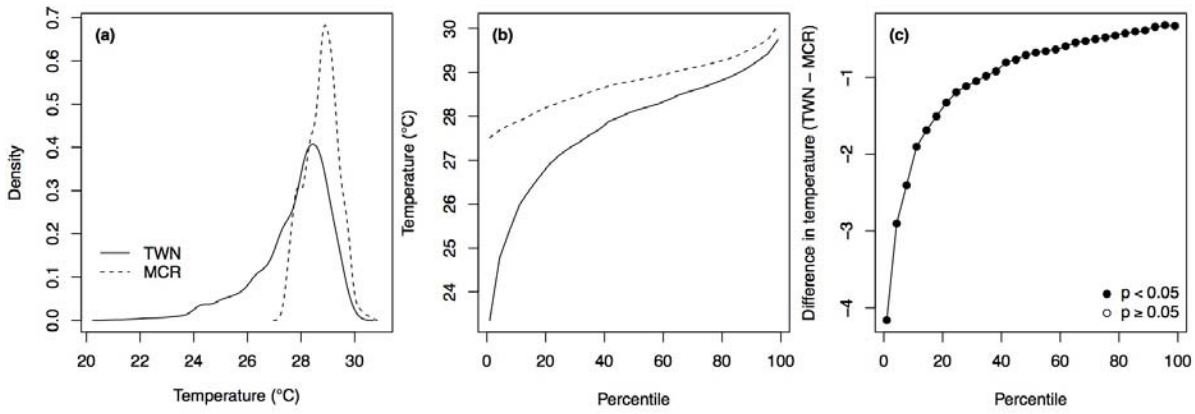

observed differences in temperature between sites were statistically significant for all quantiles (Fig. 28C). The most common and most rare temperature values were significantly higher in Moorea than in Taiwan (Fig. 26C), as suggested by the summary statistics (Table 35).

Correlation between pH and temperature variability

The correlation between pH and temperature through time was determined for time series at each site using wavelet coherence. In Moorea, pH and temperature were significantly correlated through time on a ~24-hour period, with significant intermitted correlation at lower periods (<16 hours; Fig. 29A). In Taiwan, strong correlation between pH and temperature was sometimes present on a 24-hour period, but unlike Moorea, it was not consistent throughout the length of the time series. Lower periods were also sometimes significant in Taiwan (Fig. 29B). Similar to analyses of wavelet power, areas delineated by black lines in plots of wavelet coherence show correlation between pH and temperature signals that are significantly different than what would be expected from a null model. It is important to note that strong correlation does not imply that one signal is driving the other or vice versa (Cazelles et al., 2008). Both signals could have strong independent cycles of the same period.

Dynamics of environmental salinity

A salinity time series was generated in Taiwan, characterized by strong and consistent daily fluctuations, with some larger period dips that coincide with larger decreases in temperature (Figs. 30A, 27B). The distribution of salinity values was skewed,

Figure 29. Correlation between pH and temperature fluctuations in seawater. Wavelet coherence, measuring the time-resolved correlation at each frequency or period for time series collected in (A) Moorea [MCR] and (B) Taiwan [TWN]. Warm colors indicate regions of high correlation, while cool colors indicate regions of low correlation. Black lines outline regions with significantly greater correlation.

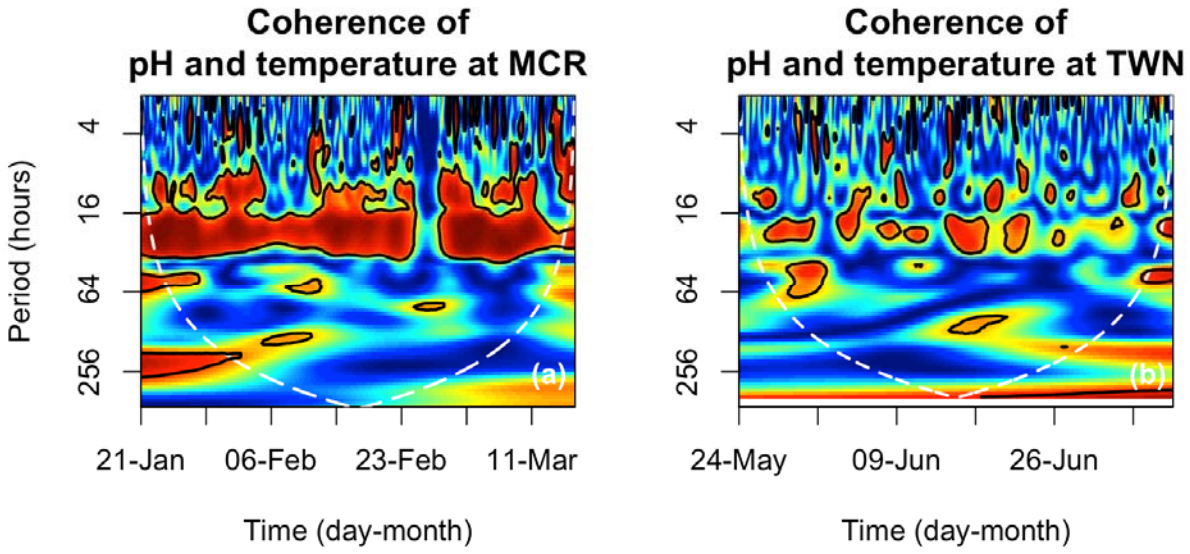

Figure 30. Time series and wavelet power analyses of seawater salinity in Taiwan. (A) Time series plot of seawater salinity collected on a fringing reef in Taiwan [TWN]. (B) Histogram of frequencies of salinity. (C) Wavelet power quantifies the changes of relative contribution of each period in the pH signal to the overall variance of the signal for time series collected in Taiwan. See Figure 25 legend for details. (D) Wavelet power integrated over time to describe changes in power over frequency. (E) Wavelet power was also integrated over period to describe changes in total variance over time. (F) Partial wavelet coherences of pH, salinity, and temperature describe correlation between the three parameters across frequency and time domains. High coherence is represented in warm colors and low power is represented in cold colors. Black contours designate regions of significantly high temporal variation. The white line represents the cone of influence – values outside of this region are less reliable due to edge effects in the analysis.

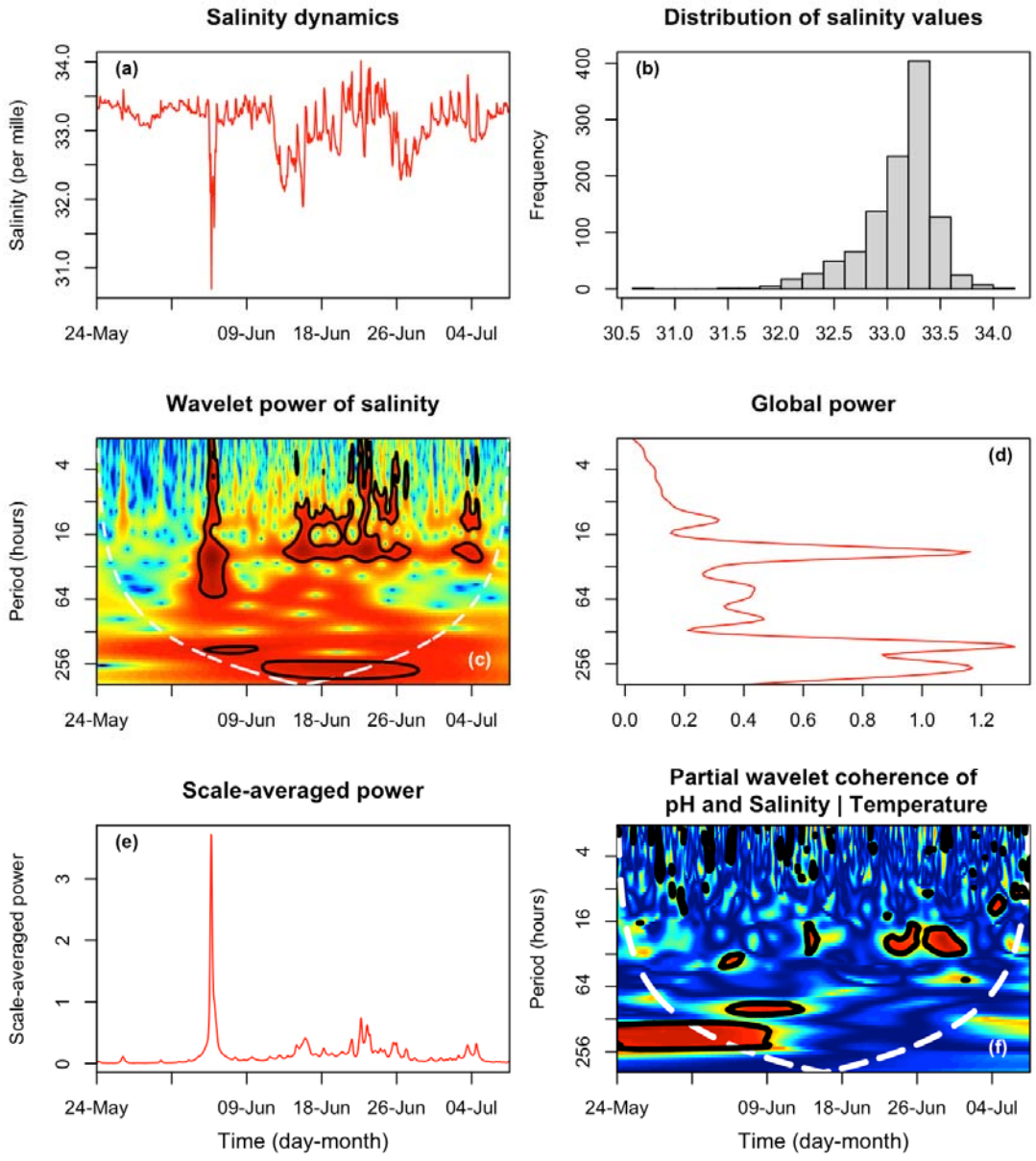

with a longer tail of lower values (Fig. 30B). The plot of wavelet power shows that salinity varied at different periods and the periodicity of the signal varied through time (Fig. 30C).

Throughout the entire time series for Taiwan, wavelet power was inconsistently high on a ~24-hour period, with intermittent significant fluctuations occurring at lower periods (< 16 hours) and at 64-hour to two-week periods (Fig. 30C). Integrating across time, the global power of salinity was concentrated at the 24-hour and two-week periods (Fig. 30D). When power was averaged over all periods, scale-averaged power was greatest for a discrete period in early June and elevated again around June 21 (Fig. 30E). The salinity time series was used to plot the correlation between pH, temperature and salinity through time at Taiwan, using partial wavelet coherence. pH, temperature, and salinity were not significantly correlated for the majority of the time-frequency space, indicated by the abundance of dark blue color in Figure 30C. However, at intermittent times, the coherence is significant around the 24-hour period (Fig. 30F).

Dynamics of seawater depth

Depth time series at both sites are characterized by strong and consistent daily fluctuations, with some larger period oscillations (Figs. 31A, B). Water depth oscillated with two minima and maxima per day at each location. However, in Moorea, each of the two oscillations had a consistent height, while in Taiwan, there was one large oscillation and one small oscillation per day (Figs. 31A, B). Based on observation of the raw time series, the signals appeared to contain strong daily and lunar tidal signals. Throughout the entire time series for Moorea, high wavelet power was observed on a ~12-hour period, with no significant fluctuations at other periods (Fig. 31C). In Taiwan, wavelet power at the 12-hour

Figure 31. Time series and wavelet power analyses of seawater depth. Time series plots of seawater depth collected on a fringing reef in (A) Moorea [MCR], French Polynesia and (B) Taiwan [TWN]. (C) Distributions of frequencies of depth values during the deployments. Wavelet power quantifies the changes of relative contribution of each period in the depth signal to the overall variance of the signal for time series collected in (C) Moorea and (D) Taiwan. See Figure 25 legend for details. (E) A comparison between sites of wavelet power integrated over time. Wavelet power was also integrated over period to describe changes in total variance over time for MCR (F) and TWN (G).

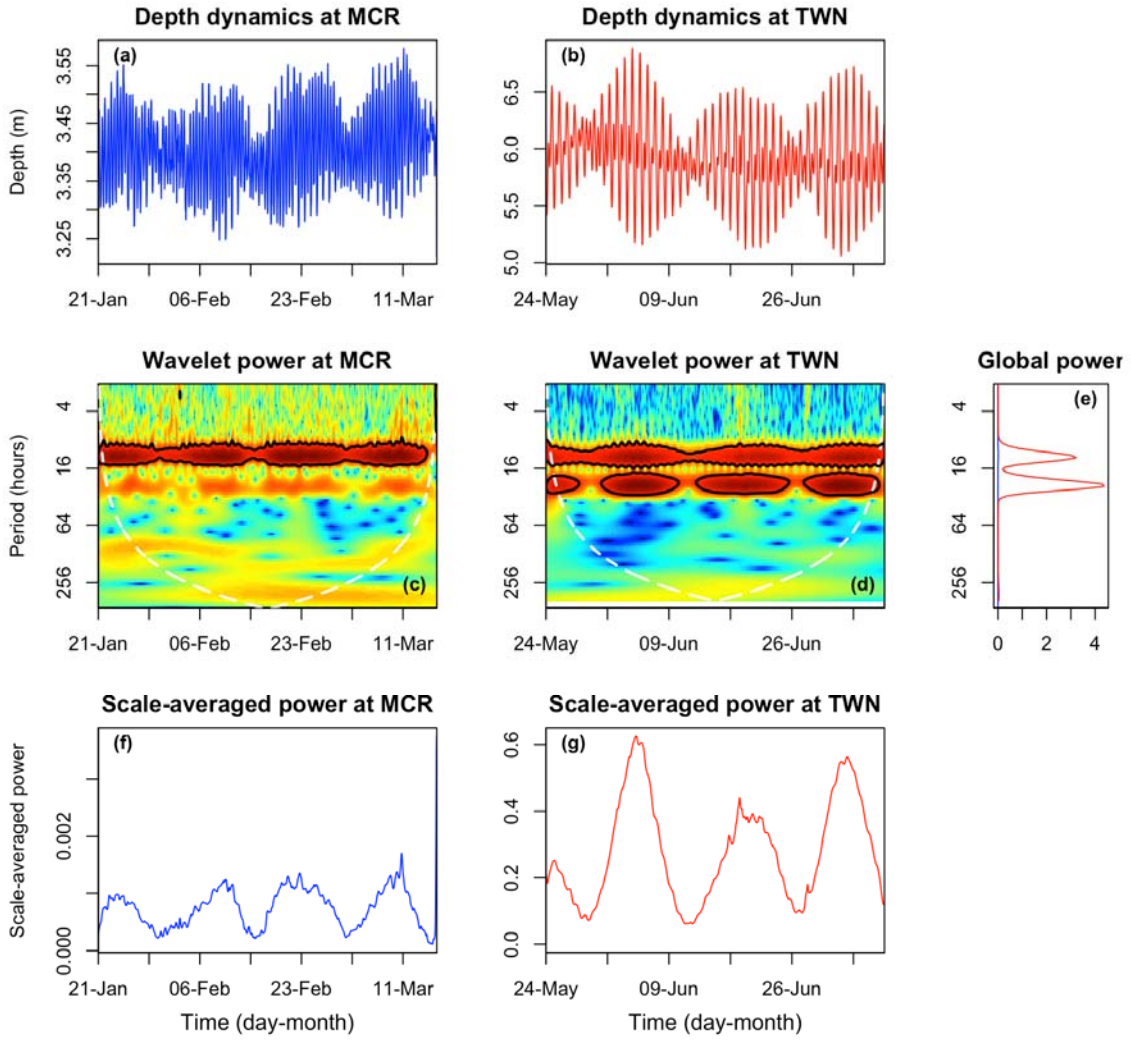

period was also consistently high, with evenly spaced high fluctuations at 24-hour periods (Figure 31D). Integrating across time, the global power in Moorea was low for all periods, while global power in Taiwan was elevated at 12- and 24-hour periods (Fig. 31E). When power was averaged over all periods, scale-averaged power was peaked every two weeks in Moorea and in Taiwan, with greater amplitudes in Taiwan (Figs. 31F, G).

When distributions of seawater depth were compared between Moorea and Taiwan, the Moorea time series contained a much narrower range of values, while the distribution in Taiwan was much wider (Fig. 32A). Plotting the data as a distribution of depth over percentiles of the dataset, seawater depth in Taiwan was greater than in Moorea for all percentiles (Fig. 32B). Monte Carlo randomizations were used to test the difference between temperature in Moorea and Taiwan for each percentile of the depth distributions. The observed differences in depth between sites were statistically significant for all quantiles (Fig. 32C). The most common and most rare depth values were significantly higher in Taiwan than in Moorea (Fig. 32C).

Discussion

In this chapter, I compared present-day environmental characteristics of the water masses bathing two fringing reefs, which contained the populations of coral used in my studies. Autonomous sensors generated datasets of pH, temperature, salinity, and depth that were analyzed to describe the abiotic conditions to which resident coral populations are potentially locally adapted or acclimatized, and further, to place the experimental treatments used in laboratory exposures in an ecologically-relevant context.

Figure 32. Comparison of seawater depth between Moorea [MCR] and Taiwan [TWN]. (A) Histogram of the frequency densities of depth values observed during the deployments. (B) Distributions of frequencies of depth values during the deployments. (C) Differences in depth (TWN – MCR) for each percentile of the distribution of seawater depth, tested whether different from zero using Monte Carlo randomizations.

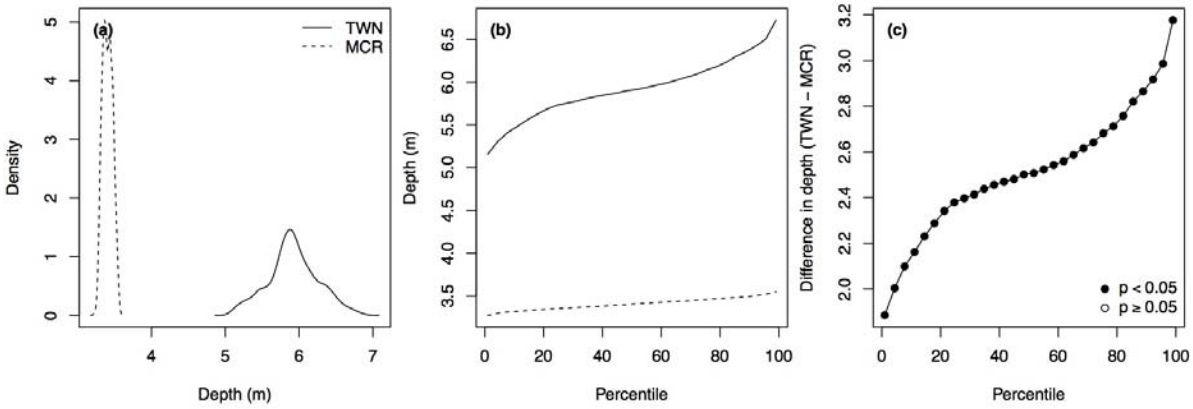

A variety of analyses all confirmed that pH and temperature regimes in Moorea and Taiwan were significantly different. The summary statistics (mean and variance) of pH and temperature differed significantly between fringing reefs in Moorea and Taiwan. In addition, the entire distribution of pH values differed between sites, not only the mean and median pH but also the extreme values (Fig. 26C). pH was higher in Moorea, for its mean and across almost all percentiles, but extreme values at this site were lower than in Taiwan. However, overall variance of pH was slightly greater in Moorea. Mean temperature was greater in Moorea, but variance of temperature was greater in Taiwan. Finally, wavelet analysis assessed composition and coherence of variance in pH, temperature, salinity, and depth across a range of frequencies at each site. For all parameters measured, changes in the contribution of the most important frequencies between sites suggest that the relative influence of biological processes versus oceanographic processes on environmental variability differs between the datasets collected in Moorea and Taiwan.

Differences in environmental variability between Moorea and Taiwan

There are several reasons why pH and temperature regimes may differ between Moorea and Taiwan. Firstly, although both time series were collected during the austral summer at each site, they did not overlap in time. Therefore, it is possible that the differences in environmental variability attributed to space may be due to temporal changes in the regimes of pH and temperature. In a small-scale study along a 32 m slope of a fringing reef at Coconut Island, Oahu, Guadayol *et al.* (2014) found that spatial changes in variability of abiotic parameters like pH and temperature exceeded temporal changes in the regime of these variables. The Hawaii study employed a spatio-temporal sampling design with more

coverage than I had in this study with one set of sensors at each location. In comparison to the Hawaii study, my study encompassed a larger biogeographic spatial scale, where ratios between the variances of pH and temperature may not be constant through time (Guadayol et al., 2014). The ~6-week deployments likely did not capture temporal changes in pH and temperature regimes across the austral summer seasons.

Different oceanographic features in Moorea and Taiwan likely contributed to the observed differences in pH and temperature regimes. In Nanwan Bay in Taiwan, upwelling induced by internal tides is known to cause large drops in temperature within a few hours, a phenomenon that is exacerbated when monsoon winds raise the thermocline in the bay (Lee et al., 1999; Jan and Chen, 2009). During this study, Typhoon Mawar in early June and supertyphoon Guchol in late June may have caused upwelling in Nanwan Bay and subsequently drove the large-period depressions in seawater temperature observed at the Taiwan reef site (Fig. 27B). Additionally, the flood and ebb eddies established near the study site in Nanwan Bay during spring tides have been reported to cause two temperature drops per day (Lee et al., 1999). This phenomenon may account for the strong power of a ~2-week period observed in fluctuations of seawater temperature in Taiwan (Fig. 27D). It was previously unknown whether the temperature-characterized upwelling in Nanwan Bay also caused changes in seawater pH. The results of this study suggest that fluctuations in temperature and pH in Taiwan at periods < 10 hours are not strongly correlated (Fig. 29B).

With respect to the site in French Polynesia, the Moorea site was more protected, due to its location inside a lagoon. Circulation patterns in Moorea are driven more by waves than by wind or tides (Hench et al., 2008). In general, the lagoon is flushed as water comes over the barrier reef and flows out through the passes (Hench et al., 2008). Because the Moorea

site is more protected, fluctuations in pH and temperature may be less affected by oceanographic features and thus dominated by a diel period attributed to biological processes and the light regime.

Differences in weather patterns between Moorea and Taiwan could have contributed to their unique environmental regimes. Due to the two typhoons, the Taiwan site experienced ~1600 mm of rainfall during May-July, 2012 (Central Weather Bureau, Taiwan). In contrast, the island adjacent to Moorea (Tahiti) experienced ~1700 mm of rainfall during the entire year of 2012 (www.tutiempo.net), suggesting that heavy rainfall may have a more dramatic effect on the pH and temperature dynamics observed in Taiwan than in Moorea. In addition to inducing upwelling, the stormy weather in Taiwan could also have reduced seawater temperature due to decreased solar heating of the surface ocean. Interestingly, the coherence between pH and temperature was not strong during this time, so upwelling enhanced by the typhoons likely did not alter the pH regime in Taiwan. Additionally, high rainfall during typhoons likely caused the observed broad decreases in salinity in Taiwan (Fig. 30A).

Water depth plays an important role in the variability of pH and temperature. Mixing, turbulence, light intensity and quality, nutrient concentrations, and the influence of waves all vary by depth. Due to constraints in the specific deployment locations of the sensors, sensor depth differed between sites. Sensors were deployed at ~3 m in Moorea and at ~6 m in Taiwan. This difference may help explain why the 24-hour period in fluctuations of pH and temperature is much stronger and more consistent in Moorea. The deeper depth in Taiwan likely dilutes the signal of photosynthesis and respiration within the overall variability of pH and temperature. Similarly, Guadayol *et al.* (2014) also found that the

importance of daily fluctuations within pH and temperature signals decreases with water depth. Water depth was also affected by semidiurnal tides present at both sites. Here, I show that changes in water depth associated with waves and tides are much more diverse in Taiwan than in Moorea (Fig. 31C). The wide range of water depth may have weakened the power of the 24-hour period in the pH and temperature fluctuations in Taiwan (Figs. 25D, 27D).

An ecological perspective

The environmental data collected at my study sites, Moorea and Taiwan, confirmed that the Ambient experimental treatments used in Chapter 4 approximated conditions experienced at the reef scale during the time the experiments were conducted as well as conditions the coral larvae may have encountered in the water column shortly after release. Additionally, these datasets revealed that the High experimental treatments used were at the maxima or outside the range of exposure to pH and temperature on these fringing reefs during the time the experiment was conducted. It is important to note that the measurements of pH and temperature presented in this chapter cannot account for gradients in pH and temperature on the meter scale (*e.g.* Guadayol et al., 2014) or within the boundary layer of the corals themselves (Shashar et al., 1993).

The time series reported in this chapter revealed reef conditions for my study populations. At both sites, the mean pCO_2 value calculated (467-473 μatm) was higher than the annual global atmospheric mean for 2012 (393 μatm; Conway and Tans, NOAA/ESRL [www.esrl.noaa.gov/gmd/ccgg/trends]). Temperature stress may be more common in Moorea, where seawater temperature passed the local bleaching threshold (30°C; Gleason,

1993) for several hours on three adjacent days in early March. In contrast, seawater temperature in Taiwan passed the local bleaching threshold (30°C; Wilkinson, 1998) only once, for 6 minutes in May. As pH and temperature fluctuated on a variety of periods, aragonite saturation state at Moorea was on average above what is adequate for coral reefs (>3.5; Kleypas et al., 1999b; Guinotte et al., 2003). However, Ω_{arag} fell as low as 2.70, an extreme level for corals where accretion rates may be depressed (Kleypas et al., 1999b). Based on the summary statistics (Table 35), the study reef in Taiwan would be considered marginal and low- Ω_{arag}, with 75% of the time spent below commonly observed levels for coral reefs (Kleypas et al., 1999b; Guinotte et al., 2003). It is important to note the limitation of our ability to conclude much about Ω_{arag} at these sites as I collected limited datasets on salinity and total alkalinity.

pH and temperature time series recorded at Moorea and Taiwan differed slightly from conditions at other coral reefs. At Moorea, the mean pCO_2 value recorded (473 µatm) was higher than recorded in winter at this site in the previous year (374 µatm; Chapter 2, Rivest and Hofmann, 2014); lower wind stress in 2012 may have enhanced seawater retention in the lagoon, allowing the biological pCO_2 signal to increase average pCO_2 levels. In 2012 at Moorea, mean pH was higher and mean temperature was lower than in 2011 (Chapter 2). Mean pH variability reported here is similar to SeaFET pH time series data collected from coral reefs in the Northern Line Islands (Price et al., 2012) but pH values at Moorea and Taiwan were lower than those reported for reef lagoons and reef flats on the Great Barrier Reef (Gagliano et al., 2010; Albright et al., 2013; Shaw and McNeil, 2014). More acidic carbonate chemistry was documented in a lagoon in Okinawa and at Heron Island, where pCO_2 reached levels predicted in a worst-case scenario by the year 2100

(Ohde and van Woesik, 1999; Santos et al., 2011; IPCC, 2013). Temperature in Taiwan was similar to that reported in (Jan and Chen, 2009) for Nanwan Bay.

Conclusion

Regimes of pH and temperature differed between fringing reef sites in Moorea and Taiwan. My in-depth comparisons showed that these differences persisted across comparisons of summary statistics, frequency distributions, and signal dynamics. It is likely that the relative importance of biological processes of the coral reef community (*i.e.* photosynthesis, respiration, and calcification), oceanographic events, and weather at each site was distinct. As a result of the unique variability of pH and temperature between Moorea and Taiwan, there is potential that corals, including *P. damicornis*, are locally adapted and seasonally acclimatized to the observed conditions (Palumbi et al., 2014). Consequent population-specific physiological differences across the biogeographic species ranges may result in a range of responses to future changes in pH and temperature at these sites. In Chapter 4, I found that Moorea and Taiwan populations exhibit different physiological responses of *P. damicornis* larvae to OA and warming. Studies as this, which present measurements of the physical environment alongside metrics of biological performance, provide a valuable insight to the potential heterogeneity of phenotypes of tolerance to global ocean change.

References

Adjeroud M, Guérécheau A, Vidal-Dupiol J, Flot J-F, Arnaud-Haond S, Bonhomme F. 2013. Genetic diversity, clonality and connectivity in the scleractinian coral *Pocillopora damicornis*: a multi-scale analysis in an insular, fragmented reef system. *Mar Biol* 161:531–541.

Alamaru A, Yam R, Shemesh A. 2009. Trophic biology of *Stylophora pistillata* larvae: evidence from stable isotope analysis. *Mar Ecol Prog Ser* 383:85–94.

Alberts B, Johnson A, Lewis J, Raff M, Roberts K, Walter P. 2002. Molecular Biology of the Cell, 4th ed. New York: Garland Science.

Albright R, Langdon C, Anthony KRN. 2013. Dynamics of seawater carbonate chemistry, production, and calcification of a coral reef flat, central Great Barrier Reef. *Biogeosciences* 10:6747–6758.

Albright R, Langdon C. 2011. Ocean acidification impacts multiple early life history processes of the Caribbean coral *Porites astreoides*. *Glob Chang Biol* 17:2478–2487.

Albright R, Mason B, Langdon C. 2008. Effect of aragonite saturation state on settlement and post-settlement growth of *Porites astreoides* larvae. *Coral Reefs* 27:485–490.

Albright R, Mason B, Miller M, Langdon C. 2010. Ocean acidification compromises recruitment success of the threatened Caribbean coral *Acropora palmata*. *Proc Natl Acad Sci U S A* 107:20400–20404.

Alleaume-Benharira M, Pen I, Ronce O. 2006. Geographical patterns of adaptation within a species' range: interactions between drift and gene flow. *J Evol Biol* 19:203–215.

Amar KO, Chadwick NE, Rinkevich B. 2007. Coral planulae as dispersion vehicles: biological properties of larvae released early and late in the season. *Mar Ecol Prog Ser* 350:71–78.

Anlauf H, D'Croz L, O'Dea A. 2011. A corrosive concoction: The combined effects of ocean warming and acidification on the early growth of a stony coral are multiplicative. *J Exp Mar Bio Ecol* 397:13–20.

Anthony KRN, Kline DI, Diaz-Pulido G, Dove S, Hoegh-Guldberg O. 2008. Ocean acidification causes bleaching and productivity loss in coral reef builders. *Proc Natl Acad Sci U S A* 105:17442–17446.

Anthony KRN, Maynard JA, Diaz-Pulido G, Mumby PJ, Marshall PA, Cao L, Hoegh-Guldberg O. 2011. Ocean acidification and warming will lower coral reef resilience. *Glob Chang Biol* 17:1798–1808.

Arai T, Kato M, Heyward A. 1993. Lipid composition of positively buoyant eggs of reef building corals. *Mar Ecol Prog Ser* 12:71–75.

Arnold KE, Findlay HS, Spicer JI, Daniels CL, Boothroyd D. 2009. Effect of CO_2-related acidification on aspects of the larval development of the European lobster, *Homarus gammarus* (L.). *Biogeosciences* 6:1747–1754.

Asada K, Takahashi M. 1987. Production and scavenging of active oxygen in photosynthesis. In: *Photoinhibition*, pp 228–287. Amsterdam: Elsevier.

Baird AH, Guest JR, Willis BL. 2009. Systematic and biogeographical patterns in the reproductive biology of scleractinian corals. *Annu Rev Ecol Evol Syst* 40:551–571.

Baker PF, Connelly CM. 1966. Some properties of the external activation site of the sodium pump in crab nerve. *J Physiol* 185:270–297.

Barshis DJ, Ladner JT, Oliver TA, Palumbi SR. 2014. Lineage-specific transcriptional profiles of *Symbiodinium* spp. unaltered by heat stress in a coral host. *Mol Biol Evol*:msu107.

Barshis DJ, Ladner JT, Oliver TA, Seneca FO, Traylor-Knowles N, Palumbi SR. 2013. Genomic basis for coral resilience to climate change. *Proc Natl Acad Sci U S A* 110:1387–1392.

Bassim K, Sammarco P. 2003. Effects of temperature and ammonium on larval development and survivorship in a scleractinian coral (*Diploria strigosa*). *Mar Biol* 142:241–252.

Battey JF, Patton JS. 1984. A reevaluation of the role of glycerol in carbon translocation in zooxanthellae-coelenterate symbiosis. *Mar Biol* 79:27–38.

Bauermeister AEM, Sargent JR. 1979. Biosynthesis of triacylglycerols in the intestines of Rainbow trout (*Salmo gairdnerii*) fed marine zooplankton rich in wax esters. *Biochim Biophys Acta - Lipids* 575:358–364.

Ben-David-Zaslow R, Benayahu Y. 2000. Biochemical composition, metabolism, and amino acid transport in planula-larvae of the soft coral *Heteroxenia fuscescens*. *J Exp Zool* 287:401–412.

Benjamini Y, Hochberg Y. 1995. Controlling the false discovery rate: a practical and powerful approach to multiple testing. *J R Stat Soc B* 57:289–300.

Benzie IF, Strain JJ. 1996. The ferric reducing ability of plasma (FRAP) as a measure of "antioxidant power": the FRAP assay. *Anal Biochem* 239:70–76.

Benzie IFF, Strain JJ. 1999. Ferric reducing/antioxidant power assay: direct measure of total antioxidant activity of biological fluids and modified version for simultaneous

measurement of total antioxidant power and ascorbic acid concentration. *Methods Enzymol* 299:15–27.

Berkelmans R, van Oppen MJH. 2006. The role of zooxanthellae in the thermal tolerance of corals: a "nugget of hope" for coral reefs in an era of climate change. *Proc R Soc B-Biological Sci* 273:2305–2312.

Bernardo J. 1996. The particular maternal effect of propagule size, especially egg size: patterns, models, quality of evidence and interpretations. *Am Zool* 36:216–236.

Bibby R, Cleall-Harding P, Rundle S, Widdicombe S, Spicer J. 2007. Ocean acidification disrupts induced defenses in the intertidal gastropod *Littorina littorea*. *Biol Lett* 3:699–701.

Black NA, Voellmy R, Szmant AM. 1995. Heat shock protein induction in *Montastraea faveolata* and *Aiptasia pallida* exposed to elevated temperatures. *Biol Bull* 188:234–240.

Blanco G, Mercer RW. 1998. Isozymes of the Na^+/K^+-ATPase: heterogeneity in structure, diversity in function. *Am J Physiol Renal Physiol* 275:F633–650.

Bligh EG, Dyer WJ. 1959. A rapid method of total lipid extraction and purification. *Can J Biochem Physiol* 37:911–917.

Boatta F, D'Alessandro W, Gagliano AL, Liotta M, Milazzo M, Rodolfo-Metalpa R, Hall-Spencer JM, Parello F. 2013. Geochemical survey of Levante Bay, Vulcano Island (Italy), a natural laboratory for the study of ocean acidification. *Mar Pollut Bull* 73:485–494.

Bradford MM. 1976. Rapid and sensitive method for quantitation of microgram quantities of protein utilizing principle of protein-dye binding. *Anal Biochem* 72:248–254.

Brading P, Warner ME, Davey P, Smith DJ, Achterberg EP, Suggett DJ. 2011. Differential effects of ocean acidification on growth and photosynthesis among phylotypes of *Symbiodinium* (Dinophyceae). *Limnol Oceanogr* 56:927–938.

Buckley LB, Kingsolver JG. 2012. Functional and phylogenetic approaches to forecasting species' responses to climate change. *Annu Rev Ecol Evol Syst* 43:205–226.

Buddemeier RW, Jokiel PL, Zimmerman KM, Lane DR, Carey JM, Bohling GC, Martinich JA. 2008. A modeling tool to evaluate regional coral reef responses to changes in climate and ocean chemistry. *Limnol Oceanogr* 6:395–411.

Burge CA, Mouchka ME, Harvell CD, Roberts S. 2013. Immune response of the Caribbean sea fan, *Gorgonia ventalina*, exposed to an *Aplanochytrium* parasite as revealed by transcriptome sequencing. *Front Physiol* 4:180.

Burnham KP, Anderson DR. 2002. Model selection and multi-model inference: a practical information-theoretic approach. New York, NY: Springer-Verlag.

Byrne M, Soars N, Selvakumaraswamy P, Dworjanyn SA, Davis AR. 2010. Sea urchin fertilization in a warm, acidified and high pCO_2 ocean across a range of sperm densities. *Mar Environ Res* 69:234–239.

Byrne M. 2011. Impact of ocean warming and ocean acidification on marine invertebrate life history stages: vulnerabilities and potential for persistence in a changing ocean. In: *Oceanography and Marine Biology: An Annual Review, Vol 49*, pp 1–42.

Cadenas E. 1989. Biochemistry of oxygen toxicity. *Annu Rev Biochem* 58:79–110.

Cazelles B, Chavez M, Berteaux D, Menard F, Vik JO, Jenouvrier S, Stenseth NC. 2008. Wavelet analysis of ecological time series. *Oecologia* 156:287–304.

Chen CA, Yang Y-W, Wei N V, Tsai W-S, Fang L-S. 2004. Symbiont diversity in scleractinian corals from tropical reefs and subtropical non-reef communities in Taiwan. *Coral Reefs* 24:11–22.

Chen W-NU, Kang H-J, Weis VM, Mayfield AB, Jiang P-L, Fang L-S, Chen C-S. 2012. Diel rhythmicity of lipid-body formation in a coral-*Symbiodinium* endosymbiosis. *Coral Reefs* 31:521–534.

Chierici M, Fransson A. 2009. Calcium carbonate saturation in the surface water of the Arctic Ocean: undersaturation in freshwater influenced shelves. *Biogeosciences* 6:2421–2431.

Childress JJ, Somero GN. 1990. Metabolic scaling - a new perspective based on scaling of glycolytic enzyme activities. *Am Zool* 30:161–173.

Chu KH, Ovsianicokoulikowsky NN. 1994. Ontogenetic changes in metabolic activity and biochemical composition in the shrimp, *Metapenaeus ensis*. *J Exp Mar Bio Ecol* 183:11–26.

Chua C-M, Leggat W, Moya A. 2013. Near-future reductions in pH will have no consistent ecological effects on the early life-history stages of reef corals. *Mar Ecol Prog Ser* 486:143–151.

Clark D, Lamare M, Barker M. 2009. Response of sea urchin pluteus larvae (Echinodermata: Echinoidea) to reduced seawater pH: a comparison among a tropical, temperate, and a polar species. *Mar Biol* 156:1125–1137.

Cohen A, Holcomb M. 2009. Why corals care about ocean acidification: uncovering the mechanism. *Oceanography* 22:118–127.

Cohen AA, Martin LB, Wingfield JC, McWilliams SR, Dunne JA. 2012. Physiological regulatory networks: ecological roles and evolutionary constraints. *Trends Ecol Evol* 27:428–435.

Coles SL, Jokiel PL. 1977. Effects of temperature on photosynthesis and respiration in hermatypic corals. *Mar Biol* 43:209–216.

Comeau S, Carpenter RC, Edmunds PJ. 2013. Coral reef calcifiers buffer their response to ocean acidification using both bicarbonate and carbonate. *Proc R Soc B-Biological Sci* 280.

Comeau S, Jeffree R, Teyssié J-L, Gattuso J-P. 2010. Response of the Arctic pteropod *Limacina helicina* to projected future environmental conditions. *PLoS One* 5:e11362.

Conover DO. 1998. Local adaptation in marine fishes: evidence and implications for stock enhancement. *Bull Mar Sci* 62:477–493.

Crane RK. 1977. The gradient hypothesis and other models of carrier-mediated active transport. *Rev Physiol Biochem Pharmacol* 78:99–159.

Crawley MJ. 2013. The R book, Second. West Sussex, UK: John Wiley & Sons.

Császár NBM, Seneca FO, van Oppen MJH. 2009. Variation in antioxidant gene expression in the scleractinian coral *Acropora millepora* under laboratory thermal stress. *Mar Ecol Prog Ser* 392:93–102.

Cumbo VR, Edmunds PJ, Wall CB. 2013a. Brooded coral larvae differ in their response to high temperature and elevated pCO_2 depending on the day of release. *Mar Biol* 160:2903–2917.

Cumbo VR, Fan T-Y, Edmunds PJ. 2012. Physiological development of brooded larvae from two pocilloporid corals in Taiwan. *Mar Biol* 159:2853–2866.

Cumbo VR, Fan T-Y, Edmunds PJ. 2013b. Effects of exposure duration on the response of *Pocillopora damicornis* larvae to elevated temperature and high pCO_2. *J Exp Mar Bio Ecol* 439:100–107.

Davies PS. 1991. Effect of daylight variations on the energy budgets of shallow-water corals. *Mar Biol* 108:137–144.

Dean JB. 2010. Hypercapnia causes cellular oxidation and nitrosation in addition to acidosis: implications for CO_2 chemoreceptor function and dysfunction. *J Appl Physiol* 108:1786–1795.

Deigweiher K, Koschnick N, Pörtner H-O, Lucassen M. 2008. Acclimation of ion regulatory capacities in gills of marine fish under environmental hypercapnia. *Am J Physiol Regul Integr Comp Physiol* 295:R1660–16670.

Delmas RP, Parrish CC, Ackman RG. 1984. Determination of lipid class concentrations in seawater by thin-layer chromatography with flame ionization detection. *Anal Chem* 56:1272–1277.

DeSalvo MK, Sunagawa S, Voolstra CR, Medina M. 2010. Transcriptomic responses to heat stress and bleaching in the elkhorn coral *Acropora palmata*. *Mar Ecol Prog Ser* 402:97–113.

DeSalvo MK, Voolstra CR, Sunagawa S, Schwarz JA, Stillman JH, Coffroth MA, Szmant AM, Medina M. 2008. Differential gene expression during thermal stress and bleaching in the Caribbean coral *Montastraea faveolata*. *Mol Ecol* 17:3952–3971.

Dickson A, Sabine C, Christian J. 2007. Guide to best practices for ocean CO_2 measurements. Sidney, British Columbia.

Dickson AG, Millero FJ. 1987. A comparison of the equilibrium constants for the dissociation of carbonic acid in seawater media. *Deep Sea Res Part A Oceanogr Res Pap* 34:1733–1743.

Doney SC. 2010. The growing human footprint on coastal and open-ocean biogeochemistry. *Science* 328:1512–1516.

Downs CA, Fauth JE, Halas JC, Dustan P, Bemiss J, Woodley CM. 2002. Oxidative stress and seasonal coral bleaching. *Free Radic Biol Med* 33:533–543.

Downs CA, Mueller E, Phillips S, Fauth JE, Woodley CM. 2000. A molecular biomarker system for assessing the health of coral (*Montastraea faveolata*) during heat stress. *Mar Biotechnol* 2:533–544.

Dupont S, Havenhand J, Thorndyke W, Peck L, Thorndyke M. 2008. Near-future level of CO_2-driven ocean acidification radically affects larval survival and development in the brittlestar *Ophiothrix fragilis*. *Mar Ecol Prog Ser* 373:285–294.

Dykens JA, Shick JM, Benoit C, Buettner GR, Winston GW. 1992. Oxygen radical production in the sea anemone *Anthopleura elegantissima* and its endosymbiotic algae. *J Exp Biol* 168:219–241.

Dykens JA, Shick JM. 1982. Oxygen production by endosymbiotic algae controls superoxide dismutase activity in their animal host. *Nature* 297:579–580.

Edmunds PJ, Brown D, Moriarty V. 2012. Interactive effects of ocean acidification and temperature on two scleractinian corals from Moorea, French Polynesia. *Glob Chang Biol* 18:2173–2183.

Edmunds PJ, Cumbo VR, Fan T-Y. 2013. Metabolic costs of larval settlement and metamorphosis in the coral *Seriatopora caliendrum* under ambient and elevated pCO_2. *J Exp Mar Bio Ecol* 443:33–38.

Edmunds PJ, Gates RD, Gleason DF. 2001. The biology of larvae from the reef coral *Porites astreoides*, and their response to temperature disturbances. *Mar Biol* 139:981–989.

Edmunds PJ, Gates RD, Leggat W, Hoegh-Guldberg O, Allen-Requa L. 2005. The effect of temperature on the size and population density of dinoflagellates in larvae of the reef coral *Porites astreoides*. *Invertebr Biol* 124:185–193.

Edmunds PJ. 2005. Effect of elevated temperature on aerobic respiration of coral recruits. *Mar Biol* 146:655–663.

Edmunds PJ. 2014. Is acclimation beneficial to scleractinian corals, *Porites* spp.? *Mar Biol*.

Eliason EJ, Clark TD, Hague MJ, Hanson LM, Gallagher ZS, Jeffries KM, Gale MK, Patterson DA, Hinch SG, Farrell AP. 2011. Differences in thermal tolerance among sockeye salmon populations. *Science* 332:109–112.

Ellis RP, Bersey J, Rundle SD, Hall-Spencer JM, Spicer JI. 2009. Subtle but significant effects of CO_2 acidified seawater on embryos of the intertidal snail, *Littorina obtusata*. *Aquat Biol* 5:41–48.

Emlet RB. 1986. Facultative planktotrophy in the tropical echinoid *Clypeaster rosaceus* (Linnaeus) and a comparison with obligate planktotrophy in *Clypeaster*. *J Exp Mar Bio Ecol* 95:183–202.

Emmett R, Hochachka PW. 1981. Scaling of oxidative and glycolytic enzymes in mammals. *Respir Physiol* 45:261–272.

Esmann M. 1988. ATPase and phosphatase activity of the Na^+,K^+-ATPase: molar and specific activity, protein determination. *Methods Enzymol* 156:105–115.

Evans TG, Chan F, Menge BA, Hofmann GE. 2013. Transcriptomic responses to ocean acidification in larval sea urchins from a naturally variable pH environment. *Mol Ecol* 22:1609–1625.

Evans TG, Hofmann GE. 2012. Defining the limits of physiological plasticity: how gene expression can assess and predict the consequences of ocean change. *Philos Trans R Soc B Biol Sci* 367:1733–1745.

Fabricius KE, Langdon C, Uthicke S, Humphrey C, Noonan S, De'ath G, Okazaki R, Muehllehner N, Glas MS, Lough JM. 2011. Losers and winners in coral reefs acclimatized to elevated carbon dioxide concentrations. *Nat Clim Chang* 1:165–169.

Fabry VJ, Seibel BA, Feely RA, Orr JC. 2008. Impacts of ocean acidification on marine fauna and ecosystem processes. *Ices J Mar Sci* 65:414–432.

Fadlallah YH. 1983. Sexual reproduction, development and larval biology in scleractinian corals. *Coral Reefs* 2:129–150.

Fan T-Y, Li J-J, Ie S-X, Fang L-S. 2002. Lunar periodicity of larval release by Pocilloporid corals in southern Taiwan. *Zool Stud* 41:288–294.

Fan T-Y, Lin K-H, Kuo F-W, Soong K, Liu L-L, Fang L-S. 2006. Diel patterns of larval release by five brooding scleractinian corals. *Mar Ecol Prog Ser* 321:133–142.

Fangue NA, O'Donnell MJ, Sewell MA, Matson PG, MacPherson AC, Hofmann GE. 2010. A laboratory-based, experimental system for the study of ocean acidification effects on marine invertebrate larvae. *Limnol Oceanogr* 8:441–452.

Faul F, Erdfelder E, Lang A-G, Buchner A. 2007. G*Power 3: a flexible statistal power analysis program for the social, behavioral, and biomedical sciences. *Behav Res Methods* 39:175–191.

Feely RA. 2008. Ocean acidification. In: *State of the Climate in 2007* (Levinson DH, Lawrimore JH, eds.), pp S1–S179. Bulletin of the American Meteorological Society.

Figueiredo J, Baird AH, Cohen MF, Flot J-F, Kamiki T, Meziane T, Tsuchiya M, Yamasaki H. 2012. Ontogenetic change in the lipid and fatty acid composition of scleractinian coral larvae. *Coral Reefs* 31:613–619.

Findlay HS, Kendall MA, Spicer JI, Widdicombe S. 2009. Post-larval development of two intertidal barnacles at elevated CO_2 and temperature. *Mar Biol* 157:725–735.

Fitt WK, McFarland FK, Warner ME, Chilcoat GC. 2000. Seasonal patterns of tissue biomass and densities of symbiotic dinoflagellates in reef corals and relation to coral bleaching. *Limnol Oceanogr* 45:677–685.

Forsman ZH, Johnston EC, Brooks AJ, Adam TC, Toonen RJ. 2013. Genetic evidence for regional isolation of *Pocillopora* corals from Moorea. *Oceanography* 26:153–155.

Fridovich I. 1998. Oxygen toxicity: a radical explanation. *J Exp Biol* 201:1203–1209.

Frieder CA, Nam SH, Martz TR, Levin LA. 2012. High temporal and spatial variability of dissolved oxygen and pH in a nearshore California kelp forest. *Biogeosciences* 9:3917–3930.

Frieder CA. 2014. Present-day nearshore pH differentially depresses fertilization in congeneric sea urchins. *Biol Bull* 226:1–7.

Gagliano M, McCormick MI, Moore JA, Depczynski M. 2010. The basics of acidification: baseline variability of pH on Australian coral reefs. *Mar Biol* 157:1849–1856.

Gaitán-Espitia JD, Hancock JR, Padilla-Gamiño JL, Rivest EB, Blanchette CA, Reed DC, Hofmann GE. 2014. Interactive effects of elevated temperature and pCO_2 on early-life-history stages of the giant kelp *Macrocystis pyrifera*. *J Exp Mar Bio Ecol* 457:51–58.

Gaither MR, Rowan R. 2010. Zooxanthellar symbiosis in planula larvae of the coral *Pocillopora damicornis*. *J Exp Mar Bio Ecol* 386:45–53.

Gallager SM, Mann R, Sasaki GC. 1986. Lipid as an index of growth and viability in three species of bivalve larvae. *Aquaculture* 56:81–103.

Gates RD, Edmunds PJ. 1999. The physiological mechanisms of acclimatization in tropical reef corals. *Am Zool* 39:30–43.

Gattuso J-P, Yellowlees D, Lesser M. 1993. Depth-dependent and light-dependent variation of carbon partitioning and utilization in the zooxanthellate scleractinian coral *Styolophora pistillata*. *Mar Ecol Prog Ser* 92:267–276.

Gibbin EM, Putnam HM, Davy SK, Gates RD. 2014. Intracellular pH and its response to CO_2-driven seawater acidification in symbiotic versus non-symbiotic coral cells. *J Exp Biol* jeb.099549.

Gillooly JF, Brown JH, West GB, Savage VM, Charnov EL. 2001. Effects of size and temperature on metabolic rate. *Science* 293:2248–2251.

Gleason MG. 1993. Effects of disturbance on coral communities: bleaching in Moorea, French Polynesia. *Coral Reefs* 12:193–201.

Glynn IM, Karlish SJD. 1975. The sodium pump. *Annu Rev Physiol* 37:13–55.

Godbold JA, Calosi P. 2013. Ocean acidification and climate change: advances in ecology and evolution. *Philos Trans R Soc Lond B Biol Sci* 368:20120448.

Gordon BR, Leggat W. 2010. Symbiodinium-invertebrate symbioses and the role of metabolomics. *Mar Drugs* 8:2546–2568.

Griffin S, Bhagooli R. 2004. Measuring antioxidant potential in corals using the FRAP assay. *J Exp Mar Bio Ecol* 302:201–211.

Grottoli AG, Rodrigues LJ, Juarez C. 2004. Lipids and stable carbon isotopes in two species of Hawaiian corals, *Porites compressa* and *Montipora verrucosa*, following a bleaching event. *Mar Biol* 145:621–631.

Guadayol O, Silbiger NJ, Donahue MJ, Thomas FIM. 2014. Patterns in temporal variability of temperature, oxygen and pH along an environmental gradient in a coral reef. *PLoS One* 9:e85213.

Guinotte JM, Buddemeier RW, Kleypas JA. 2003. Future coral reef habitat marginality: temporal and spatial effects of climate change in the Pacific basin. *Coral Reefs* 22:551–558.

Guppy M, Withers P. 1999. Metabolic depression in animals: physiological perspectives and biochemical generalizations. *Biol Rev* 74:1–40.

Halliwell B, Gutteridge J. 1999. Free Radicals in Biology and Medicine. New York: Oxford University Press.

Hall-Spencer JM, Rodolfo-Metalpa R, Martin S, Ransome E, Fine M, Turner SM, Rowley SJ, Tedesco D, Buia M-CC. 2008. Volcanic carbon dioxide vents show ecosystem effects of ocean acidification. *Nature* 454:96–99.

Hand SC, Hardewig I. 1996. Downregulation of cellular metabolism during environmental stress: mechanisms and implications. *Annu Rev Physiol* 58:539–563.

Hand SC. 1991. Metabolic dormancy in aquatic invertebrates. In: *Advances in Comparative and Environmental Physiology*, 8th ed. (Castellini, M. A., B. Fievet, S. C. Hand, R. Motais BP and REW, ed.), pp 1–50. Berlin Heidelberg: Springer-Verlag.

Hargrove JL, Hulsey MG, Beale EG. 1991. The kinetics of mammalian gene expression. *Bioassays* 13:667–674.

Harii S, Kayanne H, Takigawa H, Hayashibara T, Yamamoto M. 2002. Larval survivorship, competency periods and settlement of two brooding corals, *Heliopora coerulea* and *Pocillopora damicornis*. *Mar Biol* 141:39–46.

Harii S, Kayanne H. 2003. Larval dispersal, recruitment, and adult distribution of the brooding stony octocoral *Heliopora coerulea* on Ishigaki Island, southwest Japan. *Coral Reefs* 22:188–196.

Harii S, Nadaoka K, Yamamoto M. 2007. Temporal changes in settlement, lipid content and lipid composition of larvae of the spawning hermatypic coral *Acropora tenuis*. *Mar Ecol Prog Ser* 346:89–96.

Harii S, Yamamoto M, Hoegh-Guldberg O. 2010. The relative contribution of dinoflagellate photosynthesis and stored lipids to the survivorship of symbiotic larvae of the reef-building corals. *Mar Biol* 157:1215–1224.

Harland AD, Fixter LM, Spencer Davies P, Anderson RA. 1991. Distribution of lipids between the zooxanthellae and animal compartment in the symbiotic sea anemoneAnemonia viridis: wax esters, triglycerides and fatty acids. *Mar Biol* 110:13–19.

Harriott VJ. 1983. Reproductive seasonality, settlement, and post-settlement mortality of *Pocillopora damicornis* (Linnaeus), at Lizard Island, Great Barrier Reef. *Coral Reefs* 2:151–157.

Harrison PL, Wallace CC. 1990. Reproduction, dispersal and recruitment of scleractinian corals. In: *Ecosystems of the World, vol. 25: Coral Reefs* (Dubinsky Z, ed.), pp 133–207. New York: Elsevier.

Hauri C, Gruber N, Plattner G-K, Alin S, Feely RA, Hales B, Wheeler PA. 2009. Ocean acidification in the California Current System. *Oceanography* 22:60–71.

Havenhand J, Buttler FR, Thorndyke MC, Williamson JE. 2008. Near-future levels of ocean acidification reduce fertilization success in a sea urchin. *Curr Biol* 18:R651–R652.

Hazel JR, Prosser CL. 1974. Molecular mechanisms of temperature compensation in poikilotherms. *Physiol Rev* 54:620.

Hench JL, Leichter JJ, Monismith SG. 2008. Episodic circulation and exchange in a wave-driven coral reef and lagoon system. *Limnol Oceanogr* 53:2681–2694.

Hendriks IE, Duarte CM, Alvarez M. 2010. Vulnerability of marine biodiversity to ocean acidification: a meta-analysis. *Estuar Coast Shelf Sci* 86:157–164.

Hertwig B, Streb P, Feierabend J. 1992. Light dependence of catalase synthesis and degradation in leaves and the influence of interfering stress conditions. *Plant Physiol* 100:1547–1553.

Heyward AJ, Negri AP. 2010. Plasticity of larval pre-competency in response to temperature: observations on multiple broadcast spawning coral species. *Coral Reefs* 29:631–636.

Highsmith RC, Emlet RB. 1986. Delayed metamorphosis: Effect on growth and survival of juvenile sand dollars (Echinoidea: Clypeasteroida). *Bull Mar Sci* 39:347–361.

Hochachka PW, Somero GN. 2002. Biochemical adaptation: mechanism and process in physiological evolution. New York, NY: Oxford University Press.

Hoegh-Guldberg O, Mumby PJ, Hooten AJ, Steneck RS, Greenfield P, Gomez E, Harvell CD, Sale PF, Edwards AJ, Caldeira K, Knowlton N, Eakin CM, Iglesias-Prieto R, Muthiga N, Bradbury RH, Dubi A, Hatziolos ME. 2007. Coral reefs under rapid climate change and ocean acidification. *Science* 318:1737–1742.

Hoegh-Guldberg O. 1999. Climate change, coral bleaching and the future of the world's coral reefs. *Mar Freshw Res* 50:839–866.

Hofmann GE, Barry JP, Edmunds PJ, Gates RD, Hutchins DA, Klinger T, Sewell MA. 2010. The effect of ocean acidification on calcifying organisms in marine ecosystems: An organism-to-ecosystem perspective. *Annu Rev Ecol Evol Syst* 41:127–147.

Hofmann GE, Blanchette CA, Rivest EB, Kapsenberg L. 2013. Taking the pulse of marine ecosystems: The importance of coupling long-term physical and biological observations in the context of global change biology. *Oceanography* 26:140–148.

Hofmann GE, Evans TG, Kelly MW, Padilla-Gamino JL, Blanchette CA, Washburn L, Chan F, McManus MA, Menge BA, Gaylord B, Hill TM, Sanford E, LaVigne M, Rose JM, Kapsenberg L, Dutton JM. 2014. Exploring local adaptation and the ocean acidification seascape - studies in the California Current Large Marine Ecosystem. *Biogeosciences* 11:1053–1064.

Hofmann GE, O'Donnell MJ, Todgham AE. 2008. Using functional genomics to explore the effects of ocean acidification on calcifying organisms. *Mar Ecol Prog Ser* 373:219–225.

Hofmann GE, Smith JE, Johnson KS, Send U, Levin LA, Micheli F, Paytan A, Price NN, Peterson B, Takeshita Y, Matson PG, Crook ED, Kroeker KJ, Gambi MC, Rivest EB, Frieder CA, Yu PC, Martz TR. 2011. High-frequency dynamics of ocean pH: a multi-ecosystem comparison. *PLoS One* 6:e28983.

Hofmann GE, Todgham AE. 2010. Living in the now: physiological mechanisms to tolerate a rapidly changing environment. *Annu Rev Physiol* 72:127–145.

Holland DL, Walker G. 1975. The biochemical composition of the cyprid larva of the barnacle *Balanus balanoides* L. *ICES J Mar Sci* 36:162–165.

Hothorn T, Bretz F, Westfall P. 2008. Simultaneous inference in general parametric models. *Biometrical J* 50:346–363.

Howells EJ, Beltran VH, Larsen NW, Bay LK, Willis BL, van Oppen MJH. 2012. Coral thermal tolerance shaped by local adaptation of photosymbionts. *Nat Clim Chang* 2:116–120.

IPCC. 2013. Summary for Policymakers. In: *Climate Change 2013: The Physical Science Basis. Contribution of Working Group I to the Fifth Assessment Report of the Intergovernmental Panel on Climate Change* (Stocker T, Qin D, Plattner G-K, Tignor M, Allen S, Boschung J, Nauels A, Xia Y, Bex V, Midgley P, eds.). Cambridge, United Kingdom and New York, NY USA: Cambridge University Press.

Isomura N, Nishihira M. 2001. Size variation of planulae and its effect on the lifetime of planulae in three pocilloporid corals. *Coral Reefs* 20:309–315.

Jaeckle WB, Manahan DT. 1989a. Feeding by a nonfeeding larva - uptake of dissolved amino acids from seawater by lecithotrophic larvae of the gastropod *Haliotis rufescens*. *Mar Biol* 103:87–94.

Jaeckle WB, Manahan DT. 1989b. Growth and energy imbalance during the development of a lecithotrophic molluscan larva (*Haliotis rufescens*). *Biol Bull* 177:237–246.

Jan S, Chen C-TA. 2009. Potential biogeochemical effects from vigorous internal tides generated in Luzon Strait: A case study at the southernmost coast of Taiwan. *J Geophys Res* 114.

Jimenez IM, Kühl K, Larkum AWD, Ralph PJ. 2008. Heat budget and thermal microenvironment of shallow-water corals: Do massive corals get warmer than branching corals? *Limnol Oceanogr* 53:1548–1561.

Jokiel PL, Coles SL. 1990. Response of Hawaiian and other Indo-Pacific reef corals to elevated temperature. *Coral Reefs* 8:155–162.

Jokiel PL, Rodgers KS, Kuffner IB, Andersson AJ, Cox EF, Mackenzie FT. 2008. Ocean acidification and calcifying reef organisms: a mesocosm investigation. *Coral Reefs* 27:473–483.

Jones GP, Milicich MJ, Emslie MJ. 1999. Self-recruitment in a coral reef fish population. *Nature* 402:802–804.

Jones RJ, Larkum AWD, Schreiber U. 1998. Temperature-induced bleaching of corals begins with impairment of the CO_2 fixation mechanism in zooxanthellae. *Plant, Cell Environ* 21:1219–1230.

Kaniewska P, Campbell PR, Kline DI, Rodriguez-Lanetty M, Miller DJ, Dove S, Hoegh-Guldberg O. 2012. Major cellular and physiological impacts of ocean acidification on a reef building coral. *PLoS One* 7:e34659.

Karnauskas KB, Cohen AL. 2012. Equatorial refuge amid tropical warming. *Nat Clim Chang* 2:530–534.

Kawecki TJ, Ebert D. 2004. Conceptual issues in local adaptation. *Ecol Lett* 7:1225–1241.

Kelly MW, Hofmann GE. 2012. Adaptation and the physiology of ocean acidification. *Funct Ecol* 27:980–990.

Kelly MW, Padilla-Gamiño JL, Hofmann GE. 2013. Natural variation and the capacity to adapt to ocean acidification in the keystone sea urchin *Strongylocentrotus purpuratus*. *Glob Chang Biol* 19:2536–2546.

Kelly SA, Panhuis TM, Stoehr AM. 2012. Phenotypic plasticity: molecular mechanisms and adaptive significance. *Compr Physiol* 2:1417–1439.

Kempf S. 1981. Long-lived larvae of the gastropod *Aplysia juliana*: do they disperse and metamorphose or just slowly fade away? *Mar Ecol Prog Ser* 6:61–65.

Kempf SC, Hadfield MG. 1985. Planktotrophy by the lecithotrophic larvae of a nudibranch, *Phestilla sibogae* (Gastropoda). *Biol Bull* 169:119–130.

Kenkel CD, Meyer E, Matz M V. 2013. Gene expression under chronic heat stress in populations of the mustard hill coral (*Porites astreoides*) from different thermal environments. *Mol Ecol* 22:4322–4334.

Kenkel CD, Traylor MR, Wiedenmann J, Salih A, Matz M V. 2011a. Fluorescence of coral larvae predicts their settlement response to crustose coralline algae and reflects stress. *Proc R Soc B-Biological Sci* 278:2691–2697.

Kenkel CD et al. 2011b. Development of gene expression markers of acute heat-light stress in reef-building corals of the genus *Porites*. Voolstrag CR, ed. *PLoS One* 6:e26914.

Kiessling A, Kiessling KH, Storebakken T, Asgard T. 1991. Changes in the structure and fuction of the epaxial muscle of Rainbow trout (*Oncorhynchus mykiss*) in relation to ration and age. 2. Activity of key enzymes in energy metabolism. *Aquaculture* 93:357–372.

Kleypas JA, Buddemeier RW, Archer D, Gattuso J-P, Langdon C, Opdyke BN. 1999a. Geochemical consequences of increased atmospheric carbon dioxide on coral reefs. *Science* 284:118–120.

Kleypas JA, McManus JW, Menez LAB. 1999b. Environmental limits to coral reef development: where do we draw the line? *Integr Comp Biol* 39:146–159.

Knight-Jones EW. 1953. Decreased discrimination during setting after prolonged planktonic life in larvae of *Spirorbis borealis* (Serpulidae). *J Mar Biol Assoc United Kingdom* 32:337–345.

Kroeker KJ, Kordas RL, Crim RN, Singh GG. 2010. Meta-analysis reveals negative yet variable effects of ocean acidification on marine organisms. *Ecol Lett* 13:1419–1434.

Kuhl M, Cohen Y, Dalsgaard T, Jorgensen BB, Revsbech NP. 1995. Microenvironment and photosynthesis of zooxanthellae in scleractinian corals studied with microsensors for O_2, pH, and light. *Mar Ecol Prog Ser* 117:159–172.

Kültz D. 2005. Molecular and evolutionary basis of the cellular stress response. *Annu Rev Physiol* 67:225–257.

Kurihara H, Kato S, Ishimatsu A. 2007. Effects of increased seawater pCO_2 on early development of the oyster *Crassostrea gigas*. *Aquat Biol* 1:91–98.

Kurihara H, Shirayama Y. 2004. Effects of increased atmospheric CO_2 on sea urchin early development. *Mar Ecol Prog Ser* 274:161–169.

Kurihara H. 2008. Effects of CO_2-driven ocean acidification on the early developmental stages of invertebrates. *Mar Ecol Prog Ser* 373:275–284.

Lambert A, Brand M. 2004. Superoxide production by NADH:ubiquinone oxidoreductase (complex I) depends on the pH gradient across the mitochondrial inner membrane. *Biochem J* 382:511–517.

Lannig G, Eilers S, Pörtner H-O, Sokolova IM, Bock C. 2010. Impact of ocean acidification on energy metabolism of oyster, *Crassostrea gigas*-changes in metabolic pathways and thermal response. *Mar Drugs* 8:2318–2339.

Lee H-J, Chao S-Y, Fan K-L, Kuo T-Y. 1999. Tide-induced eddies and upwelling in a semi-enclosed basin: Nan Wan. *Estuar Coast Shelf Sci* 49:775–787.

Lee K, Tong LT, Millero FJ, Sabine CL, Dickson AG, Goyet C, Park G-H, Wanninkhof R, Feely RA, Key RM. 2006a. Global relationships of total alkalinity with salinity and temperature in surface waters of the world's oceans. *Geophys Res Lett* 33:L19605.

Lee RF, Hagen W, Kattner G. 2006b. Lipid storage in marine zooplankton. *Mar Ecol Prog Ser* 307:273–306.

Lee RF, Hirota J, Barnett AM. 1971. Distribution and importance of wax esters in marine copepods and other zooplankton. *Deep Sea Res* 18:1147–1165.

Lee RF. 1974. Lipids of zooplankton from Bute Inlet, British Columbia. *J Fish Res Board Canada* 31:1577–1582.

Leichter J. 2014. MCR LTER: Coral Reef: Benthic Water Temperature, ongoing since 2005. Moorea Coral Reef LTER; Long Term Ecol Research Network.

Lemos D, Salomon M, Gomes V, Phan V, Buchholz F. 2003. Citrate synthase and pyruvate kinase activities during early life stages of the shrimp *Farfantepenaeus paulensis* (Crustacea, Decapoda, Penaeidae): effects of development and temperature. *Comp Biochem Physiol B Biochem Mol Biol* 135:707–719.

Leong PKK, Manahan DT. 1997. Metabolic importance of Na^+/K^+-ATPase activity during sea urchin development. *J Exp Biol* 200:2881–2892.

Leong PKK, Manahan DT. 1999. Na^+/K^+-ATPase activity during early development and growth of an Antarctic sea urchin. *J Exp Biol* 202:2051–2058.

Lesser MP, Farrell JH. 2004. Exposure to solar radiation increases damage to both host tissues and algal symbionts of corals during thermal stress. *Coral Reefs* 23:367–377.

Lesser MP, Weis VM, Patterson MR, Jokiel PL. 1994. Effects of morphology and water motion on carbon delivery and productivity in the reef coral, *Pocillopora damicornis* (Linnaeus) - diffusion barriers, inorganic carbon limitation, and biochemical plasticity. *J Exp Mar Bio Ecol* 178:153–179.

Lesser MP. 1996. Elevated temperatures and ultraviolet radiation cause oxidative stress and inhibit photosynthesis in symbiotic dinoflagellates. *Limnol Oceanogr* 41:271–283.

Lesser MP. 1997. Oxidative stress causes coral bleaching during exposure to elevated temperatures. *Coral Reefs* 16:187–192.

Lesser MP. 2006. Oxidative stress in marine environments: biochemistry and physiological ecology. *Annu Rev Physiol* 68:253–278.

Logan CA, Somero GN. 2011. Effects of thermal acclimation on transcriptional responses to acute heat stress in the eurythermal fish *Gillichthys mirabilis* (Cooper). *Am J Physiol Regul Integr Comp Physiol* 300:R1373–1383.

Loram JE, Trapido-Rosenthal HG, Douglas AE. 2007. Functional significance of genetically different symbiotic algae Symbiodinium in a coral reef symbiosis. *Mol Ecol* 16:4849–4857.

Lucas MI, Walker G, Holland DL, Crisp DJ. 1979. An energy budget for the free-swimming and metamorphosing larvae of *Balanus balanoides* (Crustacea: Cirripedia). *Mar Biol* 55:221–229.

Lucu C, Pavicic D. 1995. Role of seawater concentration and major ions in oxygen consumption rate of isolated gills of the shore crab *Carcinus mediterraneus* Csrn. *Comp Biochem Physiol* 112:565–572.

Lunden JL, Rivest EB, Kapsenberg L, Martz TR, Gotschalk CC, O'Brien M, Blanchette CA, Hofmann GE. In review. The simple marine ecologist's guide to autonomous pH sensor deployment: from benchtop to benthos. *Environ Sci Technol*.

Luo YJ, Wang LH, Chen WNU, Peng SE, Tzen JTC, Hsiao YY, Huang HJ, Fang L-S, Chen C-S. 2009. Ratiometric imaging of gastrodermal lipid bodies in coral-dinoflagellate endosymbiosis. *Coral Reefs* 28:289–301.

Luo YJ. 2008. Lipid bodies in the marine endosymbiosis. Masters Thesis, National Tsing Hwa University, Taiwan.

Maina J, McClanahan TR, Venus V, Ateweberhan M, Madin J. 2011. Global gradients of coral exposure to environmental stresses and implications for local management. *PLoS One* 6.

Manly BFJ. 2006. Randomization, bootstrap and Monte Carlo methods in biology, Third. Chapman & Hall.

Marsh AG, Leong PKK, Manahan DT. 1999. Energy metabolism during embryonic development and larval growth of an Antarctic sea urchin. *J Exp Biol* 202:2041–2050.

Marsh AG, Mullineaux LS, Young CM. 2001. Larval dispersal potential of the tubeworm *Riftia pachyptila* at deep-sea hydrothermal vents. *Nature* 411:77–80.

Marshall DJ, Keough MJ. 2003. Variation in the dispersal potential of non-feeding invertebrate larvae: the desperate larva hypothesis and larval size. *Mar Ecol Prog Ser* 255:145–153.

Marshall DJ, Pechenik JA, Keough MJ. 2003. Larval activity levels and delayed metamorphosis affect post-larval performance in the colonial ascidian *Diplosoma listerianum*. *Mar Ecol Prog Ser* 246:153–162.

Martin S, Gattuso J-P. 2009. Response of Mediterranean coralline algae to ocean acidification and elevated temperature. *Glob Chang Biol* 15:2089–2100.

Martz TR, Connery JG, Johnson KS, Road EW, Glen M. 2010. Testing the Honeywell Durafet® for seawater pH applications. *Limnol Oceanogr* 8:172–184.

Marubini F, Ferrier-Pagès C, Furla P, Allemand D. 2008. Coral calcification responds to seawater acidification: a working hypothesis towards a physiological mechanism. *Coral Reefs* 27:491–499.

McCarthy DJ, Chen Y, Smyth GK. 2012. Differential expression analysis of multifactor RNA-Seq experiments with respect to biological variation. *Nucleic Acids Res* 40:4288–4297.

McCulloch M, Falter J, Trotter J, Montagna P. 2012. Coral resilience to ocean acidification and global warming through pH up-regulation. *Nat Clim Chang* 2:623–627.

Mehr SFP, DeSalle R, Kao H-T, Narechania A, Han Z, Tchernov D, Pieribone V, Gruber DF. 2013. Transcriptome deep-sequencing and clustering of expressed isoforms from *Favia* corals. *BMC Genomics* 14:546.

Mehrbach C, Culberso CH, Hawley JE, Pytkowic RM. 1973. Measurement of apparent dissociation constants of carbonic acid in seawater at atmospheric pressure. *Limnol Oceanogr* 18:897–907.

Melzner F, Goebel S, Langenbuch M, Gutowska MA, Pörtner H-O, Lucassen M. 2009a. Swimming performance in Atlantic Cod (*Gadus morhua*) following long-term (4-12 months) acclimation to elevated seawater pCO_2. *Aquat Toxicol* 92:30–37.

Melzner F, Gutowska MA, Langenbuch M, Dupont S, Lucassen M, Thorndyke MC, Bleich M, Pörtner H-O. 2009b. Physiological basis for high CO_2 tolerance in marine ectothermic animals: pre-adaptation through lifestyle and ontogeny? *Biogeosciences* 6:2313–2331.

Meyer E, Aglyamova G V, Matz M V. 2011. Profiling gene expression responses of coral larvae (*Acropora millepora*) to elevated temperature and settlement inducers using a novel RNA-Seq procedure. *Mol Ecol* 20:3599–3616.

Michaelidis B, Ouzounis C, Paleras A, Pörtner H-O. 2005. Effects of long-term moderate hypercapnia on acid-base balance and growth rate in marine mussels *Mytilus galloprovincialis*. *Mar Ecol Prog Ser* 293:109–118.

Middlebrook R, Hoegh-Guldberg O, Leggat W. 2008. The effect of thermal history on the susceptibility of reef-building corals to thermal stress. *J Exp Biol* 211:1050–1056.

Miller S. 1993. Larval period and its influence on post-larval life history: comparison of lecithotrophy and facultative planktotrophy in the aeolid nudibranch *Phestilla sibogae*. *Mar Biol* 117:635–645.

Moran AL, Manahan DT. 2003. Energy metabolism during larval development of Green and White abalone, *Haliotis fulgens* and *H. sorenseni*. *Biol Bull* 204:270–277.

Moran AL, Manahan DT. 2004. Physiological recovery from prolonged "starvation" in larvae of the Pacific oyster *Crassostrea gigas*. *J Exp Mar Bio Ecol* 306:17–36.

Morgan SG. 1995. The timing of larval release. In: *Ecology of Marine Invertebrate Larvae* (McEdward L, ed.), pp 157–191. Boca Raton, FL: CRC Press.

Morita M, Suwa R, Iguchi A, Nakamura M, Shimada K, Sakai K, Suzuki A. 2010. Ocean acidification reduces sperm flagellar motility in broadcast spawning reef invertebrates. *Zygote* 18:103–107.

Moya A, Huisman L, Ball EE, Hayward DC, Grasso LC, Chua CM, Woo HN, Gattuso J-P, Forêt S, Miller DJ. 2012. Whole transcriptome analysis of the coral *Acropora millepora* reveals complex responses to CO_2-driven acidification during the initiation of calcification. *Mol Ecol* 21:2440–2454.

Moyes CD. 2003. Controlling muscle mitochondrial content. *J Exp Biol* 206:4385–4391.

Munday PL, Crawley NE, Nilsson GE. 2009. Interacting effects of elevated temperature and ocean acidification on the aerobic performance of coral reef fishes. *Mar Ecol Prog Ser* 388:235–242.

Munday PL, Warner RR, Monro K, Pandolfi JM, Marshall DJ. 2013. Predicting evolutionary responses to climate change in the sea. *Ecol Lett* 16:1488–1500.

Murphy MP. 2009. How mitochondria produce reactive oxygen species. *Biochem J* 417:1–13.

Muscatine L, Porter J. 1977. Reef corals: mutualistic symbioses adapted to nutrient-poor environments. *Bioscience* 27:454–460.

Muscatine L. 1967. Glycerol excretion by symbiotic algae from corals and *Tridacna* and its control by the host. *Science* 156:516–519.

Nakamura M, Ohki S, Suzuki A, Sakai K. 2011. Coral larvae under ocean acidification: survival, metabolism, and metamorphosis. *PLoS One* 6:e14521.

Napolitano GE, Ratnayake WMN, Ackman RG. 1988. Fatty acid components of larval *Ostrea edulis* (L.): importance of triacylglycerols as a fatty acid reserve. *Comp Biochem Physiol B Comp Biochem* 90:875–883.

Nates SF, McKenney CL. 2000. Ontogenetic changes in biochemical composition during larval and early postlarval development of *Lepidophthalmus louisianensis*, a ghost shrimp with abbreviated development. *Comp Biochem Physiol B Biochem Mol Biol* 127:459–468.

Nevenzel JC. 1970. Occurrence, function and biosynthesis of wax esters in marine organisms. *Lipids* 5:308–319.

Nii CM, Muscatine L. 1997. Oxidative stress in the symbiotic sea anemone *Aiptasia pulchella* (Carlgren, 1943): contribution of the animal to superoxide ion production at elevated temperature. *Biol Bull* 192:444–456.

Norström A V, Sandström M. 2010. Lipid content of *Favia fragum* larvae: changes during planulation. *Coral Reefs* 29:793–795.

Nozawa Y, Harrison PL. 2007. Effects of elevated temperature on larval settlement and post-settlement survival in scleractinian corals, *Acropora solitaryensis* and *Favites chinensis*. *Mar Biol* 152:1181–1185.

O'Donnell MJ, Hammond LM, Hofmann GE. 2009. Predicted impact of ocean acidification on a marine invertebrate: elevated CO_2 alters response to thermal stress in sea urchin larvae. *Mar Biol* 156:439–446.

O'Donnell MJ, Todgham AE, Sewell MA, Hammond LM, Ruggiero K, Fangue NA, Zippay ML, Hofmann GE. 2010. Ocean acidification alters skeletogenesis and gene expression in larval sea urchins. *Mar Ecol Prog Ser* 398:157–171.

Ohde S, van Woesik R. 1999. Carbon dioxide flux and metabolic processes of a coral reef, Okinawa. *Bull Mar Sci* 65:559–576.

Oku H, Yamashiro H, Onaga K, Sakai K, Iwasaki H. 2003. Seasonal changes in the content and composition of lipids in the coral *Goniastrea aspera*. *Coral Reefs* 22:83–85.

Okubo N, Yamamoto HH, Nakaya F, Okaji K. 2008. Oxygen consumption of a single embryo/planula in the reef-building coral *Acropora intermedia*. *Mar Ecol Prog Ser* 366:305–309.

Olive PJW, Lewis C, Beardall V. 2000. Fitness components of seasonal reproduction: an analysis using *Nereis virens* as a life history model. *Oceanol Acta* 23:377–389.

Oliver TA, Palumbi SR. 2011. Do fluctuating temperature environments elevate coral thermal tolerance? *Coral Reefs* 30:429–440.

Olsen K, Ritson-Williams R, Ochrietor JD, Paul VJ, Ross C. 2013. Detecting hyperthermal stress in larvae of the hermatypic coral *Porites astreoides*: the suitability of using

biomarkers of oxidative stress versus heat-shock protein transcriptional expression. *Mar Biol* 160:2609–2618.

Padilla-Gamiño JL, Kelly MW, Evans TG, Hofmann GE. 2013. Temperature and CO_2 additively regulate physiology, morphology and genomic responses of larval sea urchins, *Strongylocentrotus purpuratus*. *Proc R Soc B-Biological Sci* 280:20130155.

Palumbi SR, Barshis DJ, Traylor-Knowles N, Bay RA. 2014. Mechanisms of reef coral resistance to future climate change. *Science* 344:895-898.

Pandolfi JM, Connolly SR, Marshall DJ, Cohen AL. 2011. Projecting coral reef futures under global warming and ocean acidification. *Science* 333:418–422.

Parker LM, Ross PM, O'Connor WA. 2009. The effect of ocean acidification and temperature on the fertilization and embryonic development of the Sydney rock oyster *Saccostrea glomerata* (Gould 1850). *Glob Chang Biol* 15:2123–2136.

Parker LM, Ross PM, O'Connor WA. 2010. Comparing the effect of elevated pCO_2 and temperature on the fertilization and early development of two species of oysters. *Mar Biol* 157:2435–2452.

Parrish CC, Ackman RG. 1985. Calibration of the Iatroscan-Chromarod system for marine lipid class analyses. *Lipids* 20:521–530.

Parrish CC. 1987. Separation of aquatic lipid classes by Chromarod thin-layer chromatography with measurement by Iatroscan flame ionization detection. *Can J Fish Aquat Sci* 44:722–731.

Patton JS, Abraham S, Benson AA. 1977. Lipogenesis in the intact coral *Pocillopora capitata* and its isolated zooxanthellae: Evidence for a light-driven carbon cycle between symbiont and host. *Mar Biol* 44:235–247.

Patton JS, Benson AA. 1975. A comparative study of wax ester digestion in fish. *Comp Biochem Physiol B Comp Biochem* 52:111–116.

Patton JS, Burris JE. 1983. Lipid synthesis and extrusion by freshly isolated zooxanthellae (symbiotic algae). *Mar Biol* 75:131–136.

Patton JS, Nevenzel JC, Benson AA. 1975. Specificity of digestive lipases in hydrolysis of wax esters and triglycerides studied in anchovy and other selected fish. *Lipids* 10:575–583.

Pechenik JA, Rittschof D, Schmidt AR. 1993. Influence of delayed metamorphosis on survival and growth of juvenile barnacles *Balanus amphitrite*. *Mar Biol* 115:287–294.

Pechenik JA. 1990. Delayed metamorphosis by larvae of benthic marine invertebrates - does it occur - is there a price to pay? *OPHELIA* 32:63–94.

Pechenik JA. 1999. On the advantages and disadvantages of larval stages in benthic marine invertebrate life cycles. *Mar Ecol Prog Ser* 177:269–297.

Phleger CF. 1998. Buoyancy in marine fishes: direct and indirect role of lipids. *Integr Comp Biol* 38:321–330.

Pinheiro JC, Bates DM. 2000. Mixed-effects models in S and S-PLUS Springer (Chambers J, Eddy W, Hardle W, Sheather S, Tierney L, eds.). New York, NY: Springer.

Polato NR, Altman NS, Baums IB. 2013. Variation in the transcriptional response of threatened coral larvae to elevated temperatures. *Mol Ecol* 22:1366–1382.

Pörtner H-O, Reipschlager A, Heisler N. 1998. Acid-base regulation, metabolism and energetics in *Sipunculus nudus* as a function of ambient carbon dioxide level. *J Exp Biol* 201:43–55.

Pörtner H-O, Reipschlager A. 1996. Ocean disposal of anthropogenic CO_2: physiological effects on tolerant and intolerant animals. In: *Ocean Storage of Carbon Dioxide. Workshop 2 - Environmental Impact* (Ormerod B, Angel M V, eds.), pp 57–81. Cheltenham, UK: IEA Greenhouse Gas R&D Programme.

Pörtner H-O. 2008. Ecosystem effects of ocean acidification in times of ocean warming: a physiologist's view. *Mar Ecol Prog Ser* 373:203–217.

Pörtner H-O. 2010. Oxygen- and capacity-limitation of thermal tolerance: a matrix for integrating climate-related stressor effects in marine ecosystems. *J Exp Biol* 213:881–893.

Price NN, Martz TR, Brainard RE, Smith JE. 2012. Diel variability in seawater pH relates to calcification and benthic community structure on coral reefs. *PLoS One* 7:e43843.

Prior R, Cao G. 1999. In vivo antioxidant capacity: comparison of different analytical methods. *Free Radic Biol Med* 27:1173–1181.

Putnam HM, Edmunds PJ, Fan T-Y. 2010. Effect of a fluctuating thermal regime on adult and larval reef corals. *Invertebr Biol* 129:199–209.

Putnam HM, Mayfield AB, Fan T-Y, Chen C-S, Gates RD. 2013. The physiological and molecular responses of larvae from the reef-building coral *Pocillopora damicornis* exposed to near-future increases in temperature and pCO_2. *Mar Biol* 160:2157–2173.

Putnam HM, Stat M, Pochon X, Gates RD. 2012. Endosymbiotic flexibility associates with environmental sensitivity in scleractinian corals. *Proc R Soc B-Biological Sci* 279:4352–4361.

Randall CJ, Szmant AM. 2009a. Elevated temperature reduces survivorship and settlement of the larvae of the Caribbean scleractinian coral, *Favia fragum* (Esper). *Coral Reefs* 28:537–545.

Randall CJ, Szmant AM. 2009b. Elevated temperature affects development, survivorship, and settlement of the elkhorn coral, *Acropora palmata* (Lamarck 1816). *Biol Bull* 217:269–282.

Rasband WS. 1997. ImageJ. US National Institutes of Health, Bethesda, MD, USA. http://imagej.nih.gov/ij.

Reynaud S, Leclercq N, Romaine-Lioud S, Ferrier-Pagès C, Jaubert J, Gattuso J-P. 2003. Interacting effects of CO_2 partial pressure and temperature on photosynthesis and calcification in a scleractinian coral. *Glob Chang Biol* 9:1660–1668.

Richier S, Sabourault C, Courtiade J, Zucchini N, Allemand D, Furla P. 2006. Oxidative stress and apoptotic events during thermal stress in the symbiotic sea anemone, *Anemonia viridis*. *FEBS J* 273:4186–4198.

Richmond RH, Jokiel PL. 1984. Lunar periodicity in larva release in the reef coral *Pocillopora damicornis* at Enewetak and Hawaii. *Bull Mar Sci* 34:280–287.

Richmond RH. 1981. Energetic considerations in the dispersal of *Pocillopora damicornis* (Linnaeus) planulae. In: *Proceedings of the 4th International Coral Reef Symposium*, pp 153–156.

Richmond RH. 1985. Reversible metamorphosis in coral planula larvae. *Mar Ecol Prog Ser* 22:181–185.

Richmond RH. 1987. Energetics, competence, and long-distance dispersal of planula larvae of the coral *Pocillopora damicornis*. *Mar Biol* 93:527–533.

Rivest EB, Hofmann GE. 2014. Responses of the metabolism of the larvae of *Pocillopora damicornis* to ocean acidification and warming. *PLoS One* 9:e96172.

Rivest EB. 2014. MCR LTER: Coral Reef: Coral larval metabolism in pH and temperature treatments. *Moorea Coral Reef LTER; Long Term Ecological Research Network*: knb–lter–mcr.2008.2.

Robbins LL, Hansen ME, Kleypas JA, Meylan SC. 2010. CO2calc - a user-friendly seawater carbon calculator for Windows, Mac OS X and iOS (iPhone). US Geological Survey Open-File Report 2010-1280.

Roberts CM. 1997. Connectivity and management of Caribbean coral reefs. *Science* 278:1454–1457.

Robinson JD, Flashner MS. 1979. The (Na^+/K^+)-ATPase enzymatic and transport properties. *Biochim Biophys Acta* 549:145–176.

Robinson MD, McCarthy DJ, Smyth GK. 2010. edgeR: a Bioconductor package for differential expression analysis of digital gene expression data. *Bioinformatics* 26:139–140.

Rodolfo-Metalpa R, Houlbrèque F, Tambutté É, Boisson F, Baggini C, Patti FP, Jeffree R, Fine M, Foggo A, Gattuso J-P, Hall-Spencer JM. 2011. Coral and mollusc resistance to ocean acidification adversely affected by warming. *Nat Clim Chang* 1:308–312.

Rodolfo-Metalpa R, Lombardi C, Cocito S, Hall-Spencer JM, Gambi MC. 2010. Effects of ocean acidification and high temperatures on the bryozoan *Myriapora truncata* at natural CO_2 vents. *Mar Ecol* 31:447–456.

Rodrigues LJ, Grottoli AG, Pease TK. 2008. Lipid class composition of bleached and recovering *Porites compressa* Dana, 1846 and *Montipora capitata* Dana, 1846 corals from Hawaii. *J Exp Mar Bio Ecol* 358:136–143.

Rodrigues LJ, Grottoli AG. 2007. Energy reserves and metabolism as indicators of coral recovery from bleaching. *Limnol Oceanogr* 52:1874–1882.

Rodriguez-Lanetty M, Harii S, Hoegh-Guldberg O. 2009. Early molecular responses of coral larvae to hyperthermal stress. *Mol Ecol* 18:5101–5114.

Rosa R, Seibel BA. 2008. Synergistic effects of climate-related variables suggest future physiological impairment in a top oceanic predator. *Proc Natl Acad Sci U S A* 105:20776–20780.

Rose JM, Feng Y, Gobler CJ, Gutierrez R, Hare CE, Leblanc K, Hutchins DA. 2009. Effects of increased pCO_2 and temperature on the North Atlantic spring bloom. II. Microzooplankton abundance and grazing. *Mar Ecol Prog Ser* 388:27–40.

Ross C, Ritson-Williams R, Olsen K, Paul VJ. 2012. Short-term and latent post-settlement effects associated with elevated temperature and oxidative stress on larvae from the coral *Porites astreoides*. *Coral Reefs* 32:71–79.

Ross C, Ritson-Williams R, Pierce R, Bullington JB, Henry M, Paul VJ. 2010. Effects of the Florida red tide dinoflagellate, *Karenia brevis*, on oxidative stress and metamorphosis of larvae of the coral *Porites astreoides*. *Harmful Algae* 9:173–179.

Roughgarden J, Gaines SD, Pacala S. 1987. Supply side ecology: the role of physical tranpsort processes. In: *Organization of communities: past and present* (Giller P, Gee J, eds.), pp 491–518. Blackwell, London: Proceedings of the British Ecologyical Society Symposium, Aberstwyth, Wales.

Rouser G, Fleischer S, Yamamoto A. 1970. Two dimensional thin layer chromatographic separation of polar lipids and determination of phospholipids by phosphorus analysis of spots. *Lipids* 5:494–496.

Sabine CL, Feely RA, Gruber N, Key RM, Lee K, Bullister JL, Wanninkhof R, Wong CS, Wallace DWR, Tilbrook B, Millero FJ, Peng T-H, Kozyr A, Ono T, Rios AF. 2004. The oceanic sink for anthropogenic CO_2. *Science* 305:367–371.

Sanford E, Kelly MW. 2011. Local adaptation in marine invertebrates. *Ann Rev Mar Sci* 3:509–535.

Santos IR, Glud RN, Maher D, Erler D, Eyre BD. 2011. Diel coral reef acidification driven by porewater advection in permeable carbonate sands, Heron Island, Great Barrier Reef. *Geophys Res Lett* 38:L03604.

Sargent JR, Gatten RR, McIntosh R. 1977. Wax esters in the marine environment — their occurrence, formation, transformation and ultimate fates. *Mar Chem* 5:573–584.

Sargent JR. 1976. The structure, metabolism, and function of lipids in marine organisms. In: *Biochemical and biophysical perspectives in marine biology. Vol. III* (Malins DC, Sargent JR, eds.), pp 149–212. London: Academic Press.

Schmidt-Roach S, Miller KJ, Lundgren P, Andreakis N. 2014. With eyes wide open: a revision of species within and closely related to the *Pocillopora damicornis* species complex (Scleractinia; Pocilloporidae) using morphology and genetics. *Zool J Linn Soc* 170:1–33.

Schwartz A, Lindenmayer GE, Allen JC. 1975. The sodinum-potassium adenosine triphosphatase: pharmacological, physiological and biochemical aspects. *Pharmacol Rev* 27:3–134.

Sebens K. 1983. The larval and juvenile ecology of the temperate octocoral Alcyonium siderium Verrill. I. Substratum selection by benthic larvae. *J Exp Mar Bio Ecol* 71:73–89.

Seneca FO, Forêt S, Ball EE, Smith-Keune C, Miller DJ, van Oppen MJH. 2010. Patterns of gene expression in a scleractinian coral undergoing natural bleaching. *Mar Biotechnol* 12:594–604.

Sewell MA. 2005. Utilization of lipids during early development of the sea urchin *Evechinus chloroticus*. *Mar Ecol Prog Ser* 304:133–142.

Shanks AL. 2009. Pelagic larval duration and dispersal distance revisited. *Biol Bull*.

Shashar N, Cohen Y, Loya Y. 1993. Extreme diel fluctuations of oxygen in diffusive boundary layers surrounding stony corals. *Biol Bull* 185:455–461.

Shaw EC, McNeil BI, Tilbrook B. 2012. Impacts of ocean acidification in naturally variable coral reef flat ecosystems. *J Geophys Res* 117:C03038.

Shaw EC, McNeil BI. 2014. Seasonal variability in carbonate chemistry and air–sea CO_2 fluxes in the southern Great Barrier Reef. *Mar Chem* 158:49–58.

Sheppard Brennand H, Soars N, Dworjanyn SA, Davis AR, Byrne M. 2010. Impact of ocean warming and ocean acidification on larval development and calcification in the sea urchin *Tripneustes gratilla*. *PLoS One* 5:e11372.

Shilling FM, Hoegh-Guldberg O, Manahan DT. 1996. Sources of energy for increased metabolic demand during metamorphosis of the abalone *Haliotis rufescens* (Mollusca). *Biol Bull* 191:402–412.

Shinzato C, Inoue M, Kusakabe M. 2014. A snapshot of a coral "holobiont": a transcriptome assembly of the scleractinian coral, porites, captures a wide variety of genes from both the host and symbiotic zooxanthellae. *PLoS One* 9:e85182.

Silverman J, Lazar B, Cao L, Caldeira K, Erez J. 2009. Coral reefs may start dissolving when atmospheric CO_2 doubles. *Geophys Res Lett* 36:L05606.

Silverman J, Lazar B, Erez J. 2007. Effect of aragonite saturation, temperature, and nutrients on the community calcification rate of a coral reef. *J Geophys Res* 112:C05004.

Sinervo B. 1990. The evolution of maternal investment in lizards: an experimental and comparative analysis of egg size and its effect on offspring performance. *Evolution* 44:279–294.

Skou J, Esmann M. 1979. Preparation of membrane-bound and of solubilized Na+ + K+)-ATPase from rectal glands of *Squalus acanthias*. *Biochim Biophys Acta* 567:436–444.

Smith PK, Krohn RI, Hermanson GT, Mallia AK, Gartner FH, Provenzano MD, Fujimoto EK, Goeke NM, Olson BJ, Klenk DC. 1985. Measurement of protein using bicinchoninic acid. *Anal Biochem* 150:76–85.

Sokolova IM, Frederich M, Bagwe R, Lannig G, Sukhotin AA. 2012. Energy homeostasis as an integrative tool for assessing limits of environmental stress tolerance in aquatic invertebrates. *Mar Environ Res* 79:1–15.

Sokolova IM. 2013. Energy-limited tolerance to stress as a conceptual framework to integrate the effects of multiple stressors. *Integr Comp Biol* 53:597–608.

Somero GN. 2010. The physiology of climate change: how potentials for acclimatization and genetic adaptation will determine "winners" and "losers." *J Exp Biol* 213:912–920.

Srere PA. 1969. Citrate synthase:[EC 4.1. 3.7. Citrate oxaloacetate-lyase (CoA-acetylating)]. *Methods Enzymol* 13:3–11.

Stat M, Gates RD. 2011. Clade D Symbiodinium in scleractinian corals: a "nugget" of hope, a selfish opportunist, an ominous sign, or all of the above? *J Mar Biol* 2011:730715.

Stearns SC. 1992. The evolution of life histories. Oxford, United Kingdom: Oxford University Press.

Stevens DJ, Hansell MH, Freel JA, Monaghan P. 1999. Developmental trade-offs in caddis flies: increased investment in larval defense alters adult resource allocation. *Proc R Soc B-Biological Sci* 266:1049–1054.

Stimson JS. 1987. Location, quantity and rate of change in quantity of lipids in tissue of Hawaiian hermatypic corals. *Bull Mar Sci* 41:889–904.

Stoddart JA, Black R. 1985. Cycles of gametogenesis and planulation in the coral *Pocillopora damicornis*. *Mar Ecol Prog Ser* 23:153–164.

Strathmann R. 1974. The spread of sibling larvae of sedentary marine invertebrates. *Am Nat* 108:29–44.

Strathmann RR. 1985. Feeding and non-feeding larval development and life-history evolution in marine invertebrates. *Annu Rev Ecol Syst* 16:339–361.

Sunday JM, Bates AE, Dulvy NK. 2012. Thermal tolerance and the global redistribution of animals. *Nat Clim Chang* 2:686–690.

Sunday JM, Calosi P, Dupont S, Munday PL, Stillman JH, Reusch TBH. 2014. Evolution in an acidifying ocean. *Trends Ecol Evol* 29:117–125.

Suwa R, Nakamura M, Morita M. 2010. Effects of acidified seawater on early life stages of scleractinian corals (Genus *Acropora*). *Fish Sci* 76:93–99.

Szmant AM, Meadows MG. 2006. Developmental changes in coral larval buoyancy and vertical swimming behavior: implications for dispersal and connectivity. *Proc 10th Int Coral Reef Symp*.

Tang C-H, Wu W-Y, Tsai S-C, Yoshinaga T, Lee T-H. 2010. Elevated Na+/K+-ATPase responses and its potential role in triggering ion reabsorption in kidneys for homeostasis of marine euryhaline milkfish (Chanos chanos) when acclimated to hypotonic fresh water. *J Comp Physiol B Biochem Syst Environ Physiol* 180:813–824.

Tans P, Keeling R. 2014. Trends in atmospheric carbon dioxide. Earth Systems Research Laboratory, Global Monitoring Division, Global Greenhouse Gas Reference Network. http://www.esrl.noaa.gov/gmd.ccgg/trends/.

Tchernov D, Gorbunov MY, de Vargas C, Narayan Yadav S, Milligan AJ, Häggblom M, Falkowski PG. 2004. Membrane lipids of symbiotic algae are diagnostic of sensitivity to thermal bleaching in corals. *Proc Natl Acad Sci U S A* 101:13531–13535.

Thorson G. 1950. Reproductive and larval ecology of marine bottom invertebrates. *Biol Rev* 25:1–45.

Thuesen E V, Childress JJ. 1994. Oxygen consumption rates and metabolic activities of oceanic California medusae in relation to body size and habitat depth. *Biol Bull* 187:84–98.

Todgham AE, Hofmann GE. 2009. Transcriptomic response of sea urchin larvae Strongylocentrotus purpuratus to CO_2-driven seawater acidification. *J Exp Biol* 212:2579–2594.

Tomanek L, Zuzow MJ, Ivanina A V, Beniash E, Sokolova IM. 2011. Proteomic response to elevated pCO_2 level in eastern oysters, *Crassostrea virginica*: evidence for oxidative stress. *J Exp Biol* 214:1836–1844.

Torda G, Lundgren P, Willis BL, Van Oppen MJH. 2013. Genetic assignment of recruits reveals short- and long-distance larval dispersal in *Pocillopora damicornis* on the Great Barrier Reef. *Mol Ecol* 22:5821–5834.

Traylor-Knowles N, Granger BR, Lubinski TJ, Parikh JR, Garamszegi S, Xia Y, Marto JA, Kaufman L, Finnerty JR. 2011. Production of a reference transcriptome and transcriptomic database (PocilloporaBase) for the cauliflower coral, *Pocillopora damicornis*. *BMC Genomics* 12:585.

Tremblay P, Fine M, Maguer JF, Grover R, Ferrier-Pagès C. 2013. Photosynthate translocation increases in response to low seawater pH in a coral–dinoflagellate symbiosis. *Biogeosciences* 10:3997–4007.

Trench RK. 1971. The physiology and biochemistry of zooxanthellae symbiotic with marine coelenterates. I. The assimilation of photosynthetic products of zooxantehllae by two marine coelenterates. *Proc R Soc B-Biological Sci* 177:237–250.

Underwood AJ, Keough MJ. 2001. Supply side ecology: the nature and consequences of variations in recruitment of intertidal organisms. In: *Marine Community Ecology* (Bertness M, Gaines S, Hay M, eds.), pp 183–200. Sutherland, MA: Sinauer.

Vavra J, Manahan DT. 1999. Protein metabolism in lecithotrophic larvae (Gastropoda: *Haliotis rufescens*). *Biol Bull* 196:177–186.

Venn A, Tambutté E, Holcomb M, Allemand D, Tambutté S. 2011. Live tissue imaging shows reef corals elevate pH under their calcifying tissue relative to seawater. *PLoS One* 6:e20013.

Venn AA, Tambutté E, Lotto S, Zoccola D, Allemand D, Tambutté S. 2009. Imaging intracellular pH in a reef coral and symbiotic anemone. *Proc Natl Acad Sci U S A* 106:16574–16579.

Veron JEN. 2000. Corals of the world. Townsville, Australia: Australian Institute of Marine Science and CCR Qld Pty Ltd.

Vidal-Dupiol J, Adjeroud M, Roger E, Foure L, Duval D, Mone Y, Ferrier-Pagès C, Tambutté E, Tambutté S, Zoccola D, Allemand D, Mitta G. 2009. Coral bleaching under thermal stress: putative involvement of host/symbiont recognition mechanisms. *BMC Physiol* 9:14.

Vidal-Dupiol J, Zoccola D, Tambutté E, Grunau C, Cosseau C, Smith KM, Freitag M, Dheilly NM, Allemand D, Tambutté S. 2013. Genes related to ion-transport and energy production are upregulated in response to CO_2-driven pH decrease in corals: new insights from transcriptome analysis. *PLoS One* 8:e58652.

Villinski JT, Villinski JC, Byrne M, Raff RA. 2002. Convergent maternal provisioning and life-history evolution in echinoderms. *Evolution* 56:1764–1775.

Waldbusser GG, Voigt EP, Bergschneider H, Green MA, Newell RIE. 2011. Biocalcification in the eastern oyster (*Crassostrea virginica*) in relation to long-term trends in Chesapeake Bay pH. *Estuaries and Coasts* 34:221–231.

Walther G-R. 2010. Community and ecosystem responses to recent climate change. *Philos Trans R Soc B Biol Sci* 365:2019–2024.

Walther K, Sartoris F, Bock C, Pörtner H-O. 2009. Impact of anthropogenic ocean acidification on thermal tolerance of the spider crab *Hyas araneus*. *Biogeosciences* 6:2207–2215.

Ward S. 1992. Evidence for broadcast spawning as well as brooding in the scleractinian coral *Pocillopora damicornis*. *Mar Biol* 112:641–646.

Weibel ER, Hoppeler H. 2005. Exercise-induced maximal metabolic rate scales with muscle aerobic capacity. *J Exp Biol* 208:1635–1644.

Weis VM. 2008. Cellular mechanisms of Cnidarian bleaching: stress causes the collapse of symbiosis. *J Exp Biol* 211:3059–3066.

Weiss M, Heilmayer O, Brey T, Lucassen M, Pörtner H-O. 2012. Physiological capacity of *Cancer setosus* larvae - adaptation to El Nino Southern Oscillation conditions. *J Exp Mar Bio Ecol* 413:100–105.

Wellington GM, Fitt WK. 2003. Influence of UV radiation on the survival of larvae from broadcast-spawning reef corals. *Mar Biol* 143:1185–1192.

Wendt D. 2000. Energetics of larval swimming and metamorphosis in four species of *Bugula* (Bryozoa). *Biol Bull* 198:346–356.

Whitehead A, Galvez F, Zhang S, Williams LM, Oleksiak MF. 2010. Functional genomics of physiological plasticity and local adaptation in killifish. *J Hered* 102:499–511.

Wilkinson C. 1998. The 1997-1998 mass bleaching event around the world. In: *Status of coral reefs of the world: 1998* (Wilkinson CR, ed.), pp 15–38. Townsville, Australia: Australian Institute of Marine Science.

Williams TD. 1994. Intraspecific variation in egg size and egg composition in birds: effects on offspring fitness. *Biol Rev* 69:35–59.

Willis BL, Oliver JK. 1990. Direct tracking of coral larvae: implications for dispersal studies of planktonic larvae in topographically complex environments. *Ophelia* 32:145–162.

Wood HL, Spicer JI, Lowe DM, Widdicombe S. 2010. Interaction of ocean acidification and temperature; the high cost of survival in the brittlestar *Ophiura ophiura*. *Mar Biol* 157:2001–2013.

Wooldridge SA. 2009. A new conceptual model for the warm-water breakdown of the coral–algae endosymbiosis. *Mar Freshw Res* 60:483–496.

Woollacott RM, Pechenik JA, Imbalzano KM. 1989. Effects of duration of larval swimming period on early colony development in *Bugula stolonifera* (Bryozoa: Cheilostomata). *Mar Biol* 102:57–63.

Wootton JT, Pfister CA, Forester JD. 2008. Dynamic patterns and ecological impacts of declining ocean pH in a high-resolution multi-year dataset. *Proc Natl Acad Sci U S A* 105:18848–18853.

Wootton JT, Pfister CA. 2012. Carbon system measurements and potential climatic drivers at a site of rapidly declining ocean pH. *PLoS One* 7:e53396.

Yakovleva I, Bhagooli R, Takemura A, Hidaka M. 2004. Differential susceptibility to oxidative stress of two scleractinian corals: antioxidant functioning of mycosporine-glycine. *Comp Biochem Physiol B Biochem Mol Biol* 139:721–730.

Yates KK, Dufore C, Smiley N, Jackson C, Halley RB. 2007. Diurnal variation of oxygen and carbonate system parameters in Tampa Bay and Florida Bay. *Mar Chem* 104:110–124.

Yates KK, Halley RB. 2006. Diurnal variation in rates of calcification and carbonate sediment dissolution in Florida Bay. *Estuaries and Coasts* 29:24–39.

Yeoh S-R, Dai C-F. 2009. The production of sexual and asexual larvae within single broods of the scleractinian coral, *Pocillopora damicornis*. *Mar Biol* 157:351-359.

Young CM. 1995. Behavior and locomotion during the dispersal phase of larval life. In: *Ecology of Marine Invertebrate Larvae* (McEdward L, ed.), pp 249–277. Boca Raton, FL: CRC Press.

Yu PC, Matson PG, Martz TR, Hofmann GE. 2011. The ocean acidification seascape and its relationship to the performance of calcifying marine invertebrates: Laboratory experiments on the development of urchin larvae framed by environmentally-relevant pCO_2/pH. *J Exp Mar Bio Ecol* 400:288–295.

Zuur AF, Ieno E, Walker N, Saveliev A, Smith G. 2009. Mixed effects models and extensions in ecology with R. New York, NY: Springer.